ARMY ENGINEER WATERWAYS EXPERIMENT STATION

VICKSBURG, MS

CORPS OF ENGINEERS

HYDRAULIC DESIGN CRITERIA . Volume I.

Volume I   [Revised January 1977]

PREFACE

(11 Jan 77)

LEVEL II

This loose-leaf data-book is based on analyses of experimental in-
vestigations, model studies, and prototype observations. The purpose is
to make the data available to offices of the Corps of Engineers for use as
hydraulic design criteria. Certain design aids based on accepted theory,
such as energy-depth curves, will be included.

The material is prepared and disseminated by authority of the Office,
Chief of Engineers, as a part of the Corps of Engineers Civil Works
Investigations - Hydraulics (Item CW 804). The cooperation of other hy-
draulic laboratories, Government agencies, and individuals in permitting
the use of their data is appreciated and every effort is being made to
credit the original source.

In order that this data-book may be of greatest service, individual
sheets and charts will be distributed as issued. Revised sheets and charts
will be issued as new data become available. The data-book is being is-
sued in loose-leaf form to facilitate the addition of new material and the
revision of previously issued sheets and charts.

The classification index presents the range of subjects intended to
be covered in this compilation. A table of contents is included to assist
in the location of specific charts. Suggestions for revisions, corrections,
or additions are invited from those who use the data-book. Correspondence
should be addressed to the Director, U. S. Army Engineer Waterways Experi-
ment Station, Vicksburg, Mississippi.

The Waterways Experiment Station has no objection to reproduction of
the U. S. Army Engineer material published in this data-book provided a
credit line is included with each reproduction. Permission to reproduce
other than U. S. Army Engineer data presented on these charts should be ob-
tained from the original sources.

(12 309)

DTIC
S ELECTE D
NOV 28 1980

D

Revised 5-59

80 10 22 082

CORPS OF ENGINEERS

HYDRAULIC DESIGN CRITERIA

CLASSIFICATION INDEX

Revised 5-59

CORPS OF ENGINEERS

HYDRAULIC DESIGN CRITERIA

CLASSIFICATION INDEX (Continued)

100-SPILLWAYS (Continued)

200-OUTLET WORKS

Revised 5-59

CORPS OF ENGINEERS

HYDRAULIC DESIGN CRITERIA

CLASSIFICATION INDEX (Continued)

300-GATES AND VALVES

CORPS OF ENGINEERS

HYDRAULIC DESIGN CRITERIA

CLASSIFICATION INDEX (Continued)

500-NAVIGATION DAMS

Revised 2-54

CORPS OF ENGINEERS

HYDRAULIC DESIGN CRITERIA

CLASSIFICATION INDEX (Continued)

600 - ARTIFICIAL CHANNELS

Revised 2-54

CORPS OF ENGINEERS

HYDRAULIC DESIGN CRITERIA

CLASSIFICATION INDEX (Continued)

700-SPECIAL PROBLEMS

CORPS OF ENGINEERS

HYDRAULIC DESIGN CRITERIA

VOLUME 1

TABLE OF CONTENTS

Chart No.

CORPS OF ENGINEERS

HYDRAULIC DESIGN CRITERIA

VOLUME 1

TABLE OF CONTENTS (Continued)

Asterisk (*) denotes Seventeenth Issue.

Revised 1-77

CORPS OF ENGINEERS

HYDRAULIC DESIGN CRITERIA

VOLUME 1

TABLE OF CONTENTS (Continued)

Asterisk (*) denotes Seventeenth Issue.

CORPS OF ENGINEERS

HYDRAULIC DESIGN CRITERIA

VOLUME 1

TABLE OF CONTENTS (Continued)

Revised 1-77

CORPS OF ENGINEERS

HYDRAULIC DESIGN CRITERIA

VOLUME 1

TABLE OF CONTENTS (Continued)

CORPS OF ENGINEERS

HYDRAULIC DESIGN CRITERIA

VOLUME 1

TABLE OF CONTENTS (Continued)

Asterisk (*) denotes Seventeenth Issue.

Revised 1-77

CORPS OF ENGINEERS

HYDRAULIC DESIGN CRITERIA

VOLUME 1

TABLE OF CONTENTS (Continued)

Revised 1-77

HYDRAULIC DESIGN CRITERIA

SHEET 000-1

PHYSICAL CONSTANTS

ACCELERATION OF GRAVITY

EFFECTS OF LATITUDE AND ALTITUDE

1. The value of acceleration of gravity commonly quoted in hydraulics textbooks is 32.2 ft/sec^2. Accordingly, the value of 2g in conversions between velocity and velocity head would be 64.4 ft/sec^2. Some engineers prefer to use 64.3 ft/sec^2 as being more representative of the acceleration of gravity for the United States.

2. Hydraulic Design Chart 000-1 was prepared to afford the engineer a convenient illustration of the nature of the variation of the acceleration of gravity with latitude and altitude. The theoretical values of acceleration of gravity at sea level are based on the international gravity formula converted to English units(2)

$$g_o = 32.08822 (1 + 0.0052884 \sin^2 \phi - 0.0000059 \sin^2 2\phi)$$

where

g_o = acceleration of gravity at sea level in ft/sec^2
ϕ = latitude in degrees.

Tabular values are given in reference (2). The correction for elevation above sea level is contained in the equation:

$$g_H = g_o - 0.000003086 \, H$$

where

g_H = acceleration of gravity at a given elevation in ft/sec^2
H = elevation above sea level in ft.

3. Chart 000-1 presents the variation of the acceleration of gravity with altitude for north latitudes from 30-50 degrees. The value of g for sea level at the equator is 32.088 ft/sec^2 and at Fairbanks, Alaska, is 32.227 ft/sec^2.

4. The values of the acceleration of gravity as measured by a pendulum are available from the Coast and Geodetic Survey.(1) The deviation of the measured value from the theoretical value, corrected for altitude, is called the free air anomaly. A plus or minus anomaly of 0.0016 ft/sec^2 may be considered large, except in high mountains or deep gorges.

5. <u>References.</u>

(1) Duerksen, J. A., <u>Pendulum Gravity Data in the United States.</u> U. S.
Coast and Geodetic Survey Special Publication No. 244, 1949.

(2) Swick, C. H., <u>Pendulum Gravity Measurements and Isostatic Reductions.</u>
U. S. Coast and Geodetic Survey Special Publication No. 232, 1942.

000-1

LATITUDE IN DEGREES

ACCELERATION OF GRAVITY IN FT/SEC²

10,000 FT ABOVE SEA LEVEL
8000
6000
4000
2000
SEA LEVEL
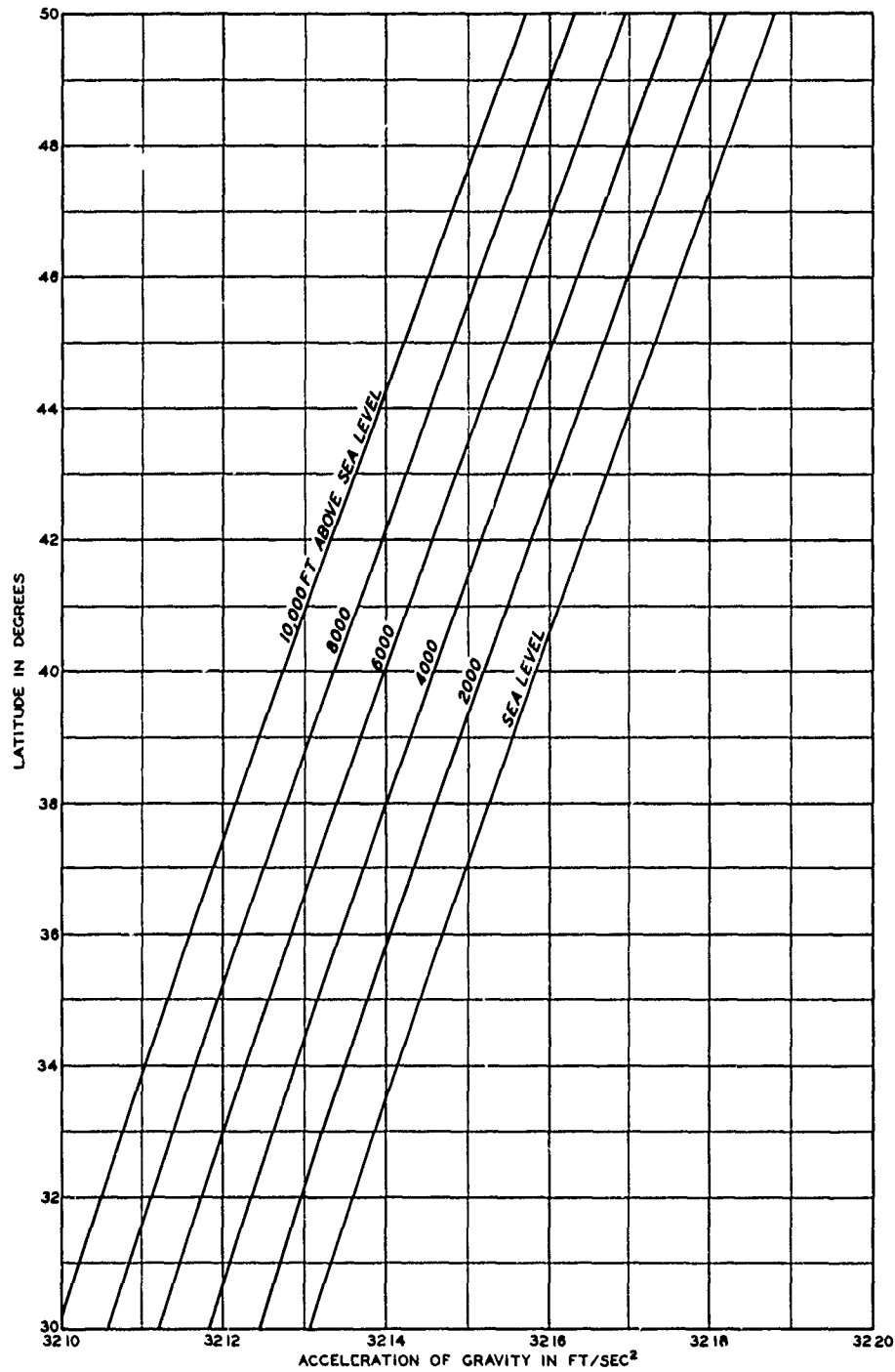
NOTE CHART PREPARED FROM INFORMATION
PUBLISHED IN USC & GS SPECIAL
PUBLICATION NO 232, "PENDULUM
GRAVITY MEASUREMENTS AND ISO-
STATIC REDUCTIONS," BY C H SWICK, 1942

PHYSICAL CONSTANTS

ACCELERATION OF GRAVITY
EFFECTS OF LATITUDE AND ALTITUDE

HYDRAULIC DESIGN CHART 000-1

HYDRAULIC DESIGN CRITERIA

SHEET 000-2

PHYSICAL CONSTANTS

BAROMETRIC DATA

ALTITUDE VS PRESSURE

1. **Cavitation.** The equation for incipient cavitation index takes into account the vapor pressure of water:

$$K_i = \frac{h_o - h_v}{V_o^2/2g}$$

where h_o is the absolute pressure in ft of water, h_v is vapor pressure of water in ft, and V_o is velocity of the water in ft per sec.

2. **Vapor Pressure.** The vapor pressure of water has been found to vary with the temperature as follows(1,2,3):

Temp, F	h_v ft of Water Absolute
32	0.20
50	0.41
70	0.84

3. **Barometric Pressure.** The value of the numerator in the above equation is also dependent upon h_o which is the barometric pressure less the negative pressure measured from atmospheric pressure. The incipient cavitation index is thus dependent upon the barometric pressure. For similar boundary geometry and similar flow conditions, the chances of cavitation occurring are somewhat greater at higher altitudes than at lower altitudes. The effect of altitude on cavitation possibilities is more marked than the effect of temperature.

4. **Chart 000-2.** The variation of barometric pressure with altitude is given on Chart 000-2. This chart was plotted using values given by King (reference 2, page 18), and agrees very closely with the values presented by the Smithsonian Institute (reference 1 page 559).

5. **Other Applications.** Barometric pressure is also of interest in the vertical limit of pump suction lines and turbine draft tubes.

6. **References.**

(1) Fowle, F. E., Smithsonian Physical Tables. Vol 88, Smithsonian Institute, Washington, D. C., 1934, p 232, p 559.

(2) King, H. W., Handbook of Hydraulics. 3d ed., McGraw-Hill Book Co.,
     Inc., New York, N. Y., 1939, table 14, p 18.

(3) National Research Council, International Critical Tables. Vol III,
     McGraw-Hill Book Co., Inc., New York, N. Y., 1928, p 211.

PRESSURE IN PSI
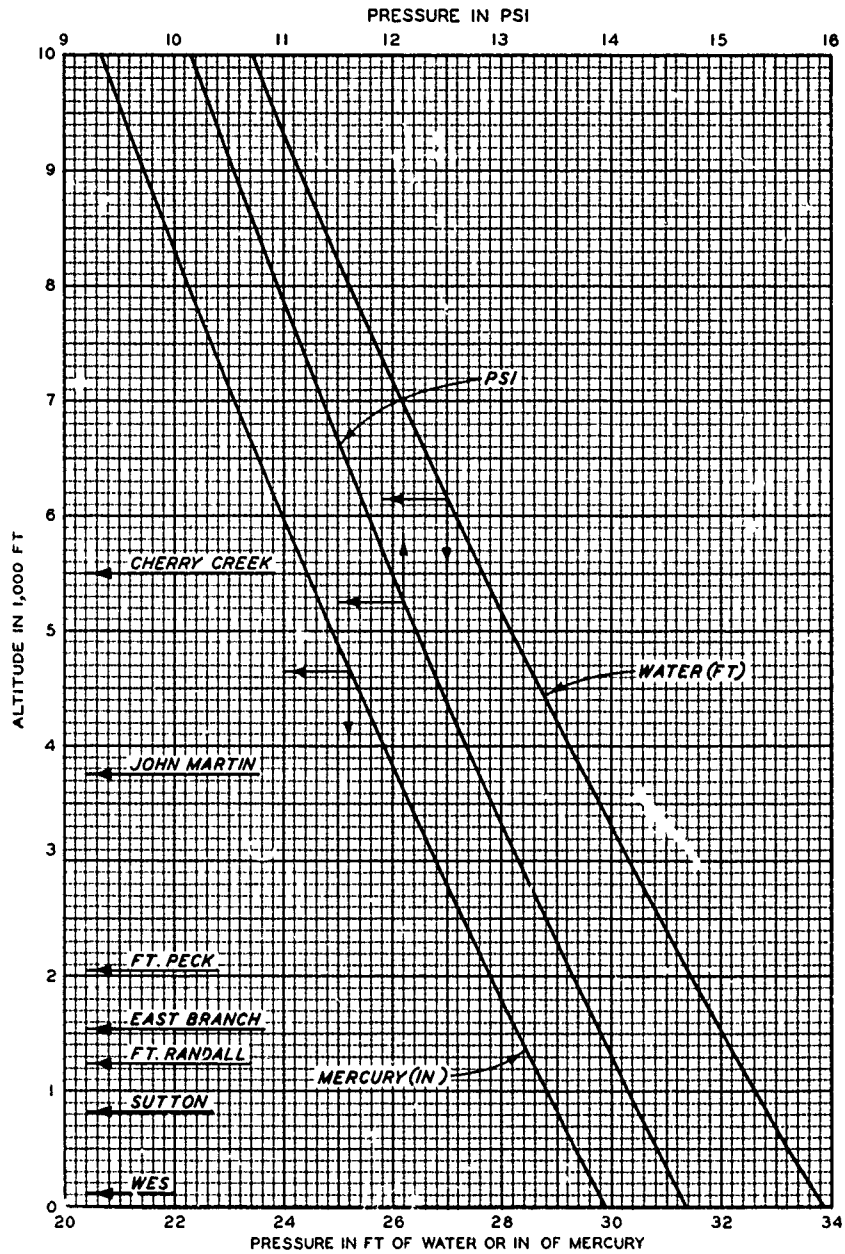
NOTE PRESSURES ARE FOR AIR TEMPERATURE OF 50 F.

PHYSICAL CONSTANTS
BAROMETRIC DATA
ALTITUDE VS. PRESSURE

HYDRAULIC DESIGN CHART 000-2

HYDRAULIC DESIGN CRITERIA

SHEETS 001-1 TO 001-5

FLUID PROPERTIES

EFFECT OF TEMPERATURE

1. Data on the fluid properties of water are required for the solution of many hydraulic problems. Hydraulic Design Charts 001-1 through 001-5 present information on those properties most commonly used in the design of hydraulic structures, and are included to afford convenient references for the design engineer.

2. Charts 001-1, 001-2, and 001-3 show the effect of temperature on kinematic viscosity, vapor pressure, and surface tension of water. The charts, in the order numbered, were prepared from data published in the International Critical Tables (4 and 5), (3), (4), respectively.

3. Chart 001-4 presents bulk modulus of water curves at atmospheric pressure for temperatures of 32 to 100 F. The Randall and Tryer curves were plotted from data published by Dorsey (1). The NBS curve was computed from Greenspan and Tschiegg (2) data on the speed of sound in water. The equation used in the computation was:

$$V = \sqrt{\frac{E}{\rho}}$$

where

V = speed of sound in water in ft per sec
E = bulk modulus in psi
ρ = density of fluid in slugs per cu ft

A change in pressure up to 10 atmospheres appears to have negligible effect on the value of the bulk modulus.

4. A curve for the Greenspan and Tschiegg data on the effect of temperature on the speed of sound in water is shown on Chart 001-5.

5. References.

(1) Dorsey, N. Ernest, Properties of Ordinary Water-Substance. Reinhold Publishing Corp., New York, N. Y., 1940, Table 105, p 243.

(2) Greenspan, M., and Tschiegg, C. E., "Speed of sound in water by a direct method." Research Paper 2795, Journal of Research of the National Bureau of Standards, vol 59, No. 4 (October 1957).

(3) International Critical Tables, vol III, First Edition, McGraw-Hill
Book Co., Inc., New York and London, 1928, p 211 (vapor pressure).

(4) _____, vol IV, First Edition, McGraw-Hill Book Co., Inc.,
New York and London, 1928, p 25 (density) and p 447 (surface tension).

(5) _____, vol V, First Edition, McGraw-Hill Book Co., Inc.,
New York and London, 1929, p 10 (dynamic viscosity).

001-1 to 001-5

WATER TEMPERATURE - F

KINEMATIC VISCOSITY ν* - SQUARE FEET PER SECOND x 10^{-5}
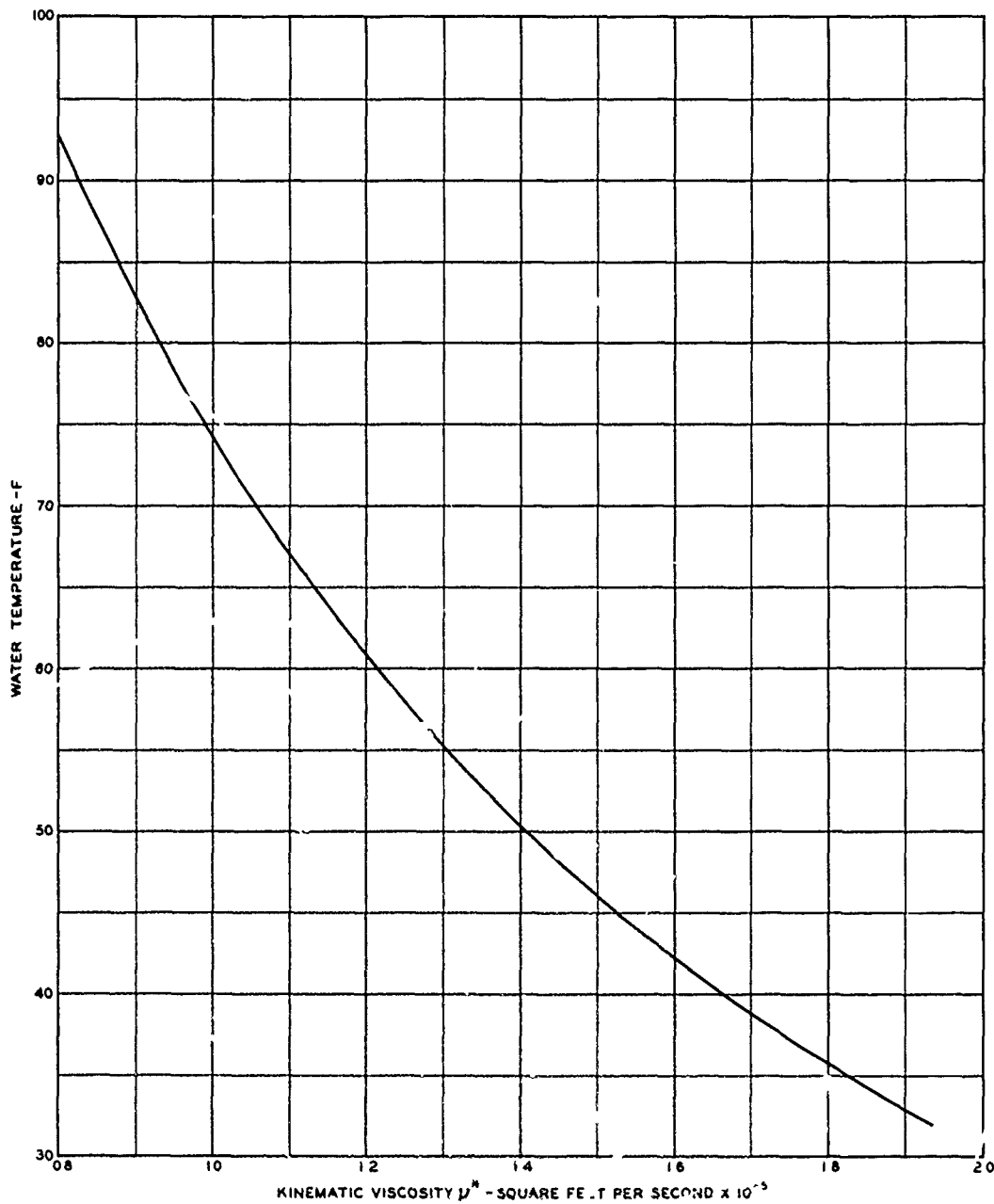
REFERENCE: INTERNATIONAL CRITICAL
TABLES, VOL. IV, PAGE 25,
AND VOL. V, PAGE 10, FIRST
EDITION

*FRESH WATER

FLUID PROPERTIES
KINEMATIC VISCOSITY OF WATER
EFFECT OF TEMPERATURE
HYDRAULIC DESIGN CHART 001-1

PREPARED BY U. S. ARMY ENGINEER WATERWAYS EXPERIMENT STATION, VICKSBURG, MISSISSIPPI   REV 8-50   WES 4-53

WATER TEMPERATURE - F
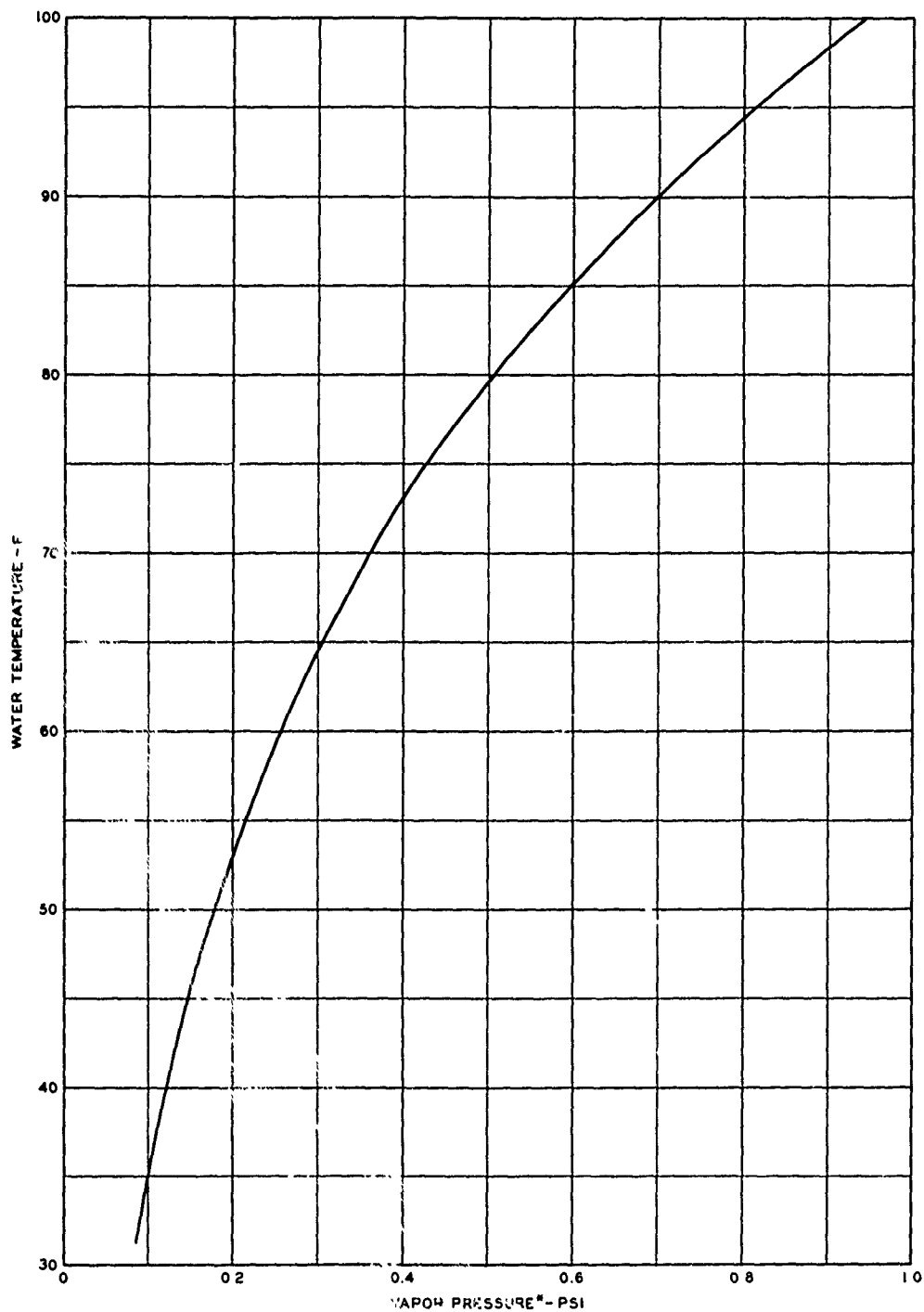
VAPOR PRESSURE* - PSI

REFERENCE: INTERNATIONAL CRITICAL
TABLES, VOL III, PAGE 211,
FIRST EDITION

*FRESH WATER

FLUID PROPERTIES
VAPOR PRESSURE OF WATER
EFFECT OF TEMPERATURE

HYDRAULIC DESIGN CHART 001-2

WES 8-60

WATER TEMPERATURE - F (y-axis)

SURFACE TENSION* - LB/FT X 10⁻³ (x-axis)
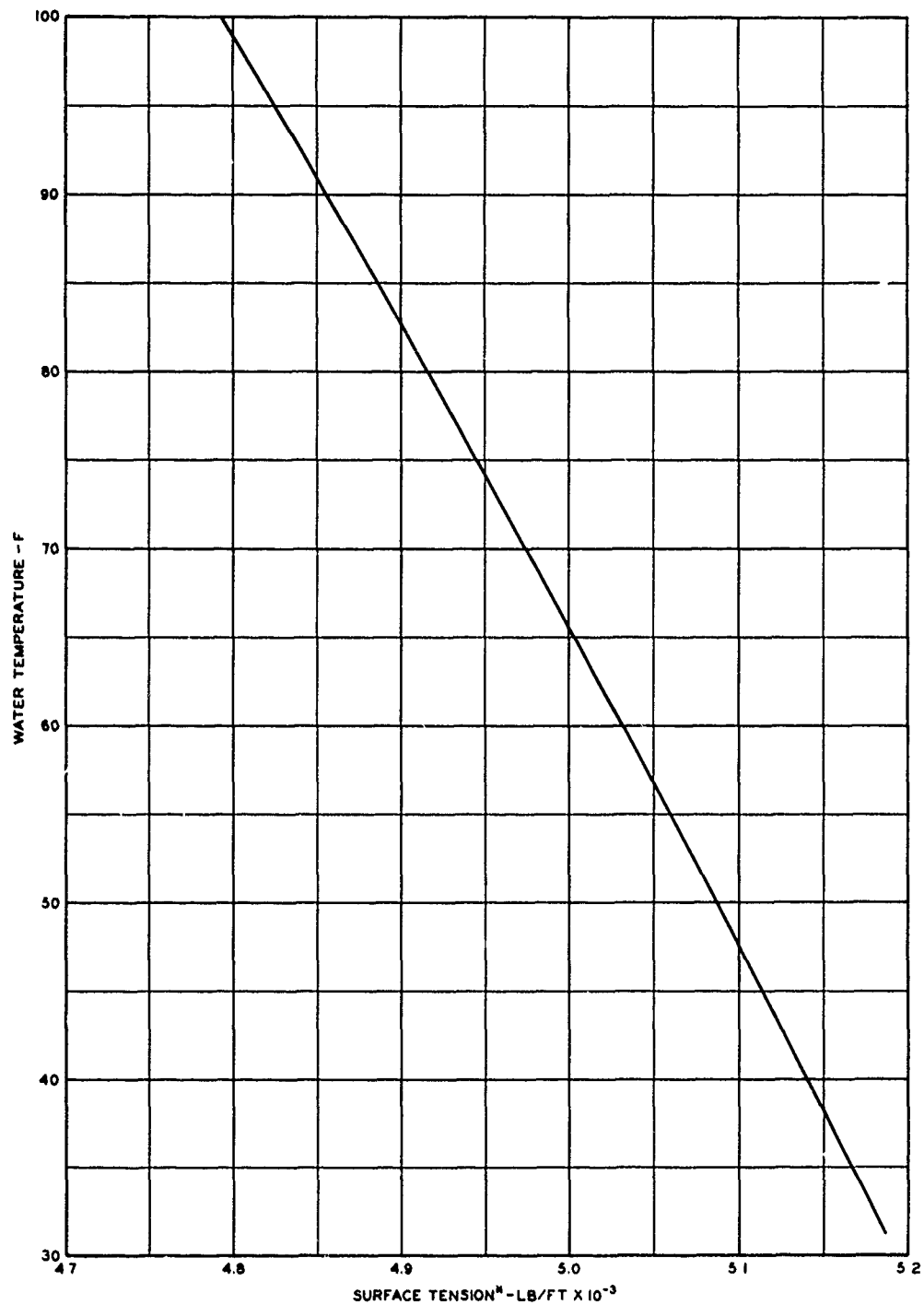
REFERENCE INTERNATIONAL CRITICAL
TABLES, VOL. IV, PAGE 447,
TABLE A-B, FIRST EDITION

*FRESH WATER

FLUID PROPERTIES
SURFACE TENSION OF WATER
EFFECT OF TEMPERATURE

HYDRAULIC DESIGN CHART 001-3

WES 8-60

WATER TEMPERATURE – F

BULK MODULUS* – PSI X 10⁵

LEGEND
TYRER
NBS
RANDALL
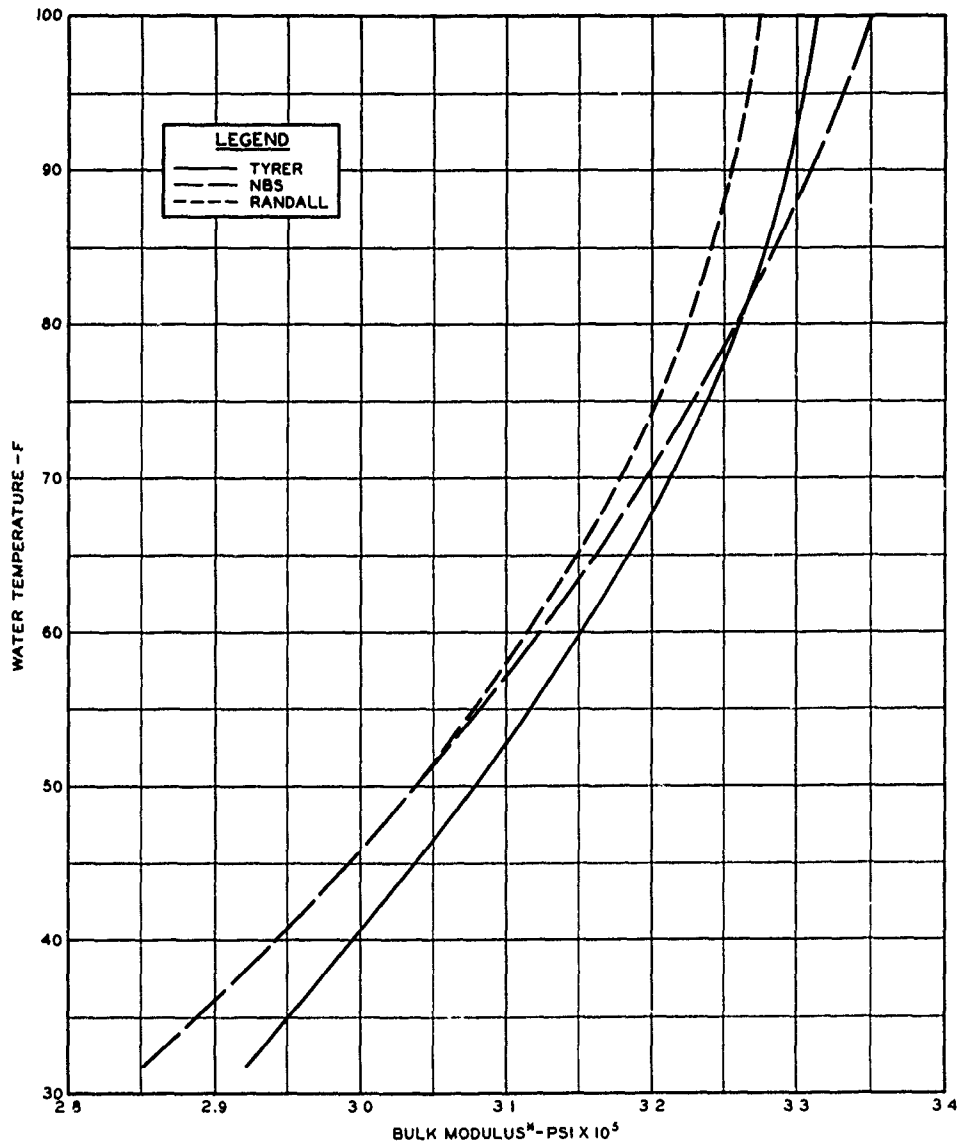
NOTE: CURVES SHOWN ARE FOR
ATMOSPHERIC PRESSURE

*FRESH WATER

FLUID PROPERTIES

BULK MODULUS OF WATER
EFFECT OF TEMPERATURE

HYDRAULIC DESIGN CHART 001-4

WES 8-60

WATER TEMPERATURE - F

100

90

80

70

60

50

40

30

46   47   48   49   50   51

SPEED-FT/SEC X 10^2
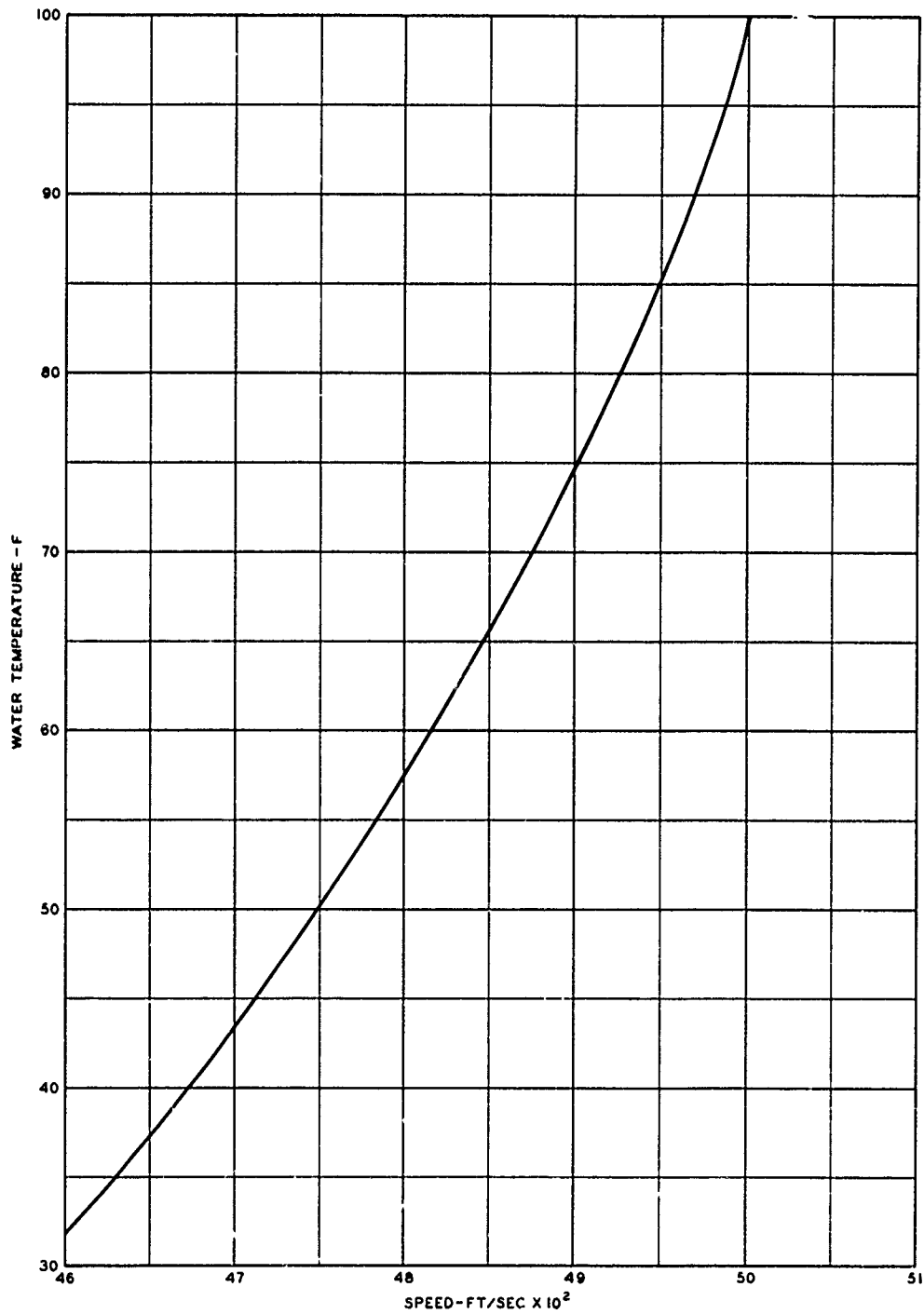
NOTE CURVE PLOTTED FROM DATA
REPORTED BY M GREENSPAN
AND C E TSCHIEGG, JOUR OF
RES , NBS, VOL 59, NO 4, 1957,
ON DISTILLED WATER

FLUID PROPERTIES
SPEED OF SOUND IN WATER
EFFECT OF TEMPERATURE

HYDRAULIC DESIGN CHART 001-5

WES 8-60

HYDRAULIC DESIGN CRITERIA

SHEET 010-1

OPEN CHANNEL FLOW

SURFACE CURVE CLASSIFICATIONS

1. Bakhmeteff's treatise on open channel flow[1] illustrates and defines classifications of surface curves of nonuniform flow. Hydraulic Design Chart 010-1 presents definition sketches of six water-surface curves encountered in many design problems. Although this schematic representation of classification of surface profiles has been presented in numerous textbooks, it is included here for ready reference. In addition, the chart presents examples of each type of surface curve chosen from problems that commonly occur in the work of the Corps of Engineers.

---

[1] B. A. Bakhmeteff, Hydraulics of Open Channel Flow, New York, N. Y., McGraw-Hill Book Company (1932), chapter VII.
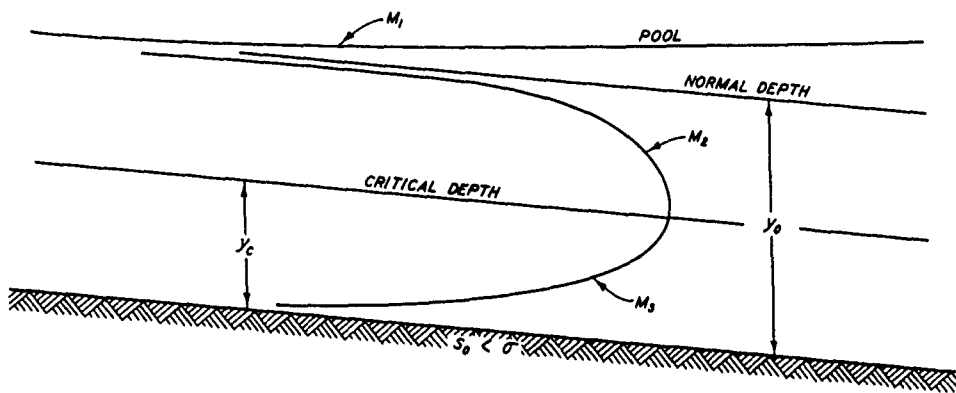
M_1 – BACKWATER FROM RESERVOIR – UNIFORM CHANNEL.
$y > y_0$, $\eta > 1$.

M_2 – DROP-DOWN TO SPILLWAY WITH SHALLOW APPROACH.
$y_0 > y > y_c$, $\eta < 1$.

M_3 – FLOW UNDER GATE ON MILD SLOPE.
$y < y_c$, $\eta < 1$.

MILD SLOPE
$$y_0 > y_c$$
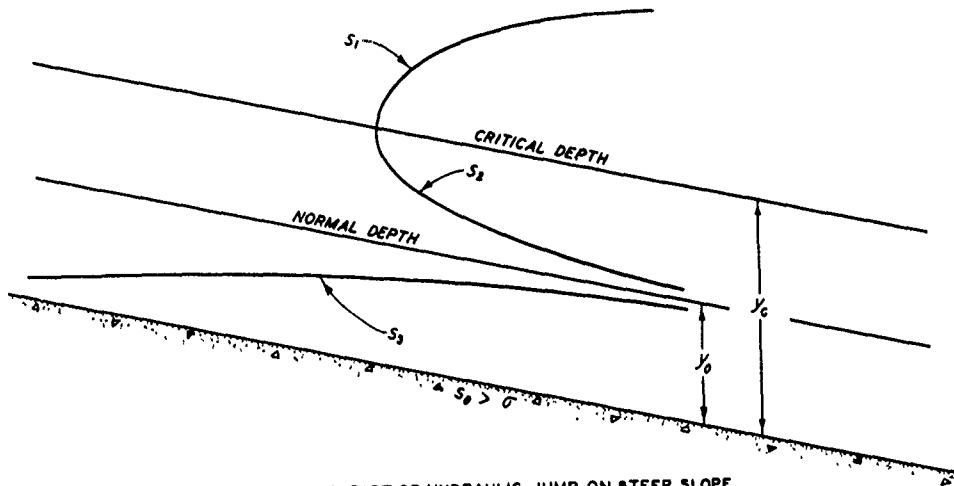
S_1 – LOWER PART OF HYDRAULIC JUMP ON STEEP SLOPE.
$y > y_c$, $\eta > 1$.

S_2 – CHUTE FLOW FROM LOW OGEE CREST.
$y_c > y > y_0$, $\eta > 1$.

S_3 – CHUTE FLOW FROM HIGH OGEE CREST. FLOW UNDER
GATE ON STEEP SLOPE.
$y < y_0$, $\eta < 1$.

STEEP SLOPE
$$y_0 < y_c$$

$$\eta = \frac{y}{y_0}$$

OPEN CHANNEL FLOW
CLASSIFICATIONS
UNIFORM SLOPES

HYDRAULIC DESIGN CHART 010-1

WES 3-56

HYDRAULIC DESIGN CRITERIA

SHEETS 010-2 TO 010-5/3

OPEN CHANNEL FLOW

BACKWATER COMPUTATIONS

1. Hydraulic Design Charts 010-2 to 010-5/3 are aids for reducing the computation effort in the design of uniform channels having nonuniform flow. It is expected that the charts will be of value in preliminary design work where various channel sizes, roughness values, and slopes are to be investigated. Other features of the charts will permit accurate determination of water-surface profiles.

2. **Basic Principle.** The theoretical water-surface profile of nonuniform flow in a uniform channel can be determined only by integrating the varied-flow equation throughout the reach under study. Such integration can be accomplished by the laborious step method or by various analytical methods such as that of Bakhmeteff[1]* and others. However, all methods are tedious and, in many cases, involve successive approximations.

3. Escoffier[3] has developed a graphical method based on the Bakhmeteff varied-flow function. This method greatly simplifies varied-flow solutions and eliminates successive approximations. The desired terminal water-surface elevation of a reach can be determined with or without intermediate water-surface points. The method is adaptable to all uniform-channel flow problems except those with horizontal or adverse bottom slopes. The more elaborate method of Keifer and Chu[4] is indicated for problems with circular section when accuracy is required. The method may be used for natural water courses if the cross section and slope are assumed uniform and hydraulic shape exponents are determined. Precise determination of the hydraulic exponent is not necessary to assure appropriate accuracy in backwater computations for natural channels. Usually an average value within the indicated range of depths will suffice.

4. The equation developed by Bakhmeteff to compute the water-surface profile is:

$$L = \frac{y_o}{S_o} \left\{ (\eta_2 - \eta_1) - (1 - \beta) \left[B(\eta_2) - B(\eta_1) \right] \right\}$$

---

* Raised numbers in parentheses refer to list of references at end of text.

where

$$L, \ y_o, \ \text{and} \ S_o = \text{length, normal depth, and bottom slope, respectively}$$

$$\eta = \text{dimensionless stage variable} \ (y/y_o)$$

$$\beta = \text{dimensionless quantity} \ (y_c/y_o)^N$$

$$B(\eta) = \text{varied flow function (Chart 010-3)}$$

$$y_c = \text{critical depth}$$

$$N = \text{hydraulic exponent (Chart 010-4)}.$$

If the equation is divided by y_o/S_o then

$$L \ \frac{S_o}{y_o} = (\eta_2 - \eta_1) - (1 - \beta) \left[B(\eta_2) - B(\eta_1) \right]$$

The term $\eta_2 - \eta_1$ is the vertical intercept of the varied-flow function plotted on Chart 010-3. The factor of the second term, $B(\eta_2) - B(\eta_1)$, is the horizontal intercept and $1 - \beta$ is a slope factor which converts the horizontal intercept into a component of the vertical. If the value of the equation computed from $L \ S_o/y_o$ is plotted vertically from a known η_1 on Chart 010-3 and the required slope line projected from the limit of this line to the curve, a value of η_2 is obtained from which the unknown depth can be computed, $y_2 = \eta_2 \ y_o$.

5. <u>Application.</u> Chart 010-2 defines the equations required in the Escoffier graphical method and outlines the required steps in the solution. It is necessary to plot the slope line, $1 - \beta$, in accordance with the horizontal and vertical scales of the chart.

6. Chart 010-4 presents graphical plots of hydraulic exponents for different channel shapes for use in conjunction with Chart 010-3. The coordinates are in dimensionless terms and are therefore applicable to channels of various sizes. The equations for trapezoidal and circular shaped channels and the method of plotting were developed by N. L. Barbarossa[2]. The general equation for hydraulic exponents applicable to all channel shapes was developed by Bakhmeteff.

7. Large-scale plots of the varied-flow function can be made where greater accuracy of results is required. Published tables[1] of the varied-flow function are given on Charts 010-5 to 010-5/3 for convenient reference. A hydraulic exponent of 3.3 is suggested for wide channels with two-dimensional flow. Tabulated values of the function for N = 3.3 were computed by the Waterways Experiment Station.

8. <u>List of References.</u>

(1) Bakhmeteff, B. A., <u>Hydraulics of Open Channel Flow.</u> McGraw-Hill Book Company, New York, N. Y., 1932.

(2) Barbarossa, N. L., Missouri River Division, CE, Omaha, Nebr., un-published data.

(3) Escoffier, F. F., <u>A Simplified Graphical Method for Determining Backwater Profiles.</u> Mobile District, CE, Mobile, Ala., un-published paper, 1955.

(4) Keifer, C. J., and Chu, H. H., "Backwater functions by numerical integration." <u>Transactions,</u> ASCE, vol 120 (1955), pp 429-448.

EQUATIONS AND DEFINITIONS

$$\eta = \frac{y}{y_o}, \text{ Where } y = \text{depth and } y_o = \text{normal depth.}$$

$$\beta = \left(\frac{y_c}{y_o}\right)^N, \text{ Where } y_c = \text{critical depth and } N = \text{hydraulic exponent.}$$

$$I = \frac{LS_o}{y_o}, \text{ Where } L = \text{length of reach and } S_o = \text{bottom slope.}$$

$$m = 1 - \beta, \text{ Where } m = \text{slope of construction line, } \left(\frac{\Delta \eta}{\Delta B(\eta)}\right).$$

GENERAL APPLICATION

1. Given channel shapes, S_o, Q, y_1 and Manning's "n." Required to find y_2 at a distance L from y_1.

2. The following charts apply:

Channel Type	Design Criteria Chart	
	y_o	y_c
Wide Channels	610-8	610-8
Rectangular Channels	610-9 and 9/1*	610-8
Trapezoidal Channels	610-2 to 4/1*	610-5 to 7
Circular Channels	224-8*	224-9

* Also requires use of Charts 610-1 and 1/1.

3. Select hydraulic exponent N from Chart 010-4.

4. Compute η_1, β, I and m from above equations.

5. Establish η_1 on curve of Chart 010-3 for proper value of exponent N.

6. Construct I in units of η vertically from η_1, upward for negative m and downward for positive m.

7. Draw slope line m through extremity of I and find η_2 where slope line intersects $B(\eta)$ curve.

8. Compute $y_2 = y_o \eta_2$.
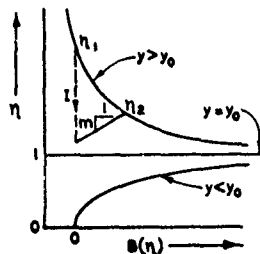
OPEN CHANNEL FLOW

DEFINITION AND APPLICATION

HYDRAULIC DESIGN CHART 010-2

WES 3-56
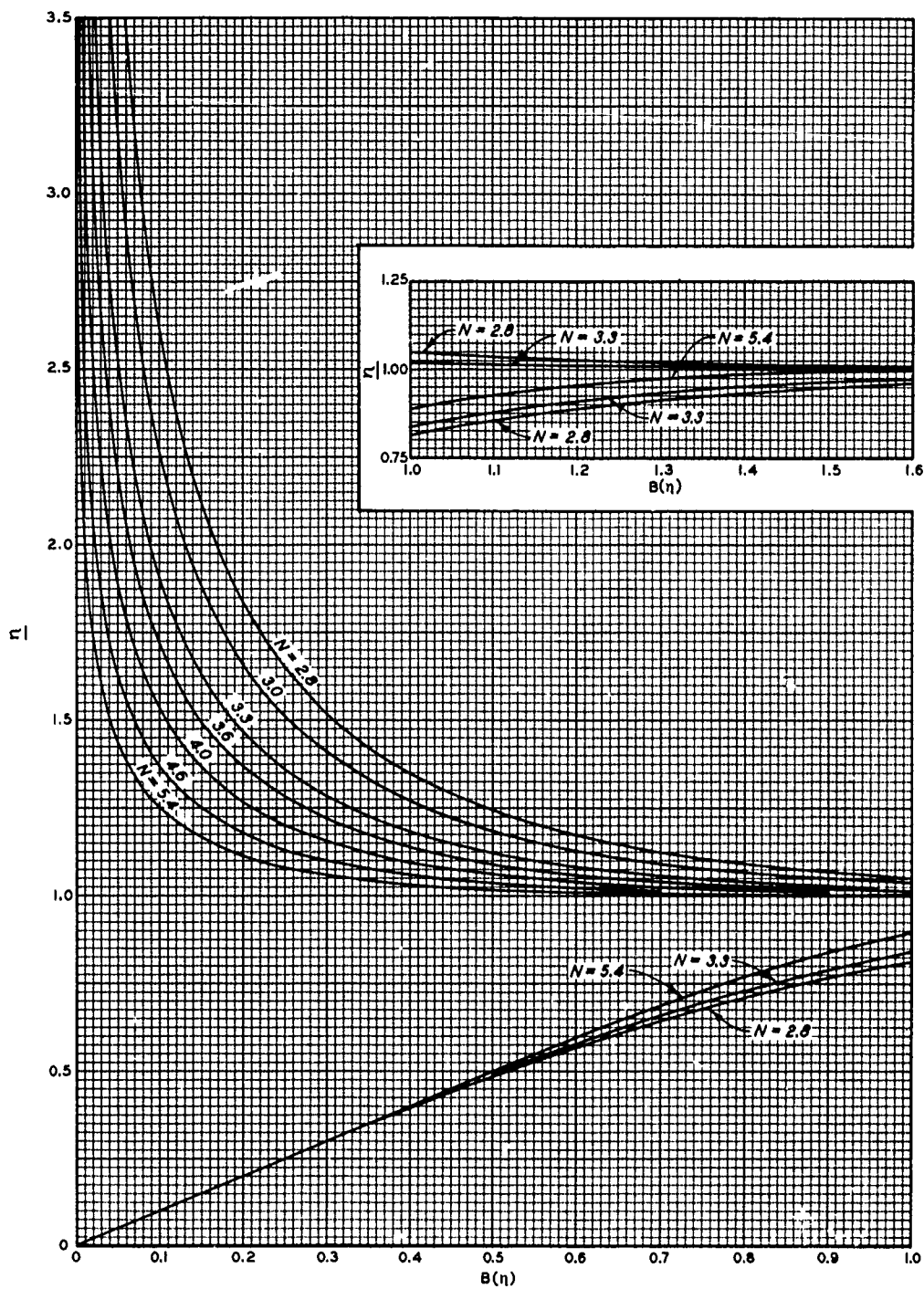
BASIC EQUATION

$$B(\eta) = -\int_0^\eta \frac{d\eta}{\eta^N - 1}$$

WHERE: $\eta = \dfrac{y}{y_0}$

N = HYDRAULIC EXPONENT
(3.3 FOR WIDE RECTANGULAR
CHANNELS)

OPEN CHANNEL FLOW

η VS $B(\eta)$

HYDRAULIC DESIGN CHART 010-3

WES 3-56

HYDRAULIC EXPONENT (N)

5.0

Z = 3

Z = 2

Z = 1.5

4.0

Z = 1

3.0

Z = 0 (RECTANGULAR)

2.0

CIRCULAR

1.0

0

| 0 | 0.5 | 1.0 | 1.5 | 2.0 | 2.5 |

DEPTH-BASE OR DEPTH-DIAMETER RATIO (α)

WS

y

1
Z

b

WS

D

y

GENERAL EQUATION

$$N = 2\frac{\log(K_2/K_1)}{\log(y_2/y_1)} = f(\alpha)$$

TRAPEZOIDAL SECTION

$$N = \frac{10}{3}\left(\frac{1+2Z\alpha}{1+Z\alpha}\right) - \frac{8}{3}\left(\frac{\alpha\sqrt{Z^2+1}}{1+2\alpha\sqrt{Z^2+1}}\right)$$

CIRCULAR SECTION

$$N = \frac{8}{3}\frac{1}{\sqrt{\alpha-\alpha^2}}\left[\frac{20\alpha^2(1-\alpha)}{\pi+4(2\alpha-1)\sqrt{\alpha-\alpha^2}+2\sin^{-1}(2\alpha-1)} - \frac{\alpha}{\pi+2\sin^{-1}(2\alpha-1)}\right]$$
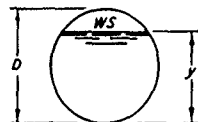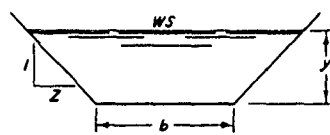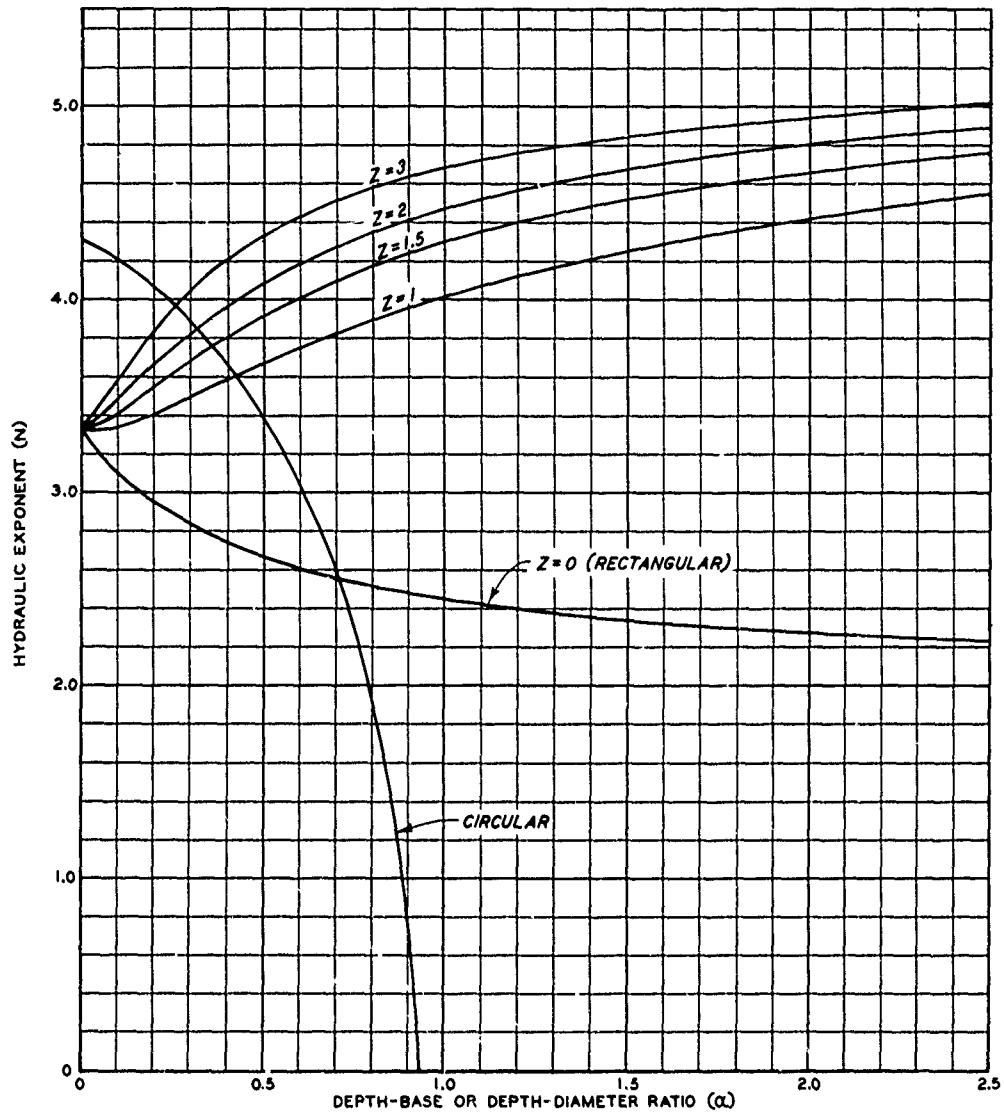
NOTE: $\alpha = \frac{y}{b}$ OR $\frac{y}{D}$

$K = \frac{1.486}{n}AR^{2/3}$ (BAKHMETEFF CONVEYANCE FACTOR)

OPEN CHANNEL FLOW
HYDRAULIC EXPONENT "N"

HYDRAULIC DESIGN CHART 010-4

	N											
η	2.8	3.0	3.2	3.3	3.4	3.6	3.8	4.0	4.2	4.6	5.0	5.4
0.00	0.000	0.000	0.000	0.000	0.000	0.000	0.000	0.000	0.000	0.000	0.000	0.000
0.02	0.020	0.020	0.020	0.020	0.020	0.020	0.020	0.020	0.020	0.020	0.020	0.020
0.04	0.040	0.040	0.040	0.040	0.040	0.040	0.040	0.040	0.040	0.040	0.040	0.040
0.06	0.060	0.060	0.060	0.060	0.060	0.060	0.060	0.060	0.060	0.060	0.060	0.060
0.08	0.080	0.080	0.080	0.080	0.080	0.080	0.080	0.080	0.080	0.080	0.080	0.080
0.10	0.100	0.100	0.100	0.100	0.100	0.100	0.100	0.100	0.100	0.100	0.100	0.100
0.12	0.120	0.120	0.120	0.120	0.120	0.120	0.120	0.120	0.120	0.120	0.120	0.120
0.14	0.140	0.140	0.140	0.140	0.140	0.140	0.140	0.140	0.140	0.140	0.140	0.140
0.16	0.160	0.160	0.160	0.160	0.160	0.160	0.160	0.160	0.160	0.160	0.160	0.160
0.18	0.180	0.180	0.180	0.180	0.180	0.180	0.180	0.180	0.180	0.180	0.180	0.180
0.20	0.201	0.200	0.200	0.200	0.200	0.200	0.200	0.200	0.200	0.200	0.200	0.200
0.22	0.221	0.221	0.220	0.220	0.220	0.220	0.230	0.220	0.220	0.220	0.220	0.220
0.24	0.241	0.241	0.241	0.240	0.240	0.240	0.240	0.240	0.240	0.240	0.240	0.240
0.26	0.262	0.261	0.261	0.261	0.261	0.260	0.260	0.260	0.260	0.260	0.260	0.260
0.28	0.282	0.282	0.281	0.281	0.281	0.281	0.280	0.280	0.280	0.280	0.280	0.280
0.30	0.303	0.302	0.302	0.301	0.301	0.301	0.301	0.300	0.300	0.300	0.300	0.300
0.32	0.324	0.323	0.322	0.322	0.322	0.321	0.321	0.321	0.321	0.320	0.320	0.320
0.34	0.344	0.343	0.343	0.342	0.342	0.342	0.341	0.341	0.341	0.340	0.340	0.340
0.36	0.366	0.364	0.363	0.363	0.363	0.362	0.362	0.361	0.361	0.361	0.360	0.360
0.38	0.387	0.385	0.384	0.383	0.383	0.383	0.382	0.382	0.381	0.381	0.381	0.380
0.40	0.408	0.407	0.405	0.404	0.404	0.403	0.403	0.402	0.402	0.401	0.401	0.400
0.42	0.430	0.428	0.426	0.425	0.425	0.424	0.423	0.423	0.422	0.421	0.421	0.421
0.44	0.452	0.450	0.448	0.447	0.446	0.445	0.444	0.443	0.443	0.442	0.441	0.441
0.46	0.475	0.472	0.470	0.469	0.468	0.466	0.465	0.464	0.463	0.462	0.462	0.461
0.48	0.497	0.494	0.492	0.490	0.489	0.488	0.486	0.485	0.484	0.483	0.482	0.481
0.50	0.521	0.517	0.514	0.512	0.511	0.509	0.508	0.506	0.505	0.504	0.503	0.502
0.52	0.544	0.540	0.536	0.534	0.534	0.531	0.529	0.528	0.527	0.525	0.523	0.522
0.54	0.568	0.563	0.559	0.557	0.556	0.554	0.551	0.550	0.548	0.546	0.544	0.543
0.56	0.593	0.587	0.583	0.580	0.579	0.576	0.574	0.572	0.570	0.567	0.565	0.564
0.58	0.618	0.612	0.607	0.604	0.603	0.599	0.596	0.594	0.592	0.589	0.587	0.585
0.60	0.644	0.637	0.631	0.628	0.627	0.623	0.620	0.617	0.614	0.611	0.608	0.606
0.61	0.657	0.650	0.644	0.641	0.639	0.635	0.631	0.628	0.626	0.622	0.619	0.617
0.62	0.671	0.663	0.657	0.653	0.651	0.647	0.643	0.640	0.637	0.633	0.630	0.628
0.63	0.684	0.676	0.669	0.666	0.664	0.659	0.655	0.652	0.649	0.644	0.641	0.638
0.64	0.698	0.690	0.683	0.678	0.677	0.672	0.667	0.664	0.661	0.656	0.652	0.649
0.65	0.712	0.703	0.696	0.692	0.689	0.684	0.680	0.676	0.673	0.667	0.663	0.660
0.66	0.727	0.717	0.709	0.705	0.703	0.697	0.692	0.688	0.685	0.679	0.675	0.672
0.67	0.742	0.731	0.722	0.718	0.716	0.710	0.705	0.701	0.697	0.691	0.686	0.683
0.68	0.757	0.746	0.737	0.732	0.729	0.723	0.718	0.713	0.709	0.703	0.698	0.694
0.69	0.772	0.761	0.751	0.746	0.743	0.737	0.731	0.726	0.722	0.715	0.710	0.706
0.70	0.787	0.776	0.766	0.760	0.757	0.750	0.744	0.739	0.735	0.727	0.722	0.717
0.71	0.804	0.791	0.781	0.775	0.772	0.764	0.758	0.752	0.748	0.740	0.734	0.729
0.72	0.820	0.807	0.796	0.790	0.786	0.779	0.772	0.766	0.761	0.752	0.746	0.741
0.73	0.837	0.823	0.811	0.805	0.802	0.793	0.786	0.780	0.774	0.765	0.759	0.753
0.74	0.854	0.840	0.827	0.820	0.817	0.808	0.800	0.794	0.788	0.779	0.771	0.766

BASIC EQUATION

$$B(\eta) = -\int_0^\eta \frac{d\eta}{\eta^N - 1}$$

WHERE:

$\eta = \dfrac{y}{y_0}$

N = HYDRAULIC EXPONENT

η = 0.00 TO 0.74 *

* FROM TABLES IN BAKHMETEFF'S
"HYDRAULICS OF OPEN CHANNEL FLOW."
N = 3.3 COMPUTED BY WES

OPEN CHANNEL FLOW
VARIED FLOW FUNCTION B(η)

HYDRAULIC DESIGN CHART 010-5

WES 3-56

η	N											
	2.8	3.0	3.2	3.3	3.4	3.6	3.8	4.0	4.2	4.6	5.0	5.4
0.75	0.872	0.857	0.844	0.836	0.833	0.823	0.815	0.808	0.802	0.792	0.784	0.778
0.76	0.890	0.874	0.861	0.853	0.849	0.839	0.830	0.823	0.817	0.806	0.798	0.791
0.77	0.909	0.892	0.878	0.870	0.866	0.855	0.846	0.838	0.831	0.820	0.811	0.804
0.78	0.929	0.911	0.896	0.887	0.883	0.872	0.862	0.854	0.847	0.834	0.825	0.817
0.79	0.949	0.930	0.914	0.905	0.901	0.889	0.879	0.870	0.862	0.849	0.839	0.831
0.80	0.970	0.950	0.934	0.924	0.919	0.907	0.896	0.887	0.878	0.865	0.854	0.845
0.81	0.992	0.971	0.954	0.943	0.938	0.925	0.914	0.904	0.895	0.881	0.869	0.860
0.82	1.015	0.993	0.974	0.964	0.958	0.945	0.932	0.922	0.913	0.897	0.885	0.875
0.83	1.039	1.016	0.996	0.985	0.979	0.965	0.952	0.940	0.931	0.914	0.901	0.890
0.84	1.064	1.040	1.019	1.007	1.001	0.985	0.972	0.960	0.949	0.932	0.918	0.906
0.85	1.091	1.065	1.043	1.030	1.024	1.007	0.993	0.980	0.969	0.950	0.935	0.923
0.86	1.119	1.092	1.068	1.055	1.048	1.031	1.015	1.002	0.990	0.970	0.954	0.940
0.87	1.149	1.120	1.095	1.081	1.074	1.055	1.039	1.025	1.012	0.990	0.973	0.959
0.88	1.181	1.151	1.124	1.109	1.101	1.081	1.064	1.049	1.035	1.012	0.994	0.978
0.89	1.216	1.183	1.155	1.139	1.131	1.110	1.091	1.075	1.060	1.035	1.015	0.999
0.90	1.253	1.218	1.189	1.171	1.163	1.140	1.120	1.103	1.087	1.060	1.039	1.021
0.91	1.294	1.257	1.225	1.206	1.197	1.173	1.152	1.133	1.116	1.088	1.064	1.045
0.92	1.340	1.300	1.266	1.245	1.236	1.210	1.187	1.166	1.148	1.117	1.092	1.072
0.93	1.391	1.348	1.311	1.289	1.279	1.251	1.226	1.204	1.184	1.151	1.123	1.101
0.94	1.449	1.403	1.363	1.339	1.328	1.297	1.270	1.246	1.225	1.188	1.158	1.134
0.95	1.518	1.467	1.423	1.397	1.385	1.352	1.322	1.296	1.272	1.232	1.199	1.172
0.96	1.601	1.545	1.497	1.468	1.454	1.417	1.385	1.355	1.329	1.285	1.248	1.217
0.97	1.707	1.644	1.590	1.558	1.543	1.501	1.464	1.431	1.402	1.351	1.310	1.275
0.975	1.773	1.707	1.649	1.615	1.598	1.554	1.514	1.479	1.447	1.393	1.348	1.311
0.980	1.855	1.783	1.720	1.684	1.666	1.617	1.575	1.536	1.502	1.443	1.395	1.354
0.985	1.959	1.880	1.812	1.772	1.752	1.699	1.652	1.610	1.573	1.508	1.454	1.409
0.990	2.106	2.017	1.940	1.894	1.873	1.814	1.761	1.714	1.671	1.598	1.537	1.487
0.995	2.355	2.250	2.159	2.105	2.079	2.008	1.945	1.889	1.838	1.751	1.678	1.617
0.999	2.931	2.788	2.663	2.590	2.554	2.457	2.370	2.293	2.223	2.101	2.002	1.917

BASIC EQUATION

$$B(\eta) = -\int_0^\eta \frac{d\eta}{\eta^N - 1}$$

WHERE:

$\eta = \dfrac{y}{y_0}$

N = HYDRAULIC EXPONENT

* FROM TABLES IN BAKHMETEFF'S
"HYDRAULICS OF OPEN CHANNEL FLOW."
N = 33 COMPUTED BY WES.

η = 0.75 TO 0.999*

OPEN CHANNEL FLOW
VARIED FLOW FUNCTION B(η)

HYDRAULIC DESIGN CHART 010-5/1

WES 3-56

η	N											
	2.8	3.0	3.2	3.3	3.4	3.6	3.8	4.0	4.2	4.6	5.0	5.4
1.001	2.399	2.184	2.008	1.905	1.856	1.725	1.610	1.508	1.417	1.264	1.138	1.033
1.005	1.818	1.649	1.506	1.422	1.384	1.279	1.188	1.107	1.036	0.915	0.817	0.737
1.010	1.572	1.419	1.291	1.217	1.182	1.089	1.007	0.936	0.873	0.766	0.681	0.610
1.015	1.428	1.286	1.166	1.097	1.065	0.978	0.902	0.836	0.778	0.680	0.602	0.537
1.02	1.327	1.191	1.078	1.013	0.982	0.900	0.828	0.766	0.711	0.620	0.546	0.486
1.03	1.186	1.060	0.955	0.894	0.866	0.790	0.725	0.668	0.618	0.535	0.469	0.415
1.04	1.086	0.967	0.868	0.811	0.785	0.714	0.653	0.600	0.554	0.477	0.415	0.365
1.05	1.010	0.896	0.802	0.747	0.723	0.656	0.598	0.548	0.504	0.432	0.374	0.328
1.06	0.948	0.838	0.748	0.696	0.672	0.608	0.553	0.506	0.464	0.396	0.342	0.298
1.07	0.896	0.790	0.703	0.653	0.630	0.569	0.516	0.471	0.431	0.366	0.315	0.273
1.08	0.851	0.749	0.665	0.617	0.595	0.535	0.485	0.441	0.403	0.341	0.292	0.252
1.09	0.812	0.713	0.631	0.584	0.563	0.506	0.457	0.415	0.379	0.319	0.272	0.234
1.10	0.777	0.681	0.601	0.556	0.536	0.480	0.433	0.392	0.357	0.299	0.254	0.218
1.11	0.746	0.652	0.575	0.531	0.511	0.457	0.411	0.372	0.338	0.282	0.239	0.204
1.12	0.718	0.626	0.551	0.508	0.488	0.436	0.392	0.354	0.321	0.267	0.225	0.192
1.13	0.692	0.602	0.529	0.487	0.468	0.417	0.374	0.337	0.305	0.253	0.212	0.181
1.14	0.669	0.581	0.509	0.468	0.450	0.400	0.358	0.322	0.291	0.240	0.201	0.170
1.15	0.647	0.561	0.490	0.451	0.432	0.384	0.343	0.308	0.278	0.229	0.191	0.161
1.16	0.627	0.542	0.473	0.434	0.417	0.369	0.329	0.295	0.266	0.218	0.181	0.153
1.17	0.608	0.525	0.458	0.419	0.402	0.356	0.317	0.283	0.255	0.208	0.173	0.145
1.18	0.591	0.509	0.443	0.405	0.388	0.343	0.305	0.272	0.244	0.199	0.165	0.138
1.19	0.574	0.494	0.429	0.392	0.375	0.331	0.294	0.262	0.235	0.191	0.157	0.131
1.20	0.559	0.480	0.416	0.380	0.363	0.320	0.283	0.252	0.226	0.183	0.150	0.125
1.22	0.531	0.454	0.392	0.357	0.341	0.299	0.264	0.235	0.209	0.168	0.138	0.114
1.24	0.505	0.431	0.371	0.337	0.322	0.281	0.248	0.219	0.195	0.156	0.127	0.104
1.26	0.482	0.410	0.351	0.319	0.304	0.265	0.233	0.205	0.182	0.145	0.117	0.095
1.28	0.461	0.391	0.334	0.303	0.288	0.250	0.219	0.193	0.170	0.135	0.108	0.088
1.30	0.442	0.373	0.318	0.288	0.274	0.237	0.207	0.181	0.160	0.126	0.100	0.081
1.32	0.424	0.357	0.304	0.274	0.260	0.225	0.196	0.171	0.150	0.118	0.093	0.075
1.34	0.408	0.342	0.290	0.261	0.248	0.214	0.185	0.162	0.142	0.110	0.087	0.069
1.36	0.393	0.329	0.278	0.250	0.237	0.204	0.176	0.153	0.134	0.103	0.081	0.064
1.38	0.378	0.316	0.266	0.238	0.226	0.194	0.167	0.145	0.127	0.097	0.076	0.060
1.40	0.365	0.304	0.256	0.229	0.217	0.185	0.159	0.138	0.120	0.092	0.071	0.056
1.42	0.353	0.293	0.246	0.219	0.208	0.177	0.152	0.131	0.114	0.087	0.067	0.052
1.44	0.341	0.282	0.236	0.211	0.199	0.169	0.145	0.125	0.108	0.082	0.063	0.049
1.46	0.330	0.273	0.227	0.202	0.191	0.162	0.139	0.119	0.103	0.077	0.059	0.046
1.48	0.320	0.263	0.219	0.195	0.184	0.156	0.133	0.113	0.098	0.073	0.056	0.043
1.50	0.310	0.255	0.211	0.188	0.177	0.149	0.127	0.108	0.093	0.069	0.053	0.040
1.55	0.288	0.235	0.194	0.171	0.161	0.135	0.114	0.097	0.083	0.061	0.046	0.035
1.60	0.269	0.218	0.179	0.157	0.148	0.123	0.103	0.087	0.074	0.054	0.040	0.030
1.65	0.251	0.203	0.165	0.145	0.136	0.113	0.094	0.079	0.067	0.048	0.035	0.026
1.70	0.236	0.189	0.153	0.134	0.125	0.103	0.086	0.072	0.060	0.043	0.031	0.023
1.75	0.222	0.177	0.143	0.124	0.116	0.095	0.079	0.065	0.054	0.038	0.027	0.020
1.80	0.209	0.166	0.133	0.116	0.108	0.088	0.072	0.060	0.049	0.034	0.024	0.017
1.85	0.198	0.156	0.125	0.108	0.100	0.082	0.067	0.055	0.045	0.031	0.022	0.015

BASIC EQUATION

$$B(\eta) = -\int_0^\eta \frac{d\eta}{\eta^N - 1}$$

WHERE;

$\eta = \frac{y}{y_0}$

N = HYDRAULIC EXPONENT

$\eta = 1.001$ TO 1.85*

* FROM TABLES IN BAKHMETEFF'S
"HYDRAULICS OF OPEN CHANNEL FLOW."
N = 3.3 COMPUTED BY WES.

OPEN CHANNEL FLOW
VARIED FLOW FUNCTION B(η)

HYDRAULIC DESIGN CHART 010-5/2

WES 3-56

η	N											
	2.8	3.0	3.2	3.3	3.4	3.6	3.8	4.0	4.2	4.6	5.0	5.4
1.90	0.188	0.147	0.117	0.101	0.094	0.076	0.062	0.050	0.041	0.028	0.020	0.014
1.95	0.178	0.139	0.110	0.094	0.085	0.070	0.057	0.046	0.038	0.026	0.018	0.012
2.00	0.169	0.132	0.104	0.089	0.082	0.066	0.053	0.043	0.035	0.023	0.016	0.011
2.1	0.154	0.119	0.092	0.079	0.073	0.058	0.046	0.037	0.030	0.019	0.013	0.009
2.2	0.141	0.107	0.083	0.070	0.065	0.051	0.040	0.032	0.025	0.016	0.011	0.007
2.3	0.129	0.098	0.075	0.063	0.058	0.045	0.035	0.028	0.022	0.014	0.009	0.006
2.4	0.119	0.089	0.068	0.057	0.052	0.040	0.031	0.024	0.019	0.012	0.008	0.005
2.5	0.110	0.082	0.062	0.052	0.047	0.036	0.028	0.022	0.017	0.010	0.006	0.004
2.6	0.102	0.076	0.057	0.047	0.043	0.033	0.025	0.019	0.015	0.009	0.005	0.003
2.7	0.095	0.070	0.052	0.043	0.039	0.029	0.022	0.017	0.013	0.008	0.005	0.003
2.8	0.089	0.065	0.048	0.039	0.036	0.027	0.020	0.015	0.012	0.007	0.004	0.002
2.9	0.083	0.060	0.044	0.036	0.033	0.024	0.018	0.014	0.010	0.006	0.004	0.002
3.0	0.078	0.056	0.041	0.033	0.030	0.022	0.017	0.012	0.009	0.005	0.003	0.002
3.5	0.059	0.041	0.029	0.023	0.021	0.015	0.011	0.008	0.006	0.003	0.002	0.001
4.0	0.046	0.031	0.022	0.017	0.015	0.010	0.007	0.005	0.004	0.002	0.001	0.000
4.5	0.037	0.025	0.017	0.013	0.011	0.008	0.005	0.004	0.003	0.001	0.001	0.000
5.0	0.031	0.020	0.013	0.010	0.009	0.006	0.004	0.003	0.002	0.001	0.000	0.000
6.0	0.022	0.014	0.009	0.007	0.006	0.004	0.002	0.002	0.001	0.000	0.000	0.000
7.0	0.017	0.010	0.006	0.005	0.004	0.002	0.002	0.001	0.001			
8.0	0.013	0.008	0.005	0.003	0.003	0.002	0.001	0.001	0.000			
9.0	0.011	0.006	0.004	0.003	0.002	0.001	0.001	0.000	0.000			
10.0	0.009	0.005	0.003	0.002	0.002	0.001	0.001	0.000	0.000			
20.0	0.006	0.002	0.001	0.001	0.001	0.000	0.000	0.000	0.000			

BASIC EQUATION

$$B(\eta) = -\int_0^\eta \frac{d\eta}{\eta^N - 1}$$

WHERE:

$$\eta = \frac{y}{y_0}$$

N = HYDRAULIC EXPONENT

* FROM TABLES IN BAKHMETEFF'S
"HYDRAULICS OF OPEN CHANNEL FLOW."
N = 3.3 COMPUTED BY WES.

η = 1.90 TO 20.0 *

OPEN CHANNEL FLOW
VARIED FLOW FUNCTION B(η)

HYDRAULIC DESIGN CHART 010-5/3

WES 3-56

HYDRAULIC DESIGN CRITERIA

SHEETS 010-6 TO 010-6/5

OPEN CHANNEL FLOW

BRIDGE PIER LOSSES

Background

1. Methods for computing head losses at bridge piers have been developed by D'Aubuisson, Nagler, Yarnell, Koch and Carstanjen, and others. Each method is based on experimental data for limited flow conditions. Complete agreement between methods is not always obtained. The energy method of Yarnell(4) and the momentum method of Koch and Carstanjen(1) have been widely used in the United States.

Equations for Classes of Flow

2. Three classes of flow conditions, A, B, and C, are encountered in the bridge pier problem. Hydraulic Design Chart 010-6 illustrates the flow condition upstream from, within, and downstream from the bridge section for each class of flow. The energy method of Yarnell is generally used for the solution of Class A flow problems, and is also used for solution of Class B flow. However, the momentum method of Koch and Carstanjen is believed more applicable to Class B flow, and is also applicable for solution of Class C flow.

3. **Energy Method, Class A Flow.** The Yarnell equation for Class A flow is

$$H_3 = 2K(K + 10\omega - 0.6)(\alpha + 15\alpha^4)\frac{V_3^2}{2g}$$

where

H_3 = drop in water surface, in ft, from upstream to downstream at the contraction

K = experimental pier shape coefficient

ω = ratio of velocity head to depth downstream from the contraction

α = horizontal contraction ratio

V_3 = velocity downstream from the contraction in ft per sec

g = acceleration, gravitational, in ft per sec^2

The values of K determined by Yarnell for different pier shapes are

Pier Shape	K
Semicircular nose and tail	0.90
Twin-cylinder piers with connecting diaphragm	0.95
Twin-cylinder piers without diaphragm	1.05
90 deg triangular nose and tail	1.05
Square nose and tail	1.25

4. __Energy Method, Class B Flow.__ The Yarnell equations for Class B flow are

$$L_B = C_B \frac{V_1^2}{2g}$$

and

$$C_B = 0.50 + K_B(5.5\alpha^3 + 0.08)$$

where

L_B = pier nose loss in ft

C_B = pier nose loss coefficient

V_1 = velocity upstream from the contraction in ft per sec

K_B = experimental pier shape coefficient

The values of K_B determined by Yarnell for different pier shapes are

Pier Shape	K_B
Square nose piers	5
Round nose piers	1

The following equation permits solution of the Yarnell equation for Class B flow by successive approximation

$$d_1 = d_L + L_B$$

where

d_1 = upstream water depth in ft

d_L = the higher depth, in ft, in the unobstructed channel which has flow of equal energy to that required for critical flow within the constricted bridge section

5. __Momentum Method, Class B Flow.__ Koch and Carstanjen applied the momentum principle to flow past bridge piers and verified their results by laboratory investigations. The total upstream momentum minus the momentum loss at the entrance equals the total momentum within the pier section. This momentum quantity is also equal to the total momentum downstream minus the static pressure on the downstream obstructed area. The general momentum equation is

$$m_1 - m_p + \frac{\gamma Q^2}{gA_1^2}(A_1 - A_p) = m_2 + \frac{\gamma Q^2}{gA_2} = m_3 - m_p + \frac{\gamma Q^2}{gA_3}$$

where

Q = discharge in cfs

m_1, m_2, m_3, m_p = total static pressure of water in the upstream section, pier section, downstream section, and on the pier ends, respectively, in lb

A_1, A_p, A_2, A_3 = cross-sectional area of the upstream channel, pier obstruction, channel within the pier section, and downstream channel, respectively, in sq ft

γ = specific weight of water, 62.5 lb/cu ft

6. **Graphical Solutions.** The U. S. Army Engineer District, Los Angeles(3), modified Yarnell's charts for solution of Class A and Class B flow, and developed a graphical solution for Class B flow by the momentum method. The U. S. Army Engineer District, Chicago (2), simplified the Los Angeles District's graphical solution for Class B flow by the energy method. Hydraulic Design Charts 010-6/2 and 010-6/3, respectively, present the Los Angeles District solutions for Class A flow by the energy method and Class B flow by the momentum method. Chart 010-6/4 presents the Chicago District's solution for Class B flow by the energy method.

Application

7. **Classification of Flow.** Flow classification can be determined from Chart 010-6/1. The intersection of the computed value of λ (the ratio of the channel depth without piers to the critical depth) and α (the horizontal contraction ratio) determines the flow classification.

8. **Class A Flow.** Chart 010-6/2 presents a graphical solution of Class A flow for five types of bridge piers. Enter the chart horizontally with a known λ_3 to a known α. Determine the value of X. The head loss through the pier section (H_3) is obtained by multiplying the critical depth in the unobstructed channel by X for round nose piers or by γX for the other pier shapes shown on the chart.

9. **Class B Flow.** Bridge pier losses by the momentum method can be determined from Chart 010-6/3. For a known value of α, the required ratio of d_1/d_c can be obtained and the upstream depth computed. Chart 010-6/4 permits solution of Class B flow for round and square nose piers by the energy method. This chart is used in the same manner as Chart 010-6/3.

10. **Class C Flow.** Class C flow is seldom encountered in practical problems. A graphical solution has not been developed, and

analytical solution by the momentum method is necessary.

11. <u>Sample Computation.</u> Chart 010-6/5 is a sample computation illustrating the use of the charts. A borderline flow condition between Class A and Class B is assumed. This permits three solutions to the problem. The most conservative solution is recommended for design purposes.

12. <u>References.</u>

(1) Koch, A., <u>Von der Bewegung des Wassers und den dabei auftretenden Kräften,</u> M. Carstanjen, ed. Julius Springer, Berlin, 1926.

(2) U. S. Army Engineer District, Chicago, CE, letter to U. S. Army Engineer Division, Great Lakes, CE, dated 22 April 1954, subject, "Analysis of Flows in Channels Constricted by Bridge Piers."

(3) U. S. Army Engineer District, Los Angeles, CE, <u>Report on Engineering Aspects, Flood of March 1938,</u> Appendix I, <u>Theoretical and Observed Bridge Pier Losses.</u> Los Angeles, Calif., May 1939.

(4) Yarnell, David L., <u>Bridge Piers as Channel Obstructions.</u> U. S. Department of Agriculture Technical Bulletin No. 442, Washington, D. C., November 1934.

PLAN

ELEVATION

CLASS A

$d_1 > d_c$

CLASS B

$d_2 > d_{c2}$

$d_3 > d_c$

$d_1 > d_c$

$d_2 = d_{c2}$

$d_3 > d_c$

CLASS C

$d_3 < d_c$

$d_1 < d_c$

$d_2 < d_{c2}$

$d_3 < d_c$

BRIDGE PIER

W_p

W_c
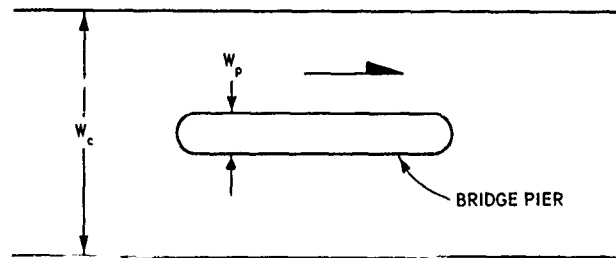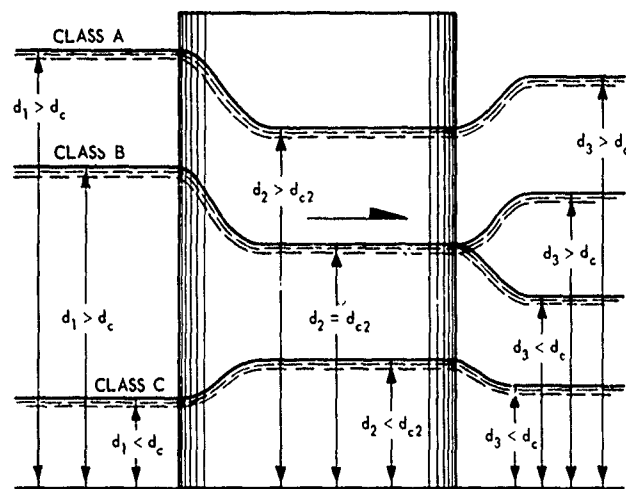
NOTE: $\alpha = W_p/W_c$ = HORIZONTAL CONTRACTION RATIO

W_p = TOTAL PIER WIDTH
W_c = GROSS CHANNEL WIDTH
d_1 = UPSTREAM DEPTH
d_2 = DEPTH WITHIN PIER SECTION
d_3 = DOWNSTREAM DEPTH
d_c = CRITICAL DEPTH WITHIN THE UNOBSTRUCTED
         CHANNEL SECTION
d_{c2} = CRITICAL DEPTH WITHIN THE PIER SECTION

OPEN CHANNEL FLOW
RECTANGULAR SECTION
BRIDGE PIER LOSSES
DEFINITION

HYDRAULIC DESIGN CHART 010-6

WES 5-59

CLASS A

LIMITING λ_3 BY MOMENTUM METHOD (KOCH-CARSTANJEN)

CLASS A OR B

LIMITING λ_3 BY ENERGY METHOD (YARNELL)

CLASS B

LIMITING λ_1 BY MOMENTUM METHOD (KOCH-CARSTANJEN)

CLASS C

$\lambda = \dfrac{d}{d_c}$

α = HORIZONTAL CONTRACTION RATIO
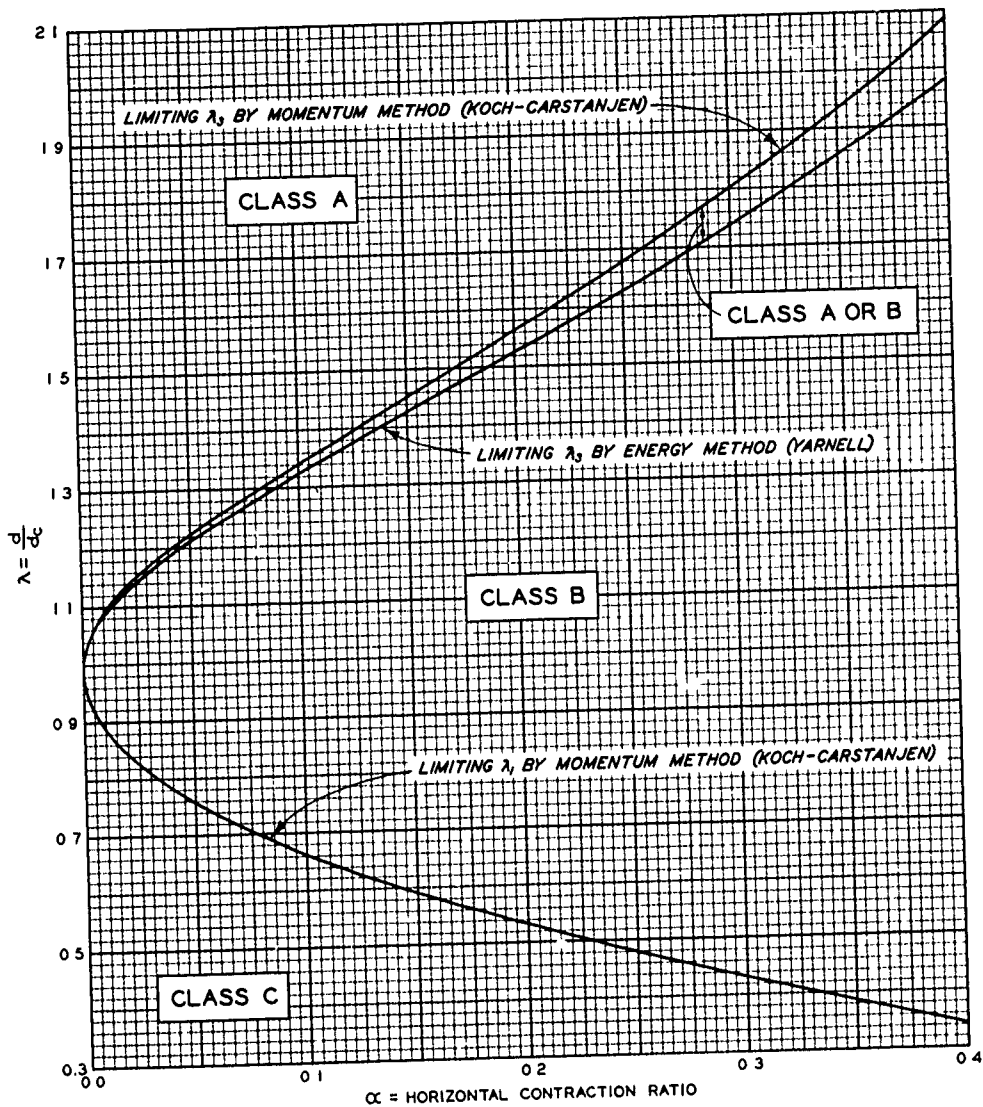
EQUATIONS FOR LIMITING λ

λ_3 – ENERGY METHOD (YARNELL)

$$\alpha = 1 - \left[\frac{3\lambda_3^3}{2\lambda_3^3 + 1}\right]^{3/2}$$

λ_3 – MOMENTUM METHOD (KOCH-CARSTANJEN)

$$\alpha = 1 - \left[\frac{3\lambda_3}{(1-\alpha)\lambda_3^3 + 2}\right]^3$$

λ_1 – MOMENTUM METHOD (KOCH-CARSTANJEN)

$$\alpha = 1 - \left[\frac{3\lambda_1}{\lambda_1^3 + 2}\right]^{3/4}$$

NOTE $\lambda_1 = d_1/d_c$
$\lambda_3 = d_3/d_c$
d_1 = UPSTREAM WATER DEPTH
d_3 = DOWNSTREAM WATER DEPTH
d_c = CRITICAL DEPTH WITHIN THE
UNOBSTRUCTED CHANNEL SECTION
α = HORIZONTAL CONTRACTION RATIO
(Σ PIER WIDTHS ÷ CHANNEL WIDTH)
d = DEPTH WITHOUT BRIDGE PIERS
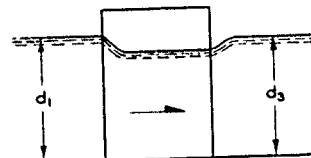
DEFINITION SKETCH

OPEN CHANNEL FLOW
RECTANGULAR SECTION
BRIDGE PIER LOSSES
CLASSIFICATION OF FLOW CONDITIONS

HYDRAULIC DESIGN CHART 010-6/1

WES 5-59

PREPARED BY U S ARMY ENGINEER WATERWAYS EXPERIMENT STATION VICKSBURG MISSISSIPPI

$\lambda_3 = \dfrac{d_3}{d_c}$

(HORIZONTAL CONTRACTION RATIO) $\alpha = 0.30$

0.28
0.26
0.24
0.22
0.20
0.18
0.16
0.14
0.12
0.10
0.08
0.06
0.04
$\alpha = 0.02$

LIMITING λ_3 FOR CLASS A FLOW

$X = \dfrac{H_3}{d_c}$ (ROUND NOSE PIERS)

90°

Υ

DEFINITION SKETCH

$d_1 > d_c$ $d_2 > d_{c2}$ $d_3 > d_c$ H_3

$d_1 = d_3 + H_3$
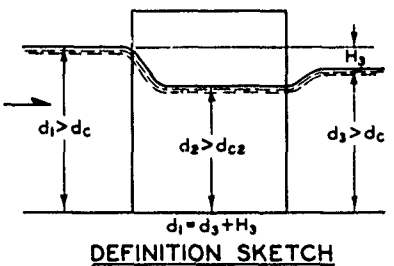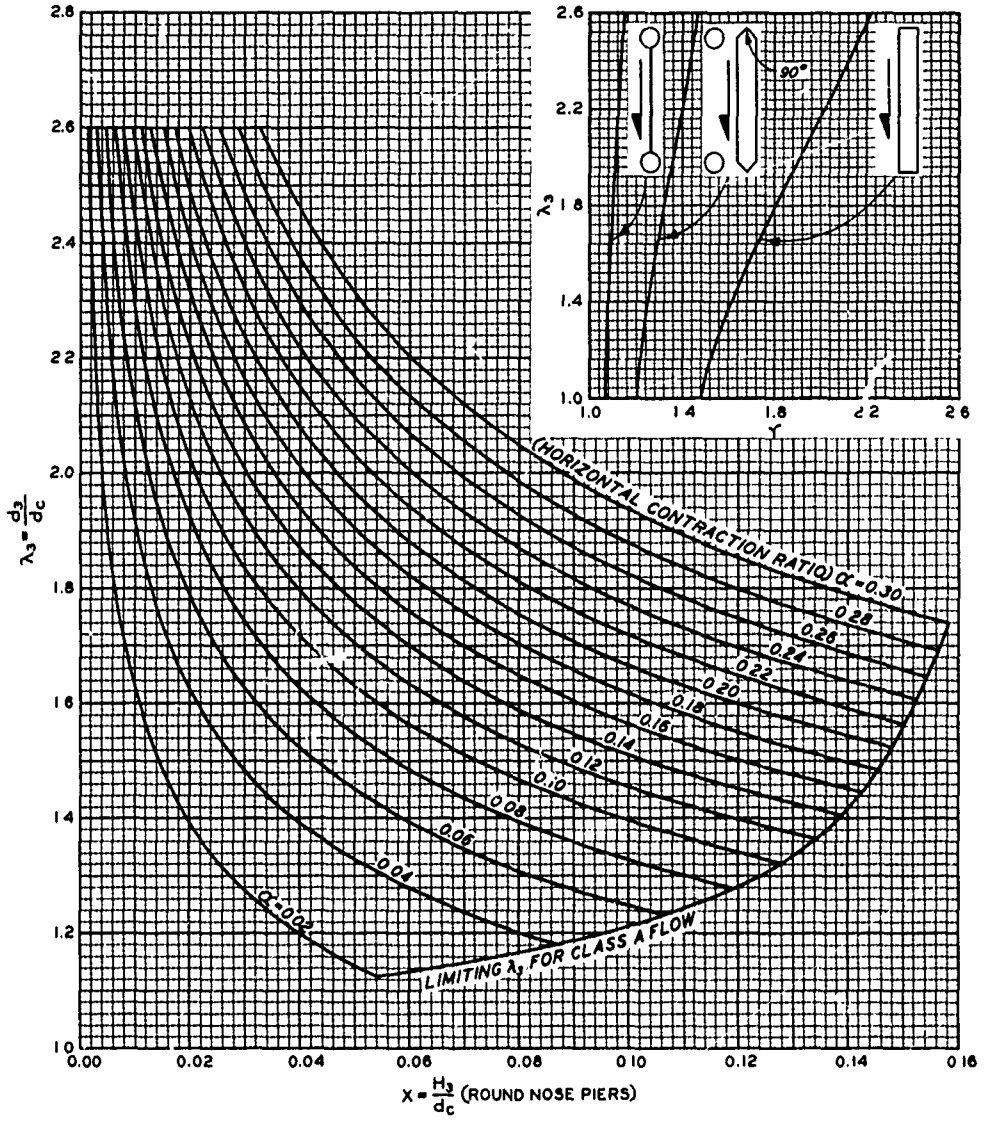
NOTE d_c = CRITICAL DEPTH WITHIN THE
               UNOBSTRUCTED CHANNEL SECTION
       d_{c2} = CRITICAL DEPTH WITHIN THE
               PIER SECTION
       $H_3 = X d_c$ (ROUND NOSE PIERS)
       $H_3 = X d_c \Upsilon$ (INDICATED SHAPES)

OPEN CHANNEL FLOW
RECTANGULAR SECTION
BRIDGE PIER LOSSES
CLASS A FLOW – ENERGY METHOD

HYDRAULIC DESIGN CHART 010-6/2

WES 5-59

DEFINITION SKETCH

$d_1 > d_c$ $d_2 = d_{c2}$ $d_3 > d_c$ $d_3 < d_c$

$$\alpha = 1 - \left[\frac{3\lambda_1}{\lambda_1^3 + 2}\right]^{3/4}$$

$\lambda_1 = \dfrac{d_1}{d_c}$

α = HORIZONTAL CONTRACTION RATIO
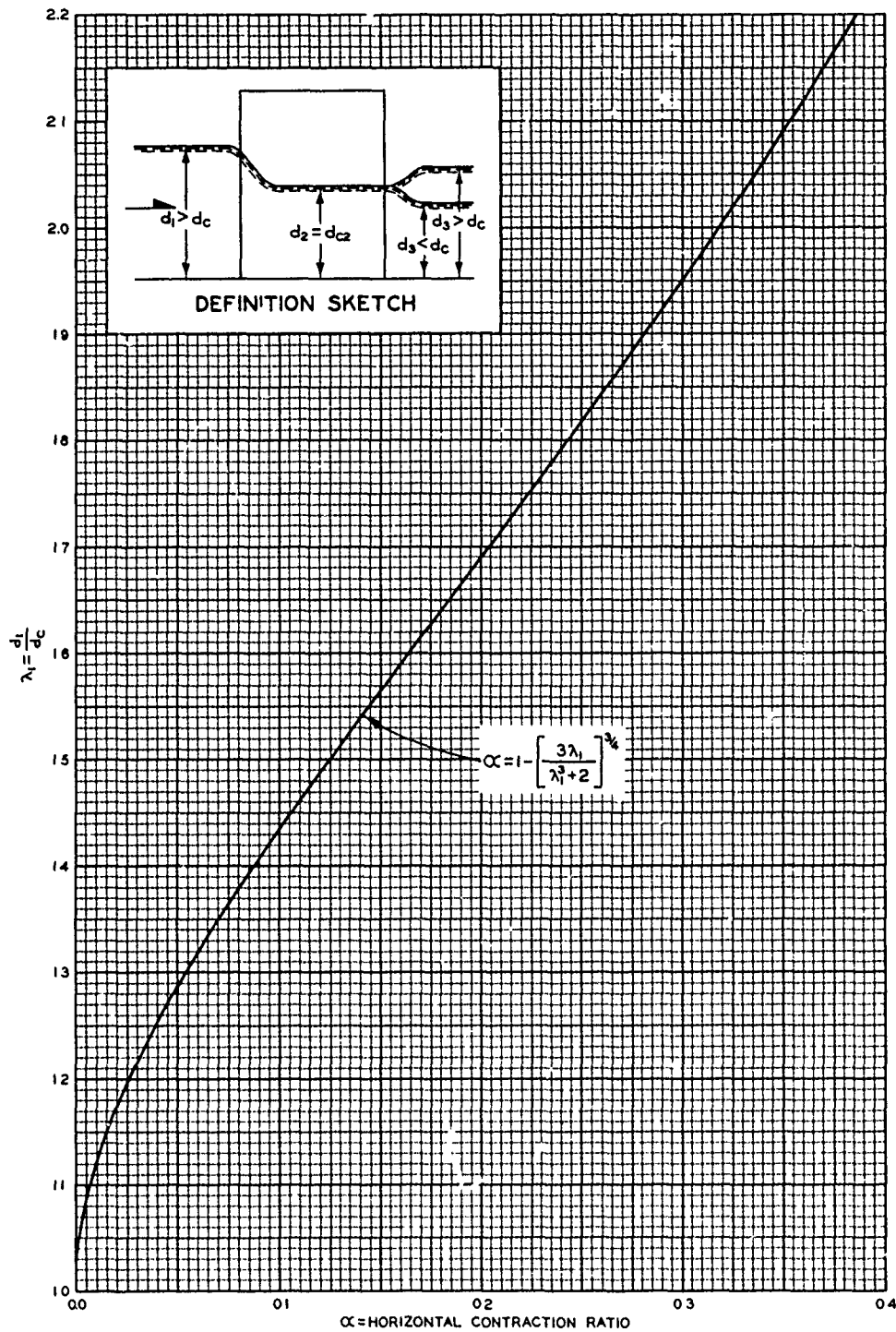
NOTE λ_1 = d_1/d_c
d_1 = UPSTREAM WATER DEPTH
d_c = CRITICAL DEPTH WITHIN THE
    UNOBSTRUCTED CHANNEL SECTION
d_{c2} = CRITICAL DEPTH WITHIN
    THE PIER SECTION
α = HORIZONTAL CONTRACTION RATIO

OPEN CHANNEL FLOW
RECTANGULAR SECTION
BRIDGE PIER LOSSES
CLASS B FLOW -- MOMENTUM METHOD

HYDRAULIC DESIGN CHART 010-6/3

WES 3-59
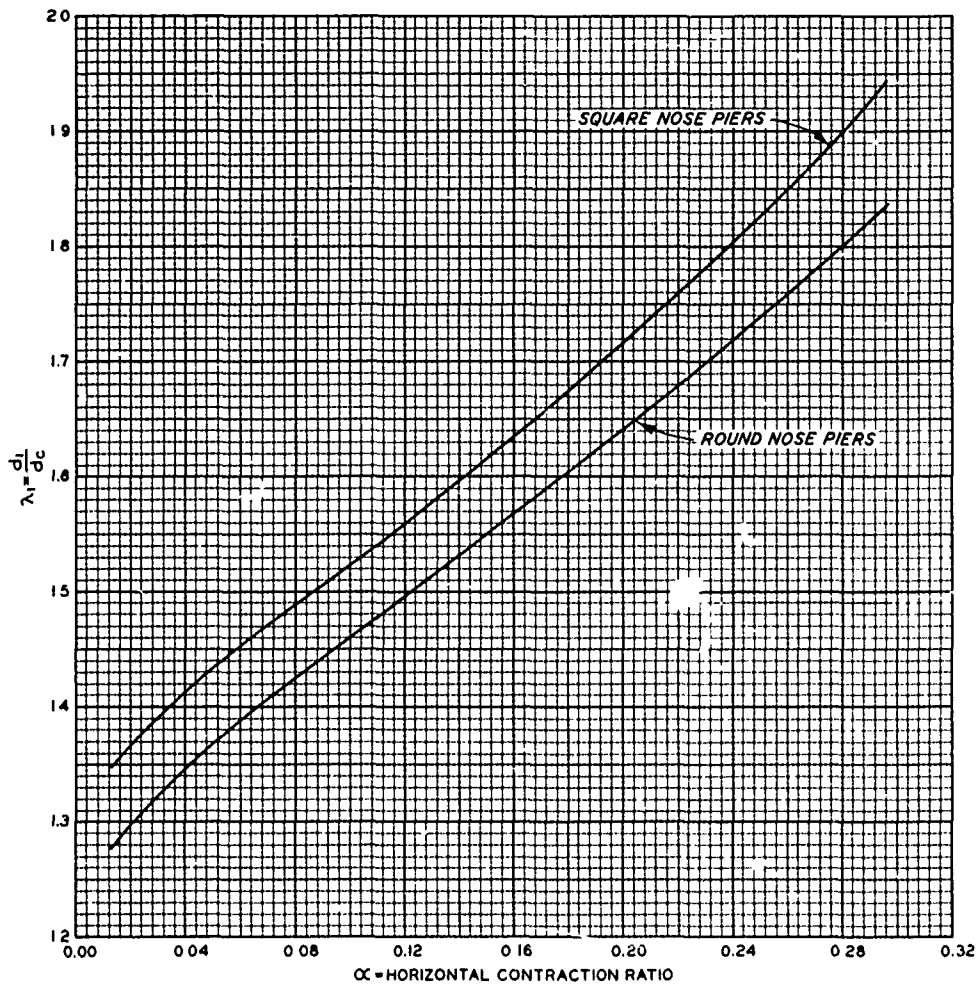
EQUATIONS

$$\frac{1}{(1-\alpha)^{2/3}} = \frac{1}{3\lambda_L^2} + \frac{2\lambda_L}{3}$$

$$\lambda_1 = \lambda_L + \frac{0.5 + K_B(5.5\alpha^3 + 0.08)}{2\lambda_1^2}$$

NOTE $\lambda_1 = d_1/d_c$

$\lambda_3 = d_3/d_c$

λ_L = LIMITING λ_3 BY ENERGY METHOD

d_1 = UPSTREAM WATER DEPTH

d_3 = DOWNSTREAM WATER DEPTH

d_c = CRITICAL DEPTH WITHIN THE UNOBSTRUCTED CHANNEL SECTION

d_{c2} = CRITICAL DEPTH WITHIN THE PIER SECTION

α = HORIZONTAL CONTRACTION RATIO

K_B = YARNELL PIER-SHAPE COEFFICIENT
(1 0 FOR ROUND NOSE)
(5 0 FOR SQUARE NOSE)
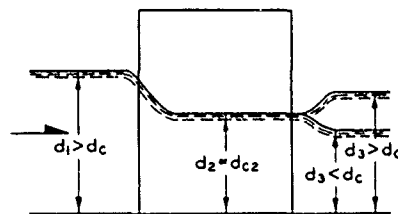
DEFINITION SKETCH

OPEN CHANNEL FLOW
RECTANGULAR SECTION
BRIDGE PIER LOSSES
CLASS B FLOW – ENERGY METHOD

HYDRAULIC DESIGN CHART 010-6/4

WES 5-59

U. S. ARMY ENGINEER WATERWAYS EXPERIMENT STATION
COMPUTATION SHEET

JOB __CW 804__ PROJECT __John Doe River__ SUBJECT __Rectangular Channel__

COMPUTATION __Bridge Pier Loss__

COMPUTED BY __MBB__ DATE __12/17/58__ CHECKED BY __WTH__ DATE __12/18/58__

GIVEN:

Rectangular channel section
Round nose piers
Channel discharge (Q) = 40,000 cfs
Channel width (W_c) = 200 ft
Total pier width (W_p) = 20 ft
Depth without bridge piers (d) = 14.3 ft
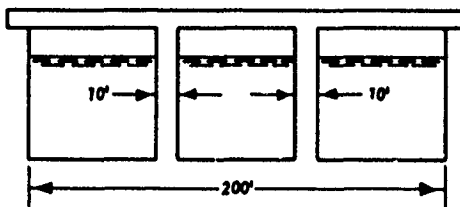
COMPUTE:

1. Horizontal contraction ratio (α)

$$\alpha = \frac{W_p}{W_c} = \frac{20}{200} = 0.10$$

2. Discharge (q) per ft of channel width

$$q = \frac{Q}{W_c} = \frac{40,000}{200} = 200 \text{ cfs}$$

3. Critical depth (d_c) in unobstructed channel
   From Chart 610-8, d_c = 10.8 ft
   for q = 200 cfs.

4. $\lambda = d/d_c = 14.3/10.8$
   = 1.324

5. Flow classification
   On Chart 010-6/1, intersection
   of α = 0.10 and λ = 1.324 is
   in zone marked Class A or B.

6. Upstream depth (d_1)
   a. Class A flow - Energy Method

      $d_1 = d_3 + H_3$ (Chart 010-6/2

      $H_3 = X d_c$

          $X = 0.127$ for α = 0.10
          and $\lambda_3 = \lambda = 1.324$

      $H_3 = 0.127 \times 10.8 = 1.37$

      $d_1 = 14.3 + 1.37 = 15.67$ ft

   b. Class B flow - Momentum Method

      $d_1 = \lambda_1 \, d_c$ (Chart 010-6/3)
          $\lambda_1 = 1.435$ for α = 0.10

      $d_1 = 1.435 \times 10.8 = 15.50$ ft

   c. Class B flow - Energy Method

      $d_1 = \lambda_1 \, d_c$ (Chart 010-6/4)
          $\lambda_1 = 1.460$ for α = 0.10

      $d_1 = 1.460 \times 10.8 = 15.77$ ft

OPEN CHANNEL FLOW
RECTANGULAR SECTION
BRIDGE PIER LOSSES
SAMPLE COMPUTATION
HYDRAULIC DESIGN CHART 010-6/5

HYDRAULIC DESIGN CRITERIA

SHEET 010-7

OPEN CHANNEL FLOW

TRASH RACK LOSSES

1. The energy loss of flow through trash racks depends upon the shape, size, and spacing of the bars and the velocity of flow. Hydraulic Design Chart 010-7 shows loss coefficient curves for different bar designs. The curves are based on tests in open channels with the racks perpendicular to the line of flow.

2. <u>Stockholm Tests.</u> Tests made in the Hydraulic Structures Laboratory of the Royal Technical University at Stockholm, Sweden, were reported by W. Fellenius(1). The publication also presents results for bar shapes and sizes not included on Chart 010-7. The effects of sloping the racks were also studied.

3. <u>Munich Tests.</u> Tests made in the Hydraulic Institute of the Technical University at Munich, Germany, were reported by O. Kirschmer(2). The tests included other bar shapes not shown on the chart. The effects of tilting the rack were also studied. Spangler(3) investigated the effects of varying the horizontal angle of approach channel to the trash rack.

4. <u>Application.</u> The loss coefficients shown on Chart 010-7 were obtained from tests in which the racks protruded above the water surface. The applicability of the data to submerged racks is not known. As stated above, numerous other shapes were tested at Stockholm and Munich. The data presented on Chart 010-7 were selected to demonstrate the general effect of bar shape on head loss.

5. <u>References.</u>

(1) Fellenius, W., "Experiments on the head loss caused by protecting racks at water-power plants." <u>Meddelande No. 5 Vattenbyggnadsinstitutionen, Vid Kungl.</u> Tekniska Hogskolan, Stockholm (1928). Summary and pertinent data also published in <u>Hydraulic Laboratory Practice,</u> ASME (1929), p 533.

(2) Kirschmer, O., "Investigation regarding the determination of head loss." <u>Mitteilungen des Hydraulischen Instituts der Technischen Hochschule Munchen,</u> Heft 1 (1926), p 21.

(3) Spangler, J., "Investigations of the loss through trash racks inclined obliquely to the stream flow." <u>Mitteilungen des Hydraulischen Instituts der Technischen Hochschule Munchen,</u> Heft 2 (1928), p 46. English translation published in Hydraulic Laboratory Practice, ASME (1929), p 461.

DEFINITION SKETCH

LEGEND
—— FELLENIUS TESTS (STOCKHOLM)
– – – KIRSCHMER TESTS (MUNICH)

$K_t = \dfrac{\Delta h}{V^2/2g}$

THE NUMBERS SHOWN ARE VALUES OF L/T

SLIGHTLY ROUNDED CORNERS

A_r
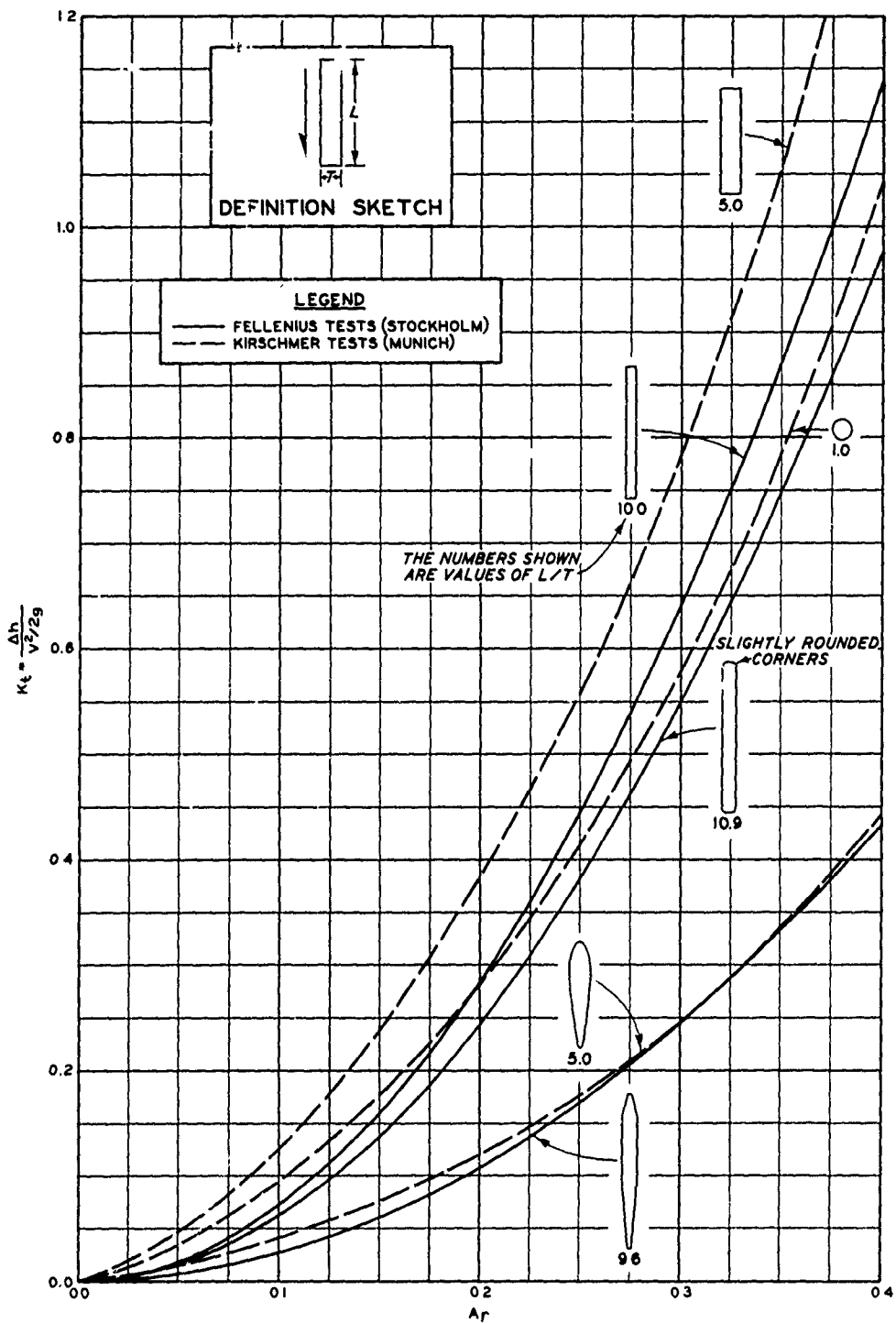
NOTE. Δh = HEAD LOSS THROUGH RACK IN FT
V = VELOCITY AT SECTION WITHOUT RACK IN FT/SEC
K_t = HEAD LOSS COEFFICIENT
$A_r = \dfrac{\text{AREA OF BARS}}{\text{AREA OF SECTION}}$

OPEN CHANNEL FLOW
TRASH RACK LOSSES
HYDRAULIC DESIGN CHART 010-7

PREPARED BY U S ARMY ENGINEER WATERWAYS EXPERIMENT STATION, VICKSBURG, MISSISSIPPI

WES 5-59

AIR DEMAND - REGULATED OUTLET WORKS

1. **Background.** The data presented are considered applicable to slide and tractor gates operating in rectangular gate chambers. Previous designs of air vents have been based on arbitrary adoption of a ratio of the cross-sectional area of the air vent to that of the conduit being aerated.

2. **Iowa Tests.** Kalinske and Robertson* have published the results of tests on the air demand of a hydraulic jump in a circular conduit. They found the ratio of air demand to water discharge (β) to be a function of the Froude number minus one. The formula which was developed is indicated in HDC 050-1.

3. **Prototype Tests.** A number of prototype tests on existing outlet works have been analyzed and compared graphically with the Kalinske and Robertson formula in HDC 050-1. In some of the prototype tests, gate openings varied from small to full opening where pressure flow existed throughout the entire system. The maximum air demand is found at some intermediate gate opening. The ratios of this gate opening (G_m) to full gate opening (G_f) are shown in table 1 together with other pertinent information.

Table 1

Dam	Max Air Velocity ft/sec	Vent Area A_v sq ft	Conduit Area A_c sq ft	$\dfrac{A_v}{A_c}$	Gate Openings ft		$\dfrac{G_m}{G_f}$
					Max Air G_m	Full G_f	
Pine Flat	280	4.91	45.0	0.109	5.5	9.0	0.611
Tygart	219	0.79	56.7	0.014	8.3	10.0	0.833
Norfork	127	2.18	24.0	0.091	5.0	6.0	0.833
Denison	57	22.33	314.2	0.071	13.0	19.0	0.685
Hulah	36	1.40	32.5	0.043	4.0	6.5	0.615

4. Extensive Corps of Engineers air-demand tests were made at Pine Flat Dam from 1952 to 1956. These tests included heads up to 370 ft

---

* A. A. Kalinske and J. W. Robertson, "Entrainment of air in flowing water--closed conduit flow." Transactions, American Society of Civil Engineers, vol 108 (1943), pp 1435-1447.

although gates are not normally operated under such high heads. The Pine Flat test data are in good agreement with other field data, as shown by the plots in HDC 050-1.

5. Recommendations. A straight line in HDC 050-1 indicates a suggested design assumption. It is suggested that the maximum air demand be assumed to occur at a gate opening ratio of 80 percent in sluices through concrete dams. A gate lip with a 45-degree angle on the bottom can be expected to have a contraction coefficient of approximately 0.80. The Froude number should be based on the effective depth at the vena contracta which, with the above-mentioned factors, would be 64 percent of the sluice depth. The suggested design curve can be used to determine the ratios of air demand to water discharge. It is further suggested that air vents be designed for velocities of not more than 150 ft per sec. The disadvantage of excessive air velocities is a high head loss in the air vent which causes subatmospheric pressures in the water conduit. Outlet works with well-streamlined water passages can tolerate lower pressures without cavitation trouble than those with less effectively streamlined water passages. The suggested design assumptions for sluices will result in area ratios of air vent to sluice of approximately 12 percent for each 150 ft of head on a 4- by 6-ft sluice, and 12 percent for each 200 ft of head on a 5-ft-8-in. by 10-ft sluice. In applying the curve to circular tunnels controlled by one or more rectangular gates, the effective depth should be based on flow in 64 percent of the area of the tunnel for maximum air demand. These are general design rules which have been devised until additional experimental data are available.

Chart axes and labels:

$\beta = \dfrac{Q_a}{Q_w}$

SUGGESTED DESIGN CURVE
$\beta = 0.03 (F_r -1)^{1.06}$

KALINSKE & ROBERTSON TESTS
$\beta = 0.0066 (F_r -1)^{1.4}$

$(F_r -1)$
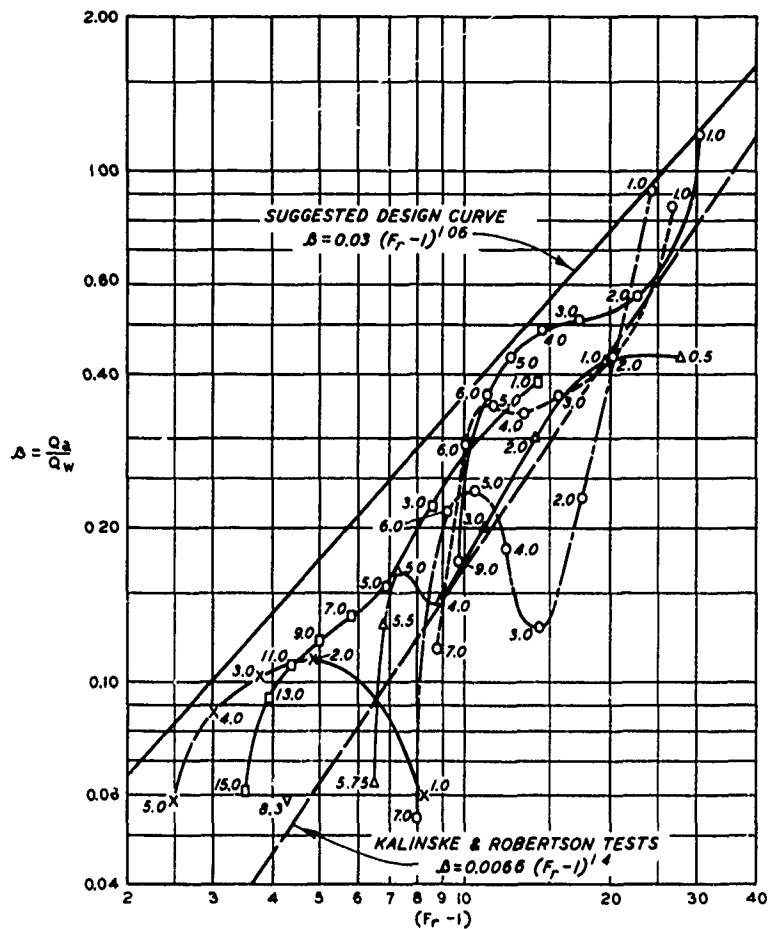
NOTE : $F_r = V/\sqrt{gy}$ (FROUDE NUMBER)
  V = WATER VELOCITY AT VENA
    CONTRACTA, FT/SEC
  y = WATER DEPTH AT VENA
    CONTRACTA, FT
  Q_a = AIR DEMAND, CFS
  Q_w = WATER DISCHARGE, CFS

LEGEND

o———o PINE FLAT – H = 370 FT
o–––––o PINE FLAT – H = 304 FT
o– – –o PINE FLAT – H = 254 FT
□———□ DENISON – H = 84 FT
x———x HULAH – H = 24 FT
△———△ NORFORK – H = 154 FT
  ∇   TYGART – H = 92 FT

H = HEAD, POOL TO CONDUIT CENTER LINE
FIGURES ON GRAPH SHOW GATE
OPENING IN FEET.

AIR DEMAND
REGULATED OUTLET WORKS

HYDRAULIC DESIGN CHART 050-1

REV 1-64   WES 4-1-52

AIR DEMAND - REGULATED OUTLET WORKS

PRIMARY AND SECONDARY MAXIMA

1. Field tests to determine air demand in regulated outlet works have indicated two gate positions at which the air demand greatly exceeds that of other gate openings. Large quantities of air are required when the gate is about 5 per cent open and again at some gate position between 50 and 100 per cent open. Hydraulic Design Chart 050-1/1 shows the observed air demand in cfs plotted against per cent of gate opening for a number of operating heads at Pine Flat, Norfork, and John H. Kerr Dams. The chart also indicates flow conditions below the gate for various openings.

2. At small gate openings the jet frays or breaks up and entrains large quantities of air. As the gate opening increases the air demand rapidly decreases and then increases to a second maximum just before the conduit flows full at the exit portal. In this phase of operation, the air demand is caused by the drag force between the water surface and the air above. With larger gate openings, a hydraulic jump forms in the conduit and the air demand is limited by the capacity of the jump to entrain and remove air. When the conduit flows full the air demand becomes zero.

3. Chart 050-1/1 is included to show the qualitative characteristics of air demand. Sufficient prototype data are not available to develop a relationship between air demand, head and other factors.

JUMP ENTRAINMENT

AIR DRAG

JET SPRAY

AIR DEMAND IN CFS

GATE OPENING IN PERCENT

PRIMARY MAXIMA

SECONDARY MAXIMA

JOHN H. KERR
68'
90'

NORFORK
154' HEAD

PINE FLAT
92'
254'
370'

	CONDUIT		AIR VENT	
	LENGTH, FT	SIZE, FT	LENGTH, FT	DIAMETER, FT
JOHN H. KERR	117	5.67 × 10	90	2.50
NORFORK	195	4 × 6	188	1.67
PINE FLAT	334	5 × 9	320	2.50
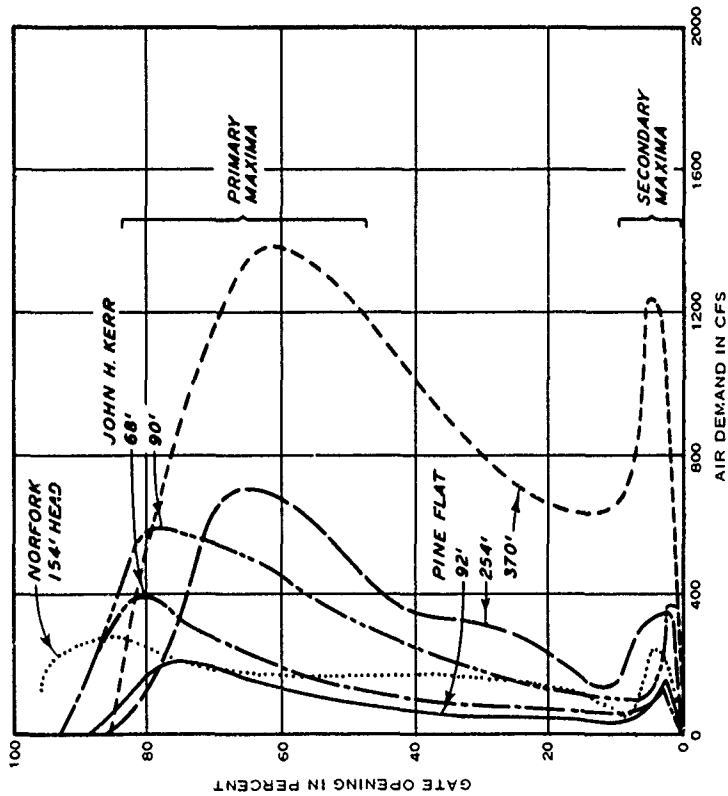
NOTE: HEADS ARE MEASURED FROM POOL TO CENTER LINE OF
CONDUIT.

AIR DEMAND

REGULATED OUTLET WORKS
PRIMARY AND SECONDARY MAXIMA

HYDRAULIC DESIGN CHART 050 1/1

WES 5-59

REV 1-64
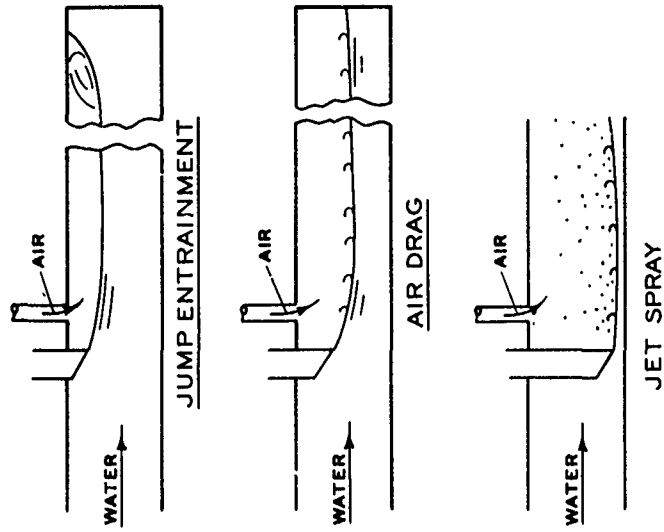
CHART 050-1/1

SAMPLE AIR VENT DESIGN COMPUTATIONS

    1. A sample computation for the design of an air vent is given on Hydraulic Design Chart 050-2. This computation is included in order to clarify the explanation given on sheet 050-1. The coefficients of discharge as given on Chart 320-1 may be considered to be contraction coefficients for determining the depth of water at the vena contracta.

U. S. ARMY ENGINEER WATERWAYS EXPERIMENT STATION

COMPUTATION SHEET

JOB: ___ES 804___ PROJECT: ___John Doe Dam___ SUBJECT: ___Air Demand___

COMPUTATION: ___Air Vent Size, Hydraulic Design___

COMPUTED BY: ___BG___ DATE: _9/5/52_ CHECKED BY: ___AAMC___ DATE: _9/5/52_

GIVEN:

Sluice size: Width (B) = 4 ft
Height (D) = 9 ft
45° gate lip

Elevation sluice invert at gate 127.0

Design pool elevation 352.0

FROM HYDRAULIC DESIGN SHEET 050-1 AND 320-1

Assume maximum air discharge (Q_a) at 80% gate opening.
Discharge coefficient (C) for 45° gate lip = 0.80.

Then:

Depth of water at vena contracta (y) = 80% × 0.80 × 9.0 = 5.76 ft

Effective head, H = 352.0 − (127.0 + 5.76) = 219.24

Water discharge (Q_w) = CAV = By $\sqrt{2gH}$ = 4.0 (5.76) $\sqrt{64.4\ (219.24)}$

Q_w = 2740 cfs

$V = \dfrac{Q_w}{A} = \dfrac{2740}{4.0 \times 5.76} = 119.0$ ft/sec velocity of water at vena contracta

$F = \dfrac{V}{\sqrt{gy}} = \dfrac{119.0}{\sqrt{32.2\ (5.76)}} = 8.75$ Froude number at vena contracta

(F − 1) = 7.75
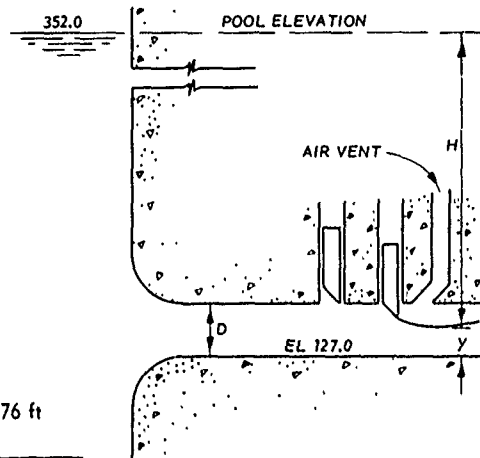
FROM HYDRAULIC DESIGN CHART 050-1. $\beta = 0.28$

$Q_a = \beta Q_w = 0.28\ (2740)$

Q_a = 767 cfs

FROM HYDRAULIC DESIGN SHEET 050-1. Maximum Air Velocity (V_a) = 150 ft/sec

$A_v - \dfrac{767}{150} = 5.1$ sq ft area of air vent required

Diameter for circular vent = 2.55 ft

AIR DEMAND
REGULATED OUTLET WORKS
SAMPLE COMPUTATION

HYDRAULIC DESIGN CHART 050-2

HYDRAULIC DESIGN CRITERIA

SHEET 050-3

AIR ENTRAINMENT

WIDE CHUTE FLOW

1. **Purpose.** The entrainment of air in flow through a chute spillway causes bulking which necessitates increasing the sidewall design height. HDC 050-3 may be used to estimate the percentage by volume of air that will be entrained in the flow at terminal velocity and its effect on flow depth.

2. **Previous Criteria.** Previous criteria for estimating air entrainment have been influenced by investigations on narrow chutes as reported by Hall.[2] The data for flows through narrow chutes show the marked effects of sidewalls on the amount of air entrained.

3. **Basic Data.** Recent tests at the University of Minnesota[3] on artificially roughened channels have afforded new information on chutes for relatively large width-depth ratios which eliminate the sidewall effect. It was found that the mean air concentration ratio of air volume to air-plus-water volume, $\overline{C}$, is a function of the shear velocity and transition depth parameter, $V_s/(d_T)^{2/3}$. This suggests that the intensity of the turbulent fluctuations causing air entrainment is increasingly damped with increasing depth. A more convenient empirical expression of this parameter is the ratio of the sine of the bottom slope to the unit discharge in cubic feet per second, $S/q^{1/5}$. This ratio is used in HDC 050-3.

4. The Minnesota laboratory data are shown in HDC 050-3 together with field data for the Kittitas chute.[2] The Minnesota data were obtained by the use of highly refined electronic equipment developed at St. Anthony Falls Hydraulic Laboratory, University of Minnesota. The Kittitas results were derived from field measurements of water-surface elevations under conditions of high velocities and great turbulence. The Kittitas data selected for use in developing HDC 050-3 were for flows with flow width exceeding five times the depth to eliminate the sidewall effect. The low concentration ratios indicated by these data appear consistent with visual observations of flows near the downstream ends of the Fort Peck[1] and Arkabutla spillway chutes.

5. **Suggested Criteria.** The curve of best fit in HDC 050-3 was determined by the least squares method using both the Minnesota and Kittitas data. The suggested design curve is believed to be a conservative basis for design. The results are applicable to flow at terminal velocity in chute spillways having width-depth ratios greater than five.

6. <u>References.</u>

(1) ASCE Committee on Hydromechanics, "Aerated flow in open channels."
     Progress Report, Task Committee on Air Entrainment in Open Channels,
     <u>Proceedings, American Society of Civil Engineers,</u> vol 87, part 1
     (Journal, Hydraulics Division, No. HY3) (May 1961).

(2) Hall, L. S., "Open channel flow at high velocities." <u>Transactions,
     American Society of Civil Engineers,</u> vol 108 (1943), pp 1394-1434 and
     1494-1513.

(3) Straub, L. G., and Anderson, A. G., "Self-aerated flow in open chan-
     nels." <u>Transactions, American Society of Civil Engineers,</u> vol 125
     (1960), pp 456-486.
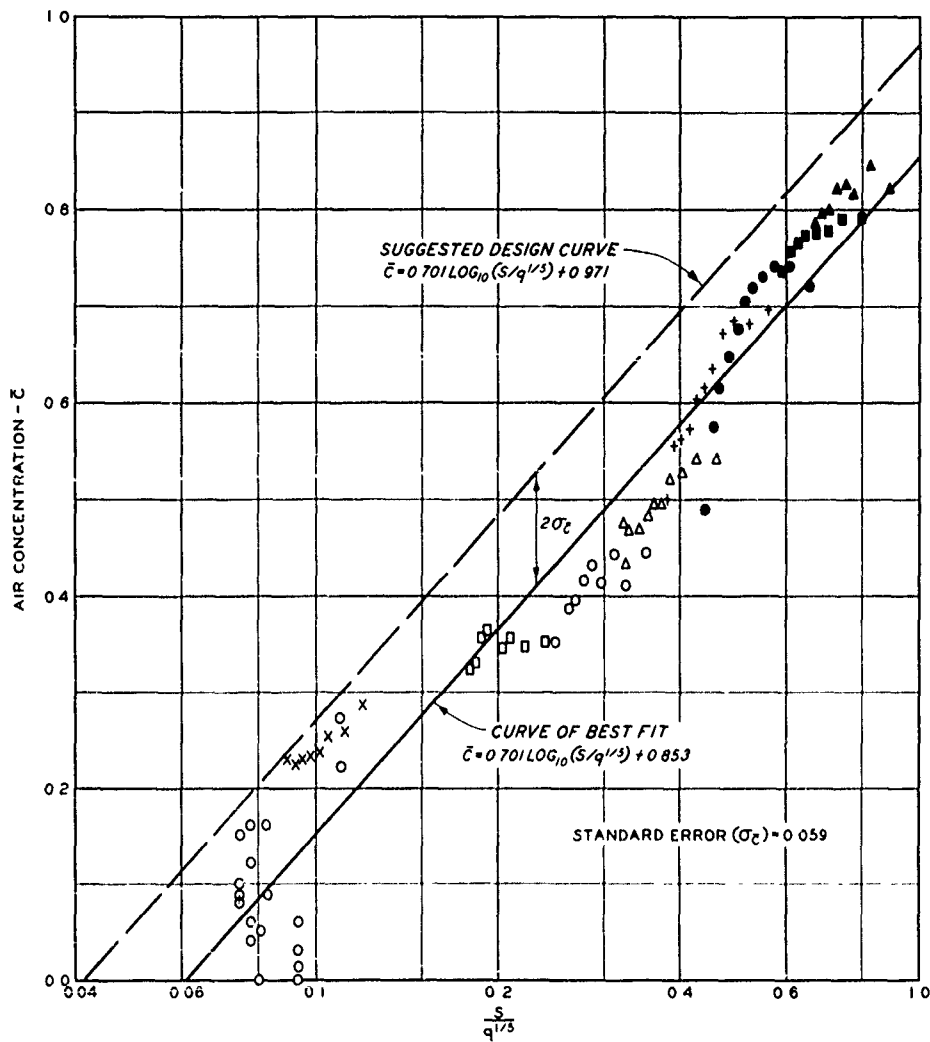
AIR ENTRAINMENT
WIDE CHUTE FLOW
CONCENTRATION ($\bar{C}$) VS $S/q^{1/5}$

HYDRAULIC DESIGN CHART 050-3

1. **Purpose.** One of the problems in the design of reservoir outlet structures is the determination of whether any disturbing frequencies are inherent in the hydraulic system that may equal or approach the natural frequency of the gate and cause resonance with resulting violent gate vibrations. Although a gate leaf may vibrate in any of several freedoms of motion including flexure, the vertical vibration of a gate on an elastic suspension is usually of most importance. Hydraulic Design Charts 060-1 to 060-1/5 are aids for estimating the vibration characteristics of elastically suspended gates.

2. **Resonance.** When the forcing frequency is exactly equal to the natural frequency a condition of "dead" resonance exists. The displacement amplitude for the vibrating system increases very rapidly for this condition of resonance and may result in rupture. The amplitude can also be increased rapidly if there is only a small difference between the forcing and natural frequencies. The transmissibility ratio, or the magnification factor, is defined by the equation:

$$T.R. = \frac{1}{1 - (f_f/f_n)^2}$$

where f_f/f_n is the ratio of the forcing frequency to natural frequency. A plot and coordinates of this function are given on Hydraulic Design Chart 060-1. Although the transmissibility ratio is negative for frequency ratios greater than one, the positive image of this part of the curve is often utilized for simplicity in plotting. The part of the curve between transmissibility ratios of unity and zero is sometimes called the isolation range with the percentage of isolation as designated. It is desirable to produce a design with a high percentage of isolation.

3. **Forcing Frequencies.** Two possible sources of disturbing frequencies are the vortex trail shed from the bottom edge of a partly opened gate and the pressure waves that travel upstream to the reservoir and are reflected back to the gate. The frequency of the vortex trail shed from a flat plate can be defined by the dimensionless Strouhal number, S_t, as follows:

$$S_t = \frac{L_p f_f}{V}$$

where L_p is the plate width, f_f is the vortex trail shedding frequency, and V is the velocity of the fluid. The Strouhal number for a flat

plate is approximately 1/7. The forcing frequency of a vortex trail shed from a gate may be estimated as:

$$f_f = \frac{\sqrt{2gH_e}}{7(2Y)}$$

where H_e is the energy head at the bottom of the gate, and Y is the projection of the gate into the conduit or half of the plate width L_p. Hydraulic Design Chart 060-1/1 can be used to estimate the forcing frequency for various combinations of energy head and gate projection. Unpublished observations of hydraulic models of gates have indicated that the vortex trail will spring from the upstream edge of a flat-bottom gate causing pressure pulsations on the bottom of the gate. The vortex trail springs from the downstream edge of a standard 45-degree gate lip, eliminating bottom pulsations.

4. The frequency of a reflected positive pressure wave may be determined from the equation:

$$f_f = \frac{C}{4L}$$

where C is the velocity of the pressure wave and L is the length of the conduit upstream from the gate. Hydraulic Design Chart 060-1/2 is a graphical solution of this equation. The pressure wave velocity is dependent upon the dimensions and elastic characteristics of the pipe or of the lining and surrounding rock of a tunnel. Data are given by Parmakian* for various combinations of these variables. Chart 060-1/2 gives frequencies for pressure wave velocities ranging from 4700 fps for a relatively inelastic conduit to 3000 fps for a relatively elastic pipe.

5. **Natural Frequency.** The natural frequency of free vertical oscillation of a cable-suspended gate can be expressed by the equation:

$$f_n = \frac{1}{2\pi}\sqrt{\frac{gE}{12\,\ell\,\sigma}}$$

where E is the modulus of elasticity of the cable, ℓ is the length of the supporting cable, and σ is the unit stress in the cable. The natural frequencies for various support lengths and typical allowable unit stresses can be estimated from Hydraulic Design Chart 060-1/3.

6. **Examples of Application.** Hydraulic Design Charts 060-1/4 and 1/5 are sample computations illustrating application of Charts 060-1 to 1/3 to the gate vibration problem. Transmissibility ratios less than 1.0 are desirable. However, ratios slightly greater than 1.0 may be satisfactory if the vibration forces are damped.

---

* John Parmakian, Waterhammer Analysis, 1st ed. (New York, Prentice-Hall, Inc., 1955), Chap. 3.

060-1 to 060-1/5

TRANSMISSIBILITY RATIO - T.R. (y-axis)

f_f/f_n (x-axis)

ISOLATION
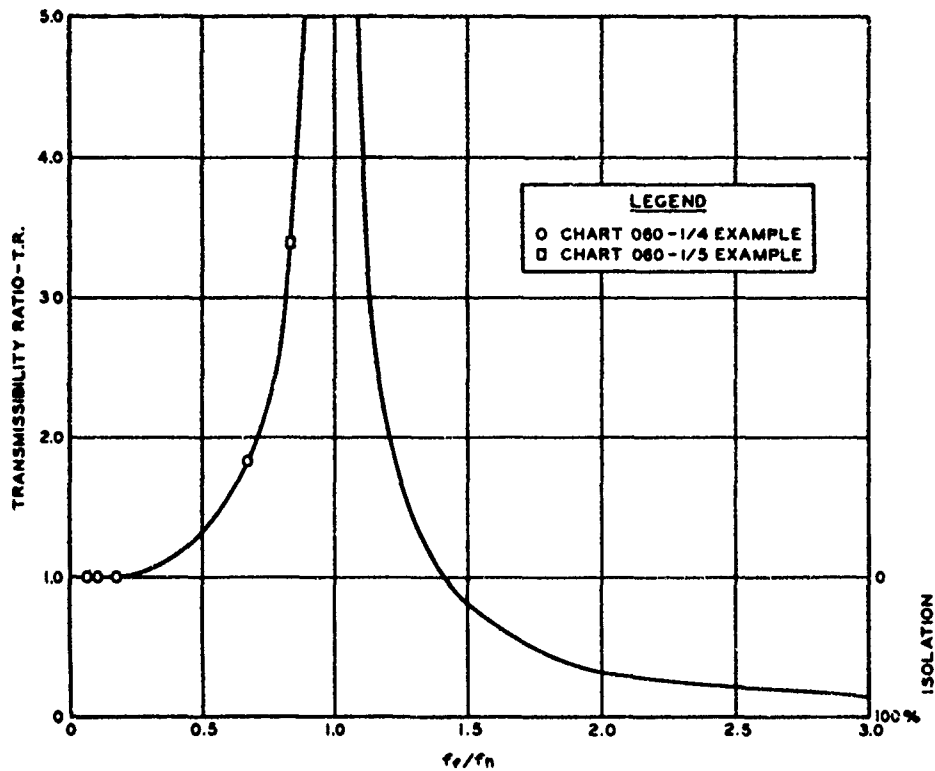
f_f/f_n	T.R.	f_f/f_n	T.R.	f_f/f_n	T.R.
0.00	1.000	0.85	3.604	1.50	0.800
0.10	1.019	0.90	5.263	1.60	0.641
0.20	1.042	0.95	10.256	1.70	0.529
0.30	1.099	1.05	9.756	1.80	0.446
0.40	1.191	1.10	4.762	1.90	0.363
0.50	1.333	1.15	3.101	2.00	0.333
0.60	1.563	1.20	2.273	2.20	0.260
0.65	1.732	1.25	1.778	2.40	0.210
0.70	1.961	1.30	1.449	2.60	0.174
0.75	2.286	1.35	1.216	2.80	0.146
0.80	2.778	1.40	1.042	3.00	0.125

BASIC EQUATION

$$T.R. = \frac{1}{1 - (f_f/f_n)^2}$$

WHERE:

T.R. = TRANSMISSIBILITY RATIO

f_f = FORCING FREQUENCY

f_n = NATURAL FREQUENCY

GATE VIBRATION
RESONANCE DIAGRAM

HYDRAULIC DESIGN CHART 060-1

WES 8-57

DEFINITION SKETCH
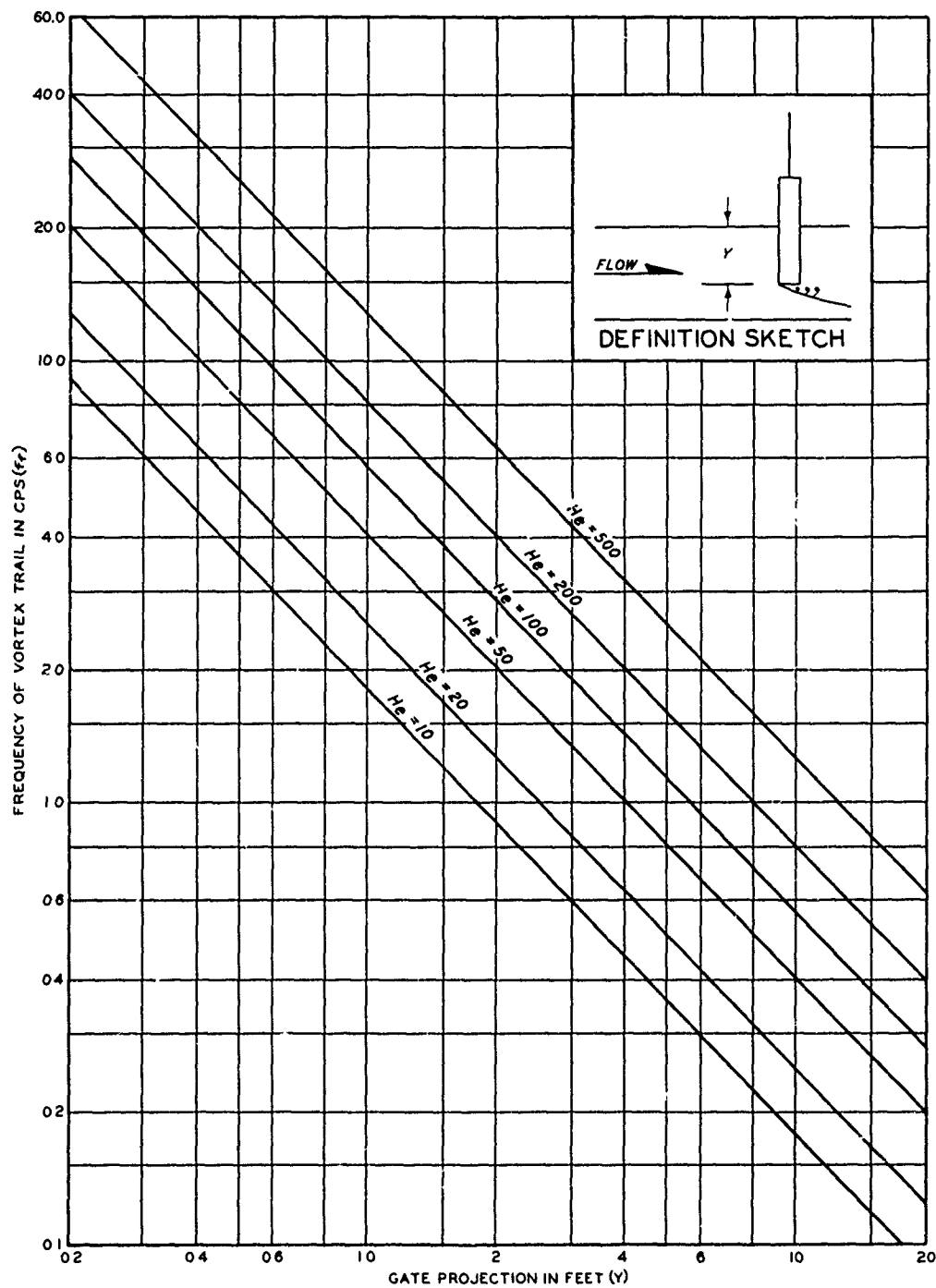
BASIC EQUATION $f_f = \dfrac{\sqrt{2gH_e}}{7(2Y)}$

WHERE

f_f = FORCING FREQUENCY IN CPS
H_e = ENERGY HEAD IN FT TO BOTTOM OF GATE
$1/7$ = STROUHAL NO FOR FLAT PLATE
Y = GATE PROJECTION IN FT

GATE VIBRATION
VORTEX TRAIL – FORCING FREQUENCY
HYDRAULIC DESIGN CHART 060-1/1

WES 6-57

FREQUENCY OF PRESSURE WAVE IN CPS (f_f)

LENGTH OF CONDUIT IN FEET (L)

C = 4700 FPS

C = 4300 FPS

C = 3000 FPS
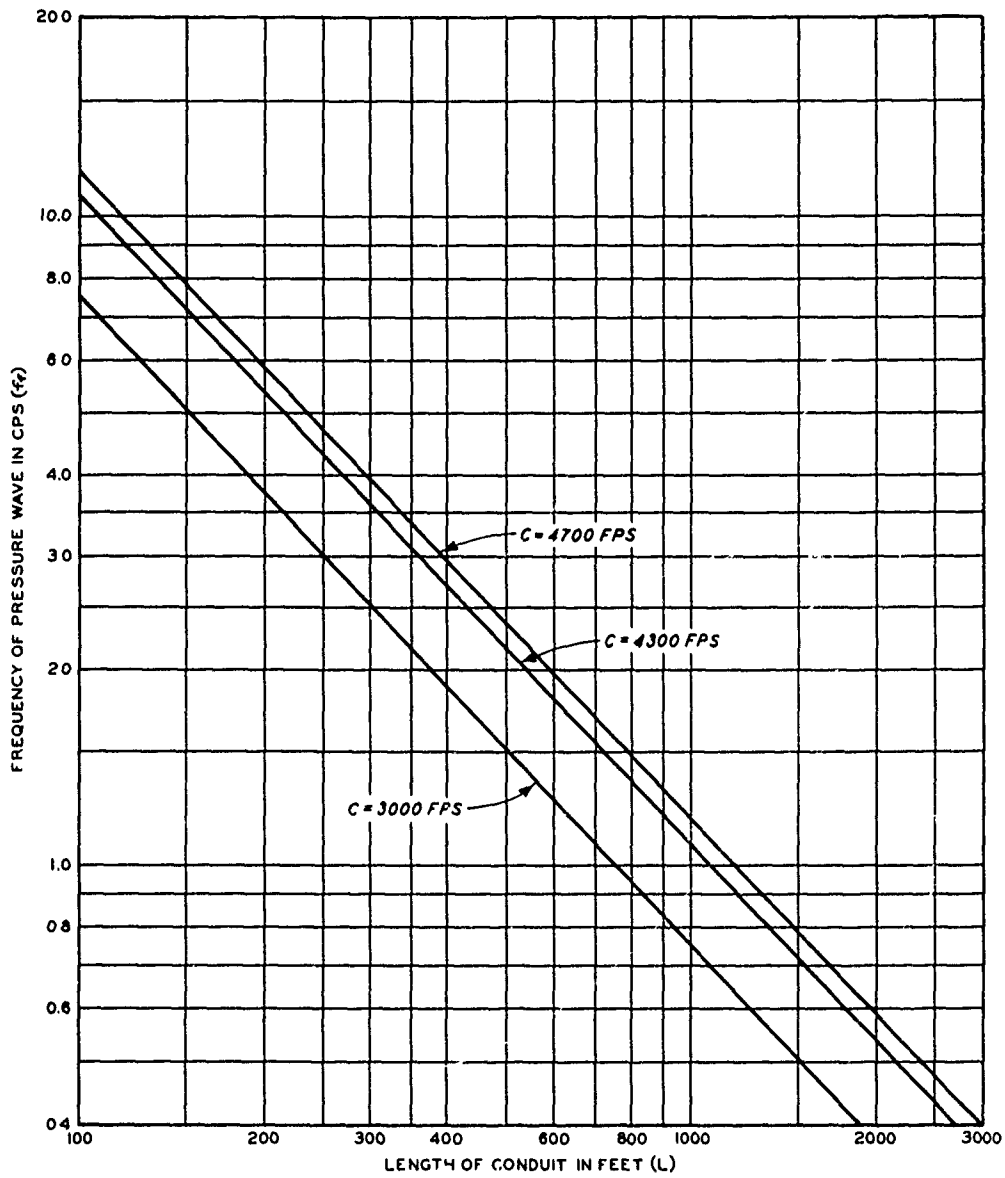
BASIC EQUATION $f_f = \dfrac{C}{4L}$

WHERE

f_f = FREQUENCY OF PRESSURE
       WAVE IN CPS
C = VELOCITY OF PRESSURE
    WAVE – FPS
L = LENGTH OF CONDUIT UP –
    STREAM FROM GATE IN FT

GATE VIBRATION
FORCING FREQUENCY
OF REFLECTED PRESSURE WAVE
HYDRAULIC DESIGN CHART 060-1/2

WES 6-57

NATURAL FREQUENCY IN CYCLES PER SEC (f_n)

σ = 6000 PSI
σ = 8500 PSI
σ = 11,000 PSI

LENGTH OF CABLE SUPPORT IN FT (ℓ)
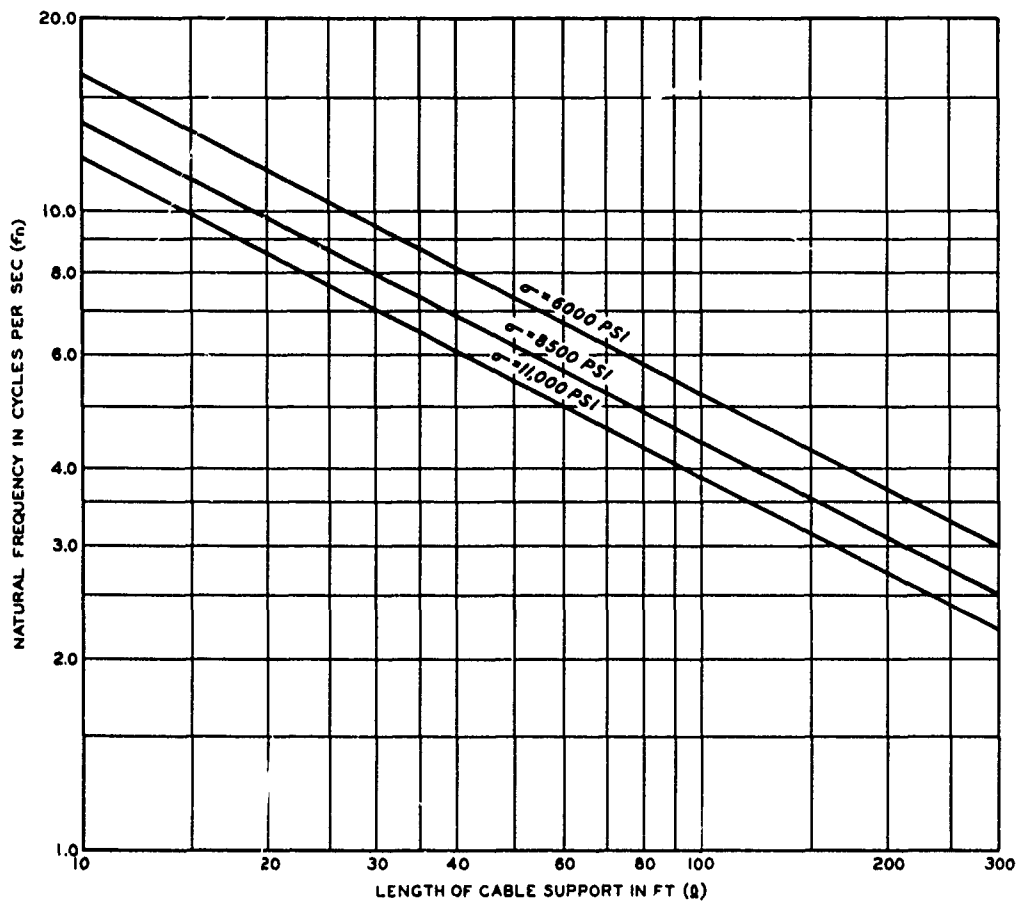
BASIC EQUATION

$$f_n = \frac{1}{2\pi}\sqrt{\frac{gE}{12\ell\sigma}}$$

WHERE:

f_n = NATURAL FREQUENCY OF SUSPENDED SYSTEM IN CYCLES PER SEC

g = ACCELERATION OF GRAVITY = 386 IN./SEC^2

E = MODULUS OF ELASTICITY OF CABLE = 20 X 10^6 PSI

ℓ = LENGTH OF CABLE SUPPORT IN FT

σ = UNIT STRESS IN CABLE STEEL IN PSI

GATE VIBRATION
NATURAL FREQUENCY
OF CABLE - SUSPENDED GATE
HYDRAULIC DESIGN CHART 060-1/3

JOB __CW 804__ PROJECT ___John Doe Dam___ SUBJECT ___Gate Vibration___

COMPUTATION __Vibration From Vortex Trail__

COMPUTED BY __RGC__ DATE __4/16/57__ CHECKED BY __RGC__ DATE __4/24/57__

GIVEN:

Gate - flat bottom
  Height $(D) = 23$ ft
  Projection (Y) into conduit
    $=$ height minus gate opening
    $= D - G_o$
  Length of cable $(\ell) = 130$ ft
  Allowable unit cable stress (σ)
    $= 8500$ psi
Total head at gate sill $= 100$ ft
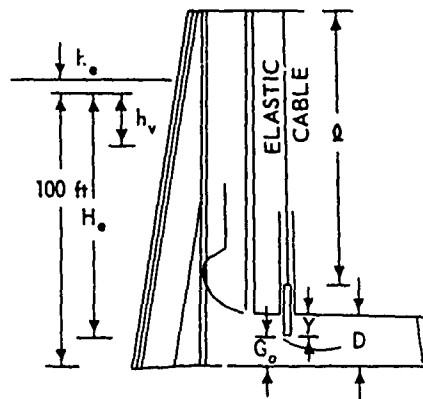
DETERMINE:

Natural frequency (f_n) for gate:
  Length of cable $(\ell) = 130$ ft
  Unit cable stress $(\sigma) = 8500$ psi
  From Chart 060-1/3 natural frequency
    $(f_n) = 3.8$ cps

Vortex trail frequency and resonance characteristics (f_f/f_n):
  Energy head (H_e) to bottom of gate $= 100$ ft $- G_o$.

Gate		H_e	Vortex Trail Frequency	Resonance Characteristics
Opening	Projection			
G_o	$Y = D - G_o$	$100 - G_o$	f_f (Chart 060 – 1/1)	(f_f/f_n)
3	20	97	0.28	0.07
9	14	91	0.39	0.10
15	8	85	0.66	0.17
21	2	79	2.54	0.67

Plot f_f/f_n on Chart 060-1:

All points plot above zero isolation line. Gate subject to vibration at all openings. Change design to 45 degree gate lip.

GATE VIBRATION

GATE BOTTOM VORTEX TRAIL
SAMPLE COMPUTATION

HYDRAULIC DESIGN CHART 060-1/4

WES 6-57

JOB ___CW 804___ PROJECT___John Doe Dam___ SUBJECT___Gate Vibration___

COMPUTATION ___Vibration From Reflected Pressure Wave___

COMPUTED BY ___RGC___ DATE ___4/22/57___ CHECKED BY ___RGC___ DATE ___4/25/57___

GIVEN:
   Conduit:
      Length upstream from
        gate (L) = 400 ft

   Gate:
      Length of supporting
        cable (ℓ) = 195 ft
      Assume unit stress in
        supporting cable (σ) = 8500 psi
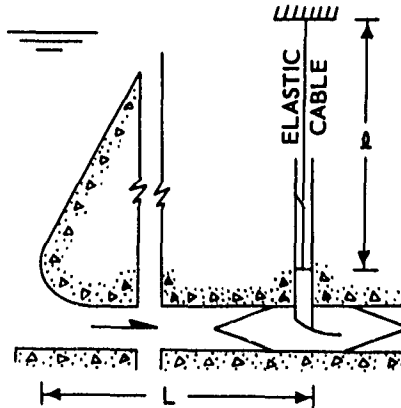
DETERMINE:
   Natural frequency (f_n) for gate:
      Length of supporting cable (ℓ) = 195 ft
      Unit stress in supporting cable (σ) = 8500 psi
      From Hydraulic Design Chart 060-1/3, natural
        frequency (f_n) = 3.2 cps

   Vibration from reflected pressure wave:
      Length of conduit upstream from gate (L) = 400 ft
      Velocity of pressure wave (C) = 4300 fps (assumed for
        concrete conduit through rock)
      From Hydraulic Design Chart 060-1/2, forcing frequency
        (f_f) = 2.7 cps

   Resonance characteristics:
      f_f/f_n = 2.7/3.2 = 0.84
      Plot f_f/f_n on Hydraulic Design Chart 060-1
      Transmissibility ratio (T.R.) = 3.4
      Isolation < 0
        Gate subject to vibration from reflected pressure wave
          if undamped. Damping forces not evaluated.

GATE VIBRATION
REFLECTED PRESSURE WAVE
SAMPLE COMPUTATION

HYDRAULIC DESIGN CHART 060-1/5

WES 6-57

HYDRAULIC DESIGN CRITERIA

SHEET 060-2

FORCED VIBRATIONS

CONSTANT FRICTION DAMPING

1. A procedure for estimating the vibration characteristics of free, elastically suspended gates is presented in HDC's 060-1 to 060-1/5. Tests at Fort Randall Dam[2] indicated that at large gate openings the flood-control tunnel gate rollers are momentarily forced away from the gate guides by pressure pulsations on the downstream face of the gate. Vertical gate vibrations of about 4 cycles per sec were observed during this interval. These vibrations were damped when the gate rollers returned to the guides. It was determined that the damping was of a Coulomb or constant friction damping character.

2. HDC 060-2 presents curves showing the effects of constant friction damping on forced vibrations. The equation and curves on the chart for the magnification factor were developed by Den Hartog[1] in 1931. The equation is only of value in the determination of the magnification factor above the dashed line on the chart. Den Hartog also successfully evaluated single points below the dashed line and constructed the curves representing high force ratios. More recently (1960) an analysis of the damping forces affecting the Fort Randall gates has been made.[3]

3. Field measurements to determine the causes, magnitudes, and frequencies of hydraulic disturbances causing gate vibration, as well as measurements of the resisting friction forces, are necessary for detail evaluation of the vibration characteristics of these hydraulic structures. HDC 060-2 is included as a supplement to HDC 060-1 to illustrate the effects of constant friction damping in the gate vibration problem.

4. References.

(1) Den Hartog, J. P., "Forced vibration with combined Coulomb and viscous friction." Transactions, American Society of Mechanical Engineers, Paper APM 53-9, presented at National Applied Mechanics Meeting, Purdue University (June 1931).

(2) U. S. Army Engineer Waterways Experiment Station, CE, Vibration and Pressure-Cell Tests, Flood-Control Intake Gates, Fort Randall Dam, Missouri River, South Dakota. Technical Report No. 2-435, Vicksburg, Miss., June 1956.

(3) _____, Vibration Problems in Hydraulic Structures, by F. B. Campbell. Miscellaneous Paper No. 2-414, Vicksburg, Miss., December 1960. Also in Proceedings, American Society of Civil Engineers, vol 87 (Journal, Hydraulics Division, No. HY2) (March 1961).
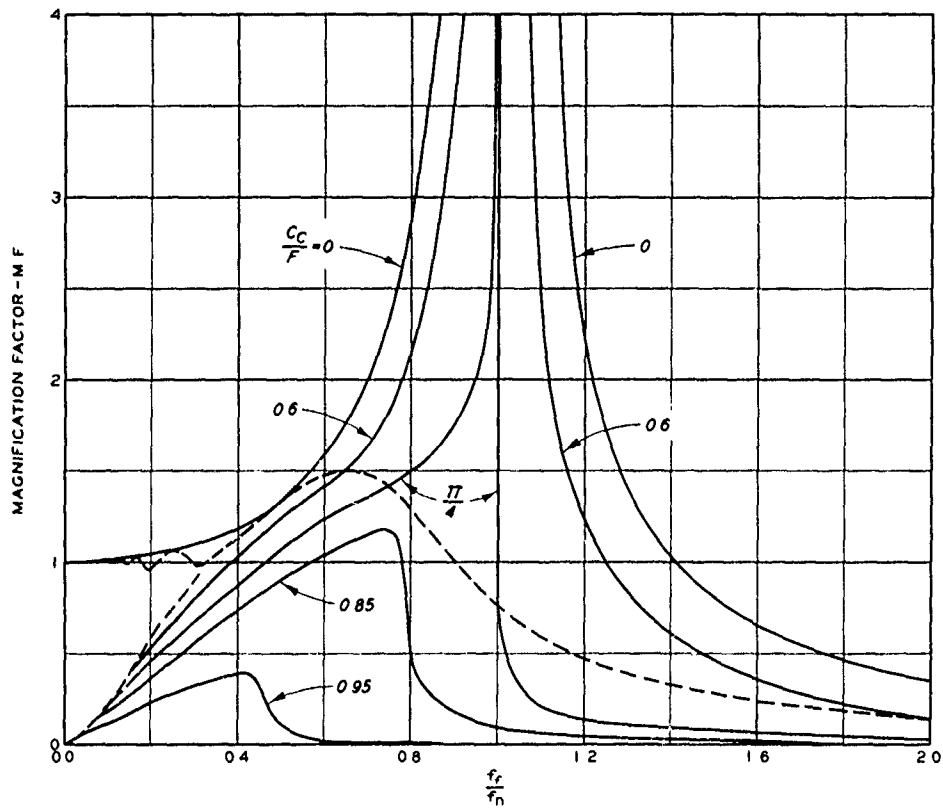
EQUATIONS

$$M F = \sqrt{A^2 - \frac{C_C^2}{F^2} B^2}$$

$$A = \frac{1}{1 - \frac{f_f^2}{f_n^2}}$$

$$B = \frac{f_n}{f_f} \text{TAN} \frac{\pi f_n}{2 f_f}$$

WHERE

M F = MAGNIFICATION FACTOR
C_C = CONSTANT FRICTION FORCE, LB
F = EXCITING FORCE, LB
f_f = FORCING FREQUENCY, CPS
f_n = NATURAL FREQUENCY, CPS

FORCED VIBRATIONS
CONSTANT FRICTION DAMPING

HYDRAULIC DESIGN CHART 060-2

WES 10-61

1. **Previous Crest Shapes.** Some early crest shapes were based on a simple parabola designed to fit the trajectory of the falling nappe. Bazin's experiments of the 19th century were the basis of many early designs. The Bureau of Reclamation conducted extensive experiments on the shape of the nappe over a sharp-crested weir.[1] Numerous crests have been designed using the coordinates of the lower surface of the nappe for the shape of the crest, without resort to an equation. The Huntington District has used an equation involving the 1.82 power of X and the Nashville District has used the 1.88 power of X .

2. **Standard Shape, Downstream Quadrant.** A comparison of the Bureau of Reclamation data with those of other experimenters was made by the Office, Chief of Engineers. On the basis of this study, Circular Letter No. 3281 was issued on 2 September 1944, suggesting the use of the 1.85 power of X . This equation is given in Hydraulic Design Charts 111-1 and 111-2 and was adopted to define the downstream quadrant shape.

3. **Point of Tangency.** The slope function graph of the tangent to the downstream quadrant is shown in Chart 111-1 to facilitate the location of the point of tangency. Although it is realized that the tangent point will often be determined analytically for the final design, this graph should be of value in the preliminary layouts in connection with stability analyses and cost estimates. In view of the fact that tables of the 1.85 and 0.85 powers are not available, the table in Chart 111-2 is issued to assist the engineer in computing the coordinates of the downstream quadrant.

4. **Standard Shape, Upstream Quadrant.** The upstream quadrant shape of circular arcs originally defined in Chart 111-1, dated 4-1-52, resulted in a surface discontinuity at the vertical spillway face. A third, short-radius arc $(R = 0.04H_d)$ recently incorporated in this design has been model tested[2] and found to result in improved pressure conditions and discharge coefficients for heads exceeding the design head. Chart 111-2/1 (revised 9-70) presents this new, recommended upstream crest quadrant design. A table of coordinates in terms of X/H_d and Y/H_d is included for design convenience.

5. **References.**

(1) U. S. Bureau of Reclamation, Part VI - Hydraulic Investigations; Bulletin 3, Studies of Crests for Overfall Dams. Boulder Canyon Project Final Reports, Denver, Colo., 1948.

(2) U. S. Army Engineer Waterways Experiment Station, CE, Investigations

of Various Shapes of the Upstream Quadrant of the Crest of a High
Spillway; Hydraulic Laboratory Investigation, by E. S. Melsheimer and
T. E. Murphy.   Research Report H-70-1, Vicksburg, Miss., January 1970.

111-1 to 111-2/1
Revised 9-70

NOTE: DOWNSTREAM QUADRANT SHAPE BASED
ON OCE CIRC LTR NO 3281, 9-2-44,
"SHAPE OF SPILLWAY CRESTS"
H_d = DESIGN HEAD BASED ON LOWER
SURFACE OF NAPPE FROM SHARP-
CRESTED WEIR

DOWNSTREAM QUADRANT

$$X^{1.85} = 2.0\, H_d^{0.85}\, Y$$

(SEE CHART III-2)

UPSTREAM QUADRANT
(SEE CHART III-2/1)
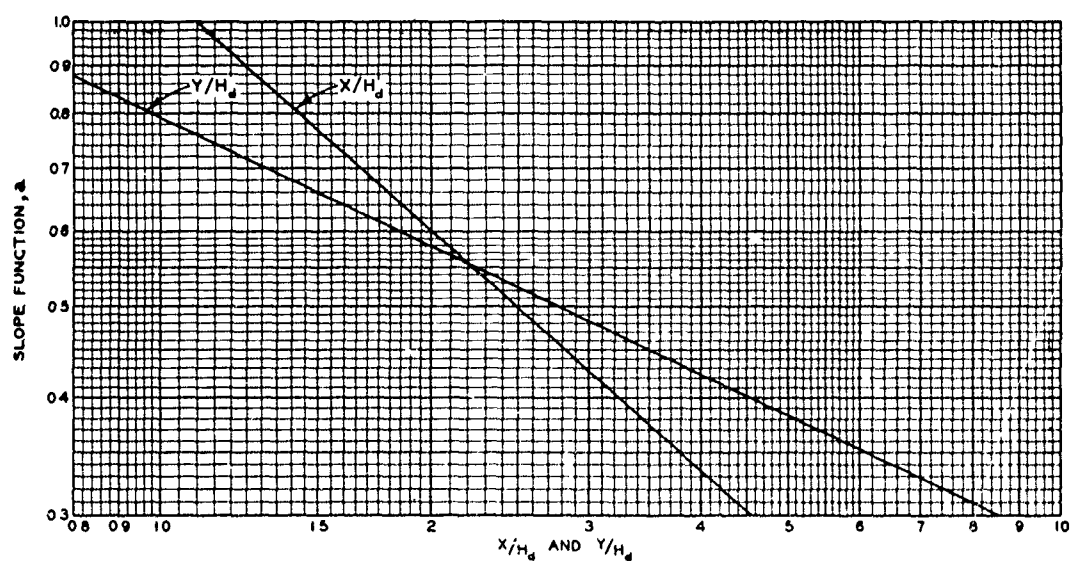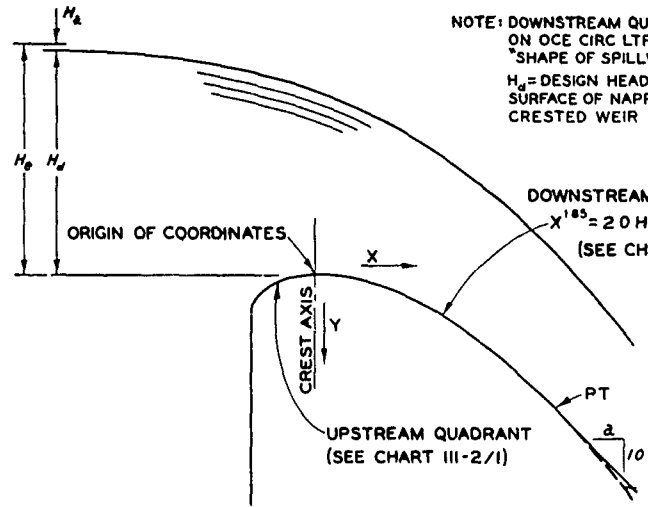
NOTE   COORDINATES OF TANGENT POINT
FOR PRELIMINARY LAYOUTS AND
ESTIMATES.

OVERFLOW SPILLWAY CREST
TANGENT ORDINATES

HYDRAULIC DESIGN CHART III-1

x	$x^{1.85}$	x	$x^{1.85}$	H_d	$2H_d^{0.85}$	H_d	$2H_d^{0.85}$	H_d	$2H_d^{0.85}$
0.10	0.0141	6	27.515	1	2.000	26	31.896	51	56.554
.15	.0299	7	36.596	2	3.605	27	32.937	52	57.495
.20	.0509	8	46.851	3	5.088	28	33.971	53	58.434
.25	.0769	9	58.257	4	6.498	29	35.000	54	59.370
.30	.1078	10	70.795	5	7.855	30	36.024	55	60.303
.35	.1434	12	99.194	6	9.172	31	37.041	56	61.234
.40	.1836	14	131.928	7	10.460	32	38.054	57	62.162
.45	.2283	16	168.897	8	11.713	33	39.063	58	63.088
.50	.2774	18	210.017	9	12.946	34	40.066	59	64.011
.60	.3887	20	255.215	10	14.159	35	41.067	60	64.932
.70	.5169	25	385.646	11	15.354	36	42.062	61	65.851
.80	.6618	30	540.349	12	16.532	37	43.053	62	66.767
.90	.8229	35	718.664	13	17.696	38	44.040	63	67.681
1.00	1.000	40	920.049	14	18.847	39	45.023	64	68.594
1.20	1.401	45	1144.045	15	19.985	40	46.002	65	69.503
1.40	1.864	50	1390.255	16	21.112	41	46.978	66	70.411
1.60	2.386	55	1658.330	17	22.229	42	47.950	67	71.317
1.80	2.967	60	1947.959	18	23.335	43	48.919	68	72.221
2.00	3.605	65	2258.863	19	24.433	44	49.884	69	73.123
2.50	5.447	70	2590.785	20	25.521	45	50.846	70	74.022
3.00	7.633	75	2943.496	21	26.602	46	51.807	71	74.920
3.50	10.151	80	3316.779	22	27.674	47	52.761	72	75.816
4.00	12.996	90	4124.285	23	28.741	48	53.714	73	76.710
4.50	16.160	100	5011.872	24	29.799	49	54.663	74	77.603
5.00	19.638			25	30.852	50	55.610	75	78.493

OVERFLOW SPILLWAY CREST EQUATIONS

$$X^{1.85} = 2H_d^{0.85}Y, \quad Y = \frac{X^{1.85}}{2H_d^{0.85}}; \text{ WHERE } H_d = \text{DESIGN HEAD}$$

NOTE: SEE CHART 111-2/1 FOR UPSTREAM
QUADRANT COORDINATES.

OVERFLOW SPILLWAY CREST
DOWNSTREAM QUADRANT
TABLE OF FUNCTIONS

HYDRAULIC DESIGN CHART 111-2

REV 6 60   WES 4-52

$0.2818H_d$

$0.2760H_d$

$0.1750H_d$

CREST AXIS ORIGIN
OF COORDINATES

X

Y

$R = 0.5H_d$

$X^{1.85} = 2.0H_d^{0.85}Y$

(SEE CHARTS III-1 AND III-2)

$0.1360H_d$

$0.1153H_d$

$0.0316H_d$

$R = 0.2H_d$

$X = -0.2418H_d$
$Y = 0.1360H_d$

$R = 0.04 H_d$

₵ CREST

$X = -0.1050H_d$
$Y = 0.2190H_d$

$X = 0.0000H_d$
$Y = 0.5000H_d$
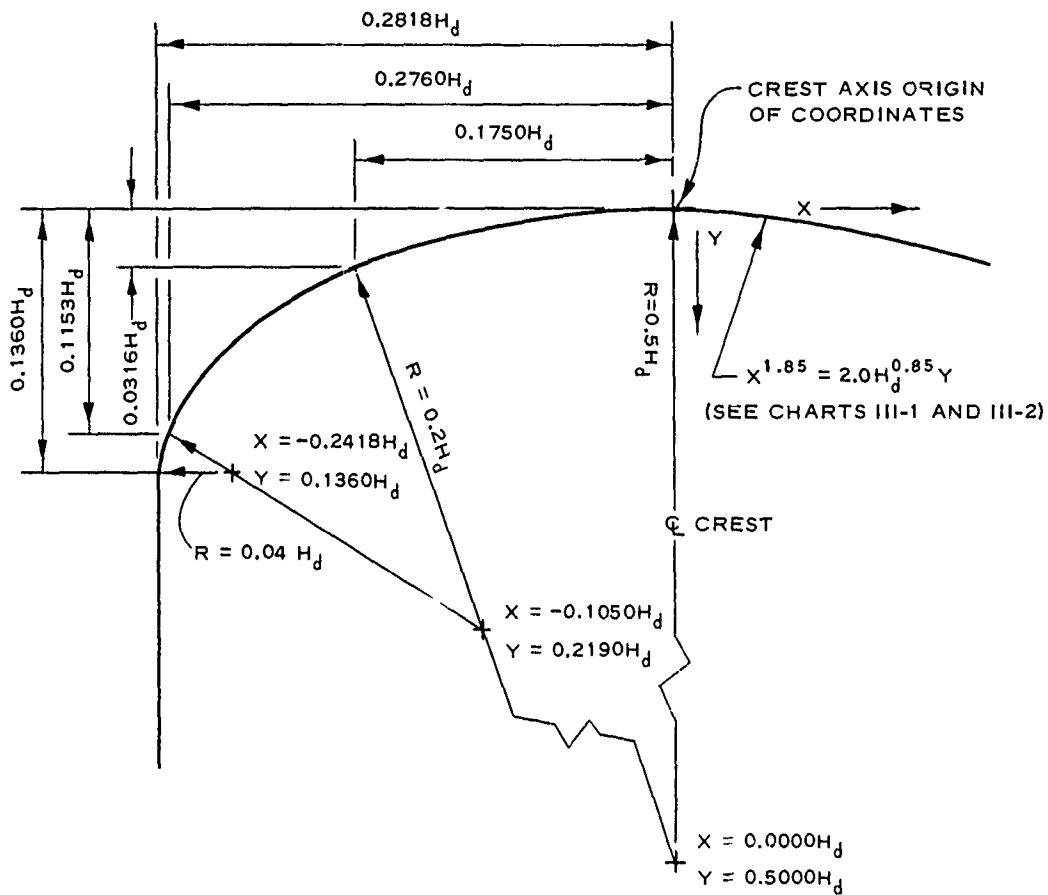
COORDINATES FOR UPSTREAM QUADRANT

$\dfrac{X}{H_d}$	$\dfrac{Y}{H_d}$	$\dfrac{X}{H_d}$	$\dfrac{Y}{H_d}$
−0.0000	0.0000	−0.2200	0.0553
−0.0500	0.0025	−0.2400	0.0714
−0.1000	0.0101	−0.2600	0.0926
−0.1500	0.0230	−0.2760	0.1153
−0.1750	0.0316	−0.2780	0.1190
−0.2000	0.0430	−0.2800	0.1241
		−0.2818	0.1360

NOTE: H_d = DESIGN HEAD BASED ON
LOWER SURFACE OF NAPPE
FROM SHARP-CRESTED WEIR
WITH NEGLIGIBLE VELOCITY
OF APPROACH AND CREST AT
$X = -0.2818H_d$, $Y = 0.1259H_d$.

OVERFLOW SPILLWAY CREST
UPSTREAM QUADRANT

HYDRAULIC DESIGN CHART III-2/1

SPILLWAY CREST

DISCHARGE COEFFICIENT

HIGH OVERFLOW DAMS

1. **General.** Discharge over an uncontrolled spillway crest is computed using the equation

$$Q = CLH_e^{3/2}$$

where

Q = total discharge, cfs

C = discharge coefficient (Hydraulic Design Chart 111-3)

L = effective crest length, ft (Hydraulic Design Sheet 111-3/1)

H_e = energy head on crest, ft

2. **Design Criteria.** Early studies of the discharge coefficient C used the relation of C to the ratio H_e/H_d . These studies indicated that C ranged from 3.90 to 4.10 at design head and decreased to 3.10 at zero head. An approximation of the upper value can be derived by transferring the sharp-crested weir coefficient to a rounded weir crest that fits the lower nappe. The head on the rounded crest is known to be 0.888 times the head on the sharp crest. Using a discharge coefficient of 3.33 for a sharp-crested weir and assuming the velocity of the approach flow to be negligible, the coefficient for design head is derived as 3.93. The lower limit of $C = 3.10$ closely approximates the theoretical broad-crested weir coefficient of 3.087. The theory, which is based on critical depth in rectangular channels, is given by King.[1] Friction can be expected to reduce the coefficient at low heads. New, smooth concrete crests should have a high coefficient at low heads compared to crests that have been roughened by weathering or other causes.

3. **Test Data.** The curve in Chart 111-3 is based primarily on data obtained from model tests conducted under Corps of Engineers Engineering Studies Item 801, General Spillway Investigation, at the U. S. Army Engineer Waterways Experiment Station (WES). Only those tests in which a deep approach channel and negligible velocity of approach existed were used in developing the curve. The plotted points from ES 801 are the basis for the curve above the H_e/H_d ratio of 0.4. Prototype test results are plotted for the low head range, and that portion of the curve is based on

the field tests indicated in the legend. More prototype observations are needed for the newer design shapes that approximate the spillway crest defined in Hydraulic Design Criteria 111-1 and 111-2/1.

4. The open-circle data points are from tests on the originally published crest shape (Charts 111-1 and 111-2, dated 4-1-52). The open-triangle points are from recent laboratory tests[2] in which a third short-radius curve ($R = 0.04H_d$, Chart 111-2/1) was added to the upstream quadrant shape to eliminate the surface discontinuity in the original design where the curve intersected the vertical face of the spillway.

5. References.

(1) King, H. W., Handbook of Hydraulics; For the Solution of Hydraulic Problems, 3d ed. (1939), pp 379-380 and 4th ed. (1954, revised by E. F. Brater), pp 8-8 and 8-9, McGraw-Hill, New York.

(2) U. S. Army Engineer Waterways Experiment Station, CE, Investigations of Various Shapes of the Upstream Quadrant of the Crest of a High Spillway; Hydraulic Laboratory Investigation, by E. S. Melsheimer and T. E. Murphy. Research Report H-70-1, Vicksburg, Miss., January 1970.

LEGEND

O	1949 WES TESTS	MODEL
▽	1969 WES TESTS	
●	FORT GIBSON	
▲	FORT RANDALL	
▼	HARLAN COUNTY	PROTOTYPE
+	PINE FLAT	
■	WOLF CREEK	
X	DALE HOLLOW	

Vertical axis: $\dfrac{H_e}{H_d}$ (0 to 1.8)

Horizontal axis: $C = \dfrac{Q}{LH_e^{3/2}}$ (3.0 to 4.4)
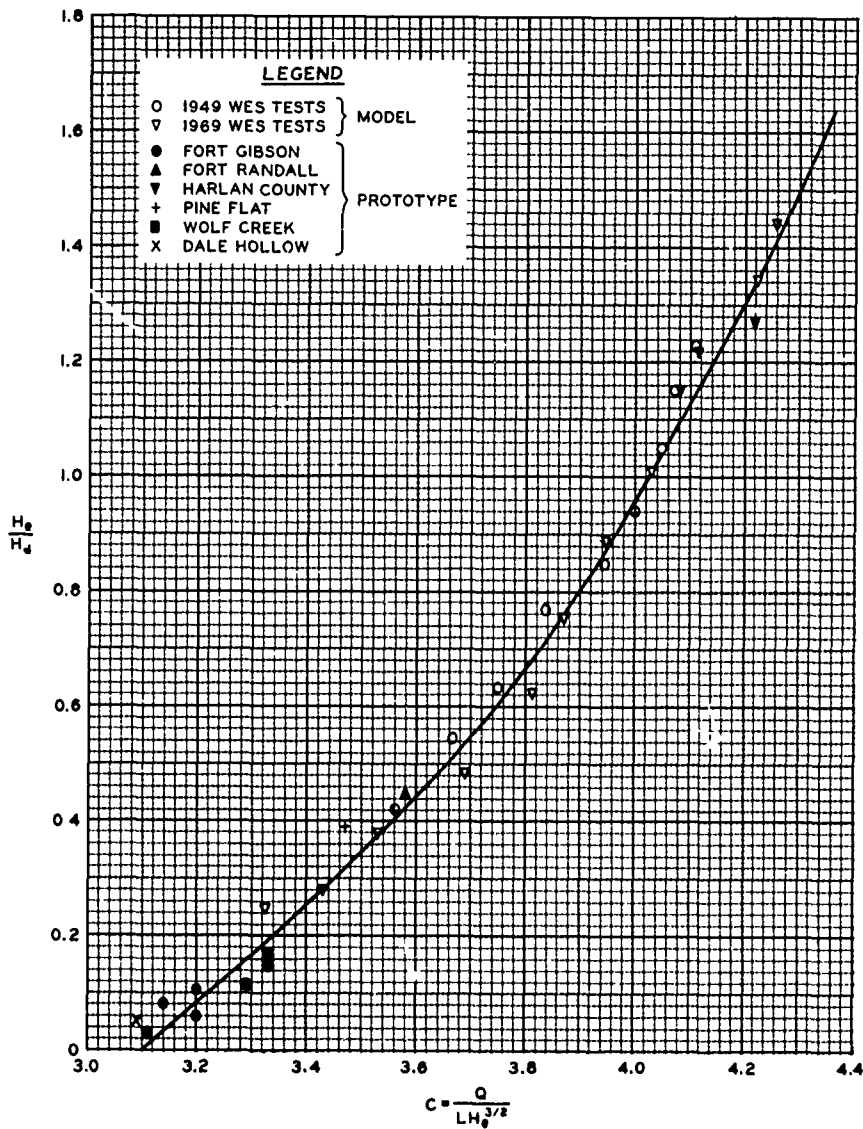
NOTE: H_e = ENERGY HEAD ON CREST, FT
H_d = DESIGN HEAD ON CREST, FT
C = DISCHARGE COEFFICIENT
Q = DISCHARGE, CFS
L = NET LENGTH OF CREST, FT

SPILLWAY CREST
DISCHARGE COEFFICIENT

HIGH OVERFLOW DAMS

HYDRAULIC DESIGN CHART III-3

OVERFLOW SPILLWAY CREST WITH ADJACENT CONCRETE SECTIONS

ABUTMENT CONTRACTION COEFFICIENT

1. The effective length L of a spillway crest used in uncontrolled-spillway discharge computations is expressed by the equation:

$$L = L' - 2 \left(NK_p + K_a \right) H_e$$

where

      L' = net length of crest, ft

      N = number of piers

      K_p = pier contraction coefficient

      K_a = abutment contraction coefficient

      H_e = energy head on crest, ft

2. HDC 111-3/1 presents a suggested abutment contraction coefficient design curve for high overflow spillways with adjacent concrete sections. Discharge and pier contraction coefficients from appropriate HDC charts were used with model discharge data to compute the plotted abutment contraction coefficients. These abutment contraction coefficients include the weir end contraction and the effect of approach flow angularity, if any, on all elements of the spillway. The coefficient K_a is plotted in terms of the ratio of the energy head on the spillway H_e to the abutment radius R . Pertinent information concerning each project is tabulated in HDC 111-3/1. An abutment contraction coefficient of 0.1 is suggested for design purposes for spillways with adjacent concrete nonoverflow sections when the approach flow is normal to the spillway crest. Higher coefficients should be assumed for projects involving extreme angularity of approach flow. It is also suggested that the maximum design head-abutment radius ratio be limited to 5.0.

3. <u>References.</u>

(1) U. S. Army Engineer Waterways Experiment Station, CE, <u>Model Studies of Spillway and Bucket for Center Hill Dam, Caney Fork River, Tennessee.</u> Technical Memorandum No. 202-1, Vicksburg, Miss., August 1946.

(2) _____ , <u>Spillway for Philpott Dam, Smith River, Virginia; Model Investigation.</u> Technical Memorandum No. 2-321, Vicksburg, Miss., December 1950.

(3) _____ , <u>Spillway and Conduits for Pine Flat Dam, Kings River,</u>

California; Hydraulic Model Investigation. Technical Memorandum No. 2-375, Vicksburg, Miss., December 1953.

(4) U. S. Army Engineer Waterways Experiment Station, CE, Folsom Dam Spillway, Uncontrolled. (Unpublished data.)

(5) _____, General Spillway Tests (ES 801). (Unpublished data.)
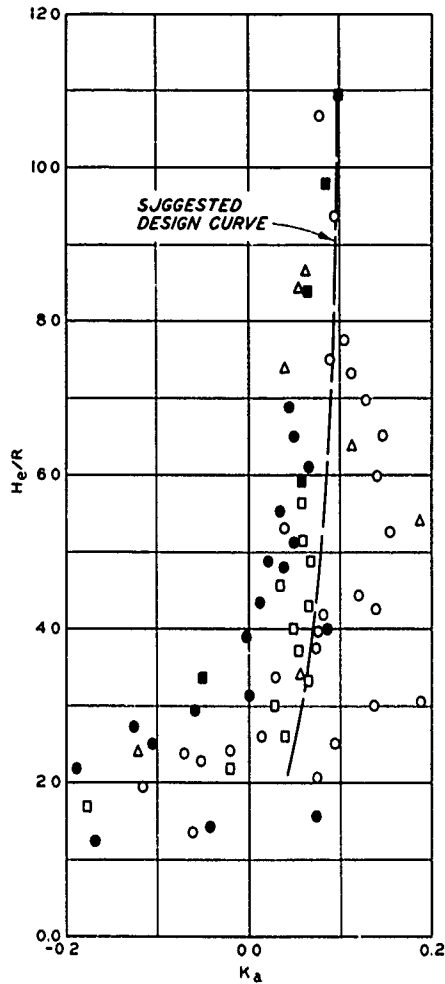
BASIC EQUATION

$$Q = C \left[L' - 2 \left(N K_P + K_a \right) H_e \right] H_e^{3/2}$$

WHERE:
Q = DISCHARGE, CFS.
C = DISCHARGE COEFFICIENT.
L' = NET LENGTH OF CREST, FT.
N = NUMBER OF PIERS.
K_P = PIER CONTRACTION COEFFICIENT.
K_a = ABUTMENT CONTRACTION COEFFICIENT.
H_e = TOTAL HEAD ON CREST, FT.

LEGEND

SYMBOL	PROJECT	R	W/L	W/H
○	CW 801	4	1 55	0 96
●	FOLSOM	8	2.10	3 77
□	PHILPOTT	5	2.67	1 42
■	PINE FLAT*	4	2.12	1 77
△	CENTER HILL*	5	3 83	9 45

*GATED SPILLWAY WITH PIERS

NOTE R = RADIUS OF ABUTMENT, FT
W = WIDTH OF APPROACH REPRODUCED IN MODEL, FT.
L = GROSS WIDTH OF SPILLWAY, FT.
H = DEPTH OF APPROACH IN MODEL, FT.

SUGGESTED DESIGN CURVE

(H_e/R vs K_a plot)
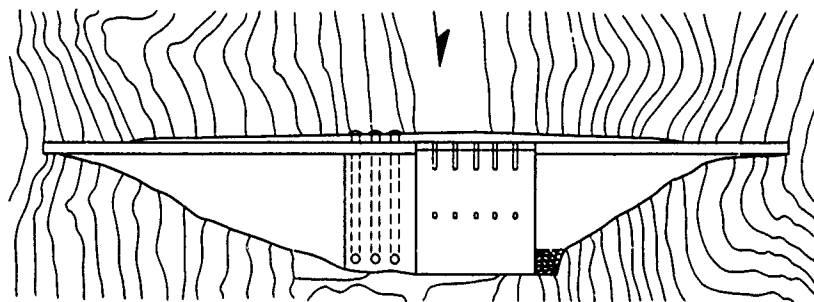
OVERFLOW SPILLWAY CREST WITH ADJACENT CONCRETE SECTIONS

ABUTMENT CONTRACTION COEFFICIENT

HYDRAULIC DESIGN CHART III-3/1

OVERFLOW SPILLWAY CREST WITH ADJACENT EMBANKMENT SECTIONS

ABUTMENT CONTRACTION COEFFICIENT

1. The effective length of a spillway crest used in uncontrolled-spillway discharge computations is expressed by the equation given in HDC Sheet 111-3/1.

2. HDC 111-3/2 presents a suggested abutment contraction coefficient design curve for spillways with adjacent earth embankment sections. Discharge and pier contraction coefficients from appropriate HDC charts were used with model discharge data to compute the plotted abutment contraction coefficients. These abutment contraction coefficients include the contractive effects of the upstream rounding of the embankments, the weir end contraction, and the effects of approach flow angularity on all elements of the spillway. The coefficient K_a is plotted in terms of the ratio of the energy head on the spillway to the spillway design head. This parameter is believed to be more representative of the composite abutment contraction effects than the energy head-abutment radius ratio used on the original HDC 111-3/2 dated August 1960. Pertinent information concerning each project is tabulated in the chart.

3. An abutment contraction coefficient of 0.2 is suggested for design purposes for spillways with adjacent nonoverflow earth embankments. Higher coefficients should be assumed for projects involving extreme angularity of approach flow. An abutment contraction coefficient of 0.74 was measured during the model study[4] of John Redmond Dam spillway for a design head of 41 ft and a weir height of 0.0 ft.

4. References.

(1) U. S. Army Engineer District, Portland, CE, Spillway for Dorena Dam, Row River, Oregon; Hydraulic Model Investigation. Bonneville Hydraulic Laboratory Report No. 27-1, Bonneville, Oreg., May 1953.

(2) U. S. Army Engineer Waterways Experiment Station, CE, Walter F. George Lock and Dam, Chattahoochee River, Alabama and Georgia; Hydraulic Model Investigation. Technical Report No. 2-519, Vicksburg, Miss., August 1959.

(3) _____, Carlyle Dam, Kaskaskia River, Illinois; Hydraulic Model Investigation. Technical Report No. 2-568, Vicksburg, Miss., June 1961.

(4) _____, Spillway for John Redmond Dam, Grand (Neosho) River, Kansas; Hydraulic Model Investigation. Technical Report No. 2-611, Vicksburg, Miss., November 1962.

(5) _____, Red Rock Dam Model Tests. (Unpublished data.)
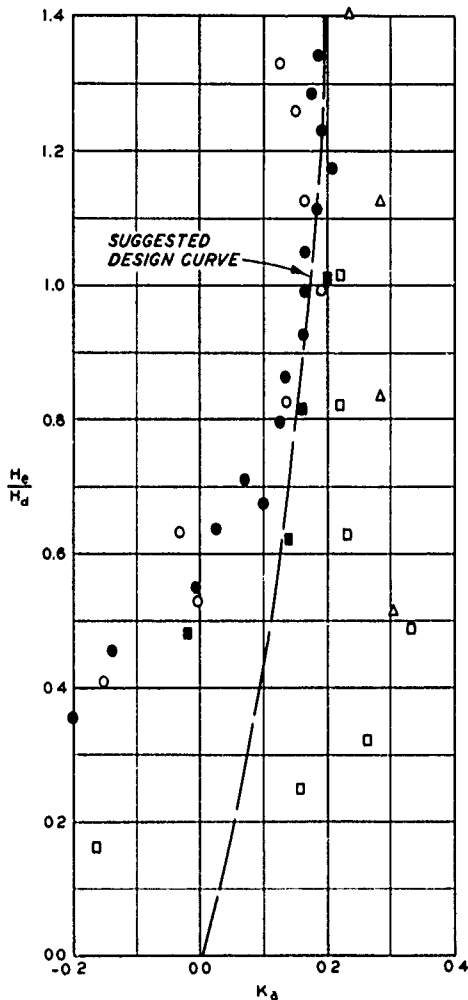
BASIC EQUATION

$$Q = C\left[L' - 2(NK_P + K_a)H_e\right]H_e^{3/2}$$

WHERE:
- Q = DISCHARGE, CFS
- C = DISCHARGE COEFFICIENT
- L' = NET LENGTH OF CREST, FT
- N = NUMBER OF PIERS
- K_P = PIER CONTRACTION COEFFICIENT
- K_a = ABUTMENT CONTRACTION COEFFICIENT
- H_e = ENERGY HEAD ON CREST, FT

LEGEND

SYMBOL	PROJECT	R	W/L	W/H
⊓	DORENA	2	5 60	10 7
■	DORENA	4	5 60	10 7
○	RED ROCK*	7.8	3 42	16 5
●	CARLYLE*	9	8 44	75.5
△	WALTER F. GEORGE*	4	5 44	55.3

*GATED SPILLWAY WITH PIERS

NOTE: R = RADIUS OF ABUTMENT, FT
W = WIDTH OF APPROACH REPRODUCED IN MODEL, FT
L = GROSS WIDTH OF SPILLWAY, FT
H = DEPTH OF APPROACH IN MODEL, FT
H_d = DESIGN HEAD ON CREST, FT
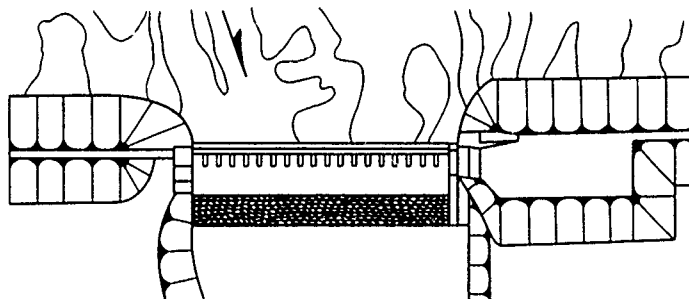
OVERFLOW SPILLWAY CREST WITH ADJACENT EMBANKMENT SECTIONS

ABUTMENT CONTRACTION COEFFICIENT

HYDRAULIC DESIGN CHART III-3/2

HYDRAULIC DESIGN CRITERIA

SHEET 111-3/3

OVERFLOW SPILLWAYS

STAGE-DISCHARGE RELATION

UNCONTROLLED FLOW

1. <u>Purpose.</u> Hydraulic Design Chart 111-3/3 provides a method for developing an uncontrolled spillway flow rating curve when the spillway discharge and head for any unsubmerged, uncontrolled flow are known or can be computed. It also provides a means of optimizing spillway design through extensive use of the sharp-crested weir data published by the USBR.[1] Its use is limited to unsubmerged flow conditions.

2. <u>Theory.</u> When flow over a spillway is controlled only by the head on the spillway, the relation between the head and discharge can be expressed by the following equation:

$$Q = CLH_e^{3/2} \qquad (1)$$

where

Q = spillway discharge, cfs

C = total flow coefficient combining the approach channel and crest shape, abutment, and pier effects

L = net spillway length, ft

H_e = energy head on the spillway, ft

3. A comparable equation for the spillway design flow is

$$Q_d = C_d L H_d^{3/2} \qquad (2)$$

where the subscript d refers to the spillway design flow. Division of equation 1 by equation 2 results in the equation

$$\frac{Q}{Q_d} = u \left(\frac{H_e}{H_d} \right)^{3/2} \qquad (3)$$

where $u = \dfrac{C}{C_d}$. Model data for ten widely varying spillway designs have been analyzed in accordance with the parameters of equation 3. The results are shown in Chart 111-3/3. The spillway design features for each project are tabulated below.

Project	Ref No.	Upstream Face Slope	Abutment Condition	No. of Bays	Approach Depth (H_d/P)	Downstream Quad Shape
Proctor*	2	3V on 2H	None	2	2.00	$x^{1.81}$
Pine Flat	3	Vertical	Concrete	6	0.11	$x^{1.85}$
Gavins Point	4	3V on 2H	Earth	14	1.64	$x^{1.78}$
Two-Dimensional	5	Vertical	None	--	0.3-0.4	$x^{1.85}$
Oakley	6	3V on 3H	Earth	4	2.2	$x^{1.747}$
Hugo	7	Vertical	Earth	6	4.3	$x^{1.85}$
Fort Randall	8	Vertical	Earth	21	1.7	$x^{1.85}$
John Redmond	9	Vertical	Earth	14	8.2	$x^{1.776}$
Kaysinger Bluff**	10	1V on 0.5H	Earth and concrete	4	0.74	$x^{1.825}$
Clarence Cannon†	11	Vertical	Concrete	4	0.40	$x^{1.85}$

* Section model (1 full and 2 half bays).
** Includes effects of 90-deg approach channel bend.
† Includes effects of adjacent outlet works and water quality weir.

   4. The plotted points on Chart 111-3/3 can be expressed by the general equation:

$$\frac{Q}{Q_d} = u\left(\frac{H_e}{H_d}\right)^n \tag{4}$$

For $Q/Q_d = 1.0$ and $H_e/H_d = 1.0$, the value of u is 1.0 and the value of n has been graphically determined to be 1.60. Therefore, the equation fitting all the data within experimental accuracy limits is

$$Q = Q_d \left(\frac{H_e}{H_d}\right)^{1.60} \tag{5}$$

   5. Application.

   a. Design. The spillway design flow Q_d is computed using

appropriate coefficients and equations given in Charts 111-3 to 111-3/2, 111-5, 111-6, 122-1 to 122-2, and 122-4 for the spillway design head H_d. Equation 5 is then solved for the desired ratios of H_e/H_d using the computed Q_d value. In a graphical solution, values of Q/Q_d are read from the chart for the selected values of H_e/H_d. These discharge ratios are then multiplied by Q_d to obtain the required Q values.

b. Operation. The theoretical or model rating curve of a spillway can be checked for the full range of spillway heads provided one accurate prototype discharge and corresponding spillway head measurement are available. Equation 5 is solved for the design discharge Q_d using the measured discharge Q, and the ratio of the measured head H to the design H_d. The derived value of Q_d is then used in equation 5 with selected values of H/H_d to obtain the required discharge quantities. If preferred, a graphical solution similar to that described in 5a above can be used.

6. References.

(1) U. S. Bureau of Reclamation, Studies of Crests for Overfall Dams; Hydraulic Investigations. Bulletin 3, Part VI, Boulder Canyon Project Final Reports, Denver, Colo., 1948.

(2) U. S. Army Engineer Waterways Experiment Station, CE, Spillway for Proctor Dam, Leon River, Texas; Hydraulic Model Investigation. Technical Report No. 2-645, Vicksburg, Miss., March 1964.

(3) _____, Spillway and Conduits for Pine Flat Dam, Kings River, California; Hydraulic Model Investigation. Technical Memorandum No. 2-375, Vicksburg, Miss., December 1953.

(4) _____, Spillway for Gavins Point Dam, Missouri River, Nebraska; Hydraulic Model Investigation. Technical Memorandum No. 2-404, Vicksburg, Miss., May 1955.

(5) _____, Investigation of Various Shapes of the Upstream Quadrant of the Crest of a High Spillway; Hydraulic Laboratory Investigation, by E. S. Melsheimer and T. E. Murphy. Research Report H-70-1, Vicksburg, Miss., January 1970.

(6) _____, Spillway for Oakley Dam, Sangamon River, Illinois; Hydraulic Model Investigation, by E. S. Melsheimer. Technical Report H-70-13, Vicksburg, Miss., November 1970.

(7) _____, Spillway for Hugo Dam, Kiamichi River, Oklahoma; Hydraulic Model Investigation, by B. P. Fletcher and J. L. Grace, Jr., Technical Report H-69-15, Vicksburg, Miss., November 1969.

(8) _____, Spillway and Outlet Works, Fort Randall Dam, Missouri River, South Dakota; Hydraulic Model Investigation. Technical Report No. 2-528, Vicksburg, Miss., October 1959.

(9) U. S. Army Engineer Waterways Experiment Station, CE, <u>Spillway for John Redmond Dam, Grand (Neosho) River, Kansas; Hydraulic Model Investigation.</u> Technical Report No. 2-611, Vicksburg, Miss., November 1962.

(10) _____, <u>Spillway for Kaysinger Bluff Dam, Osage River, Missouri; Hydraulic Model Investigation.</u> Technical Report No. 2-809, Vicksburg, Miss., January 1968.

(11) _____, <u>Spillway for Clarence Cannon Reservoir, Salt River, Missouri; Hydraulic Model Investigation,</u> by B. P. Fletcher. Technical Report H-71-7, Vicksburg, Miss., October 1971.

$$Q = Q_d \left(\frac{H_e}{H_d}\right)^{1.60}$$

WHERE:
Q = DISCHARGE, CFS
Q_d = DISCHARGE AT SPILLWAY
    DESIGN HEAD, CFS
H_e = ENERGY HEAD ON SPILLWAY, FT
H_d = SPILLWAY DESIGN HEAD, FT

LEGEND

O   OAKLEY
△   JOHN REDMOND
▽   PINE FLAT
X   GAVINS POINT
◇   PROCTOR
⬭   HUGO
●   FORT RANDALL
■   KAYSINGER BLUFF
▲   CLARENC. CANNON
▼   TWO DIMENSIONAL
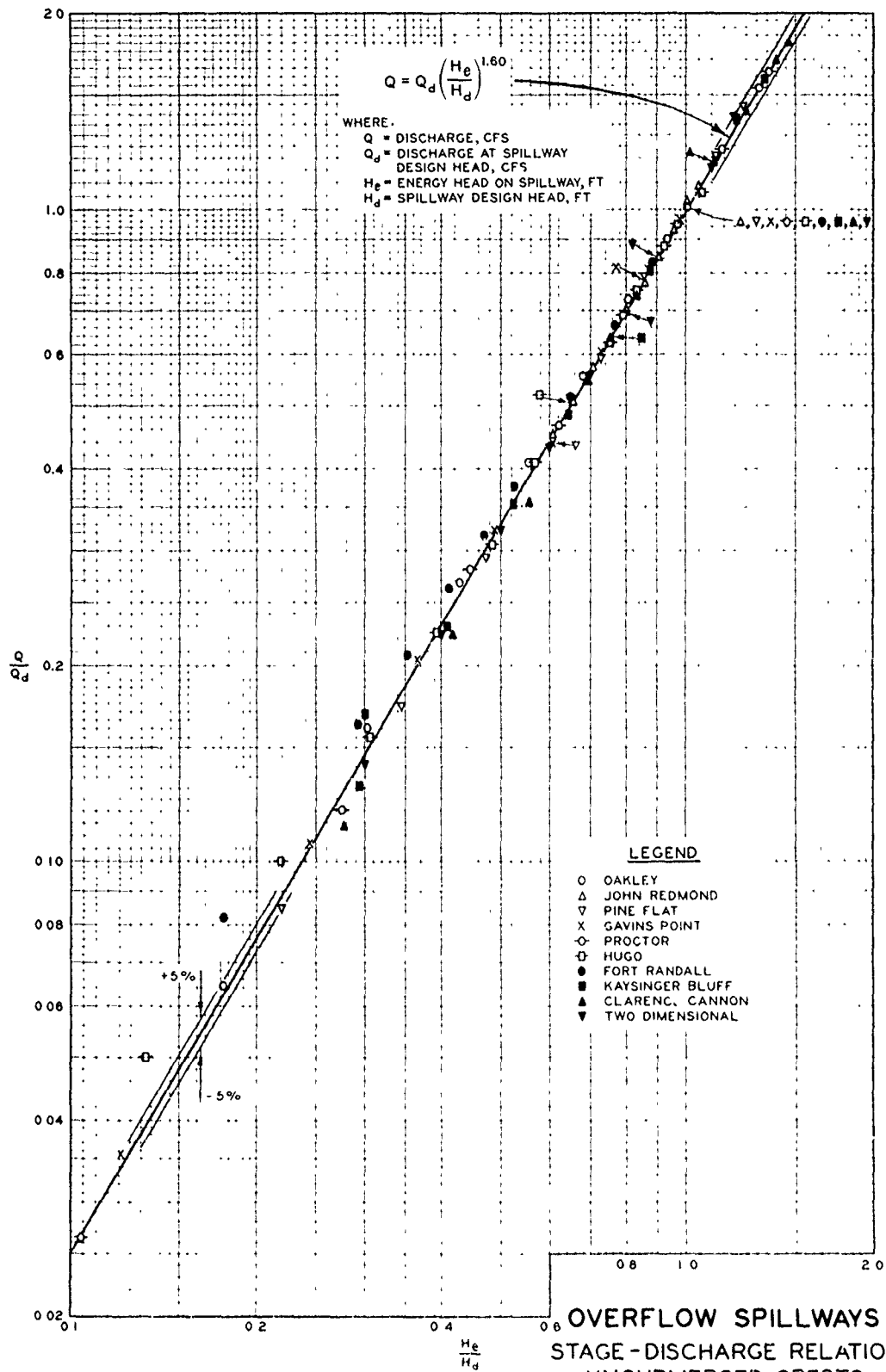
OVERFLOW SPILLWAYS
STAGE-DISCHARGE RELATION
UNSUBMERGED CRESTS

HYDRAULIC DESIGN CHART III-3/3

WES 2 72

SUBMERGED CREST COEFFICIENTS

OVERFLOW DAMS

1. **Background.** A number of important experiments on submerged, sharp-crested weirs were made in the nineteenth century. The submerged weir coefficients based on Herschel's analysis and republished in King's Handbook of Hydraulics have been widely used. Coefficients for the more modern shapes of submerged, round-crested weirs have been determined by various experimenters. However, the results have not been widely publicized and are not generally available to the design engineer. The experiments of Cox[1] were published, and the extensive test program of the U. S. Bureau of Reclamation was reported by Bradley[2].

2. **Bureau of Reclamation Tests.** The form of plotting of the variables used on Hydraulic Design Chart 111-4 was devised by Bradley. The family of curves shows various reductions in per cent from the coefficient for free or unsubmerged flow as presented on Hydraulic Design Chart 122-1. The general pattern of the curves shows that for low ratios of total drop from upper pool to apron floor divided by head on the crest, $(h_d + d)/H_e$, the flow is supercritical and the decrease in coefficient is principally affected by this ratio. The cross section B-B in the upper right-hand corner of the graph shows the variations of $(h_d + d)/H_e$ at h_d/H_e of 0.78. For large values of $(h_d + d)/H_e$ the decrease in coefficient is principally affected by the ratio h_d/H_e. For values of h_d/H_e less than 0.10, the jet is on the surface and no jump occurs. The cross section A-A shows the variations of h_d/H_e at $(h_d + d)/H_e$ of 5.0.

(1) G. N. Cox, "The Submerged Weir as a Measuring Device," University of Wisconsin, Engineering Experiment Station, Bulletin No. 67, 1928.

(2) J. N. Bradley, "Studies of Flow Characteristics, Discharge and Pressures Relative to Submerged Dams," Hydraulic Laboratory Report No. 182, Bureau of Reclamation, 1945. Also "Studies of Crests for Overfall Dams, Boulder Canyon Project," Final Reports, Part VI, Bulletin 3, Bureau of Reclamation, 1948.

3. **Current Analysis.** The experimental observations of the Bureau of Reclamation were plotted on the same graph with those of other experimenters[3]. The combined data produced 201 experimental observations. The complete plot of the test points nearly obliterates the coefficient reduction curves and for this reason was omitted from the chart. The current analysis results in some deviation from the Bradley curves which were omitted from the chart for the sake of clarity and utility.

4. **Application.** The curves shown on Chart 111-4 were based on three different test conditions of the individual experimenters as follows: the approach and apron floors at the same constant elevation, both floors at the same elevation but varied with respect to the crest, and the approach floor elevation held constant with the apron elevation varied. The decrease in the coefficient was based on the unsubmerged coefficient for the condition tested. The general agreement of the percentage decreases in coefficients from the five independent studies indicates that these values may be used in combination with Chart 122-1 to determine coefficients for higher velocities of approach.

(3) H. J. Koloseus, "Discharge Characteristics of Submerged Spillways," Colorado Agricultural and Mechanical College Thesis, Dec. 1951.
M. Bar Shany, "Pressure Distribution on Downstream Face of a Submerged Weir," State University of Iowa Thesis, June 1950.
"Spillway and Lock Approach, Jim Woodruff Dam, Apalachicola River, Florida; Model Investigation," Waterways Experiment Station, Technical Memorandum No. 2-340, Vicksburg, Miss., May 1952.
"Morgantown Spillway, Special Tests," Waterways Experiment Station, Vicksburg, Miss., 1949, unpublished.

SUBMERGED CREST COEFFICIENTS
OVERFLOW CRESTS
HYDRAULIC DESIGN CHART III-4

WES 4-1-53
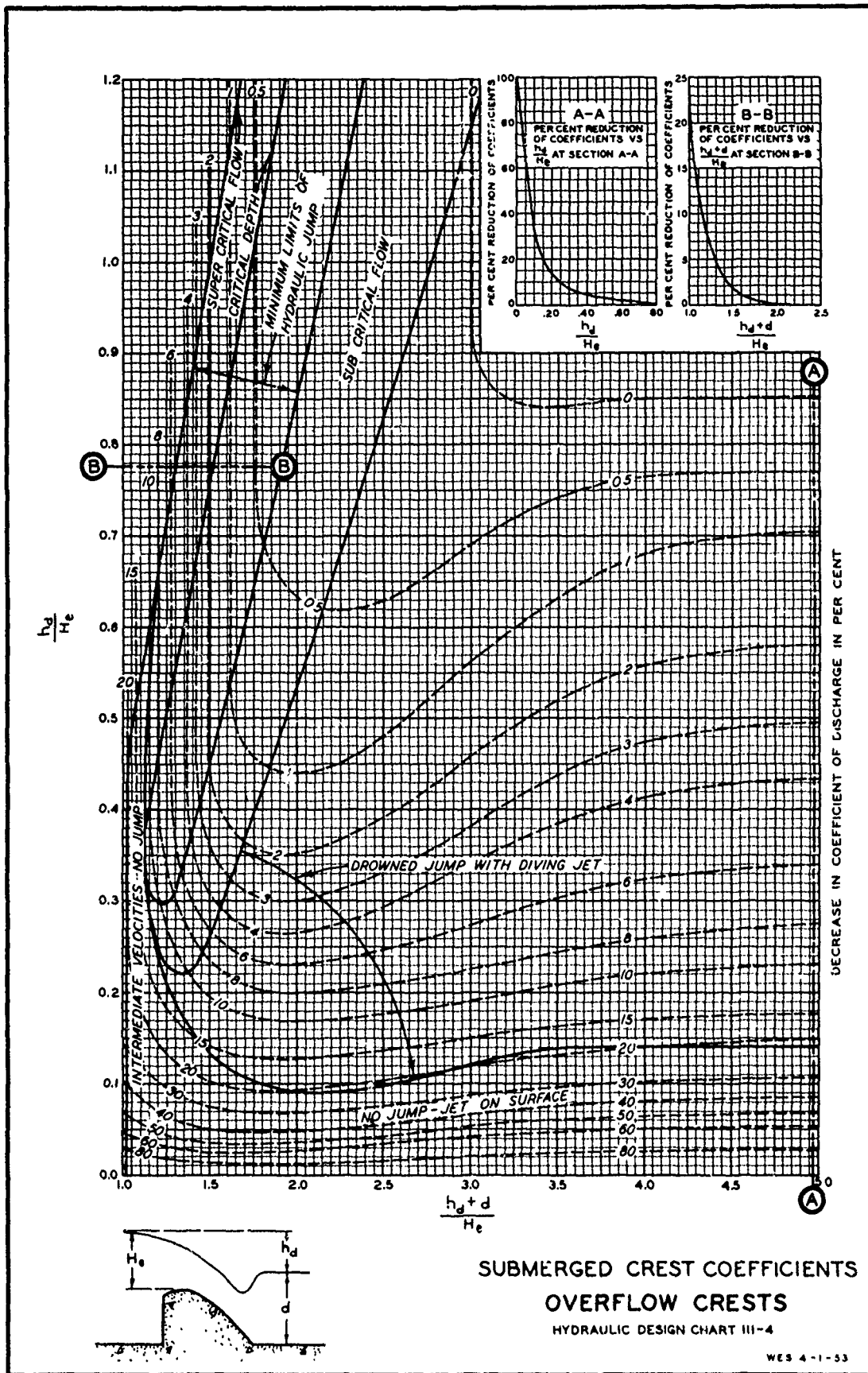
HYDRAULIC DESIGN CRITERIA

SHEETS 111-5 AND 111-6

GATED OVERFLOW SPILLWAYS

PIER CONTRACTION COEFFICIENTS

1. **General.** The basic equation for computing flow over a spillway crest is given in Hydraulic Design Criteria (HDC) Sheet 111-3. The crest length L to be used in the equation is defined in paragraph 1 of Sheet 111-3/1. The length L includes both abutment and pier effects which result in a reduction of the net crest length. The net crest length is the gross spillway width less the combined thicknesses of the crest piers.

2. Abutment effects are described in Sheets 111-3/1 and 111-3/2, and design criteria are given in Hydraulic Design Charts 111-3/1 and 111-3/2. Design criteria for the effects of piers are given in HDC 111-5, 111-6, and 122-2. Both abutment and pier effects increase proportionally with skewness of flow and with velocity of approach. In such cases, increasing the contraction coefficients is recommended.

3. When spillways are operated with one or more bays closed, the piers adjacent to these bays produce abutment-type effects and result in greater flow contractions than when the flow is evenly divided around the piers. HDC 111-3/1 should be used to estimate contraction coefficients when piers function essentially as abutments because of closed bays.

4. **Previous Criteria.** Many gated spillways have been designed according to Creager and Justin[1] who recommended a coefficient K_p of 0.1 for thick, blunt piers to 0.04 for thin or pointed piers. The research of Escande and Sabathe[2] indicated that the coefficient can be smaller than 0.04, and their observations were verified in general by the Center Hill spillway model tested at the U. S. Army Engineer Waterways Experiment Station (WES). The data for types 1, 2, 3, and 4 piers presented in the accompanying charts are based on results of tests conducted in 1949 at the WES under Corps of Engineers Engineering Studies Item 801, General Spillway Investigation. The type 3A pier coefficient curve results from 1969 studies.[3]

5. **1949 Tests.** The 1949 tests were made with a standard spillway crest shape essentially as defined in Chart 111-2/1, but without the short radius of 0.04 H_d. A model design head of 0.75 ft was used. The spillway crest shape was installed in a glass flume having parallel sidewalls to eliminate the effects of end or abutment contraction. The piers were 0.2 ft thick and the clear distance between piers was 1.0 ft. Thus the prototype design head would be 30 ft, the pier thickness 8 ft, and the clear span 40 ft if a 1:40-scale ratio was adopted. Tests for other ratios of pier thickness to gate width were not made. Type 4 pier

(Chart 111-5) resulted in the most favorable pier contraction coefficient curve. However, type 4 pier and type 1 pier are the least desirable from the standpoint of development of negative pressures and are not recommended for high heads unless a thorough investigation of pressure conditions is made.

6. 1969 Tests.[3] The 1969 tests were similar to the 1949 tests except the upstream quadrant of the spillway terminated with the short radius $(R = 0.04 H_d)$ shown in Chart 111-2/1 to eliminate a surface discontinuity at the spillway vertical face. A design head of 1.0 ft was used. Tests were limited to type 3A pier shape.

7. Application. Chart 111-5 gives the contraction coefficients for five different pier-nose shapes plotted against the ratio of H_e/H_d . In each case the pier nose was at the plane of the upstream face of the spillway. Types 2, 3, and 3A are recommended for general use with high heads. Chart 111-6 represents tests on pier type 2 nose shape located at variable distances upstream from the crest. Similar data are not available for the other three nose shapes. The noses of pier types 2A, 2B, and 2C were 0.133 H_d , 0.267 H_d , and 0.533 H_d upstream from the spillway face, respectively. The data apply to the condition of adjacent gates being open.

8. References.

(1)   Creager, W. P. and Justin, J. D., Hydroelectric Handbook, 1st ed., John Wiley & Sons, New York, 1927, p 132.

(2)   Escande, L. and Sabathe, G., "On the use of aerodynamic profiles for piers of overfall weirs, movable dams and bridges." Revue General de l'Hydraulique (July-August 1936).

(3)   U. S. Army Engineer Waterways Experiment Station, CE, Investigations of Various Shapes of the Upstream Quadrant of the Crest of a High Spillway; Hydraulic Laboratory Investigation, by E. S. Melsheimer and T. E. Murphy. Research Report H-70-1, V cksburg, Miss., January 1970.
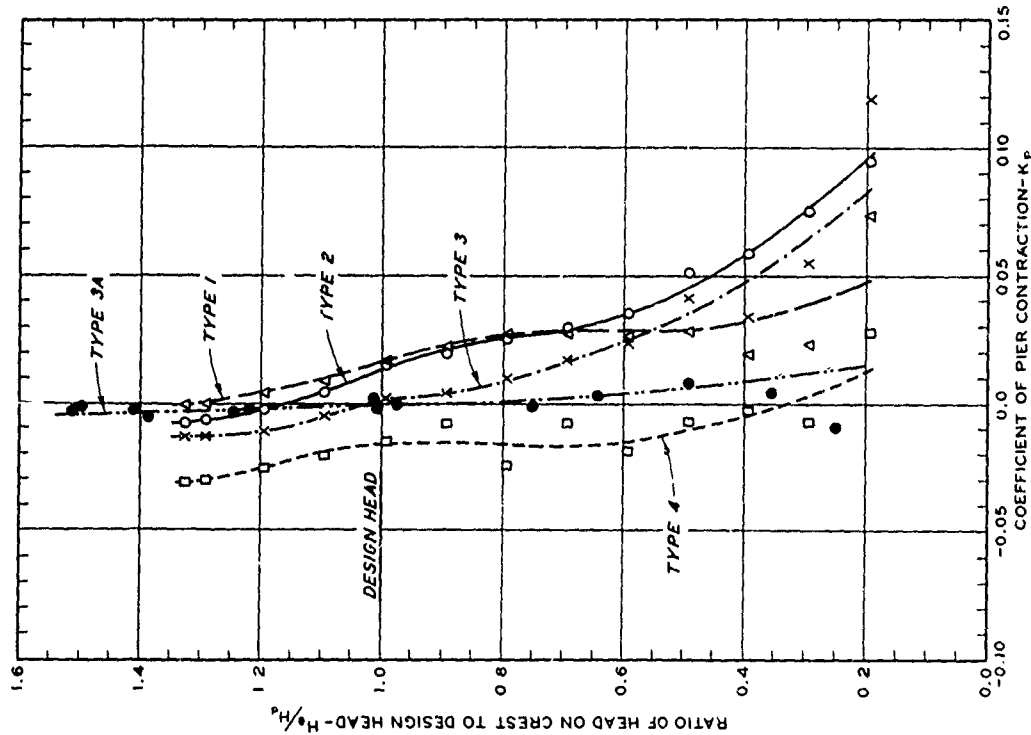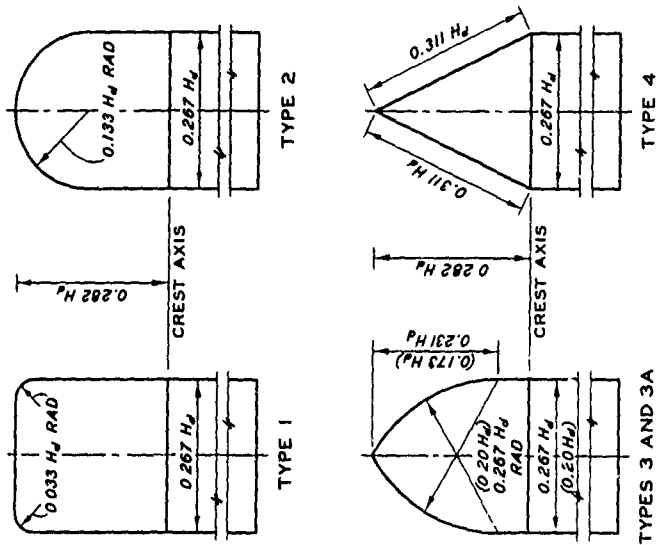
PIER NOSE SHAPES

NOTE: PIER NOSE LOCATED IN SAME PLANE
AS UPSTREAM FACE OF SPILLWAY.
DIMENSIONS IN PARENTHESES ARE FOR
TYPE 3A.

HIGH GATED OVERFLOW CRESTS
PIER CONTRACTION COEFFICIENTS
EFFECT OF NOSE SHAPE
HYDRAULIC DESIGN CHART III-5

WES 4-53

REV 9-70
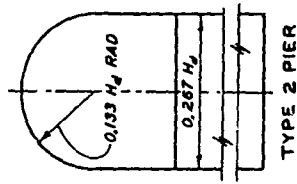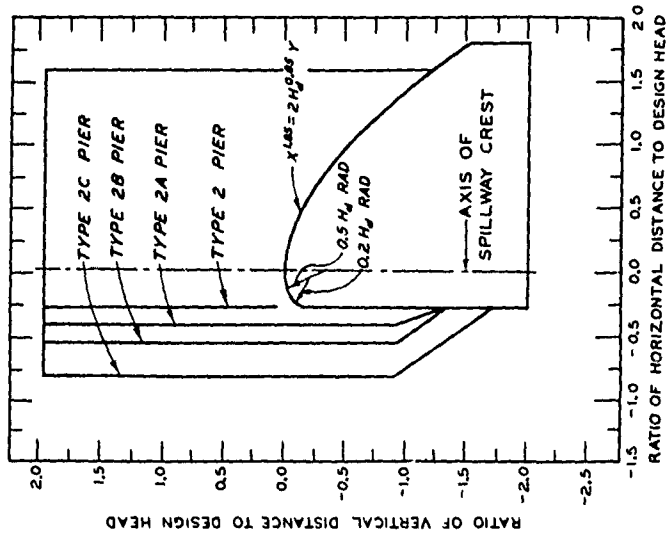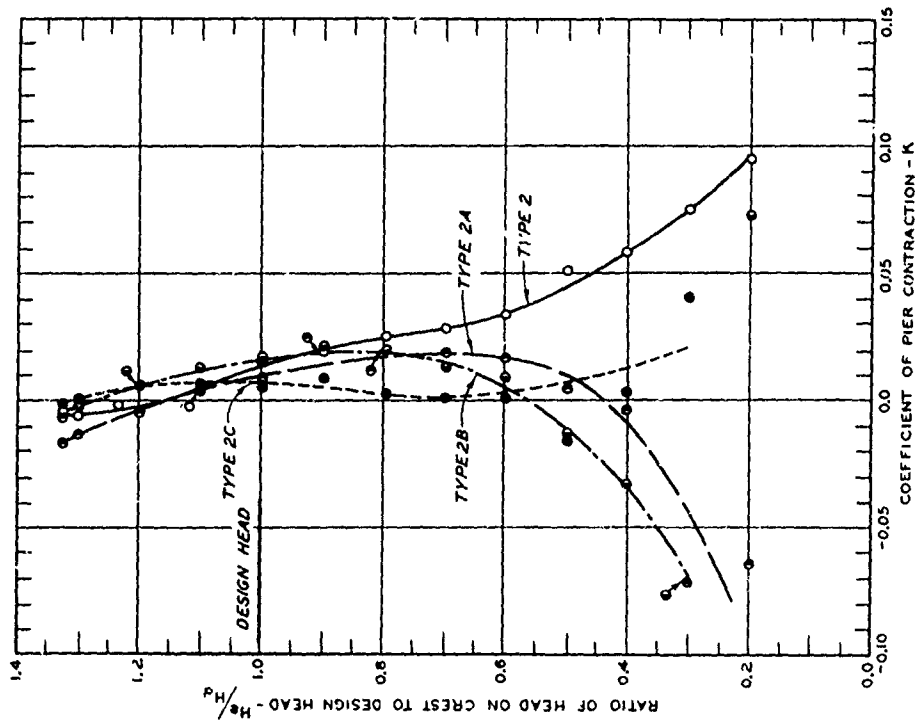
HIGH GATED OVERFLOW CRESTS
PIER CONTRACTION COEFFICIENTS
EFFECT OF PIER LENGTH

HYDRAULIC DESIGN CHART III-6

WES 4-1-53

CHART III-6

HYDRAULIC DESIGN CRITERIA

SHEETS 111-7 to 111-10

OVERFLOW SPILLWAY CRESTS WITH SLOPING UPSTREAM FACES

1. HDC 111-7 to 111-10 supplement HDC 111-1 and 111-2. These charts present suggested shapes for spillway crests with sloping upstream faces and negligible velocity of approach flows, and are based on Bureau of Reclamation data.[1,2]

2. **Crest Shapes.**

a. **3-on-1 and 3-on-2 Upstream Face Slopes.** The crest shapes presented in HDC 111-7 and 111-8 apply to spillways with upstream faces sloped 3 on 1 and 3 on 2, respectively. Equations for the downstream face of the spillway result from the best fit of the general equation $X^n = KH_d^{n-1}Y$ to the experimental data published by the Bureau of Reclamation (USBR).[1] Because the derived equations involve powers for which tables are not available, each chart contains tables of functions necessary for solution of the equations. The shape of the crest upstream from the axis results from fitting circular arcs to the experimental data.

b. **3-on-3 Upstream Face Slope.** The downstream quadrant crest shape presented in HDC 111-9 applies to spillways with 3-on-3 upstream face slopes. The equation for the downstream shape is based on curves published by the USBR[2] and reproduced in HDC 122-3/1. The published curves have been confirmed by an independent WES study of the USBR data for weirs sloping 45 degrees downstream. Tables of functions necessary for solution of the equation are included in HDC 111-9. A tabulation of the slope of the downstream crest shape is given to aid in locating the beginning of the toe curve or the sloping tangent face. A WES study to determine equations for upstream quadrant shapes of spillways having 45-degree sloping upstream faces is summarized in paragraph 5 of HDC Sheets 122-3 to 122-3/5, and the general results are presented in HDC 122-3/4. The upstream quadrant coordinates listed below are based on this study and have their origins at the apex of the spillway. The X and Y coordinates are considered positive to the right and downward, respectively.

Upstream Quadrant Coordinates

X/H_d	Y/H_d	X/H_d	Y/H_d
-0.000	0.0000	-0.150	0.0239
-0.020	0.0004	-0.155	0.0257
-0.040	0.0016	-0.160	0.0275
-0.060	0.0036	-0.165	0.0293
-0.080	0.0065	-0.170	0.0313
-0.100	0.0103	-0.175	0.0333
-0.110	0.0125	-0.180	0.0354
-0.120	0.0150	-0.185	0.0376
-0.130	0.0177	-0.190	0.0399
-0.140	0.0207	-0.195	0.0424
-0.145	0.0223	-0.200	0.0450

3. <u>Intermediate Shapes.</u> HDC 111-1C shows computed values of n and K for the equation $X^n = KH_d^{n-1}Y$ for the vertical and sloping weirs shown in HDC 111-1 and 111-7 to 111-9. Values of n and K which apply to intermediate slopes can be approximated using the curves shown in HDC 111-10. Upstream quadrant data for intermediate slopes are not presently available. However, the circular arcs given in HDC 111-7 and 111-8 and the coordinates given in the above tabulation should serve for interpolating the approximate shape for design purposes.

4. The crest shapes defined in HDC 111-7 to 111-10 have not been studied in a model to determine pressure and discharge coefficients.

5. <u>Application.</u> The shapes shown are intended for use with overflow dams with negligible velocity of approach flows. Model tests of spillways with vertical faces have shown that pressures and discharge coefficients are approximately the same for approach depth-design head ratios P/H_d greater than 1. It is therefore suggested that the shapes in HDC 111-7 to 111-9 be used in this range, unless in a particular case it is especially desired to keep pressures as close to atmospheric pressure as possible. In the latter case, the USBR data[1,2] or appropriate charts in the HDC 122-3 series should be used to develop a more suitable shape. For P/H_d ratios less than 1, it is necessary to use the USBR data or the data in HDC 122-3/2 to 122-3/5 to avoid excessive negative pressures.

6. <u>References.</u>

(1) U. S. Bureau of Reclamation, <u>Studies of Crests for Overfall Dams, Boulder Canyon Project.</u> Final Reports, Part VI-Hydraulic Investigations, Bulletin 3, Denver, Colo., 1948.

(2) _____, <u>Design of Small Dams.</u> U. S. Government Printing Office, 1960.
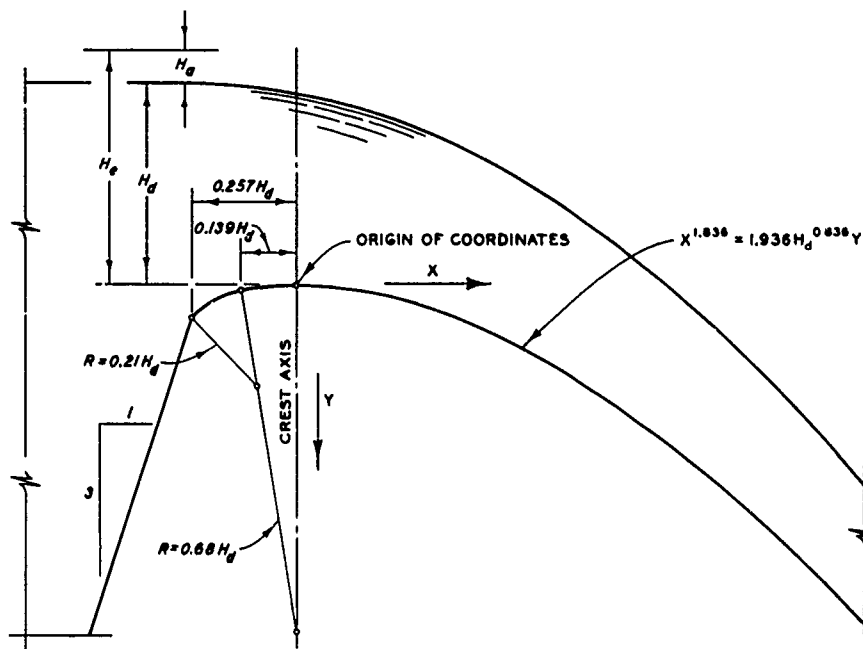
$$X^{1.836} = 1.936 H_d^{0.836} Y$$

X	$X^{1.836}$	X	$X^{1.836}$	H_d	$1.936 \times H_d^{0.836}$	H_d	$1.936 \times H_d^{0.836}$	H_d	$1.936 \times H_d^{0.836}$
.10	.0146	6	26.834	1	1.936	26	29.500	51	51.812
.15	.0307	7	35.612	2	3.456	27	30.446	52	52.660
.20	.0521	8	45.507	3	4.851	28	31.386	53	53.506
.25	.0785	9	56.492	4	6.169	29	32.320	54	54.348
.30	.1097	10	68.549	5	7.434	30	33.249	55	55.188
.35	.1455	12	95.803	6	8.659	31	34.173	56	56.026
.40	.1859	14	127.143	7	9.849	32	35.092	57	56.861
.45	.2308	16	162.467	8	11.013	33	36.007	58	57.694
.50	.2801	18	201.688	9	12.152	34	36.917	59	58.525
.60	.3915	20	244.732	10	13.271	35	37.822	60	59.353
.70	.5195	25	368.653	11	14.372	36	38.724	61	60.178
.80	.6639	30	515.221	12	15.456	37	39.621	62	61.002
.90	.8241	35	683.768	13	16.526	38	40.514	63	61.824
1.00	1.000	40	873.740	14	17.582	39	41.403	64	62.643
1.20	1.398	45	1084.673	15	18.626	40	42.289	65	63.460
1.40	1.855	50	1316.161	16	19.659	41	43.171	66	64.275
1.60	2.370	55	1567.855	17	20.681	42	44.050	67	65.089
1.80	2.942	60	1839.441	18	21.693	43	44.925	68	65.899
2.00	3.570	65	2130.631	19	22.696	44	45.797	69	66.709
2.50	5.378	70	2441.180	20	23.690	45	46.665	70	67.516
3.00	7.517	75	2770.847	21	24.676	46	47.530	71	68.321
3.50	9.975	80	3119.415	22	25.655	47	48.393	72	69.125
4.00	12.746	90	3872.480	23	26.626	48	49.252	73	69.927
4.50	15.823	100	4698.941	24	27.591	49	50.108	74	70.727
5.00	19.200			25	28.548	50	50.962	75	71.525

NOTE: EQUATION BASED ON DATA FOR NEGLIGIBLE VELOCITY OF APPROACH PUBLISHED IN BULLETIN 3, BOULDER CANYON REPORT, USBR, 1948.

OVERFLOW SPILLWAY CREST
3 ON 1 UPSTREAM FACE
HYDRAULIC DESIGN CHART III-7

Figure (schematic): Overflow spillway crest geometry with labels: H_e, H_0, H_d, $0.214H_d$, $0.115H_d$, ORIGIN OF COORDINATES, X, Y, CREST AXIS, $R=0.22H_d$, $R=0.48H_d$, slope 3-on-2, and equation $X^{1.810} = 1.939 H_d^{0.810} Y$
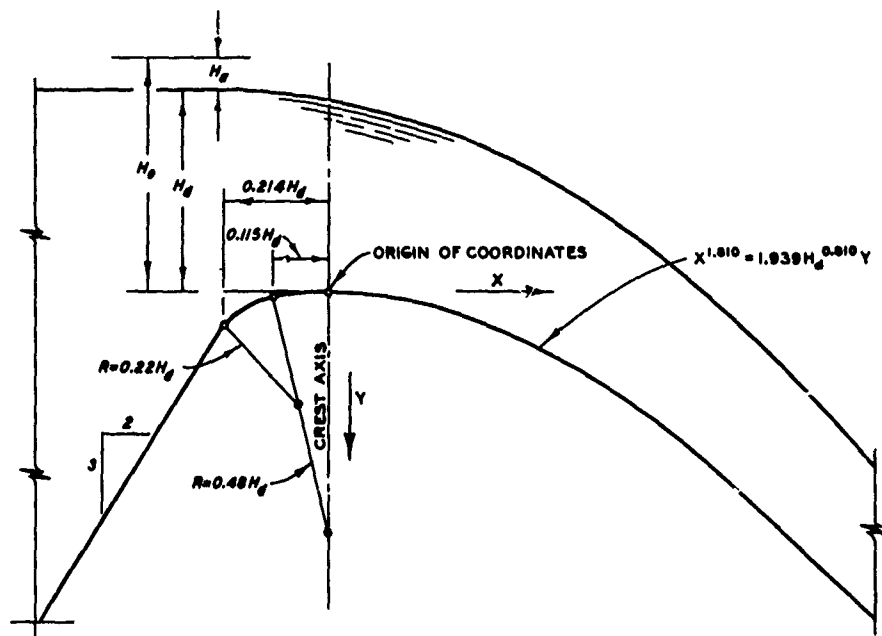
X	$X^{1.810}$	X	$X^{1.810}$	H_d	$1.939 \times H_d^{0.810}$	H_d	$1.939 \times H_d^{0.810}$	H_d	$1.939 \times H_d^{0.810}$
.10	.0155	6	25.613	1	1.939	26	27.146	51	46.850
.15	.0323	7	33.855	2	3.399	27	27.989	52	47.593
.20	.0543	8	43.111	3	4.721	28	28.825	53	48.333
.25	.0813	9	53.355	4	5.960	29	29.657	54	49.070
.30	.1131	10	64.565	5	7.141	30	30.482	55	49.805
.35	.1495	12	89.809	6	8.277	31	31.303	56	50.537
.40	.1904	14	118.711	7	9.378	32	32.118	57	51.267
.45	.2357	16	151.167	8	10.449	33	32.929	58	51.994
.50	.2852	18	187.087	9	11.495	34	33.735	59	52.719
.60	.3967	20	226.394	10	12.519	35	34.536	60	53.442
.70	.5244	25	339.056	11	13.524	36	35.333	61	54.162
.80	.6677	30	471.617	12	14.512	37	36.126	62	54.880
.90	.8284	35	623.395	13	15.484	38	36.915	63	55.596
1.00	1.000	40	793.832	14	16.442	39	37.700	64	56.310
1.20	1.391	45	982.459	15	17.386	40	38.481	65	57.021
1.40	1.839	50	1169.874	16	18.320	41	39.258	66	57.731
1.60	2.341	55	1412.721	17	19.242	42	40.032	67	58.438
1.80	2.898	60	1653.689	18	20.153	43	40.804	68	59.144
2.00	3.506	65	1911.496	19	21.056	44	41.569	69	59.847
2.50	5.251	70	2185.885	20	21.949	45	42.333	70	60.549
3.00	7.304	75	2476.829	21	22.834	46	43.093	71	61.249
3.50	9.655	80	2783.511	22	23.710	47	43.851	72	61.947
4.00	12.295	90	3444.918	23	24.580	48	44.605	73	62.643
4.50	15.217	100	4168.694	24	25.442	49	45.356	74	63.337
5.00	18.413			25	26.297	50	46.105	75	64.029

NOTE: EQUATION BASED ON DATA FOR NEGLIGIBLE VELOCITY OF APPROACH PUBLISHED IN BULLETIN 3, BOULDER CANYON REPORT USBR, 1948.

OVERFLOW SPILLWAY CREST
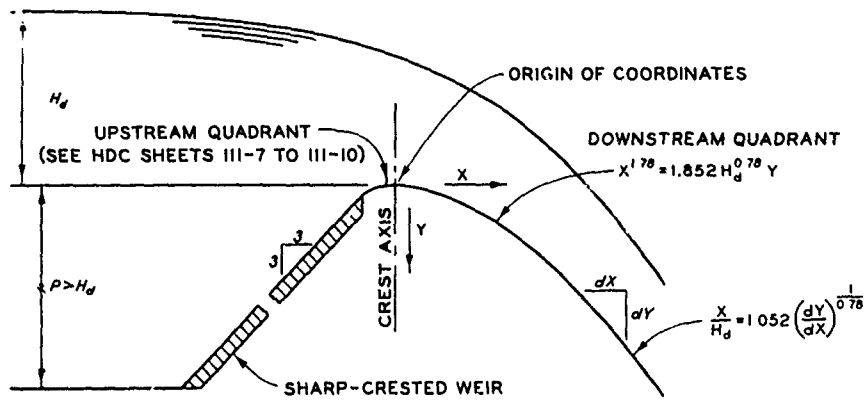### 3-ON-2 UPSTREAM FACE
HYDRAULIC DESIGN CHART III-8

WES 2-54

ORIGIN OF COORDINATES

UPSTREAM QUADRANT
(SEE HDC SHEETS III-7 TO III-10)

DOWNSTREAM QUADRANT

$X^{1.78} = 1.852 H_d^{0.78} Y$

H_d

$P > H_d$

CREST AXIS

$\dfrac{X}{H_d} = 1.052 \left(\dfrac{dY}{dX}\right)^{\frac{1}{0.78}}$

SHARP-CRESTED WEIR

NOTE: EQUATION BASED ON USBR
CURVES, HDC 122-3/1,
$h_a/H_d = 0.00$.

DOWNSTREAM QUADRANT DATA | | | | | | | | SLOPE DATA

X	$X^{1.78}$	X	$X^{1.78}$	H_d	$1.852 \times H_d^{0.78}$	H_d	$1.852 \times H_d^{0.78}$	$\frac{dY}{dX}$	$\frac{X}{H_d}$
0.10	0.0165	6	24.272	1	1.852	26	23.512	1.00	1.052
0.15	0.0341	7	31.936	2	3.180	27	24.214	1.05	1.120
0.20	0.0569	8	40.504	3	4.363	28	24.911	1.10	1.189
0.25	0.0847	9	49.952	4	5.460	29	25.602	1.15	1.258
0.30	0.1172	10	60.256	5	6.498	30	26.288	1.20	1.329
0.35	0.1543	12	83.357	6	7.40?	31	26.969	1.25	1.400
0.40	0.1957	14	109.675	7	8.449	32	27.645	1.30	1.473
0.45	0.2413	16	139.102	8	9.376	33	28.317	1.35	1.546
0.50	0.2911	18	171.548	9	10.278	34	28.984	1.40	1.619
0.60	0.4028	20	206.935	10	11.159	35	29.647	1.45	1.694
0.70	0.5299	25	307.846	11	12.020	36	30.306	1.50	1.769
0.80	0.6722	30	425.869	12	12.864	37	30.960	1.55	1.845
0.90	0.8289	35	560.326	13	13.692	38	31.611	1.60	1.922
1.00	1.0000	40	710.668	14	14.507	39	32.258	1.65	1.999
1.20	1.383	45	876.432	15	15.309	40	32.901	1.70	2.077
1.40	1.820	50	1057.223	16	16.100	41	33.541	1.75	2.156
1.60	2.309	55	1252.696	17	16.879	42	34.178	1.80	2.235
1.80	2.847	60	1462.545	18	17.649	43	34.811		
2.00	3.434	65	1686.498	19	18.409	44	35.440		
2.50	5.109	70	1924.308	20	19.161	45	36.067		
3.00	7.068	75	2175.750	21	19.904	46	36.691		
3.50	9.300	80	2440.620	22	20.639	47	37.311		
4.00	11.794	90	3009.897	23	21.368	48	37.929		
4.50	14.546	100	3630.780	24	22.089	49	38.544		
5.00	17.546			25	22.803	50	39.156		

OVERFLOW SPILLWAY CREST

3-ON-3 UPSTREAM FACE

HYDRAULIC DESIGN CHART III-9

TANGENT β

3 ON 3

3 ON 2

n CURVE

K CURVE

3 ON 1

VERTICAL

VALUES OF n AND K

$X^n = K H_d^{n-1} Y$
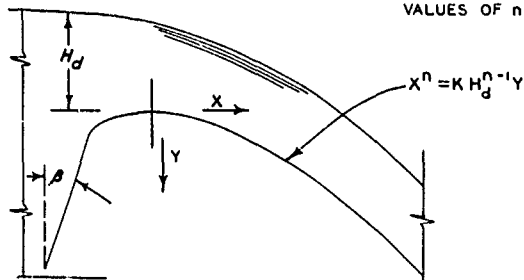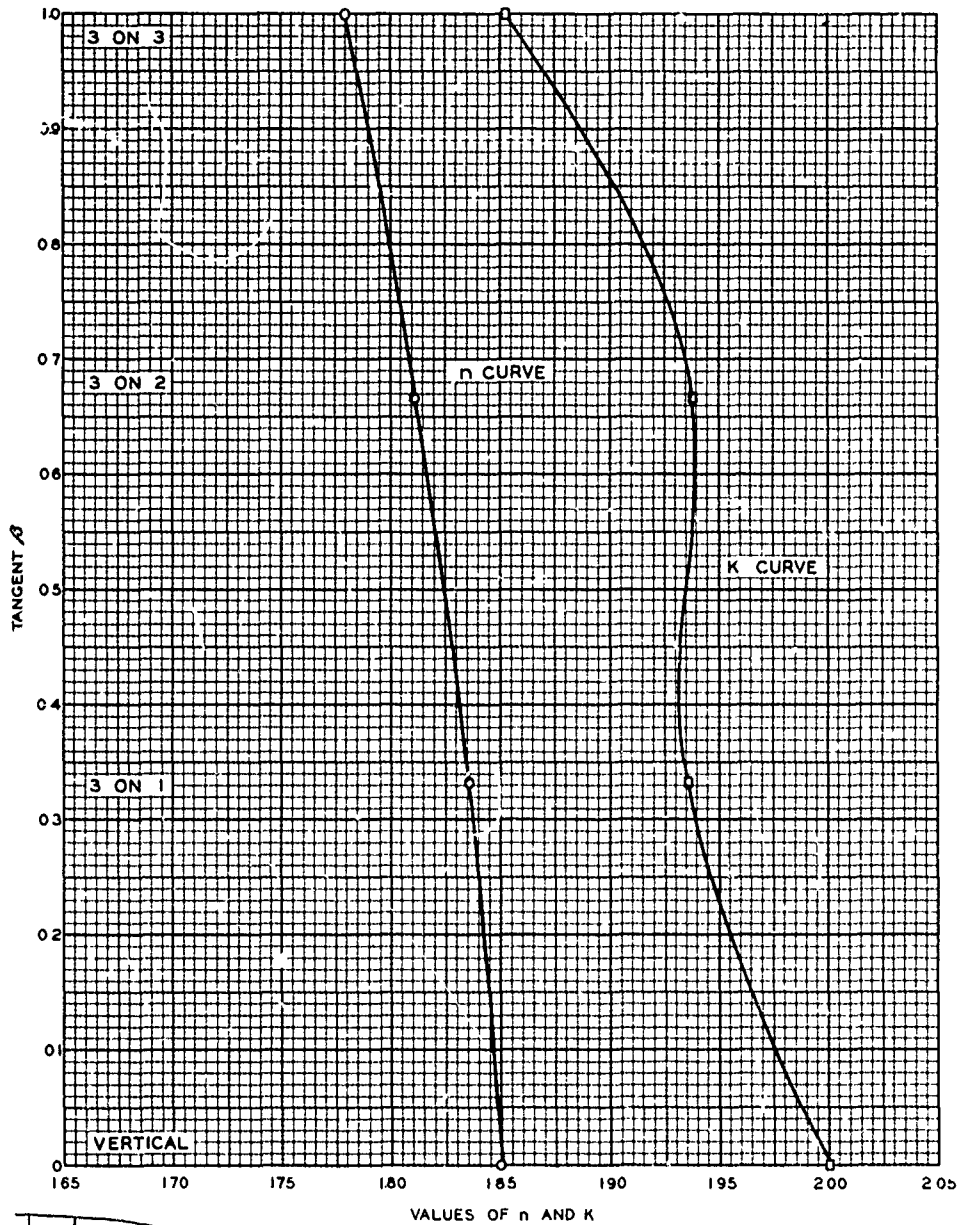
NEGLIGIBLE VELOCITY OF APPROACH FLOW

OVERFLOW SPILLWAY CREST

n AND K CURVES

HYDRAULIC DESIGN CHART III-10

REVISED 1-64   WES 2-54

HYDRAULIC DESIGN CRITERIA

SHEETS 111-11 TO 111-14/1

OVERFLOW SPILLWAY CRESTS

UPPER NAPPE PROFILES

1. The shapes of upper nappe profiles for overflow spillway crests are used in the design of spillway abutment walls and in the selection of trunnion elevations for tainter gates. Hydraulic Design Charts 111-11 to 111-14/1 give nappe profile data for spillways without and with abutments and piers and for a sampling of irregular approach flow conditions.

2. Charts 111-11 to 111-12/1 present tabulated coordinates of upper nappe profiles in terms of the design head (H_d) for gated and ungated spillways with head ratios (H/H_d) of 0.50, 1.00, and 1.33. Chart 111-11 is applicable to standard spillway crests of high overflow dams without piers or abutment effects. Charts 111-12 and 12/1 are applicable to center bays of gated spillways without abutment effects. Profiles for intermediate head ratios may be obtained by plotting Y/H_d vs H/H_d for a given X/H_d. The profile coordinates are based on investigations for negligible velocity of approach conducted under CW 801, "General Spillway Tests."

3. Charts 111-13 and 13/1 present graphically upper nappe profiles for three gate bays adjacent to abutments and show the abutment effects on the nappe profiles, based on Pine Flat Dam model test data.[1] The observations were not in sufficient detail to justify definition of the shapes by tabular coordinates.

4. Charts 111-14 and 14/1 present graphically upper nappe profiles along left and right abutments for varying abutment radii and the effects of approach channel irregularities near the abutment (i.e., a water-quality control tower, a power house, and a relatively shallow and irregular approach channel). Chart 111-14 is based on Rowlesburg Dam[2] model test data and Chart 111-14/1 is based on Alum Creek Dam[3] and Clarence Cannon Dam[4] model test data. The observations were not in sufficient detail to justify definition of the shapes by tabular coordinates.

5. References.

(1)   U. S. Army Engineer Waterways Experiment Station, CE, Spillway and Conduits for Pine Flat Dam, Kings River, California, Technical Manual No. 2-375, Vicksburg, Miss., December 1953.

(2) U. S. Army Engineer Waterways Experiment Station , CE, Spillway and Outlet Works, Rowlesburg Dam, Cheat River, West Virginia; Hydraulic Model Investigation, by J. H. Ables, Jr. and M. B. Boyd. Technical Report H-70-7, Vicksburg, Miss., June 1970.

(3) U. S. Army Engineer Waterways Experiment Station, CE, Spillway for Alum Creek Dam, Alum Creek, Ohio; Hydraulic Model Investigation, by G. A. Pickering. Technical Report H-70-4, Vicksburg, Miss., April 1970.

(4) U. S. Army Engineer Waterways Experiment Staiton, CE, Spillway for Clarence Cannon Reservoir, Salt River, Missouri; Hydraulic Model Investigation, by B. P. Fletcher. Technical Report H-71-7, Vicksburg, Miss., October 1971.

NO PIERS

$H/H_d = 1.33$

$H/H_d = 1.00$

$H/H_d = 0.50$

ORIGIN OF COORDINATES

X/H_d

Y/H_d

CREST AXIS

$X^{1.85} = 2.0\, H_d^{0.85}\, Y$
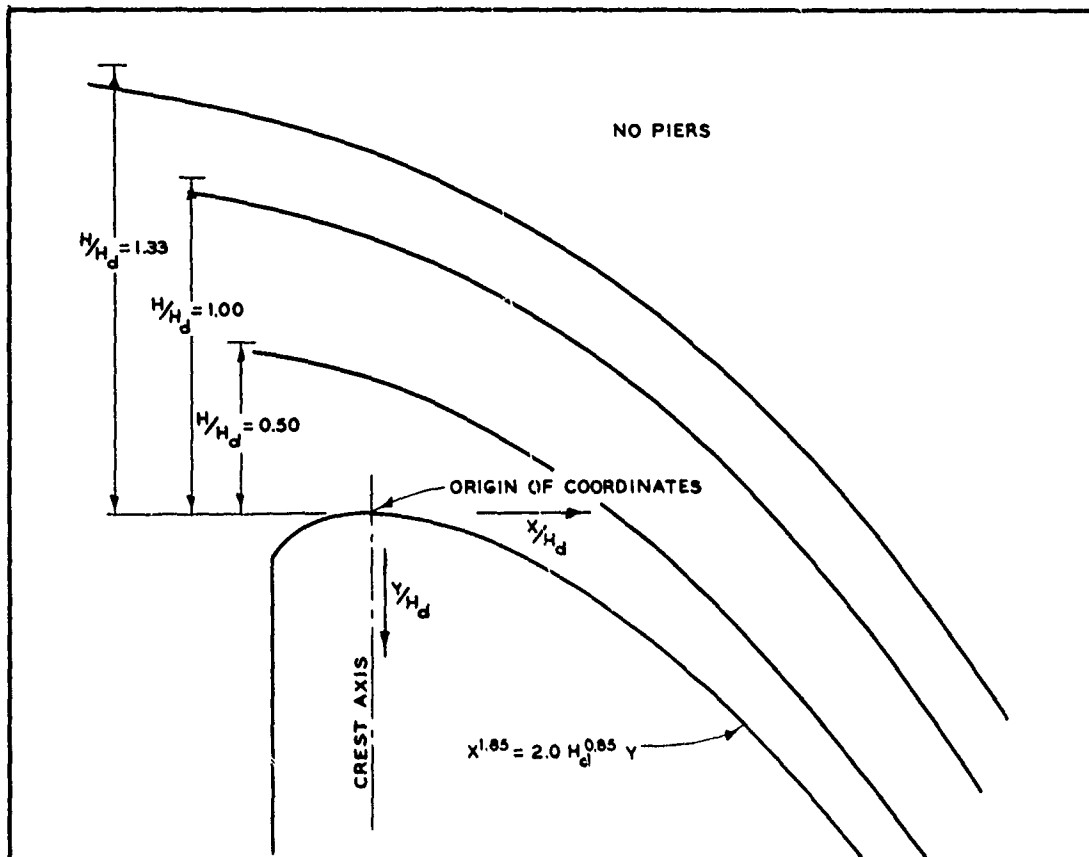
COORDINATES FOR UPPER NAPPE WITH NO PIERS*

$H/H_d = 0.50$		$H/H_d = 1.00$		$H/H_d = 1.33$	
X/H_d	Y/H_d	X/H_d	Y/H_d	X/H_d	Y/H_d
-1.0	-0.490	-1.0	-0.933	-1.0	-1.210
-0.8	-0.48^	-0.8	-0.915	-0.8	-1.185
-0.6	-0.475	-0.6	-0.893	-0.6	-1.151
-0.4	-0.460	-0.4	-0.865	-0.4	-1.110
-0.2	-0.425	-0.2	-0.821	-0.2	-1.060
0.0	-0.371	0.0	-0.755	0.0	-1.000
0.2	-0.300	0.2	-0.631	0.2	-0.919
0.4	-0.200	0.4	-0.588	0.4	-0.821
0.6	-0.075	0.6	-0.465	0.6	-0.705
0.8	0.075	0.8	-0.320	0.8	-0.569
1.0	0.258	1.0	-0.145	1.0	-0.411
1.2	0.470	1.2	0.055	1.2	-0.220
1.4	0.705	1.4	0.294	1.4	-0.002
1.6	0.972	1.6	0.563	1.6	0.243
1.8	1.269	1.8	0.857	1.8	0.531

*BASED ON ES 801 TESTS FOR
NEGLIGIBLE VELOCITY OF APPROACH

OVERFLOW SPILLWAY CREST
UPPER NAPPE PROFILES
WITHOUT PIERS

HYDRAULIC DESIGN CHART 111-11

TYPE 2 PIER
(CHART III-5)

LEGEND
——— ℄ OF BAY
- - - - ℄ WITHOUT PIERS

$H/H_d = 1.33$

$H/H_d = 1.00$

$H/H_d = 0.50$

ORIGIN OF COORDINATES

X/H_d

CREST AXIS

Y/H_d

$X^{1.85} = 2.0 H_d^{0.85} Y$
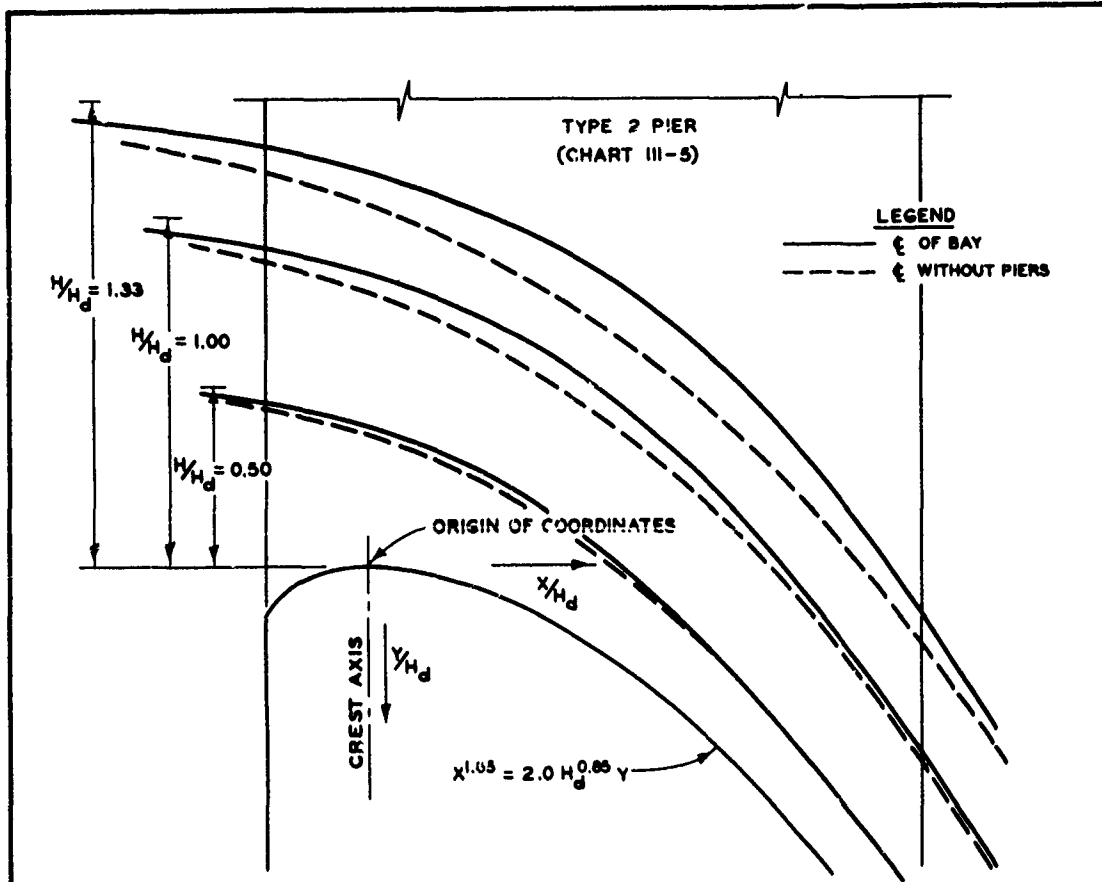
COORDINATES FOR UPPER NAPPE AT ℄ OF BAY WITH TYPE 2 PIERS*

$H/H_d = 0.50$		$H/H_d = 1.00$		$H/H_d = 1.33$	
X/H_d	Y/H_d	X/H_d	Y/H_d	X/H_d	Y/H_d
-1.0	-0.482	-1.0	-0.941	-1.0	-1.230
-0.8	-0.480	-0.8	-0.932	-0.8	-1.215
-0.6	-0.472	-0.6	-0.913	-0.6	-1.194
-0.4	-0.457	-0.4	-0.890	-0.4	-1.165
-0.2	-0.431	-0.2	-0.855	-0.2	-1.122
0.0	-0.384	0 0	-0.805	0.0	-1.071
0.2	-0.313	0.2	-0.735	0.2	-1.015
0.4	-0.220	0.4	-0.647	0.4	-0.944
0.6	-0.088	0.6	-0.539	0.6	-0.847
0.8	0.075	0.8	-0.389	0.8	-0.725
1.0	0.257	1.0	-0.202	1.0	-0.564
1.2	0.462	1.2	0.015	1.2	-0.356
1.4	0.705	1.4	0.266	1.4	-0.102
1.6	0.977	1.6	0.521	1.6	0.172
1.8	1.278	1.8	0.860	1.8	0.465

OVERFLOW SPILLWAY CREST

UPPER NAPPE PROFILES
CENTER LINE OF PIER BAY

HYDRAULIC DESIGN CHART III-12

*BASED ON CW 801 TESTS FOR
NEGLIGIBLE VELOCITY OF APPROACH

WES 9-54

TYPE 2 PIER
(CHART III-5)

——— ALONG PIERS
– – – ¢ OF BAY

$H/H_d = 1.33$

$H/H_d = 1.00$

$H/H_d = 0.50$

ORIGIN OF COORDINATES

X/H_d

Y/H_d

CREST AXIS

$X^{1.85} = 2.0 H_d^{0.85} Y$

COORDINATES FOR UPPER NAPPE ALONG PIERS*

$H/H_d = 0.50$		$H/H_d = 1.00$		$H/H_d = 1.33$	
X/H_d	Y/H_d	X/H_d	Y/H_d	X/H_d	Y/H_d
-1.0	-0.495	-1.0	-0.950	-1.0	-1.235
-0.8	-0.492	-0.8	-0.940	-0.8	-1.221
-0.6	-0.490	-0.6	-0.929	-0.6	-1.209
-0.4	-0.482	-0.4	-0.930	-0.4	-1.218
-0.2	-0.440	-0.2	-0.925	-0.2	-1.244
0.0	-0.383	0.0	-0.779	0.0	-1.103
0.2	-0.265	0.2	-0.651	0.2	-0.950
0.4	-0.185	0.4	-0.545	0.4	-0.821
0.6	-0.076	0.6	-0.425	0.6	-0.689
0.8	0.060	0.8	-0.285	0.8	-0.549
1.0	0.240	1.0	-0.121	1.0	-0.389
1.2	0.445	1.2	0.067	1.2	-0.215
1.4	0.675	1.4	0.286	1.4	0.011
1.6	0.925	1.6	0.521	1.6	0.208
1.8	1.177	1.8	0.779	1.8	0.438

*BASED ON ES 801 TESTS FOR
NEGLIGIBLE VELOCITY OF APPROACH

OVERFLOW SPILLWAY CREST
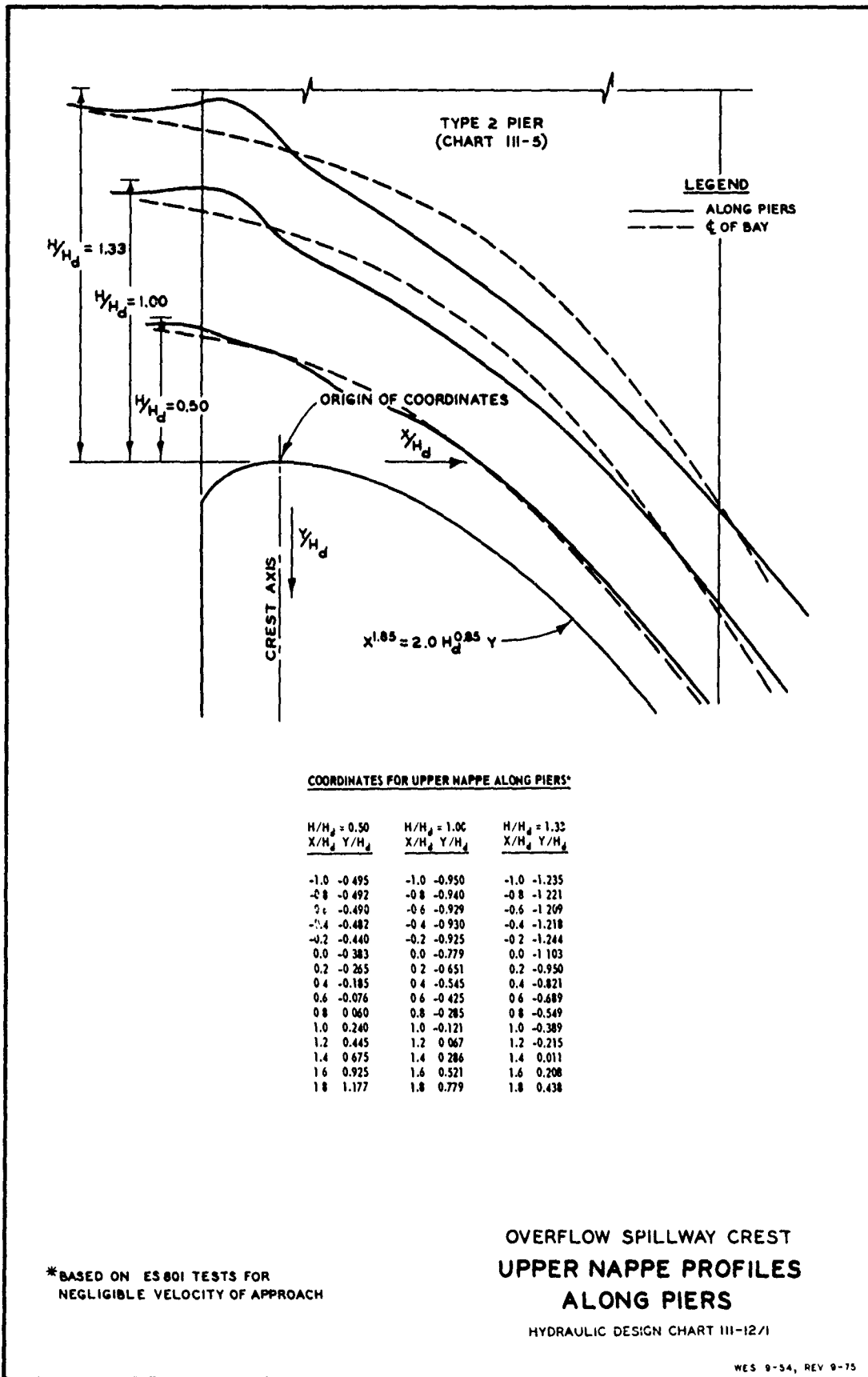**UPPER NAPPE PROFILES
ALONG PIERS**

HYDRAULIC DESIGN CHART III-12/1
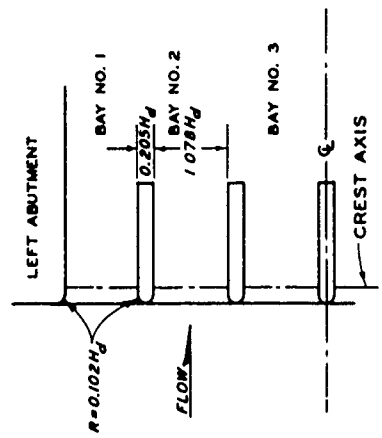
OVERFLOW SPILLWAY CREST
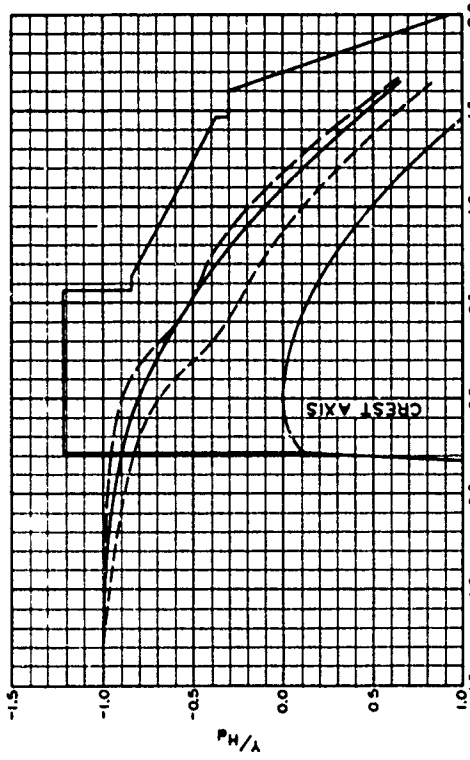UPPER NAPPE PROFILES
ABUTMENT EFFECTS
HYDRAULIC DESIGN CHART III-13

$H/H_d = 1.00$

LEGEND

——— LEFT SIDE OF BAY
——— ₵ OF BAY
——— RIGHT SIDE OF BAY

PROFILES ARE BASED ON PINE FLAT MODEL TESTS FOR SPILLWAY HAVING PIERS SIMILAR TO TYPE 2 (HYDRAULIC DESIGN CHART III-5).
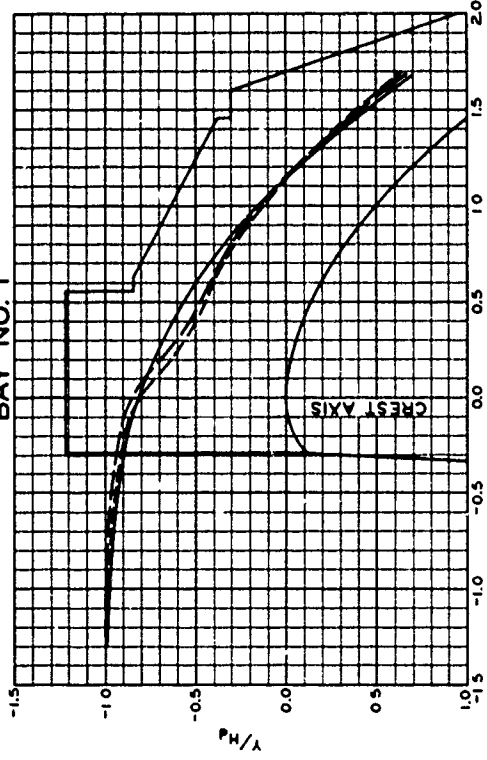
WES 9-54, REV 8-75

CHART III-13

OVERFLOW SPILLWAY CREST
UPPER NAPPE PROFILES
ABUTMENT EFFECTS
HYDRAULIC DESIGN CHART III-13/1

$H/H_d = 1.35$

WES 9-54, REV 9-73

CHART III-13/1

PROFILES ALONG ABUTMENTS
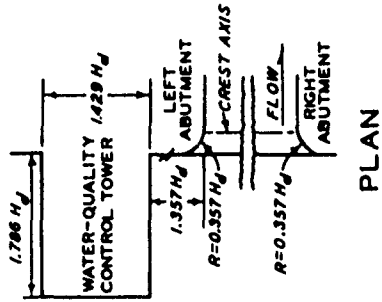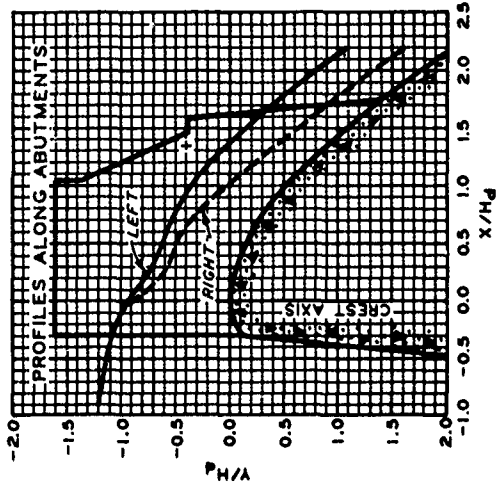
$H/H_d = 1.34$

NOTE: PROFILES BASED ON ROWLESBURG MODEL TESTS FOR SPILLWAYS HAVING SEVEN 1.607 H_d-WIDE BAYS SEPARATED BY 0.357 H_d-WIDE PIERS SIMILAR TO TYPE 3 (HYDRAULIC DESIGN CHART III-5).

OVERFLOW SPILLWAY CREST
UPPER NAPPE PROFILES
ALONG ABUTMENTS
APPROACH CHANNEL AND
ABUTMENT CURVATURE EFFECTS
HYDRAULIC DESIGN CHART III-14

WES 7-73

CHART III-14

PROFILES ALONG ABUTMENTS

$H/H_d = 1.14$

CREST AXIS

LEFT

RIGHT

X/H_d

P_H/λ

PROFILES ALONG ABUTMENTS

$H/H_d = 0.92$

LEFT

RIGHT

CREST AXIS

X/H_d

P_H/λ

PROFILES ALONG ABUTMENTS

$H/H_d = 1.35$

LEFT

RIGHT

CREST AXIS

X/H_d

P_H/λ

1V ON 4.5H

1V ON 2H

$R=0.160\ H_d$

CREST AXIS

$P/H_d = 1.12$

$\mathbb{C}$ SPILLWAY

$P/H_d = 1.12$

1V ON 2H

1V ON 4.5H

$P/H_d = 1.76$

2V ON 1H

P_H

$4.78\ H$

$R=0.240\ H_d$

FLOW
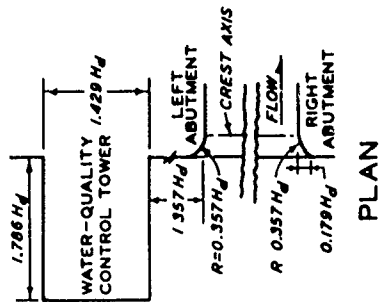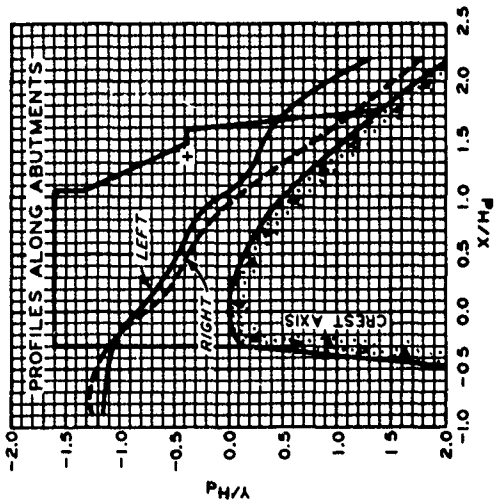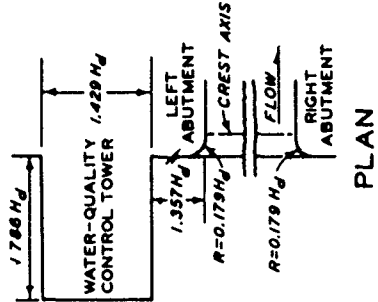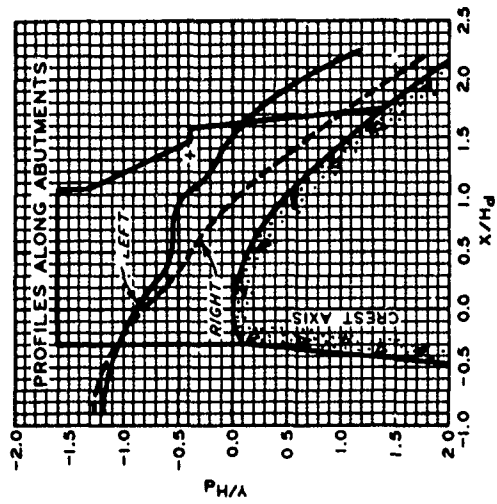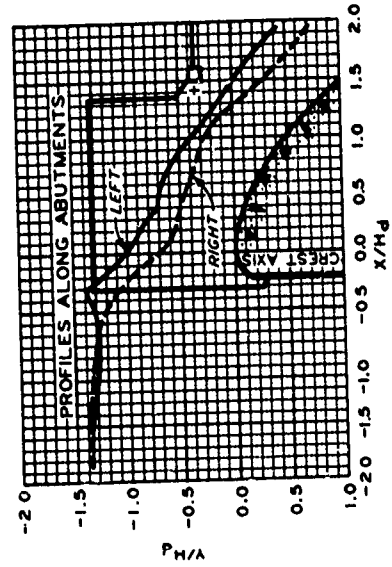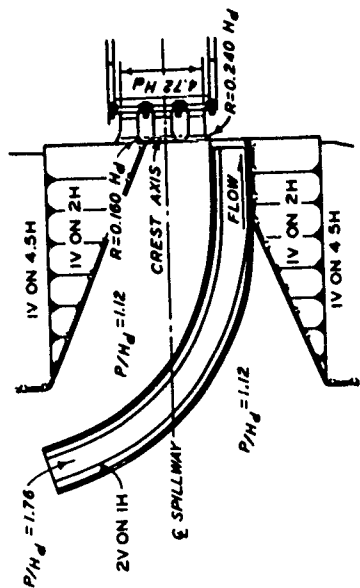
PLAN

NOTE: PROFILES BASED ON ALUM CREEK MODEL TESTS FOR SPILLWAY HAVING THREE 1.360 H_d -WIDE BAYS SEPARATED BY 0.320 H_d - WIDE PIERS SIMILAR TO TYPE 2 (HYDRAULIC DESIGN CHART III-5)

POWERHOUSE

$0.083\ H_d$

$0.270\ H_d$

LEFT ABUTMENT

$0.639\ H_d$

$R=0.139\ H_d$

FLOW

CREST AXIS

$R=0.139\ H_d$

RIGHT ABUTMENT
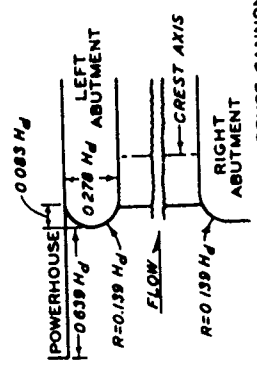
PLAN

NOTE: PROFILE BASED ON CLARENCE CANNON MODEL TESTS FOR SPILLWAY HAVING FOUR 1.389 H_d - WIDE BAYS SEPARATED BY 0.278 H_d - WIDE PIERS SIMILAR TO TYPE 2 (HYDRAULIC DESIGN CHART III-5)

OVERFLOW SPILLWAY CREST
UPPER NAPPE PROFILES
ALONG ABUTMENTS
APPROACH CHANNEL AND
ABUTMENT CURVATURE EFFECTS
HYDRAULIC DESIGN CHART III-14/1

WES 6-75

CHART III-14/1

HYDRAULIC DESIGN CRITERIA

SHEETS 111-16 TO 111-16/2

HIGH OVERFLOW DAMS

CREST PRESSURES

1. Hydraulic Design Charts 111-16 to 111-16/2 present plots of crest pressures for H/H_d values of 0.50, 1.00, 1.17, 1.33, and 1.50. The charts are based on rece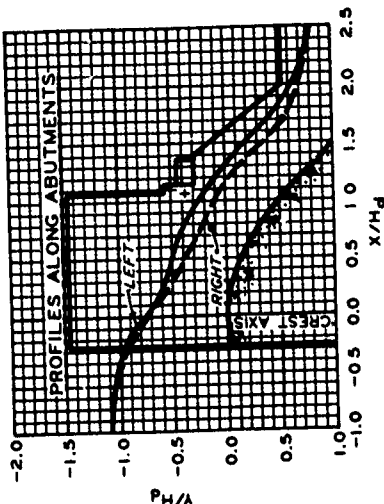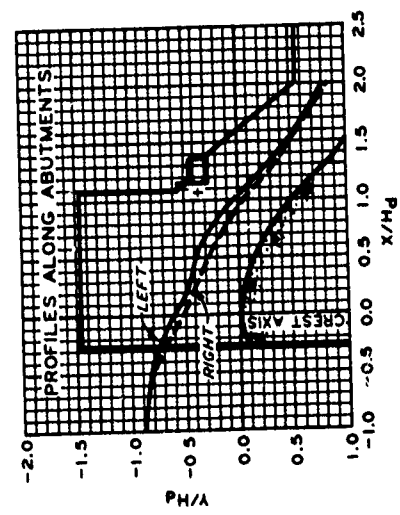nt ES 801 test data* for crests with and without piers: Chart 111-16 represents pressures on crests without piers; Chart 111-16/1, pressures midway between piers; and Chart 111-16/2, pressures adjacent to piers. Piezometers used for measuring the last condition were located immediately adjacent to the pier face.

2. The data shown are applicable to high overflow dams with standard crests. Data are plotted in terms of the dimensionless factors, pressure divided by design head (h_p/H_d) and horizontal distance divided by design head (X/H_d), to permit ready conversion to any selected design head. Pressures for intermediate head ratios can be obtained by plotting h_p/H_d versus H/H_d for a given X/H_d .

3. It is recommended that the spillway design head H_d be selected so that the minimum crest pressure for the maximum expected head H be no lower than -20 ft of water to ensure cavitation-free operation.

---

* U. S. Army Engineer Waterways Experiment Station, CE, Investigations of Various Shapes of the Upstream Quadrant of the Crest of a High Spillway; Hydraulic Laboratory Investigation, by E. S. Melsheimer and T. E. Murphy. Research Report H-70-1, Vicksburg, Miss., January 1970.

PRESSURE / DESIGN HEAD $\left(\dfrac{h_p}{H_d}\right)$

HORIZONTAL DISTANCE / DESIGN HEAD $\left(\dfrac{x}{H_d}\right)$

$H/H_d = 0.50$

$H/H_d = 1.00$

$H/H_d = 1.17$

$H/H_d = 1.33$

$H/H_d = 1.50$

AXIS BOTH QUADRANTS

X

$X^{1.85} = 2 H_d^{0.85} Y$

R = 0.20 H_d
R = 0.04 H_d
R = 0.50 H_d
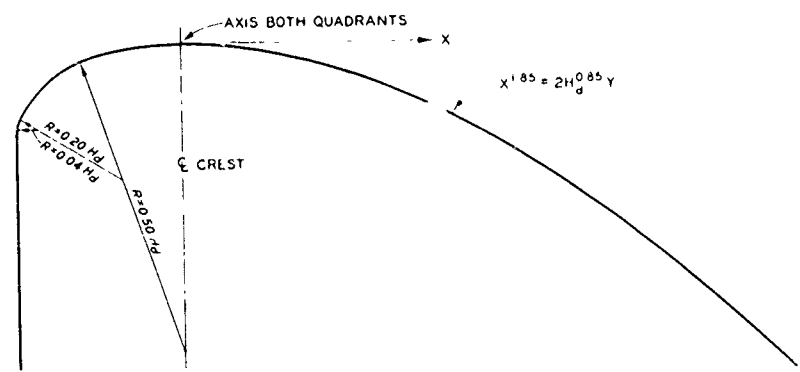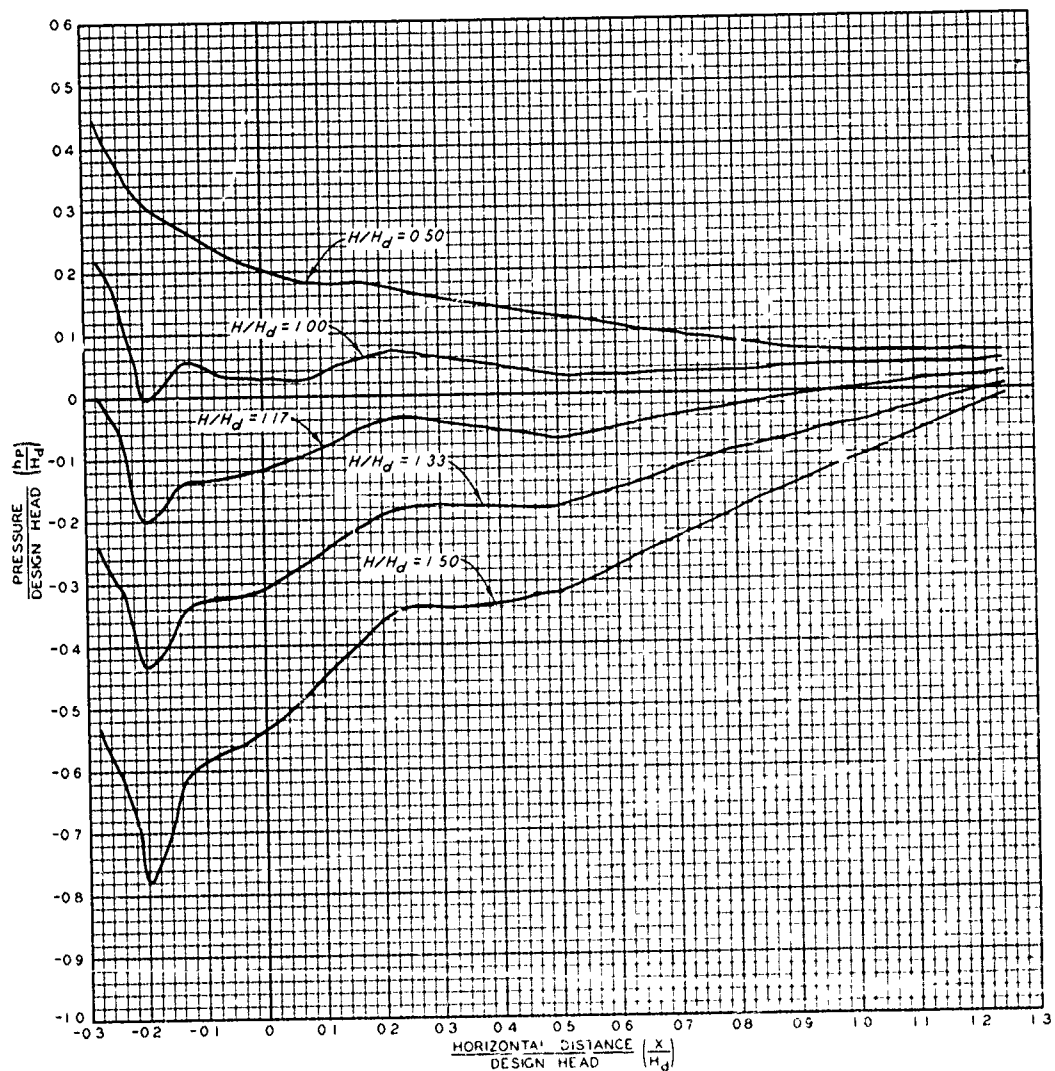
¢ CREST

NOTE DATA BASED ON ES801 TESTS

HIGH OVERFLOW DAMS
CREST PRESSURES
NO PIERS

HYDRAULIC DESIGN CHART III-16

REV 3-55, 9-70   WES 9-54

PRESSURE / DESIGN HEAD ($\frac{h_p}{H_d}$)

HORIZONTAL DISTANCE / DESIGN HEAD ($\frac{X}{H_d}$)

$H/H_d = 0.50$

$H/H_d = 1.00$

$H/H_d = 1.17$

$H/H_d = 1.33$

$H/H_d = 1.50$

AXIS BOTH QUADRANTS

X

$X^{1.85} = 2H_d^{0.85} Y$

R = 0.20 H_d

R = 0.04 H_d

R = 0.50 H_d
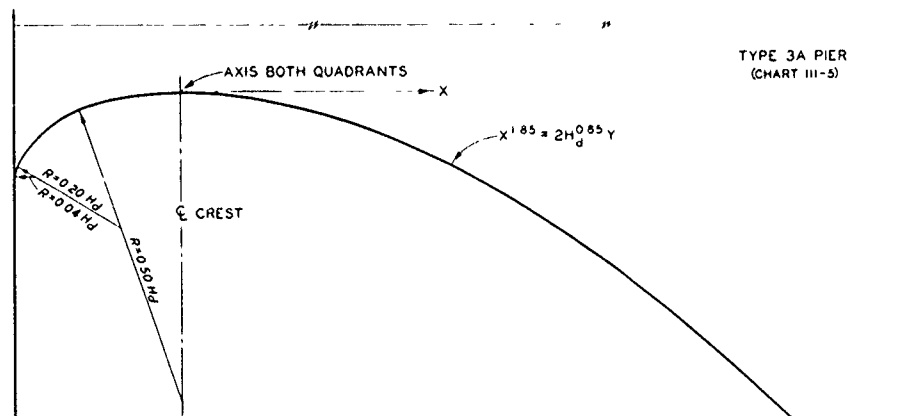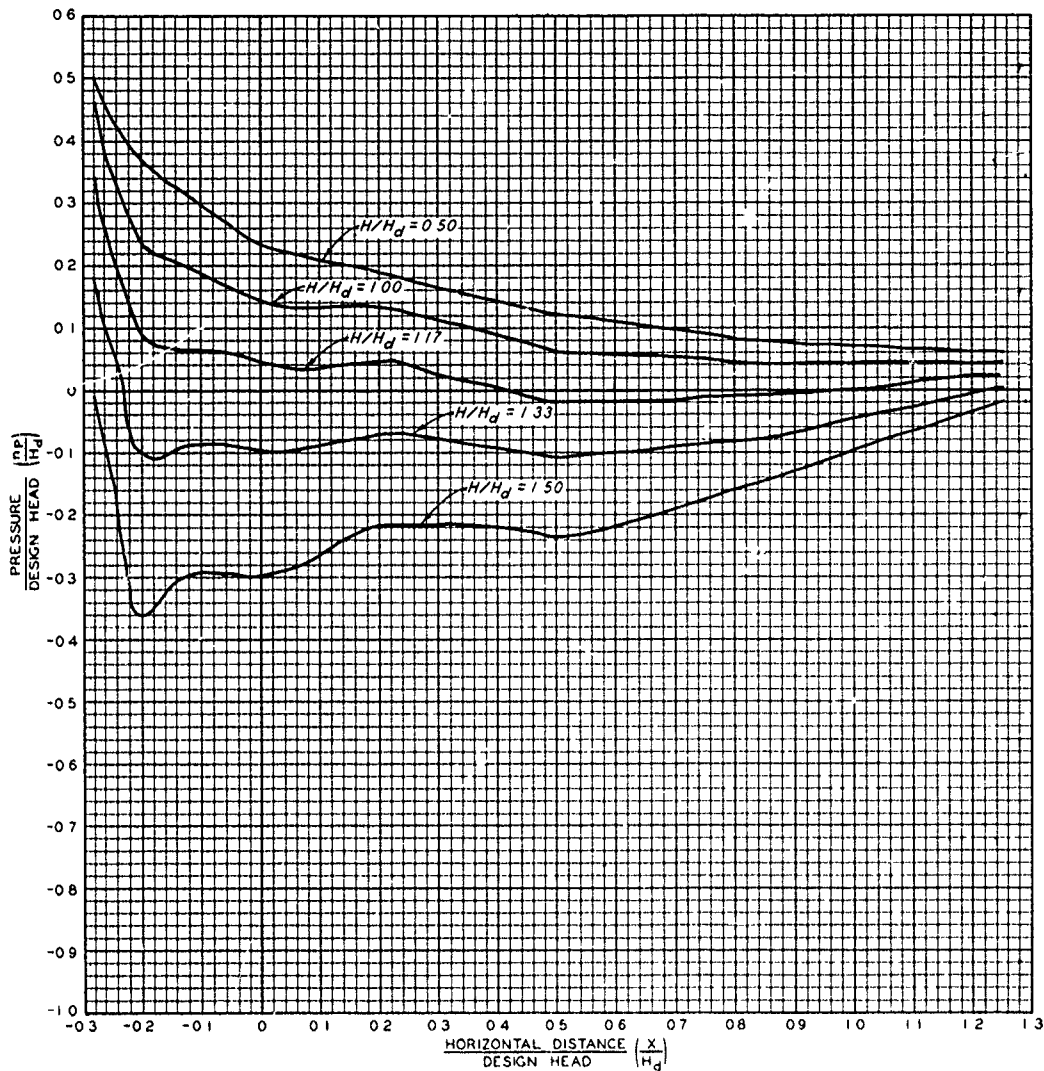
$\mathcal{C}$ CREST

TYPE 3A PIER
(CHART III-5)

NOTE   DATA BASED ON ES801 TESTS

HIGH OVERFLOW DAMS
CREST PRESSURES
CENTER LINE OF PIER BAY

HYDRAULIC DESIGN CHART III-16/1

REV 9-70   WES 3-55

PRESSURE / DESIGN HEAD $\left(\dfrac{h_P}{H_d}\right)$

0.6
0.5
0.4
0.3
0.2
0.1
0
-0.1
-0.2
-0.3
-0.4
-0.5
-0.6
-0.7
-0.8
-0.9
-1.0

-0.3 -0.2 -0.1 0 0.1 0.2 0.3 0.4 0.5 0.6 0.7 0.8 0.9 1.0 1.1 1.2 1.3

HORIZONTAL DISTANCE / DESIGN HEAD $\left(\dfrac{X}{H_d}\right)$

$H/H_d = 0.50$
$H/H_d = 1.00$
$H/H_d = 1.17$
$H/H_d = 1.33$
$H/H_d = 1.50$

AXIS BOTH QUADRANTS

X

$X^{1.85} = 2 H_d^{0.85} Y$

TYPE 3A PIER
(CHART III-5)

R = 0.20 H_d
R = 0.04 H_d
R = 0.50 H_d
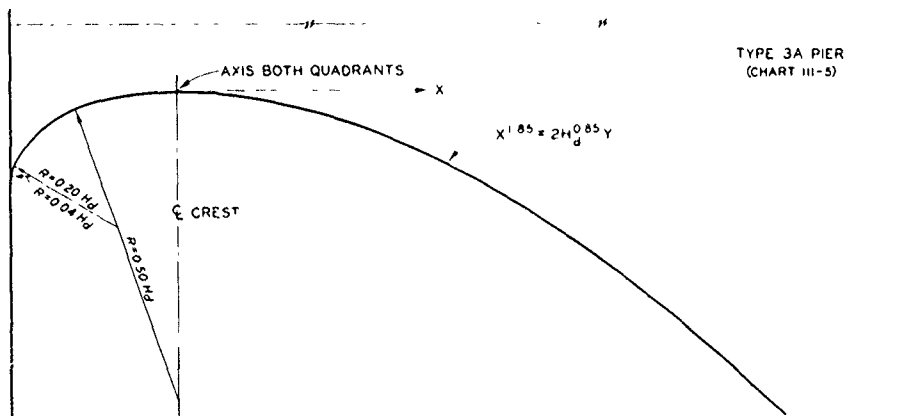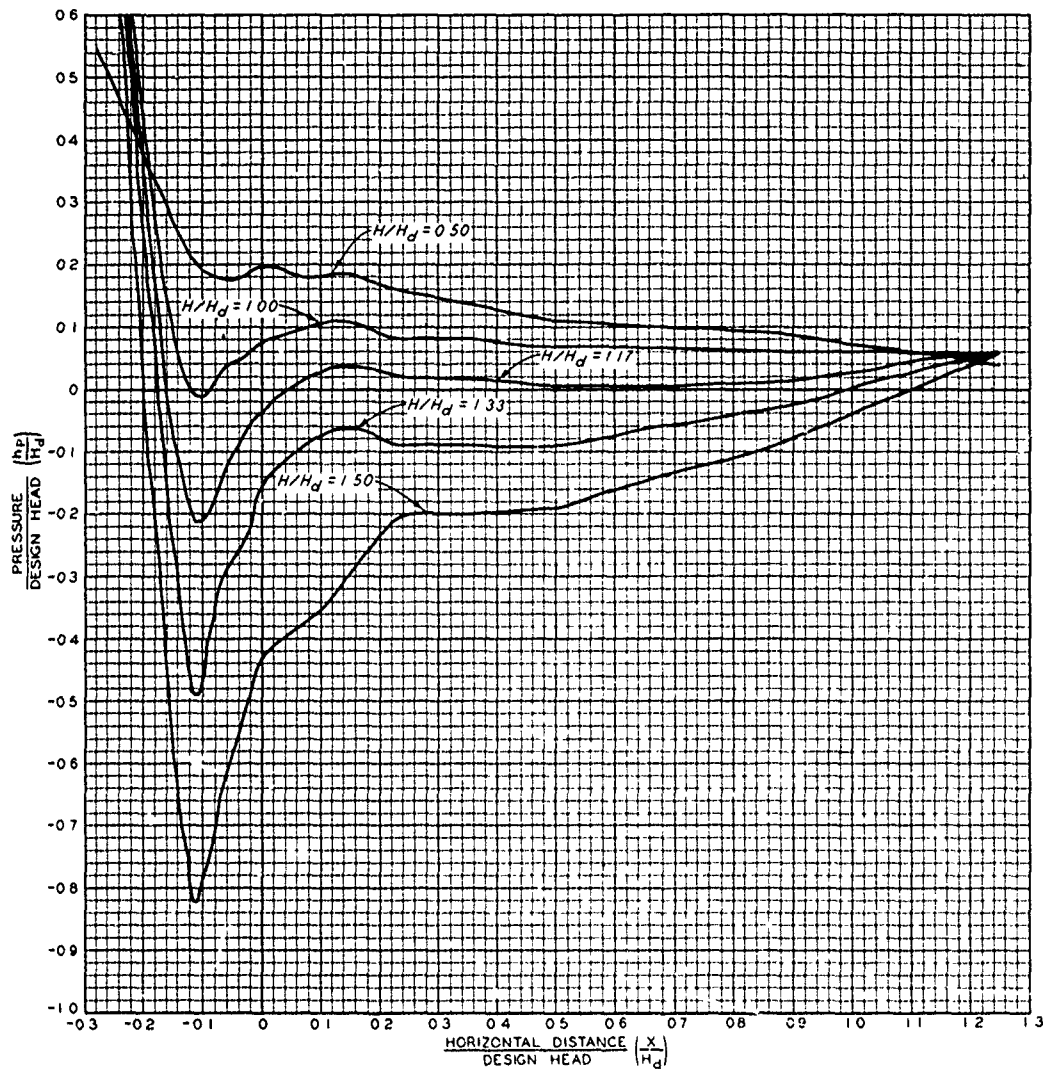
℄ CREST

NOTE   DATA BASED ON ES80I TESTS

HIGH OVERFLOW DAMS
CREST PRESSURES
ALONG PIERS

HYDRAULIC DESIGN CHART III-16/2

HYDRAULIC DESIGN CRITERIA

'SHEET 111-17

HIGH OVERFLOW DAMS

PRESSURE RESULTANTS

1.   In certain stability problems it is desirable to determine the actual pressure forces acting on the upstream face of the dam rather than to assume straight-line pressure distribution near the crest. Hydraulic Design Chart 111-17 presents a plot of experimental data showing pressure distribution in terms of the design head. The data presented are based on CW 801 tests for crests without piers and on USBR tests[1] of pressures on a sharp-crested weir for $H/H_d = 1.00$. The location and magnitude (in terms of the design head) of three resultants based on integration of the pressure plot between the limits of $0 < y < 1.5\ H_d$ are also shown. The cross-hatched area (R_1) is a pressure reduction to be applied to the normally assumed pressure acting on the vertical face of the dam. Sufficient pressure data on the vertical face are not available to allow computation of the resultant (R_1) for H/H_d values of 0.50 and 1.33. R_2 is the vertical pressure resultant effected by flow over the curved surface of the crest. R_3 is the horizontal pressure resultant effected by the flow downstream from the spillway crest.

---

(1)   "Studies of Crests for Overfall Dams, Boulder Canyon Project," Final Reports, Part VI, Bulletin 3, Bureau of Reclamation, 1948.

HIGH OVERFLOW DAMS
PRESSURE RESULTANTS
NO PIERS

HYDRAULIC DESIGN CHART III-17

REVISED 8-58   WES 9-54

CHART III-17
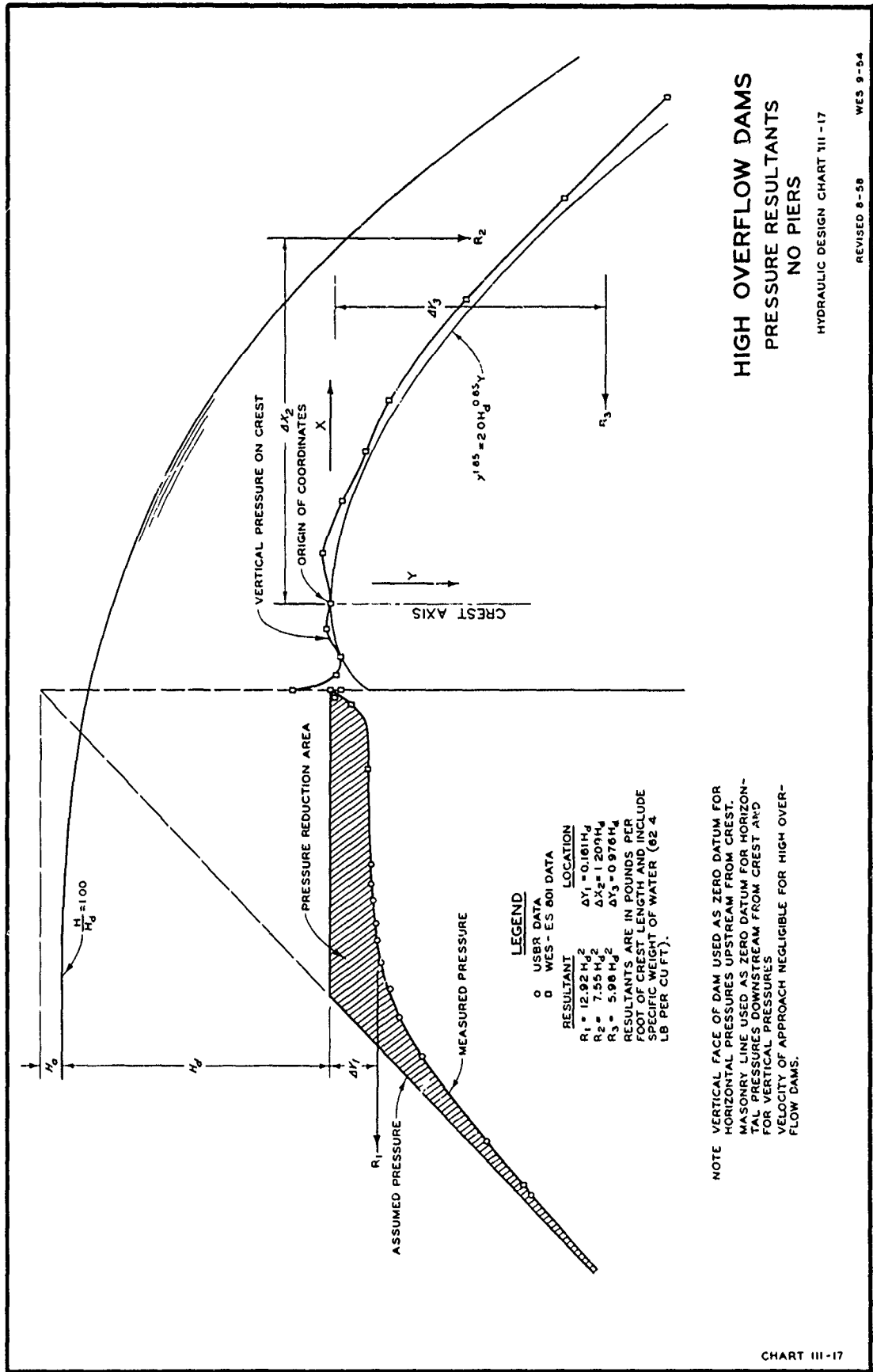
HYDRAULIC DESIGN CRITERIA

SHEETS 111-18 TO 111-18/5

SPILLWAY ENERGY LOSSES

1. An estimate of the loss of energy on the downstream face of a high overflow spillway may be important in the design of energy-dissipating devices at the foot of the spillway. If the losses are substantial, their evaluation is desirable in order to design an economical stilling basin or to estimate the throw of a jet from a flip bucket. The problem is twofold: (a) determination of energy loss during development of the turbulent boundary layer, and (b) determination of energy loss in the fully developed turbulent flow. For a large head on the crest with the spillway design flow, usually only (a) need be considered. HDC 111-18 to 111-18/5 apply to the condition of turbulent boundary layer development.

2. **Previous Design Criteria.** It has been common practice to use the Manning equation or some other open-channel equation to determine spillway energy losses. Gumensky[1] based an analysis on the Manning equation and published a graph which has been widely used. Jansen[2] proposed an empirical equation based on Randolph's[3] observation on Madden Dam. Bradley and Peterka[4] published a graph which reflects spillway losses as indicated by tests on Shasta and Grand Coulee Dams. In general, the results obtained by these methods do not agree.

3. **Boundary Layer Theory.** The concepts of displacement thickness and momentum thickness of the boundary layer are discussed in modern fluid mechanics textbooks.[5] The concept of energy thickness, which is useful in the spillway energy-loss problem, has appeared in the literature only recently. Schlichting[6] makes reference to the use of the energy thickness by Wieghardt.[7] The decrease in energy flux in the boundary layer caused by friction is found by:

$$\frac{1}{2} \rho \int_0^\delta u \left(U^2 - u^2\right) dy \tag{1}$$

where δ is the boundary layer thickness as indicated in the definition sketch in HDC 111-18, u is the velocity at a distance y from the boundary, and U is the potential flow velocity. By definition, the energy thickness δ_3 is the thickness of a layer of fluid with velocity U which represents the loss of energy flux in the boundary layer:

$$\frac{1}{2} \rho U^3 \delta_3 = \frac{1}{2} \rho \int_0^\delta u \left(U^2 - u^2\right) dy \tag{2}$$

$$\delta_3 = \int_0^\delta \frac{u}{U} \left(1 - \frac{u^2}{U^2}\right) dy \tag{3}$$

If δ_3 can be estimated, the energy flux loss upstream from any point on the spillway face can be found from:

$$E_L = \frac{1}{2} \rho U^3 \delta_3 \quad (\text{lb/sec}) \tag{4}$$

Division of equation 4 by $q\gamma$, where q is the unit discharge and γ is the specific weight, results in defining the energy loss in terms of feet of head:

$$H_L = \frac{\delta_3 U^3}{2gq} \quad (\text{feet of head}) \tag{5}$$

where g is the acceleration due to gravity. The evaluation of δ_3 and U is discussed below.

4. **Turbulent Boundary Layer Investigations.** During spillway discharge, the turbulent boundary layer continues to develop until it reaches the free water surface or until the flow enters the energy dissipator at the toe of the structure. Bauer[8,9] made extensive laboratory tests and correlated boundary layer thickness and development length (X) with surface roughness. His analysis included limited prototype data.[10] Keulegan[11] reanalyzed Bauer's data and proposed the equation

$$\frac{\delta}{X} = 0.96 \left(\frac{X}{k} \right)^{-1/4} \tag{6}$$

where X is the distance from an assumed origin and k is the absolute surface roughness height.

5. **Spillway Energy Losses.** A study of Bauer's[8,9] data, Keulegan's[11] reanalysis, additional prototype data,[12] and photographs* has been made by the Waterways Experiment Station[13,14] to develop design criteria for estimating spillway energy losses. This study resulted in the curve given in HDC 111-18 which is applicable for estimating the boundary layer thickness in flows over spillways. The equation of the curve is:

$$\frac{\delta}{L} = 0.08 \left(\frac{L}{k} \right)^{-0.233} \tag{7}$$

where L is the length along the spillway crest from the beginning of the crest curve (HDC 111-18). A roughness k value of 0.002 ft is recommended for concrete.

---

* Unpublished photographs by the U. S. Army Engineer District, Vicksburg, Miss., of flow over the spillway of Arkabutla Dam, Coldwater River, Mississippi.

6. The relations between boundary layer thickness δ, displacement thickness δ_1, and energy thickness δ_3, based on Bauer's data for screen roughness, have been found to be:

$$\delta_1 = 0.18\delta \tag{8}$$

$$\delta_3 = 0.22\delta \tag{9}$$

The use of these relations in conjunction with the potential flow depth and equations 5 and 7 are recommended for estimating spillway flow depths and energy losses. Modifications to equations 7, 8, and 9 may prove desirable as additional data become available.

7. **Application.**

   a. **Case 1.** The boundary layer thickness δ, the flow depth d, and the spillway energy loss H_L for design heads of 20, 30, and 40 ft can be estimated directly from HDC 111-18/2 and 111-18/3 for the standard crest shape defined by HDC 111-1 to 111-2/1. The use of HDC 111-18/2 and 111-18/3 is applicable to spillways with tangent face slopes of 1:0.7 and a surface roughness k of 0.002 ft. HDC 111-18/4 illustrates the required computations. The computations indicate that the boundary layer has not reached the free-water surface. Therefore, no bulking of the flow is to be expected from air entrainment caused by turbulence generated at the spillway face.

   b. **Case 2.** For the standard crest shapes with face slopes other than 1:0.7, HDC 111-1, 111-18, and 111-18/1 and equations 5, 8, and 9 should be used in the manner illustrated by the sample computation given in HDC 111-18/5. If the computed boundary layer thickness is indicated to become greater than the summation of the displacement thickness and the potential flow depth, the intersection of the free-water surface and the boundary layer, sometimes called the critical point, can be located. This can be done by plotting the flow depth d and boundary layer thickness δ as functions of the boundary length as shown in HDC 111-18/2. Air entrainment begins beyond the critical point, and the energy-loss mechanism is not well understood.

   c. **Case 3.** For other than the standard crest shape, the curved crest length L_c is determined graphically or analytically. The computation procedure is then similar to that for Case 2.

8. **References.**

(1) Gumensky, D. B., "Air entrained in fast water affects design of training walls and stilling basins." Civil Engineering, vol 19 (December 1949), pp. 831-833, 889.

(2) Jansen, R. B., "Flow characteristics on the ogee spillway." <u>ASCE Hydraulics Division, Journal,</u> vol 83 (December 1957), pp 1452-1 to 1452-11.

(3) Randolph, R. R., Jr., "Hydraulic tests on the spillway of the Madden Dam." <u>Transactions, American Society of Civil Engineers,</u> vol 103 (1938), pp 1080-1112.

(4) Bradley, J. N., and Peterka, A. J., "Hydraulic design of stilling basins." <u>ASCE Hydraulics Division, Journal,</u> vol 83, HY 5 (October 1957), pp 1401-1 to 1406-17.

(5) Rouse, Hunter, <u>Advanced Mechanics of Fluids.</u> John Wiley & Sons, Inc., New York, N. Y., 1959.

(6) Schlichting, H., <u>Boundary Layer Theory.</u> English translation by J. Kestin. McGraw-Hill Book Co., Inc., New York, N. Y., 1960.

(7) Wieghardt, K., "Ueber einen Energiesatz zur Berechnung laminarer Grenzschichten (Concerning an energy principle for calculation of laminar boundary layer)." <u>Ingenieur-Archiv,</u> vol 16 (1948), p 231.

(8) Bauer, W. J., <u>The Development of the Turbulent Boundary Layer on Steep Slopes.</u> A dissertation submitted to State University of Iowa, August 1951.

(9) _____, "Turbulent boundary layer on steep slopes." <u>Transactions, American Society of Civil Engineers,</u> vol 119 (1954), pp 1212-1233.

(10) Hickox, G. H., "Air entrainment on spillway faces." <u>Civil Engineering,</u> vol 15 (December 1945), pp 562-563.

(11) U. S. Army Engineer Waterways Experiment Station, CE, <u>Turbulent Boundary Layer Development on Spillways,</u> by G. H. Keulegan. Miscellaneous Paper No. 2-587, Vicksburg, Miss., July 1963.

(12) Michels, V., and Lovely, M., "Some prototype observations of air entrainment flow." <u>Proceedings, Minnesota International Hydraulics Convention</u> (August 1953), pp 403-414.

(13) U. S. Army Engineer Waterways Experiment Station, CE, <u>A Study of Spillway Energy Losses During Development of the Turbulent Boundary Layer.</u> Miscellaneous Paper No. 2-642. Vicksburg, Miss., April 1964.

(14) Office, Chief of Engineers, Department of the Army, <u>Engineering and Design; Hydraulic Design of Spillways.</u> Engineer Manual EM 1110-2-1603, Washington, D. C., March 1965.

LEGEND

●	BAUER	20° SLOPE,	K = 0.0014 FT
X	BAUER	40° SLOPE,	K = 0.0014 FT
O	BAUER	60° SLOPE,	K = 0.0014 FT
□	NORRIS	55° SLOPE,	K = 0.0020 FT
▽	ARKABUTLA	59° SLOPE,	K = 0.0020 FT
△	GLENMAGGIE	18° SLOPE,	K = 0.0020 FT

$$\frac{\delta}{L} = 0.08 \left(\frac{L}{k}\right)^{-0.233}$$

$\dfrac{\delta}{L}$

$\dfrac{L}{k}$
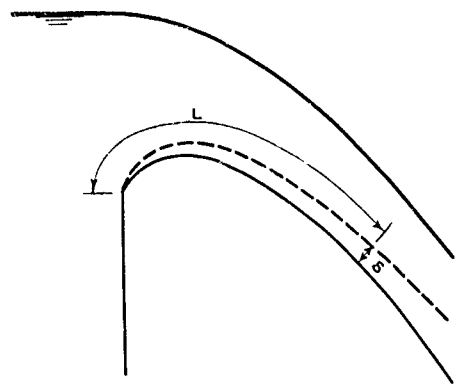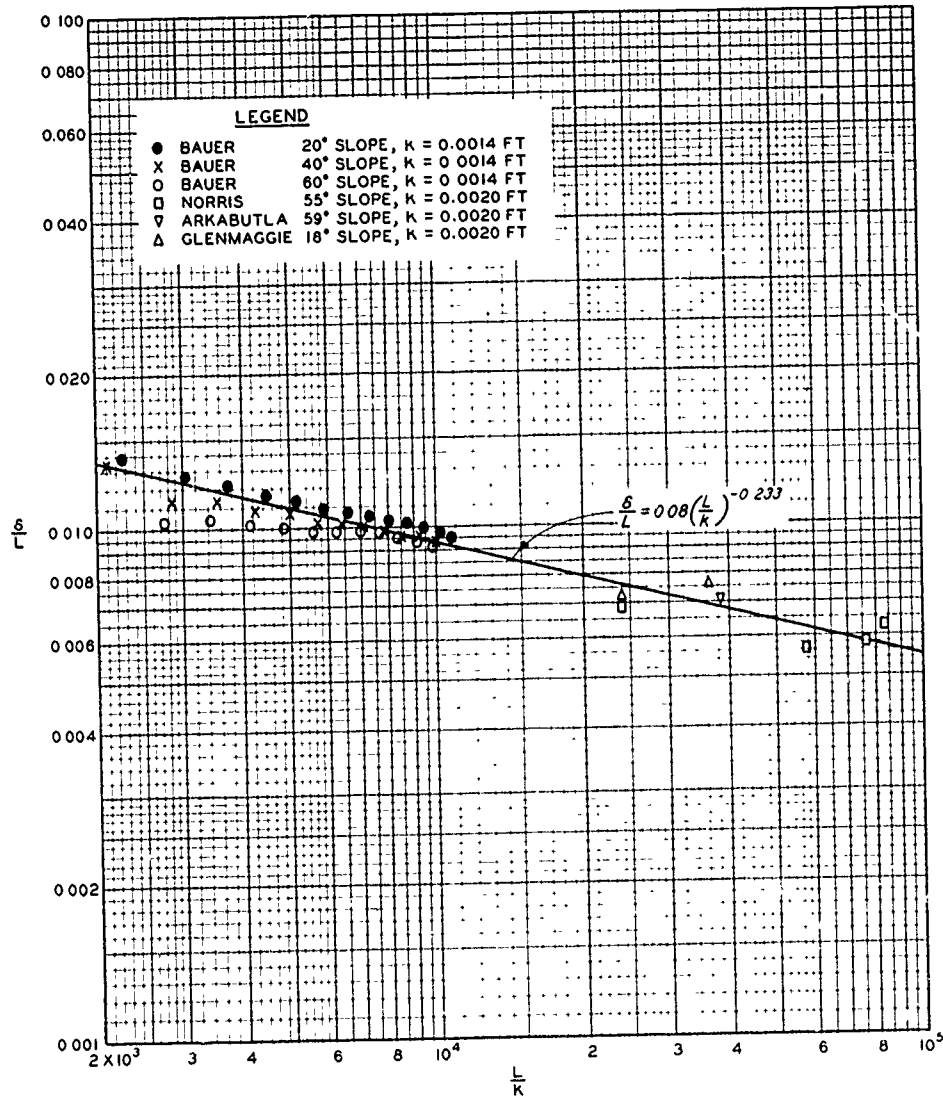
δ = BOUNDARY LAYER THICKNESS, FT
L = SURFACE LENGTH, FT
k = ABSOLUTE SURFACE ROUGHNESS HEIGHT, FT

DEFINITION SKETCH

HIGH OVERFLOW DAMS
SPILLWAY ENERGY LOSS
BOUNDARY LAYER DEVELOPMENT

HYDRAULIC DESIGN CHART III-18

WES 1-66

NOTE CURVE APPLICABLE TO CREST SHAPE
DEFINED BY HDC III-I TO III-2/I.

$\frac{L_c}{H_d}$

UPSTREAM QUADRANT LENGTH = 0.315 H_d

$\frac{X}{H_d}$

DEFINITION SKETCH
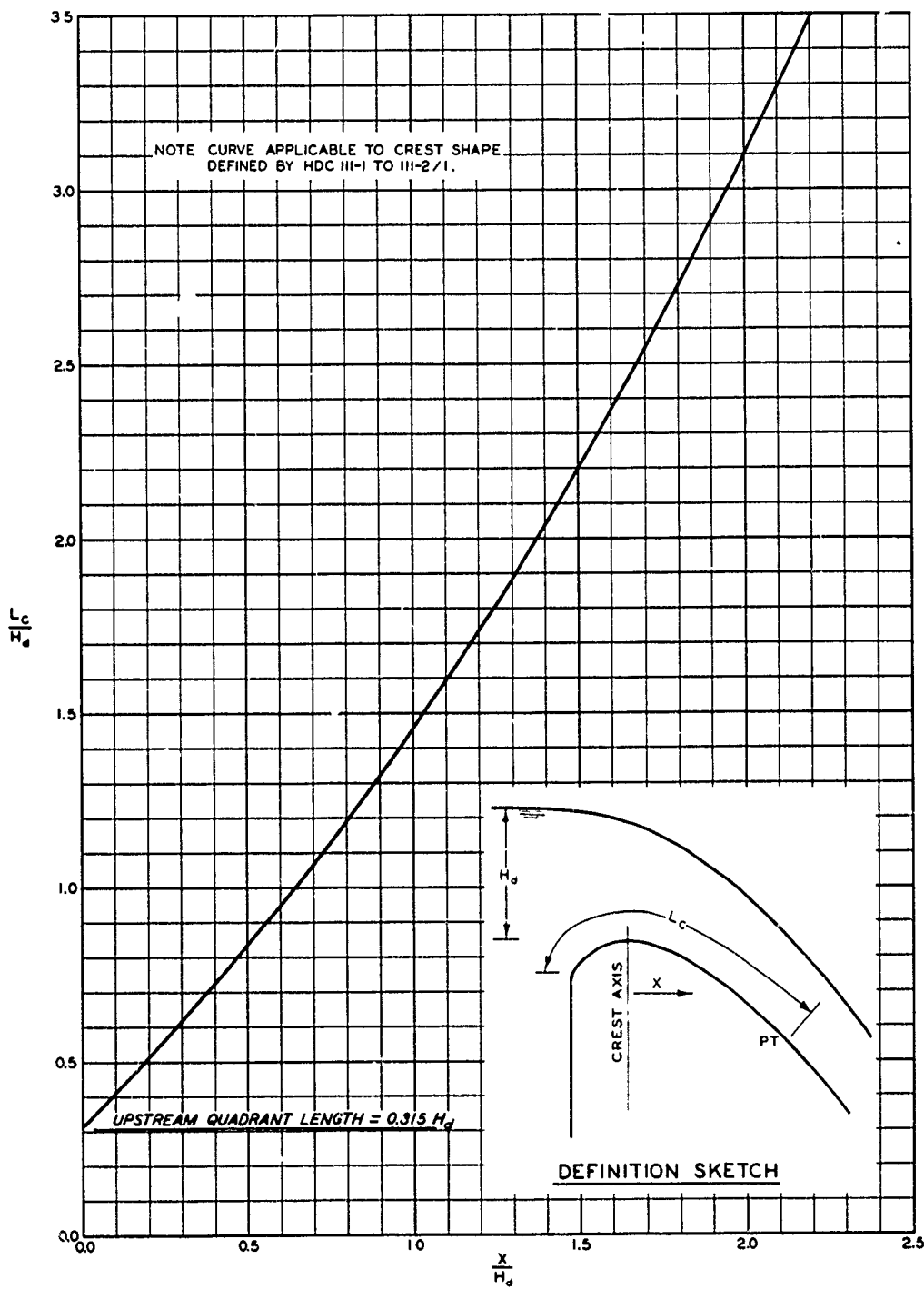
NOTE. L_c = LENGTH ALONG CURVED CREST, FT
      X = HORIZONTAL COORDINATE, FT
      H_d = SPILLWAY DESIGN HEAD, FT

HIGH-OVERFLOW DAMS
SPILLWAY ENERGY LOSS
STANDARD CREST LENGTH

HYDRAULIC DESIGN CHART III-18/I

WES 1-66
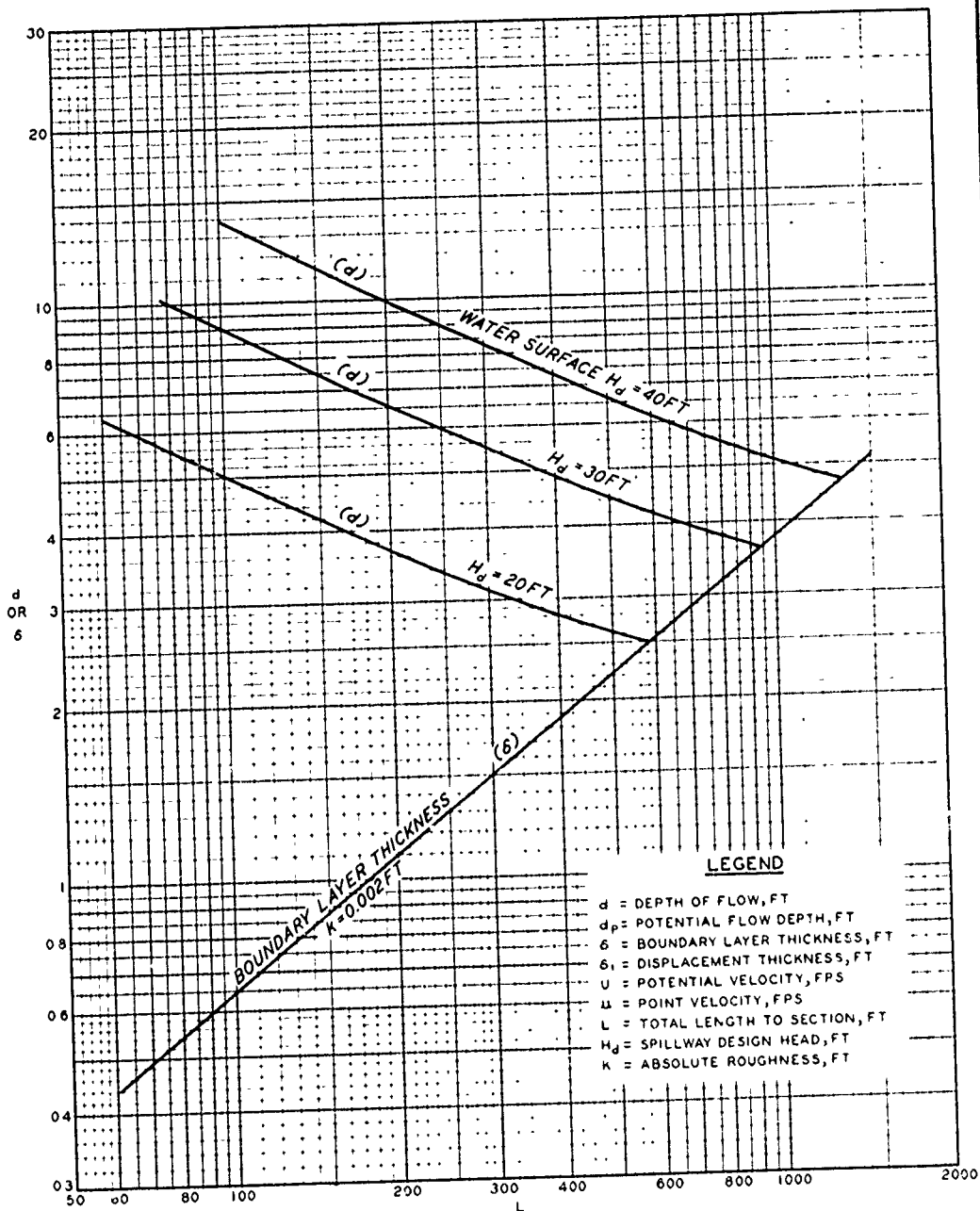
LEGEND

d = DEPTH OF FLOW, FT
d_P = POTENTIAL FLOW DEPTH, FT
δ = BOUNDARY LAYER THICKNESS, FT
δ_1 = DISPLACEMENT THICKNESS, FT
U = POTENTIAL VELOCITY, FPS
u = POINT VELOCITY, FPS
L = TOTAL LENGTH TO SECTION, FT
H_d = SPILLWAY DESIGN HEAD, FT
K = ABSOLUTE ROUGHNESS, FT

NOTE CURVES APPLICABLE TO STANDARD
SPILLWAY CREST (HDC III-1 TO III-2/1)
WITH 1 0 7 TANGENT FACE SLOPE
DEPTH (d) IS POTENTIAL FLOW DEPTH
PLUS DISPLACEMENT THICKNESS
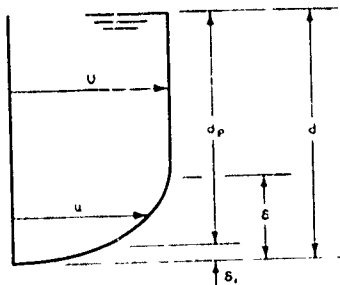
DEFINITION SKETCH

HIGH-OVERFLOW DAMS
SPILLWAY ENERGY LOSS
STANDARD CREST
LOCATION OF CRITICAL POINT

HYDRAULIC DESIGN CHART III-18/2

WES 1-68

PREPARED BY U S ARMY ENGINEER WATERWAYS EXPERIMENT STATION VICKSBURG, MISSISSIPPI

Chart plot: vertical axis H_L (1 to 100), horizontal axis L (40 to 1000), with three curves labeled $H_d = 20\,FT$, $H_d = 30\,FT$, $H_d = 40\,FT$.

NOTE CURVES APPLICABLE TO STANDARD
SPILLWAY CREST (HDC III-1 TO III-2/1)
WITH 1 0 7 TANGENT SECTION

ENERGY LOSS BASED ON ENERGY
THICKNESS FOR ABSOLUTE ROUGH-
NESS k OF 0002 FT

LEGEND

H_L = ENERGY HEAD LOSS, FT
L = TOTAL LENGTH TO SECTION, FT
H_d = SPILLWAY DESIGN HEAD, FT

HIGH-OVERFLOW DAMS

SPILLWAY ENERGY LOSS
STANDARD CREST
FACE SLOPE 1.0.7

HYDRAULIC DESIGN CHART III-18/3

WES 1-66

GIVEN:

$H_d = 30$ ft

$H = 250$ ft

$k = 0.002$ ft (Surface roughness)

Face slope = 1:0.7

$x^{1.85} = 2H_d^{0.85} Y$

COMPUTE:

1. Boundary Geometry

   a. Length of curved crest, L_c

   $$\frac{X_1}{H_d} = 1.67 \text{ (HDC 111-1)}$$

   $$\frac{L_c}{H_d} = 2.50 \text{ (HDC 111-18/1)}$$

   $$L_c = 2.50 H_d = 75.0 \text{ ft}$$

   b. Length of tangent, L_T

   $$\frac{Y_1}{H_d} = 1.32 \text{ (HDC 111-1)}$$

   $$Y_1 = 1.32 H_d = 39.6 \text{ ft}$$

   $$Y_2 - Y_1 = 250 - 39.6 = 210.4 \text{ ft}$$

   $$X_2 - X_1 = \frac{0.7}{1.0}(Y_2 - Y_1) = 147.3 \text{ ft}$$

   $$L_T = \sqrt{(210.4)^2 + (147.3)^2}$$
   $$= 256.9 \text{ ft}$$

   c. Total crest length, L

   $$L = L_c + L_T$$
   $$= 75.0 + 256.9 = 331.9 \text{ ft}$$

Note: Computed H_b is satisfactory and no bulking of flow from air entrainment since $\delta < d$.
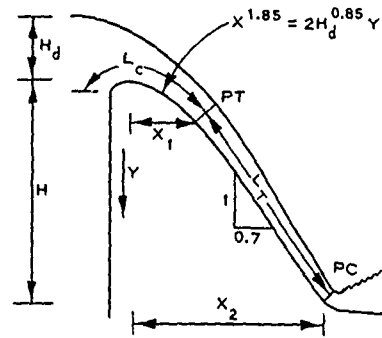
2. Hydraulic Computation

   a. Spillway energy loss, H_L

   For $L = 331.9$ ft and $H_d = 30$ ft

   $$H_L = 20.0 \text{ ft (HDC 111-18/3)}$$

   b. Energy head entering stilling basin, H_b

   $$H_b = H + H_d - H_L$$
   $$= 250 + 30 - 20 = 260 \text{ ft}$$

   c. Depth of flow, d, and boundary layer thickness, δ, at PC of toe curve

   $$d = 5.30 \text{ ft (HDC 111-18/2)}$$
   $$\delta = 1.62 \text{ ft (HDC 111-18/2)}$$

HIGH OVERFLOW DAMS
SPILLWAY ENERGY LOSS
SAMPLE COMPUTATION
FACE SLOPE 1.0.7

HYDRAULIC DESIGN CHART 111-18/4

WES 1-68

GIVEN:

$H_d = 30$ ft
$H = 350$ ft
$k = 0.002$ ft (Surface roughness)
Face slope = 1:0.78

COMPUTE ENERGY HEAD
ENTERING STILLING BASIN:

1. Boundary Geometry

   a. Length of curved crest, L_c

   $$\frac{X_1}{H_d} = 1.47 \text{ (HDC 111-1)}$$

   $$\frac{L_c}{H_d} = 2.15 \text{ (HDC 111-18/1)}$$

   $$L_c = 2.15 H_d = 64.5 \text{ ft}$$

   b. Length of tangent, L_T

   $$\frac{Y_1}{H_d} = 1.04 \text{ (HDC 111-1)}$$

   $$Y_1 = 1.04 H_d = 31.2 \text{ ft}$$

   $$Y_2 - Y_1 = 350 - 31.2 = 318.8 \text{ ft}$$

   $$\text{Tan } \alpha = \frac{1.0}{0.78} = 1.2821$$

   $$\text{Sin } \alpha = 0.7885$$

   $$L_T = \frac{Y_2 - Y_1}{\text{Sin } \alpha} = 404.4 \text{ ft}$$

   c. Total crest length, L

   $$L = L_c + L_T$$
   $$= 64.5 + 404.4 = 468.9 \text{ ft}$$

2. Hydraulic computation

   a. Boundary layer thickness, δ

   $$\frac{L}{k} = \frac{468.9}{0.002} = 2.344 \times 10^5$$

   $$\frac{\delta}{L} = 0.08 \left(\frac{L}{k}\right)^{-0.233} \text{ (HDC 111-18)}$$
   $$= 0.08 (0.0561)$$
   $$= 0.00449$$
   $$\delta = 2.10 \text{ ft}$$

   b. Energy thickness, δ_3

   $$\delta_3 = 0.22\,\delta \text{ (Eq 9, sheets 111-18 to 111-18/5)}$$
   $$= 0.462 \text{ ft}$$

   c. Unit discharge, q

   $$q = C H_d^{3/2}$$
   $$C = 4.03 \text{ (HDC 111-3)}$$
   $$q = 4.03 (30)^{3/2} = 662 \text{ cfs}$$
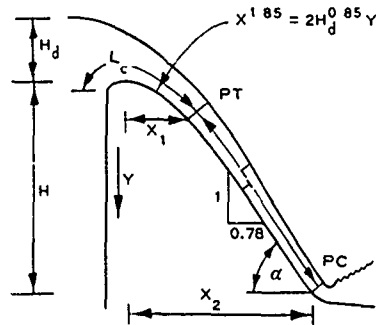
d. Potential flow depth d_p and velocity U at PC of toe curve

$$H_T = d_p \cos \alpha + \frac{U^2}{2g}$$
$$\text{Cos } \alpha = 0.6150$$
$$H_T = H + H_d = 350 + 30 = 380 \text{ ft}$$

By trial

U	$\frac{U^2}{2g}$	$H_T - \frac{U^2}{2g}$	$d_p = \dfrac{H_T - \frac{U^2}{2g}}{0.6150}$	$q = U d_p$
(ft)	(ft)	(ft)	(ft)	(cfs)
156.0	377.9	2.1	3.41	532 < 662
155.9	377.4	2.6	4.23	659 ≈ 662

e. Spillway energy loss

$$H_L = \frac{\delta_3 U^3}{2gq} \text{ (Eq 5, sheets 111-18 to 111-18/5)}$$

$$= \frac{0.462 (155.9)^3}{64.4 (662)} = 41 \text{ ft}$$

f. Energy head entering stilling basin

$$H_b = H + H_d - H_L$$
$$= 350 + 30 - 41 = 339 \text{ ft}$$

g. Depth of flow, d, at PC of toe curve

$$d = d_p + \delta_1$$
$$\delta_1 = 0.18\,\delta \text{ (Eq 8, sheets 111-18 to 111-18/5)}$$
$$= 0.18 (2.10) = 0.38 \text{ ft}$$
$$d = 4.23 + 0.38 = 4.61 \text{ ft}$$

Note: Computed H_b satisfactory and no bulking of flow from air entrainment since $\delta < d$.

HIGH OVERFLOW DAMS
SPILLWAY ENERGY LOSS
SAMPLE COMPUTATION
FACE SLOPE 1 0 78

HYDRAULIC DESIGN CHART 111-18/5

PREPARED BY U S ARMY ENGINEER WATERWAYS EXPERIMENT STATION VICKSBURG MISSISSIPPI

WES 1-66

HYDRAULIC DESIGN CRITERIA

SHEETS 111-19 TO 111-19/2

HIGH OVERFLOW DAMS

SPILLWAY CREST WITH OFFSETS AND RISERS

CREST SHAPES

1. **Purpose.** Use of spillway crests with offsets and risers may effect appreciable economies in the construction of concrete gravity spillways provided the concrete mass eliminated from the standard crest shape defined in HDC 111-1 to 111-2/1 is not required for structural stability. The scheme has also been adopted for the high arch dam Monteynard.[1] HDC 111-19 to 111-19/2 should serve for developing crest shapes for preliminary economic studies. It is suggested that the final spillway shape be model-tested.

2. **Background.** A laboratory study of overhanging crests produced by an offset in a sharp-crested weir was reported by the U. S. Bureau of Reclamation (USBR).[2] A recent analysis of unpublished USBR test data was made by the Waterways Experiment Station (WES). In this study the dimensionless quantity of the ratio of the riser height to the head on the rounded crest M/H_d was selected as the basic shape variable. The offset dimension N does not appear to be very effective until the ratio M/H_d becomes very small. One limiting case is the offset weir with no riser ($M = 0$), which forms a 45-degree backward-sloping weir. The lower nappe of the flow over a 45-degree backward-sloping, sharp-crested weir may extend initially slightly upstream of the sharp crest. The other limiting case is a high spillway with no offset ($N = 0$) described in HDC 111-1 to 111-2/1. The test data selected for the WES study were from experiments with negligible velocity of approach, a condition representative of a high dam for which substantial savings in concrete would result from undercutting the upstream face. These data were for M/H_d test values of 0.240 to 0.396 having N/H_d values of 0.079 to 0.240. The resulting M/N values are 1.0 to 5.0. Sections having M/N values less than 0.5 are not recommended.[2] The results of this study are summarized in HDC 111-19 to 111-19/2 and generally define spillway crest geometry for riser-design head ratios of $0 < M/H_d < 1.0$.

3. **Crest Location.** The USBR lower-nappe coordinates are in terms of the head on the sharp-crested weir and have their origin at the weir. For design purposes, it is more convenient to have the coordinates in terms of the head H_d on the round crest with their origin at the crest apex. HDC 111-19 gives curves for estimating the distance X_e of the round crest from the sharp crest and the height Y_e of the round crest above the sharp crest. The curves are in terms of the design head H_d on the round crest and are plotted as a function of the ratio of the riser height to design head M/H_d. The values of X_e/H_d and Y_e/H_d were found to be 0.287 and 0.166, respectively, for the limiting case of $M/H_d = 0$. HDC 111-2/1

gives values of 0.270 and 0.126 for X_e/H_d and Y_e/H_d, respectively, for the case of $M/H_d \geq 1.0$. These limiting cases are plotted in HDC 111-19 and were used as guides in defining the general shape of the curves given in the chart.

4. **Downstream Quadrant.** The standard form of the equation for the downstream quadrant with the head on the round crest is:

$$\frac{Y}{H_d} = K \left(\frac{X}{H_d}\right)^n \tag{1}$$

Values of the constant K and the exponent n for various ratios of M/H_d were determined graphically and by electronic computer. Values of n and K resulting in best correlation with the basic data are plotted in graphs a and b in HDC 111-19/1. Data points appropriate for the limiting cases discussed in paragraph 3 are also shown. The vertical-face spillway defined in HDC 111-1 has n and K values of 1.85 and 0.50, respectively. It is reasoned that the values of n and K should approach these limits asymptotically as the riser height M becomes larger in relation to the design head H_d.

5. **Upstream Quadrant.** The standard form of the equation defined in HDC 111-1 to 111-2/1 for the upstream quadrant of the vertical-face weir was used as a basis for the case of weirs with offsets and risers:

$$\frac{Y_w}{H_w} = K_1 \left(\frac{X}{H_w}\right)^{n_1} - K_2 \left(\frac{X}{H_w}\right)^{n} \tag{2}$$

The subscript w refers to the sharp-crested weir. The conditions established for developing the exponents and constants of the equations included:

a. Curve slopes $\dfrac{dY_w}{dX_w}$ of zero at the round crest and of infinity at the sharp-crested riser for the selected values of X_e/H_d and Y_e/H_d.

b. For M/H_d values > 0.24, the exponent n_1 of the first term has the value of 0.625 developed for the vertical-face weir using relaxation data of McNown and others[3] discussed in HDC 111-1 to 111-2/1.

c. The exponent n of the second term is the same as that developed for the downstream quadrant.

d. The constants K_1 and K_2 developed to provide a reasonable fit to the experimental data.

6. Computed values of exponents and constants for equation 2 based on the selected USBR data are plotted in graphs a and c in HDC 111-19/1. The plotted points meet the conditions established in paragraph 5.

7. **Application.** The crest shape defined in HDC 111-1 to 111-2/1 should be applicable to overhanging spillways having riser heights $\geq 0.6H_d$. Use of the curves in HDC 111-19 and 111-19/1 is suggested for preliminary design purposes should there be design reasons for making the riser smaller than $0.6H_d$. The curves on these charts should be used in the manner indicated by the sample computation given in HDC 111-19/2. The final design should be model-tested. The use of a curvature of appreciable radius to connect the riser to the sloping overhang is recommended if model tests indicate pressure pulsations on the crest resulting from flow separations around the riser.

8. **References.**

(1) Bowman, W. G., "French high arch dam is all-in-one (Monteynard Dam)." Engineering News-Record, vol 169 (25 October 1962), pp 30-37.

(2) U. S. Bureau of Reclamation, "Studies of crests for overfall dams." Boulder Canyon Project Final Reports, Part VI, Hydraulic Investigations, Bulletin 3, Denver, Colo. (1948).

(3) McNown, J. S., Hsu, En-Yun, and Yih, Chia-Shun, "Applications of the relaxation technique in fluid mechanics." Transactions, American Society of Civil Engineers, vol 120 (1955), pp 650-669.
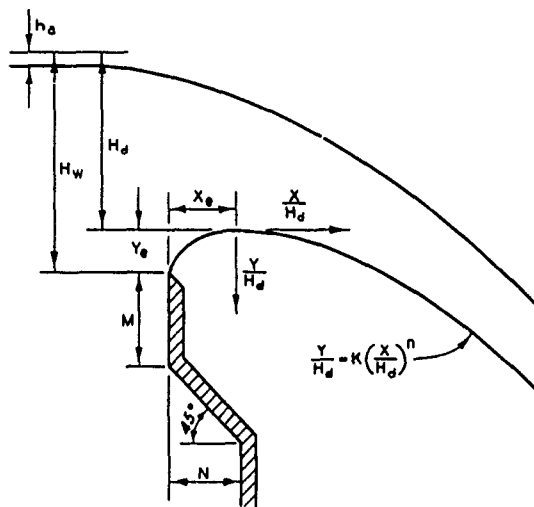
DOWNSTREAM QUADRANT

UPSTREAM QUADRANT

$$\frac{Y}{H_d} = K\left(\frac{X}{H_d}\right)^n$$

$$\frac{Y}{H_W} = K_1\left(\frac{X}{H_W}\right)^{n_1} - K_2\left(\frac{X}{H_W}\right)^n$$
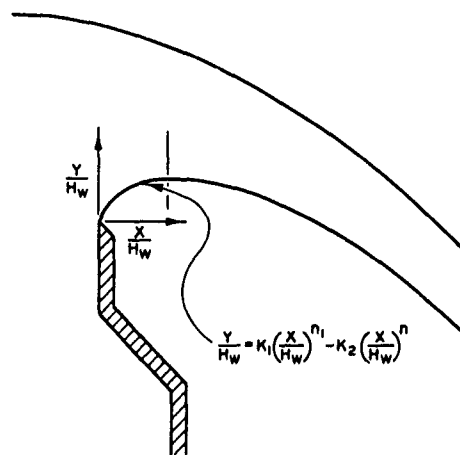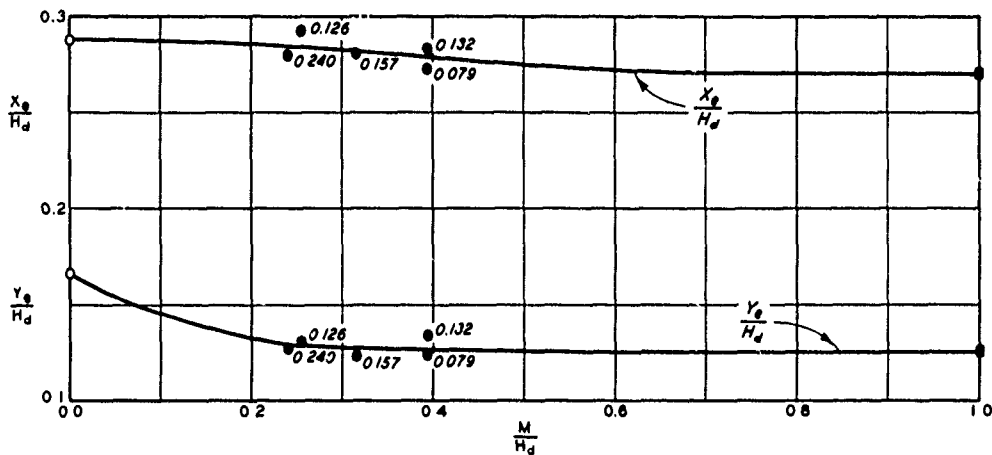
LEGEND

● BASED ON UNPUBLISHED USBR DATA
○ BASED ON PUBLISHED USBR DATA
▇ HDC 111-2/1

NOTE NUMBERS ON GRAPH ARE VALUES OF N/H_d.
H_d IS DESIGN HEAD BASED ON LOWER
SURFACE OF NAPPE FROM SHARP-CRESTED
WEIR WITH NEGLIGIBLE VELOCITY OF APPROACH.

HIGH-OVERFLOW DAMS
SPILLWAY CRESTS
WITH OFFSET AND RISER

CREST LOCATION

HYDRAULIC DESIGN CHART 111-19
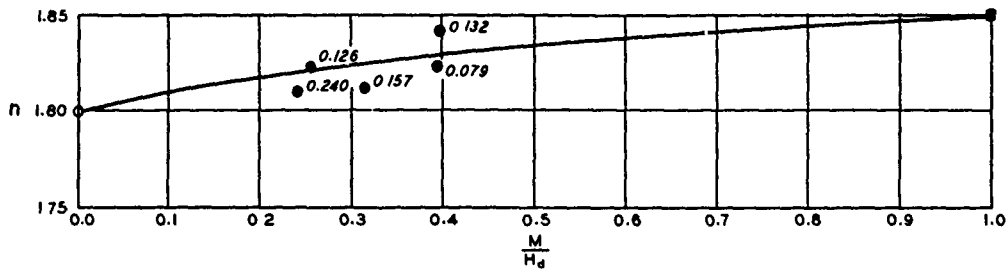
a. EXPONENT n, DOWNSTREAM QUADRANT
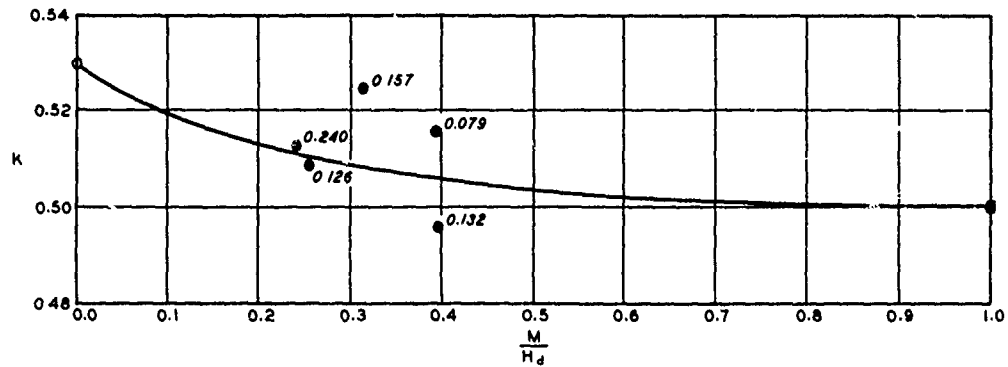
b. COEFFICIENT K, DOWNSTREAM QUADRANT
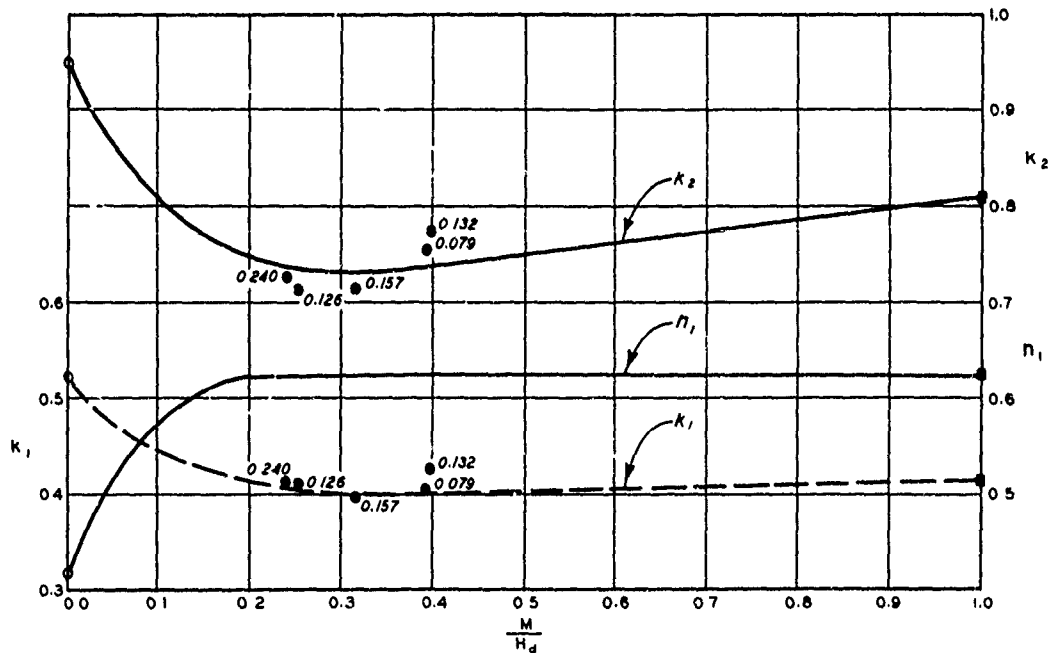
c. COEFFICIENTS AND EXPONENTS, UPSTREAM QUADRANT

HIGH-OVERFLOW DAMS

SPILLWAY CRESTS
WITH OFFSET AND RISER

CREST SHAPE

HYDRAULIC DESIGN CHART III-19/1

WES 1-66

GIVEN:

$H_d = 40$ ft

$\dfrac{M}{H_d} = 0.30$ ft

$\dfrac{N}{H_d} = 0.25$ ft

Negligible velocity of approach
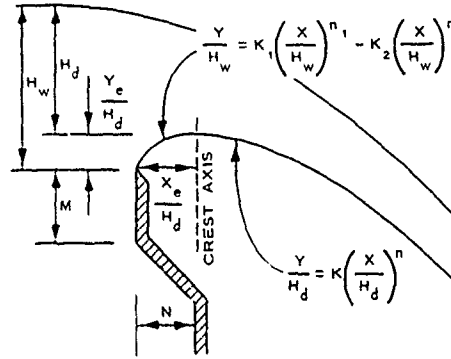
COMPUTE:

1. Downstream Quadrant Equation

$$\frac{Y}{H_d} = K\left(\frac{X}{H_d}\right)^n$$

   $K = 0.508$, $n = 1.825$ (HDC 111-19/1)

$$\frac{Y}{H_d} = 0.508\left(\frac{X}{H_d}\right)^{1.825}$$

2. Upstream Quadrant Equation

$$\frac{Y}{H_w} = K_1\left(\frac{X}{H_w}\right)^{n_1} - K_2\left(\frac{X}{H_w}\right)^n$$

$\left.\begin{array}{l} K_1 = 0.405,\ K_2 = 0.730 \\ n_1 = 0.625,\quad n = 1.825 \end{array}\right\}$ (HDC 111-19/1)

$$\frac{Y}{H_w} = 0.405\left(\frac{X}{H_w}\right)^{0.625} - 0.730\left(\frac{X}{H_w}\right)^{1.825}$$

3. Check for Zero Slope at Crest

$\dfrac{X_e}{H_d} = 0.282$, $\dfrac{Y_e}{H_d} = 0.130$ (HDC 111-19)

$H_w = H_d + Y_e = H_d + 0.130 H_d = 1.130 H_d$

$\dfrac{X_e}{H_w} = \dfrac{X_e}{1.130 H_d} = \dfrac{0.282}{1.130} = 0.250$, $\dfrac{Y_e}{H_w} = \dfrac{Y_e}{1.130 H_d} = 0.115$

$$\frac{d\left(\dfrac{Y}{H_w}\right)}{d\left(\dfrac{X}{H_w}\right)} = K_1 n_1 \left(\frac{X}{H_w}\right)^{n_1 - 1} - K_2 n \left(\frac{X}{H_w}\right)^{n - 1}$$

$$= \frac{0.405 \times 0.625}{(0.250)^{0.375}} - 0.730 \times 1.825 (0.250)^{0.825}$$

$$= \frac{0.253}{0.594} - 1.331(0.319) = 0.002 \approx 0.000$$

4. Solve for Values of K_1 and K_2 Giving Zero Slope at the Crest for $\dfrac{X_e}{H_w} = 0.250$

$$\frac{Y_e}{H_w} = K_1\left(\frac{X_e}{H_w}\right)^{n_1} - K_2\left(\frac{X_e}{H_w}\right)^n$$

$0.115 = K_1 (0.250)^{0.625} - K_2 (0.250)^{1.825}$

$0.115 = 0.421 K_1 - 0.080 K_2$ (1)

$$\frac{d\left(\dfrac{Y_e}{H_w}\right)}{d\left(\dfrac{X_e}{H_w}\right)} = 0.625 K_1 (0.250)^{-0.375}$$

$$\qquad\qquad - 1.825 K_2 (0.250)^{0.825} = 0$$

$1.05 K_1 - 0.583 K_2 = 0$

$K_1 = 0.554 K_2$ (2)

Substitute Equation 2 into Equation 1

$0.115 = 0.421 \times 0.554 K_2 - 0.080 K_2$

$K_2 = 0.752$, $K_1 = 0.416$

Upstream Quadrant Equation

$$\frac{Y}{H_w} = 0.416\left(\frac{X}{H_w}\right)^{0.625} - 0.752\left(\frac{X}{H_w}\right)^{1.825}$$

Note: For final design greater accuracy of computations is recommended.

HIGH-OVERFLOW DAMS

SPILLWAY CRESTS
WITH OFFSET AND RISER
CREST GEOMETRY
SAMPLE COMPUTATION

HYDRAULIC DESIGN CHART 111-19/2

HYDRAULIC DESIGN CRITERIA

SHEETS 112-1 AND 112-2

SPILLWAY STILLING BASINS

HYDRAULIC JUMP

1. **General.** The principle of conservation of linear momentum results in the classical hydraulic jump equation

$$D_2 = -\frac{D_1}{2} + \sqrt{\frac{2V_1^2 D_1}{g} + \frac{D_1^2}{4}}$$

Tables for the evaluation of D_2 may be found in the Corps of Engineers Hydraulic Tables, 2d Edition, 1944.

2. **Spillway Stilling Basins.** The purpose of Hydraulic Design Charts 112-1 and 112-2 is the determination of the elevation of the apron or stilling basin floor when headwater and tailwater elevations are known for a given discharge. The form of the graphs was devised by Irwin.* On each chart families of D_1 and D_2 curves are shown for various discharges per foot of basin width and heads. Chart 112-1 covers a head range of 5 to 500 ft and a discharge range of 10 to 250 cfs. Chart 112-2 covers a similar range of heads but has a discharge range of 100 to 2500 cfs. The head (H) as defined by the sketch at the foot of each chart is the difference between the headwater and tailwater elevations. In the development of these charts friction losses were neglected. Recent experiments at State University of Iowa** for the Waterways Experiment Station indicate that friction losses in accelerating flow down the face of a spillway may be considerably less than the normal friction loss in well-developed turbulent flow. Two lines depicting the Froude number squared ($F^2 = 3$ and $F^2 = 12$) are shown to define the jump characteristics. The line $F^2 = 3$ marks the boundary between jumps of the undular and shock types. Model studies indicate that a strong hydraulic jump forms in the region above the line $F^2 = 12$.

---

* R. L. Irwin, "Diagram for hydraulic jump," Civil Engineering (June 1942), p 335.

** W. J. Bauer, "The Development of the Turbulent Boundary Layer on Steep Slopes," Dissertation, University of Iowa, Iowa City, August 1951.

H = DIFFERENCE IN ELEVATION BETWEEN UPPER POOL AND TAILWATER FOR HIGH DAMS OR BETWEEN ENERGY GRADIENT UPSTREAM FROM JUMP AND TAILWATER FOR LOW DAMS AND OPEN CHANNELS IN FEET

q = DISCHARGE PER FOOT OF BASIN WIDTH IN CFS
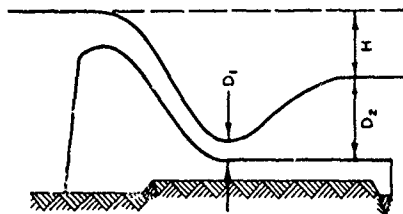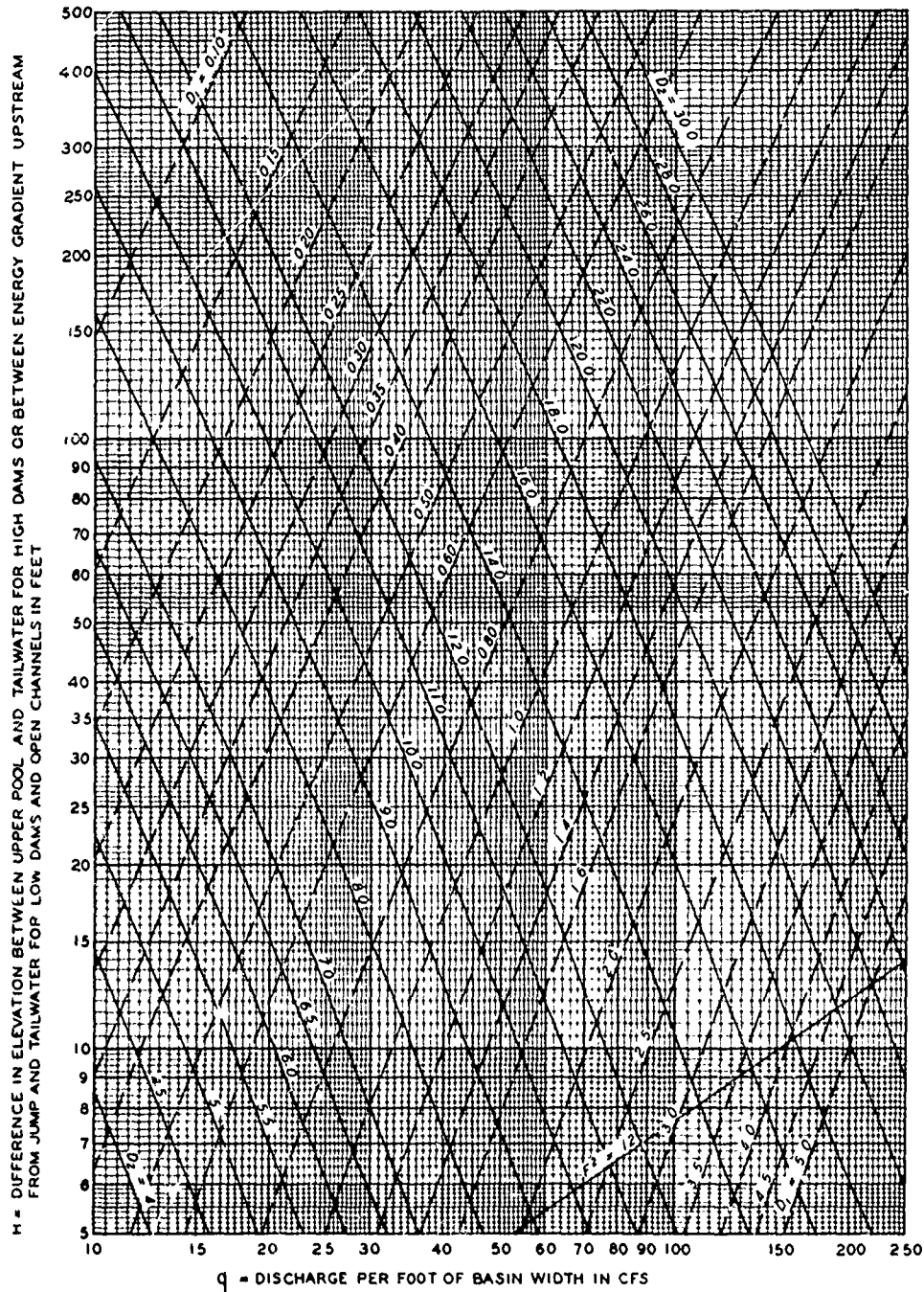
FORMULA: $H = \dfrac{2q^2}{gD_2^2\left[\sqrt{\dfrac{8q^2}{gD_2^3}+1}-1\right]^2} + \dfrac{D_2}{2}\left[\sqrt{\dfrac{8q^2}{gD_2^3}+1}-1\right] - D_2$

SPILLWAY STILLING BASINS
HYDRAULIC JUMP
$10 < q < 250$

HYDRAULIC DESIGN CHART 112-1

WES 4-1-53

H = DIFFERENCE IN ELEVATION BETWEEN UPPER POOL AND TAILWATER FOR HIGH DAMS OR BETWEEN ENERGY GRADIENT UPSTREAM FROM JUMP AND TAILWATER FOR LOW DAMS AND OPEN CHANNELS IN FEET

q = DISCHARGE PER FOOT OF BASIN WIDTH IN CFS
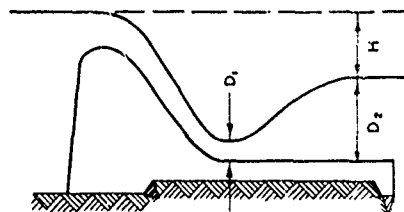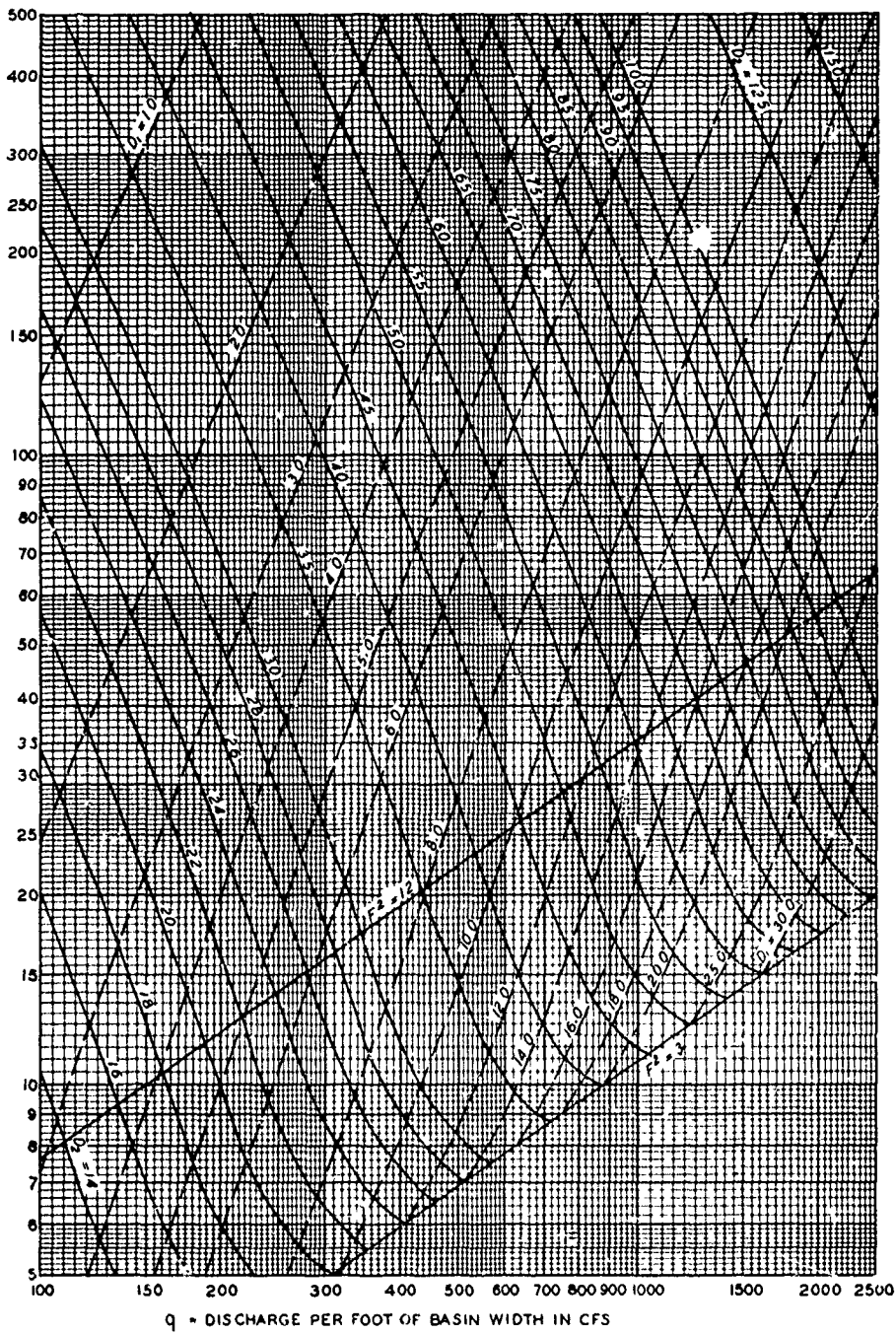
FORMULA. $H = \dfrac{2q^2}{gD_2^2\left[\sqrt{\dfrac{8q^2}{gD_2^3}+1}-1\right]^2} + \dfrac{D_2}{2}\left[\sqrt{\dfrac{8q^2}{gD_2^3}+1}-1\right]-D_2$

SPILLWAY STILLING BASINS
HYDRAULIC JUMP
$100 < q < 2500$

HYDRAULIC DESIGN CHART 112-2

WES 4-1-59

SPILLWAY STILLING BASINS

HYDRAULIC JUMP

VELOCITY DISTRIBUTION

1. The balance of pressure-plus-momentum upstream and downstream from the jump is the basis for the theoretical equation of the hydraulic jump. This equation is given in HDC 112-3. When an end sill or baffle piers are added there is an additional force in the upstream direction. U. S. Army Corps of Engineers EM 1110-2-1603[8] suggests that a satisfactory jump will occur for $0.9d_2$ by the use of an end sill and baffles although more shallow basins have been demonstrated to perform satisfactorily in the laboratory.

2. If the drag force of baffles is to be estimated, the effective velocity against the baffle and the drag coefficient must be known. The drag coefficient of the isolated cube referred to in HDC 712-1 has been estimated to be 1.33 based on State University of Iowa air tunnel tests.[1] The drag coefficient of a single cube in open channel flow has been computed to be about 1.5.[7] Tests at Massachusetts Institute of Technology[3] indicate that the drag coefficient is about 0.7 for a single row of stepped piers and about 0.4 for a double row of Bluestone Dam type baffle piers.[6]

3. HDC 112-2/1 can be used as a guide in selecting baffle pier height and location as well as in estimating the velocity in the vicinity of the baffles. HDC 112-2/1 presents vertical velocity distribution curves in the hydraulic jump at X/d_2 stations of 1, 2, and 3 from the toe of the jump. The curves result from experimental data by Rouse[4] and Mahoning Dam model study tests.[5] Curves for Froude numbers of entering flow of 2, 3, 4, 6, 8, and 10 are given. The local velocity V is expressed in terms of the entering velocity V_1. The distance y above the floor is in terms of the depth downstream from the jump d_2.

4. The force exerted on the baffle piers and the resulting reduction in total downstream pressure and momentum can be estimated by use of HDC 112-2/1 and an estimated drag coefficient. Available data indicate that the pier spacing as well as pier size and geometry has an effect upon the drag coefficient. The designer is also sometimes concerned with the force exerted on baffle piers by logs and other debris passing through the basi..

5. **References.**

(1) Chien, Ning, Fing, Yin, Wang, Huang-Ju, and Siao, Tien-To, Wind Tunnel Studies of Pressure Distribution on Elementary Building Forms. Iowa

Institute of Hydraulic Research, for Office of Naval Research, 1951.

(2) Harleman, D. R. F., "Effect of baffle piers on stilling basin performance." _Journal, Boston Society of Civil Engineers,_ vol 42, No. 2 (April 1955), pp 84-99.

(3) Newman, J. B., III, and La Boon, F. A., _Effects of Baffle Piers on the Hydraulic Jump._ M.S. thesis, Massachusetts Institute of Technology, 1953.

(4) Rouse, H., Siao, Tien-To, and Nagaratnam, S., "Turbulence characteristics of the hydraulic jump." _Transactions, American Society of Civil Engineers,_ vol 124 (1959), pp 926-966.

(5) U. S. Army Engineer District, Pittsburgh, CE, _Report on Hydraulic Model Studies on the Spillway and Outlet Works of Mahoning Dam, on Mahoning Creek, near Punxsutawney, Pennsylvania._ Case Institute of Technology, May 1938.

(6) U. S. Army Engineer Waterways Experiment Station, CE, _A Laboratory Development of Cavitation-free Baffle Piers, Bluestone Dam, New River, West Virginia._ Technical Memorandum No. 2-243, Vicksburg, Miss., March 1948.

(7) _____, unpublished data. 1957.

(8) U. S. Army, Office, Chief of Engineers, _Hydraulic Design, Spillways._ EM 1110-2-1603, March 1953.
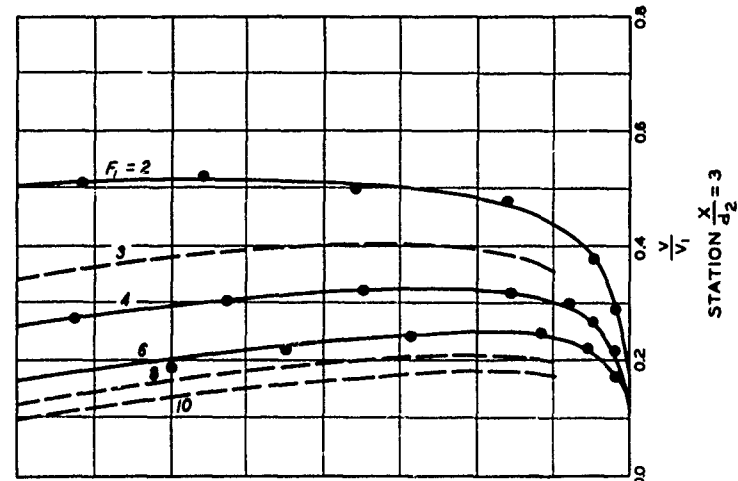
STATION $\frac{x}{d_2} = 3$
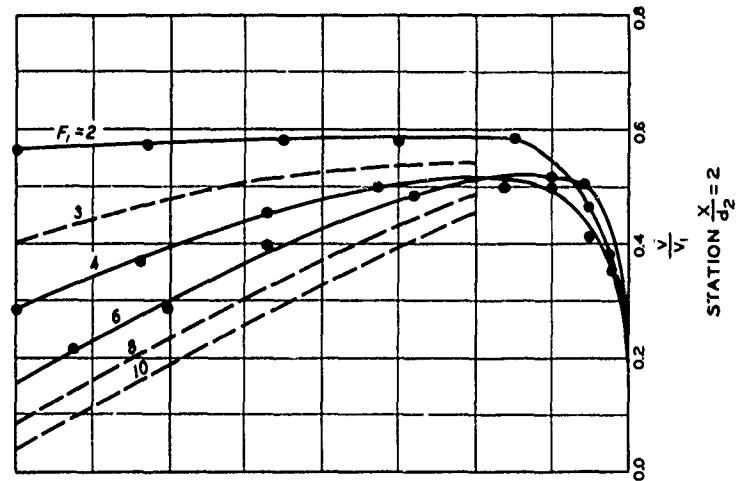
STATION $\frac{x}{d_2} = 2$

STATION $\frac{x}{d_2} = 1$

$F_i = 2$

$F_i = 2$

$F_i = 2$

$\frac{v}{v_i}$

$\frac{y}{d_2}$
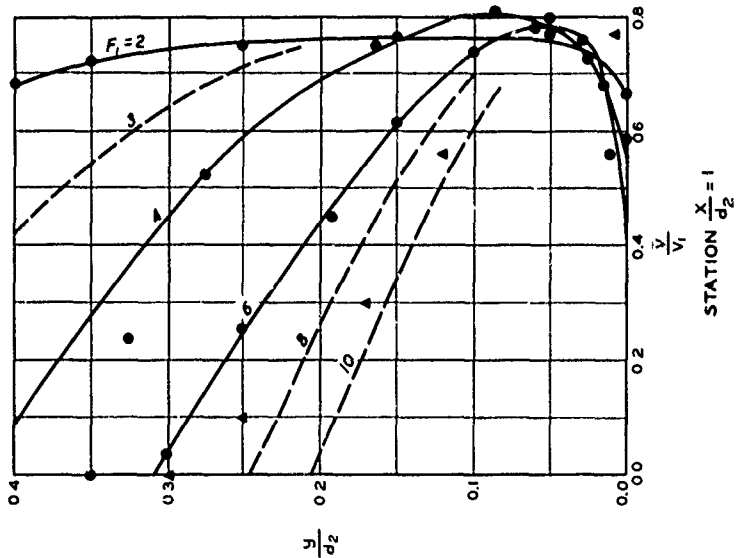
DEFINITION SKETCH

LEGEND

SYMBOL	SOURCE	FROUDE NO (F_i)
●———	ROUSE, SIAO, NAGARATNAM	2, 4, 6
▲	MAHONING MODEL	9
– – –	INTERPOLATED	3, 8, 10
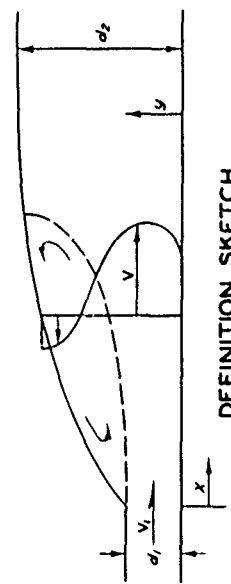
SPILLWAY STILLING BASINS
HYDRAULIC JUMP
VELOCITY DISTRIBUTION

HYDRAULIC DESIGN CHART 112-2/1

WES 10-61

PREPARED BY U S ARMY ENGINEER WATERWAYS EXPERIMENT STATION, VICKSBURG, MISSISSIPPI

CHART 112-2/1

SPILLWAY STILLING BASINS

SEQUENT DEPTH CURVES FOR RECTANGULAR CHANNEL

1. The conventional hydraulic jump equation is based on the principles of conservation of momentum and continuity of flow. The equation is

$$D_2 = -\frac{D_1}{2} + \sqrt{\frac{2 V_1^2 D_1}{g} + \frac{D_1^2}{4}}$$

where D_1 and D_2 are sequent depths upstream and downstream, respectively, from the jump. V_1 and V_2 are the corresponding sequent velocities.

2. Tables have been published by King(3) and the Corps of Engineers(6) that give the D_2 value when the D_1 and V_1 values are known.

3. A log-log graph, devised by E. W. Lane(5) and published by the National Resources Committee(4), is given as Chart 112-3. It may be used to determine D_2 and V_2 when D_1 and V_1 are known.

4. A graph on Cartesian coordinates was devised by Douma(2) and republished by Abbett(1). This graph gives the solution for D_2 when D_1 and V_1 are known. The graph was prepared for a range of values of $10 < V_1 < 100$ in Chart 112-4 and of $6 < V_1 < 40$ in Chart 112-5.

5. **List of References.**

(1) Abbett, R. W., American Civil Engineering Practice. Vol II, John Wiley & Sons., Inc., New York, N. Y., sec 17, p 56.

(2) Douma, J. H., Hydraulic Model Studies of the Wickiup Outlet Works Stilling Basin, Deschutes Project, Oregon. U. S. Bureau of Reclamation, Memorandum to Chief Designing Engineer, Denver, Colo., 30 June 1939, Appendix 1, fig. 17. (Available on loan only)

(3) King, H. W., Handbook of Hydraulics. 3d ed., McGraw-Hill Book Co., Inc., New York, N. Y., 1939, table 133, p. 444-445.

(4) National Resources Committee, Low Dams. Washington, D. C., 1938, p. 105.

(5) U. S. Bureau of Reclamation, Drawing No. X-D-931. 14 October 1933.

(6) War Department, Corps of Engineers, Hydraulic Tables. 2d ed.,
U. S. G. P. O., Washington, D. C., 1944, table 3, p. 16-56.
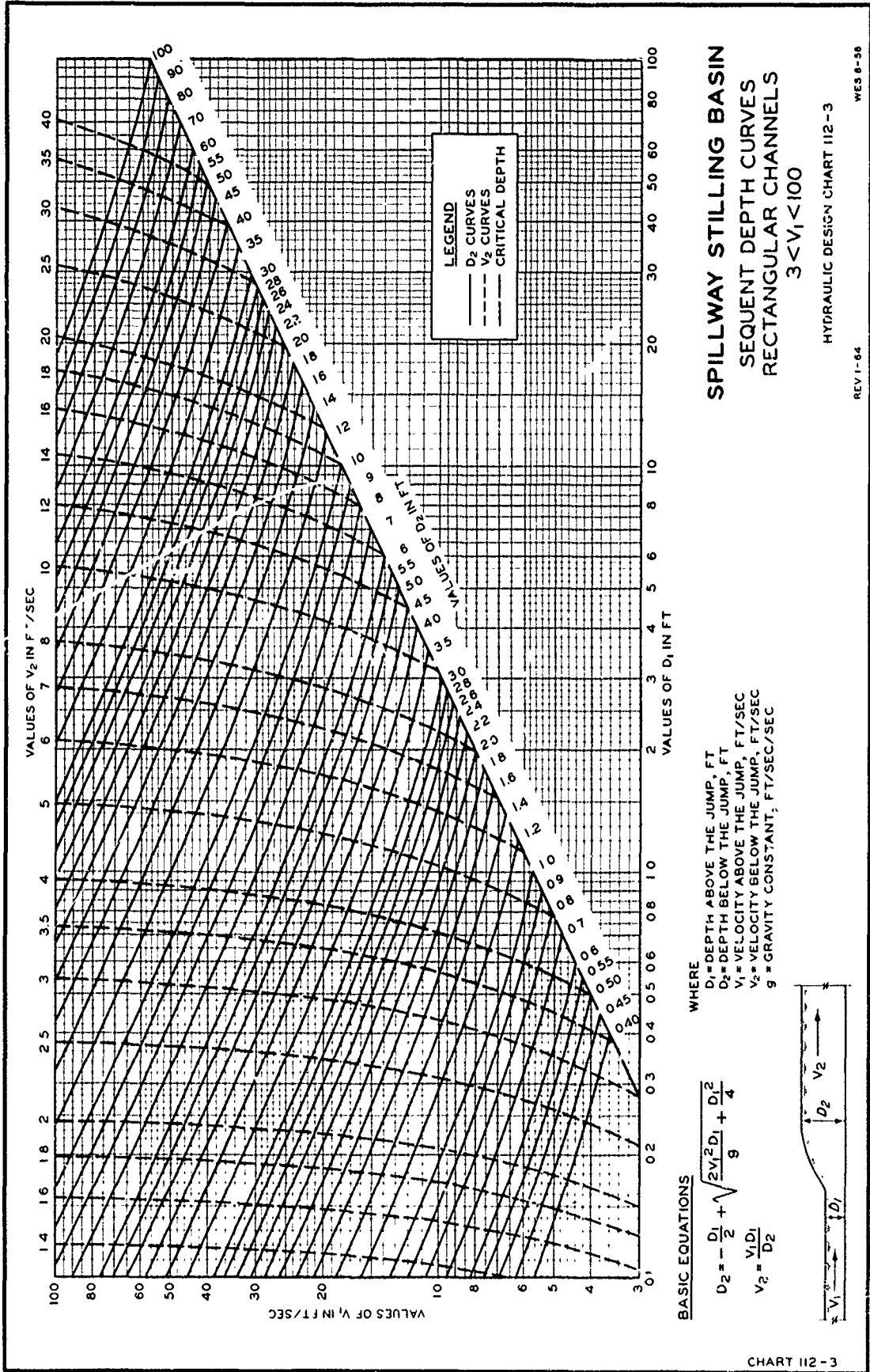
SPILLWAY STILLING BASIN
SEQUENT DEPTH CURVES
RECTANGULAR CHANNELS
$3 < V_1 < 100$

VALUES OF V_2 IN FT/SEC

VALUES OF D_2 IN FT

VALUES OF D_1 IN FT

VALUES OF V_1 IN FT/SEC

LEGEND
— D_2 CURVES
— — V_2 CURVES
— · — CRITICAL DEPTH

BASIC EQUATIONS

$$D_2 = -\frac{D_1}{2} + \sqrt{\frac{2V_1^2 D_1}{g} + \frac{D_1^2}{4}}$$

$$V_2 = \frac{V_1 D_1}{D_2}$$

WHERE
D_1 = DEPTH ABOVE THE JUMP, FT
D_2 = DEPTH BELOW THE JUMP, FT
V_1 = VELOCITY ABOVE THE JUMP, FT/SEC
V_2 = VELOCITY BELOW THE JUMP, FT/SEC
g = GRAVITY CONSTANT, FT/SEC/SEC

WES 8-56

HYDRAULIC DESIGN CHART 112-3

REV 1-64

CHART 112-3

BASIC EQUATION

$$D_2 = -\frac{D_1}{2} + \sqrt{\frac{2V_1^2 D_1}{g} + \frac{D_1^2}{4}}$$

WHERE
D_1 = DEPTH ABOVE THE JUMP – FT
D_2 = DEPTH BELOW THE JUMP – FT
V_1 = VELOCITY ABOVE THE JUMP – FT/SEC
g = GRAVITY CONSTANT – FT/SEC^2

VALUES OF D_2 IN FT

$V_1 = 100$
95
90
85
80
75
70
65
60
55
50
45
40
35
30
25
20
15
$V_1 = 10$

CRITICAL DEPTH

VALUES OF D_1 IN FT

V_1 D_1 D_2 V_2
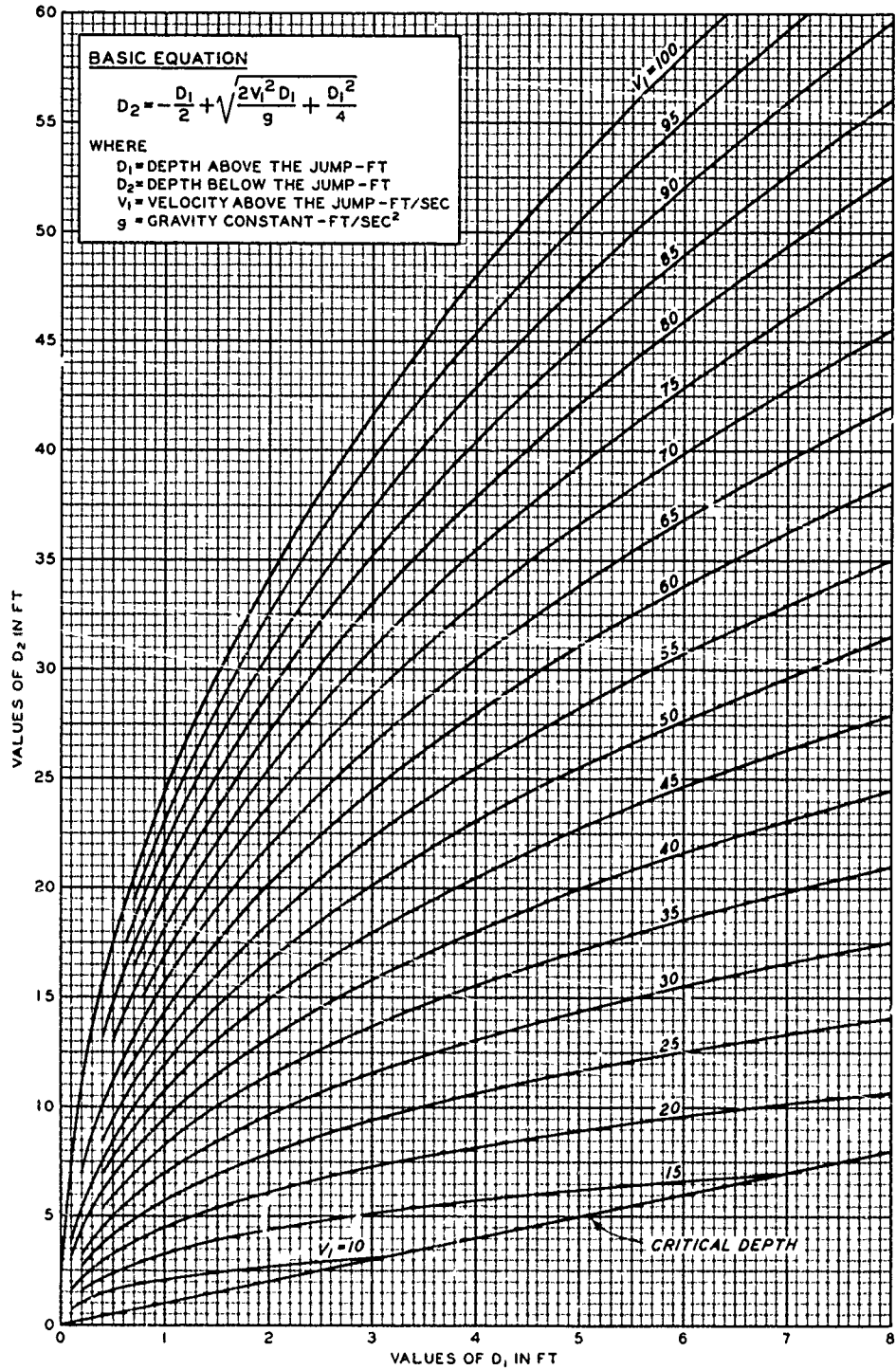
SPILLWAY STILLING BASIN
SEQUENT DEPTH CURVES
RECTANGULAR CHANNELS
$10 < V_1 < 100$

HYDRAULIC DESIGN CHART 112-4

WES 8-58

BASIC EQUATION

$$D_2 = -\frac{D_1}{2} + \sqrt{\frac{2V_1^2 D_1}{g} + \frac{D_1^2}{4}}$$

WHERE:
D_1 = DEPTH ABOVE THE JUMP - FT
D_2 = DEPTH BELOW THE JUMP - FT
V_1 = VELOCITY ABOVE THE JUMP - FT/SEC
g = GRAVITY CONSTANT - FT/SEC^2

VALUES OF D_2 IN FT

VALUES OF D_1 IN FT

CRITICAL DEPTH

$V_1 = 40$, 38, 36, 34, 32, 30, 28, 26, 24, 22, 20, 18, 16, 14, 12, 10, 8, $V_1 = 6$
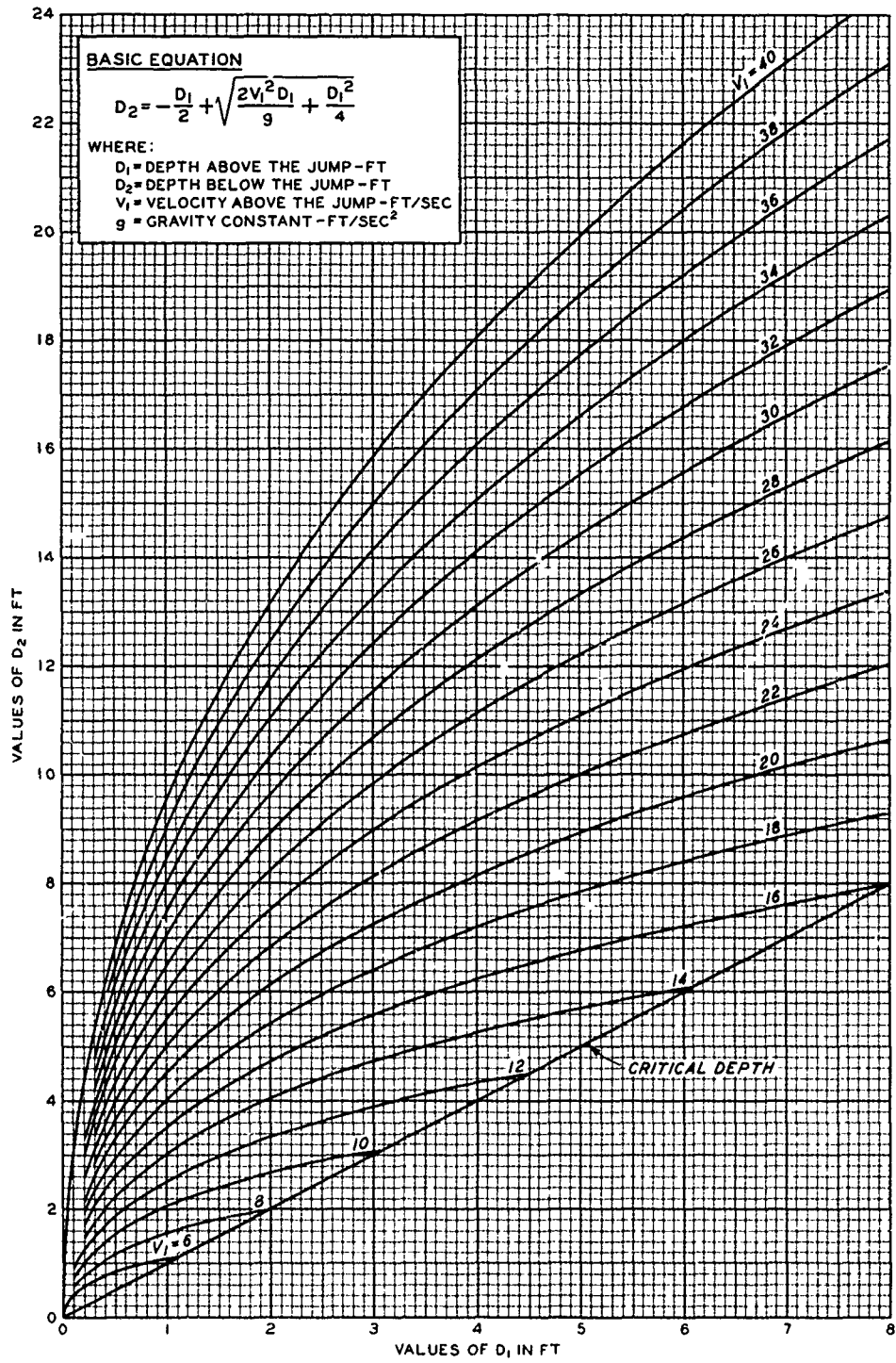
SPILLWAY STILLING BASIN

SEQUENT DEPTH CURVES
RECTANGULAR CHANNELS
$6 < V_1 < 40$

HYDRAULIC DESIGN CHART 112-5

WES 8-58

SPILLWAY STILLING BASINS

END SILL

TAILWATER REDUCTION

1. An end sill is commonly used as the terminal wall of a stilling basin. Where a tailwater deficiency prevents satisfactory hydraulic jump performance and accompanying energy dissipation, the stilling basin floor is set lower than the riverbed and an end sill forms a step, or rise, to the elevation of the bed of the channel. Hydraulic Design Chart 112-5/1 can be used to determine the relation between the Froude number of the entering jet, the sill height, and the downstream depth required for stabilizing the hydraulic jump when baffle piers are not used.

2. The effects of end sill height upon the reduction of flow depth downstream from a sill have been investigated experimentally by Forster and Skrinde.* Chart 112-5/1 reproduces the data and curves published by Forster and Skrinde. The ratio of the depth d_3 over the end sill to the entering depth d_1 is plotted against the Froude number F_1 of the entering flow. The curves represent various ratios of sill height to the upstream depth h/d_1 for basin lengths of $5(h + d_3)$. The dashed line labeled $h/d_1 = 0$ is the theoretical hydraulic jump curve for sequent depths.

3. The design criteria above apply to a stilling basin that requires a vertical end sill or downstream channel invert sufficiently high to produce the tailwater required for formation of the hydraulic jump. The end sill may act as a critical-depth control, and flow into the downstream channel may be very turbulent with supercritical velocities. Excessive wave action, surges, and supercritical velocities may require that increased protection be provided for 100 ft or more downstream of the stilling basin to prevent channel erosion. Careful consideration should be given to the need for increased riprap protection downstream of the stilling basin. In extreme cases lowering of the basin elevation and use of a standard-type stilling basin may be more economical than extensive riprap protection.

---

* J. W. Forster and R. A. Skrinde, "Control of the hydraulic jump by sills." Transactions, American Society of Civil Engineers, vol 115, paper 2415 (1950), pp 973-987.
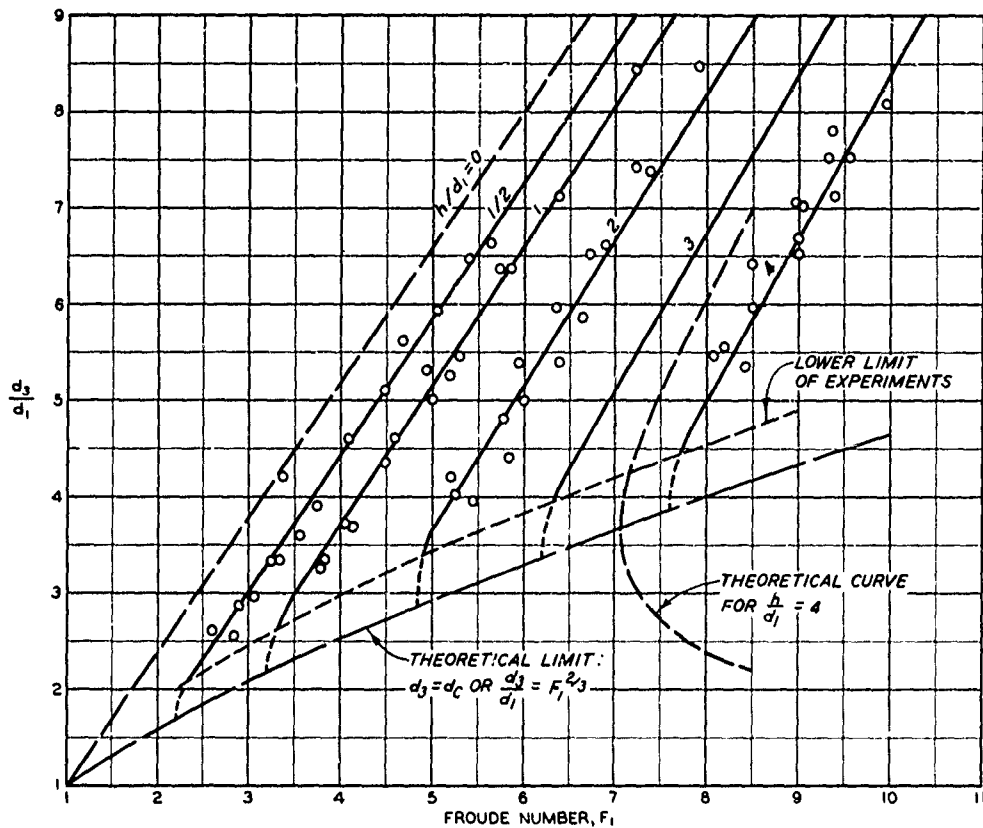
LEGEND

$$F_1 = \frac{V_1}{\sqrt{g\,d_1}}$$

d_c = CRITICAL DEPTH

NOTE CURVES AND DATA BY FORSTER AND SKRINDE
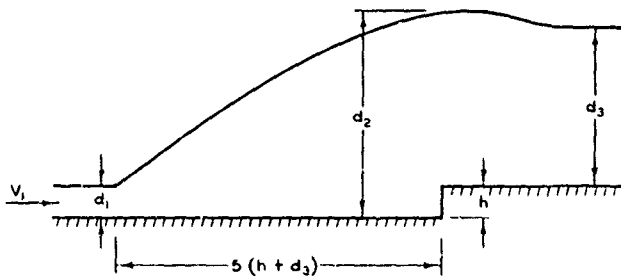
DEFINITION SKETCH

SPILLWAY STILLING BASINS
END SILL
TAILWATER REDUCTION

HYDRAULIC DESIGN CHART 112-5/1

WES 1-6t

HIGH OVERFLOW DAMS

BUCKET-TYPE ENERGY DISSIPATOR

1. Bucket-type energy dissipators are used where excessive tailwater depths prevent adequate energy dissipation by means of a hydraulic jump on a horizontal stilling basin floor. HDC 112-6 and 112-6/1 can be used to estimate probable roller and surge heights for preliminary design purposes.

2. The design curves shown in the charts were developed by McPherson and Karr[1] from extensive laboratory tests wherein the discharge was distributed uniformly over the bucket. The test data have been omitted from the charts in the interest of clarity. The data points shown are from Waterways Experiment Station (WES) studies[2-6] and are in reasonably good agreement with McPherson's and Karr's curves for q parameters $\leq 26 \times 10^{-3}$. The agreement is less satisfactory for higher q parameters. The charts are therefore not considered applicable for q parameter values $> 26 \times 10^{-3}$, and the final design for large structures should be developed by hydraulic model study.

3. The streambed was generally at the same elevation as the bucket invert in the McPherson and Karr tests. In the WES tests, the streambed elevation varied from bucket-lip elevation to below the bucket-invert elevation. However, it is believed that the channel-bed elevation has negligible effect on roller and surge heights.

4. The discharge parameter of the design curves can be related to the Froude number of the entering jet in the following manner:

$$q = V\,d \quad \text{and} \quad V = F\sqrt{gd}$$

Then

$$q = F\,d^{3/2}\,g^{1/2}$$

and

$$\frac{q}{g^{1/2}\,h_1^{3/2}} = \frac{F}{(h_1/d)^{3/2}}$$

where   F = Froude number of entering jet

q = discharge per ft of bucket width, cfs

h_1 = available energy head (pool to bucket invert), ft

d = depth of flow entering bucket, ft

V = velocity of flow entering bucket, fps

5. HDC 112-6/2 illustrates application of HDC 112-6 and 112-6/1 for the preliminary design of bucket-type energy dissipators. The sample computation is for a specific spillway discharge. The full range of spillway flows should be investigated.

6. The WES model data shown in HDC 112-6 indicate that good energy dissipation is obtained when the bucket roller depth h_b is between 75 and 90 percent of the tailwater depth h_2 . For this condition, the surge height is 105 to 130 percent of the tailwater depth.

7. <u>References.</u>

(1) McPherson, M. B., and Karr, M. H., "A study of bucket-type energy dissipator characteristics." <u>ASCE, Hydraulics Division, Journal,</u> vol 83, Paper 1266, No. HY 3 (June 1957); vol 83, Paper 1348, No. HY 4 (August 1957), Corrections, pp 57-64; vol 84, Paper 1832, No. HY 5 (October 1958), Closure, pp 41-48.

(2) U. S. Army Engineer Waterways Experiment Station, CE, <u>Model Studies of Spillway and Regulating Sluices for Wolf Creek Dam, Cumberland River, Kentucky.</u> Technical Memorandum No. 201-1, Vicksburg, Miss., January 1944.

(3) _____, <u>Model Studies of Spillway and Bucket for Center Hill Dam, Caney Fork River, Tennessee.</u> Technical Memorandum No. 202-1, Vicksburg, Miss., August 1946.

(4) _____, <u>Model Study of Spillway and Bucket, Stewarts Ferry Dam, Stones River, Tennessee.</u> Technical Memorandum No. 2-239, Vicksburg, Miss., September 1947.

(5) _____, <u>Spillway for Osceola Dam, Osage River, Missouri; Model Investigation.</u> Technical Memorandum No. 2-261, Vicksburg, Miss., October 1948.

(6) _____, <u>Spillway Design for Whitney Dam, Brazos River, Texas; Model Investigation.</u> Technical Memorandum No. 2-263, Vicksburg, Miss., October 1948.

FIGURES SHOWN ARE
VALUES OF $\dfrac{q}{\sqrt{g}\,h_1^{3/2}} \times 10^3$

LEGEND

		WES			McPHERSON AND KARR	
SYMBOL	PROJECT	$\dfrac{q}{\sqrt{g}\,h_1^{3/2}} \times 10^3$	$\dfrac{h_1}{R}$	$\dfrac{q}{\sqrt{g}\,h_1^{3/2}} \times 10^3$	$\dfrac{h_1}{R}$
○	CENTER HILL (TYPE 1 - HIGH)	14-53	3 9-4 4	5	6
□	CENTER HILL (TYPE 1 -LOW)	13-48	4 1-4 7	10	6-7
△	OSCEOLA (ORIGINAL)	30-106	1 7-2 1	15	3-8
▽	OSCEOLA (TYPE 1)	30-106	2 1-2 6	26	3-6
■	STEWARTS FERRY (TYPE 1)	24-75	2 7-3 2	40	2-6
▲	WHITNEY (TYPE 1)	8-77	2 4-3 0	60	2-6
▼	WOLF CREEK (TYPE 1)	11-47	4 0-4 5	90	2-5

NOTE DESIGN CURVES SHOWN DEVELOPED BY McPHERSON AND
KARR FROM EXPERIMENTAL DATA THESE DATA
OMITTED TO SIMPLIFY CHART

RANGES OF VARIABLES

	WES	McPHERSON AND KARR
SPILLWAY SLOPE	1 41-1 67 1	1 1
LIP ANGLE	45°	45°
H/h_1	0 68-0 93	>0 75
h_1/R	SEE LEGEND	
$q/\sqrt{g}\,h_1^{3/2} \times 10^3$	SEE LEGEND	

DEFINITION SKETCH

HIGH OVERFLOW DAMS
BUCKET-TYPE ENERGY DISSIPATOR
ROLLER DEPTH

HYDRAULIC DESIGN CHART 112-6

LEGEND

		WES		McPHERSON AND KARR	
SYMBOL	PROJECT	$\dfrac{q}{\sqrt{g}h_1^{3/2}} \times 10^3$	$\dfrac{h_1}{R}$	$\dfrac{q}{\sqrt{g}h_1^{3/2}} \times 10^3$	$\dfrac{h_1}{R}$
O	CENTER HILL (TYPE 1-HIGH)	14-53	3 9-4 4	5	6
□	CENTER HILL (TYPE 1-LOW)	13-48	4 1-4.7	10	6-7
▲	OSCEOLA (ORIGINAL)	30-106	1 7-2 1	13	3 8
▼	OSCEOLA (TYPE 1)	30-106	2 1-2 6	26	3-6
▣	STEWARTS FERRY (TYPE 1)	24-75	2 7-3 2	40	2-6
▲	WHITNEY (TYPE 1)	8-77	2 4-3 0	60	2-6
▼	WOLF CREEK (TYPE 1)	11-47	4 0-4 5	90	2-5

FIGURES SHOWN ARE VALUES
OF $\dfrac{q}{\sqrt{g}h_1^{3/2}} \times 10^3$

$h_b = h_s$

$h_b = 0.15\, h_s$

FREE JET

vertical axis: $\dfrac{h_b}{h_1}$

horizontal axis: $\dfrac{h_s}{h_1}$

NOTE: DESIGN CURVES SHOWN DEVELOPED BY McPHERSON
AND KARR FROM EXPERIMENTAL DATA THESE
DATA OMITTED TO SIMPLIFY CHART

RANGES OF VARIABLES

	WES	McPHERSON AND KARR
SPILLWAY SLOPE	1 41-1 67 1	1 1
LIP ANGLE	45°	45°
H/h₁	0 68-0 93	>0 75
h₁/R	SEE LEGEND	
q/√gh₁³/²×10³	SEE LEGEND	

POOL
ROLLER
SURGE
TW

DEFINITION SKETCH

HIGH OVERFLOW DAMS
BUCKET-TYPE ENERGY DISSIPATOR
SURGE HEIGHT

HYDRAULIC DESIGN CHART 112-6/1

REV 1-66

WES 5-59

COMPUTATION FOR PRELIMINARY DESIGN

GIVEN:
- Discharge (q) per ft of basin width = 450 cfs
- Pool elevation = 765 ft
- Tailwater elevation = 650 ft
- Radius of bucket = 50 ft
- Slope of bucket lip = 45 deg
- Spillway slope = 10:6.1
- Ratio of H to h_1 >0.75

ASSUME:
- Bucket invert elevation = 550 ft
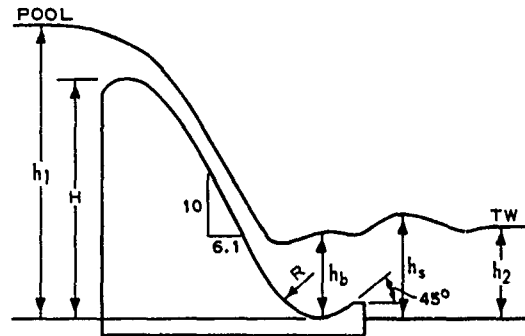
COMPUTE:

1. h_1 = pool elevation − bucket invert elevation
   = 765 − 550 = 215 ft

2. h_2 = tailwater elevation − bucket invert elevation
   = 650 − 550 = 100 ft

3. $h_2/h_1 = 100/215 \approx 0.465$

4. Discharge parameter

$$\frac{q}{\sqrt{g}\, h_1^{3/2}} \times 10^3 = \frac{450 \times 10^3}{\sqrt{32.2}\,(215)^{3/2}}$$

$$= \frac{450 \times 10^3}{5.68 \times \;\; ?}$$

$$\approx 25$$

5. From Chart 112-6 read $h_b/h_1 = 0.42$ for $h_2/h_1 = 0.465$ and

$$\frac{q}{\sqrt{g}\, h_1^{3/2}} \times 10^3 = 25$$

Note: Good energy dissipation is indicated if the roller height (h_b) is between 75 and 90 percent of the tailwater depth (h_2).

6. $h_b \approx 0.42 \times h_1$
   $\approx 0.42 \times 215 = 90$ ft

7. From Chart 112-6/1 read $h_s/h_1 = 0.52$ for $h_b/h_1 = 0.42$ and

$$\frac{q}{\sqrt{g}\, h_1^{3/2}} \times 10^3 = 25$$

8. $h_s \approx 0.52 \times h_1$
   $\approx 0.52 \times 215 = 112$ ft

9. Compute h_b and h_s for full range of spillway flows.

10. Determine maximum elevation of bucket roller and surge.

HIGH OVERFLOW DAMS
BUCKET−TYPE ENERGY DISSIPATOR
SAMPLE COMPUTATION
HYDRAULIC DESIGN CHART 112 - 6/2

HIGH OVERFLOW DAMS

ENERGY DISSIPATORS

FLIP BUCKET AND TOE CURVE PRESSURES

1. Hydraulic forces acting on high, overflow spillway flip buckets and toe curves are of interest in the structural design of these devices. Theoretical studies and model and prototype data indicate that the bottom pressures change continuously throughout the curve and are influenced by the curve radius, the total head, and the unit discharge. It has also been shown that the pressures immediately upstream and, in the case of the toe curve, downstream of the curve are influenced by the curvature. Rouse[3] illustrates the application of the flow net solution to this problem.

2. **Flip Buckets.** Approximate techniques, including use of the centrifugal force equation[2] and a vortex analogy,[1,2] have been suggested for computing the pressures on spillway flip buckets. A recent WES study[7] using a theoretical approach similar to vortex analogy suggested by Douma[2] indicated that, for relatively high dams, bucket pressures could be expressed as:

$$\frac{h_p}{H_T} = f\left(\frac{q}{R\sqrt{2g\,H_T}} \,,\, \frac{\alpha}{\alpha_T}\right)$$

where

h_p = pressure head against boundary, ft

H_T = total head (point to energy gradient), ft

q = unit discharge, cfs

R = radius of curve, ft

g = acceleration due to gravity, ft per sec per sec

α = angle of rotation from beginning of curve, degrees

α_T = total deflection angle, degrees

The term α/α_T defines the relative position along the curve.

3. HDC 112-7 presents dimensionless flip bucket pressure curves based on Pine Flat[4] and Hartwell[5] model spillway data analyzed in

accordance with the preceding expression. Spillway energy losses were assumed negligible in the analysis. The plotted data for α/α_T from 0.25 to 0.75 indicate that the pressure in the middle portion of the bucket is nearly constant. Therefore, the pressure distribution through the bucket can be adequately defined by the four curves shown in the chart. The curve for $\alpha/\alpha_T = 1.0$ coincides with the axis of the chart ordinates since the pressure on the lower nappe of the jet leaving the bucket is atmospheric. The Pine Flat[6] prototype data plotted on the chart indicate satisfactory correlation with the model data. Allowances were made for spillway energy losses in computing the total head H_T for the prototype data.

4. <u>Toe Curves.</u> The available data[8] from model tests conducted under the Corps of Engineers Engineering Studies Item 801 which are plotted in HDC 112-7 indicate that for a high dam the flip bucket pressure distribution curves generally apply to spillway toe curves. However, the data show that the pressure at the end of the toe curve approximates that at the beginning of the curve if the toe curve is not submerged.

5. HDC 112-7 can be used to estimate the pressure distribution on spillway flip buckets or toe curves associated with high overflow dams. However, for design purposes, allowance for spillway energy losses should be included in the computations of H_T required for use of the chart. The user is cautioned that the curves are not applicable to toe curves affected by submergence.

6. <u>References.</u>

(1) Balloffet, A., "Pressures on spillway flip buckets." <u>Journal of the Hydraulics Division, American Society of Civil Engineers</u> (September 1961), pp 87-96.

(2) Douma, J. H., discussion of paper, "Design of side walls in chutes and spillways," by D. B. Gumensky. <u>Transactions, American Society of Civil Engineers</u>, vol 119 (1954), pp 364-367.

(3) Rouse, H., <u>Engineering Hydraulics.</u> John Wiley and Sons, Inc., New York, N. Y., 1950, p 47.

(4) U. S. Army Engineer Waterways Experiment Station, CE, <u>Spillway and Conduits for Pine Flat Dam, Kings River, California; Hydraulic Model Investigation.</u> Technical Memorandum No. 2-375, Vicksburg, Miss., December 1953.

(5) _____, <u>Sluice Outlet Portal and Spillway Flip Bucket, Hartwell Dam, Savannah River, Georgia; Hydraulic Model Investigation.</u> Technical Memorandum No. 2-393, Vicksburg, Miss., August 1954.

(6) _____, <u>Prototype Tests of Spillway Crest and Flip Bucket, Pine Flat Dam, Kings River, California.</u> Technical Report No. 2-511, Vicksburg, Miss., June 1959.

(7) U. S. Army Engineer Waterways Experiment Station, CE, <u>An Investigation of Spillway Bucket and Toe Curve Pressures.</u> Miscellaneous Paper No. 2-625, Vicksburg, Miss., February 1964.

(8) _____, unpublished ES 801 data.

α/α_T = 1.0 (FLIP BUCKETS)

$\frac{q}{R\sqrt{2gH_T}}$

α/α_T = 0 (TOE CURVES)
α/α_T = 1.0 (TOE CURVES)
α/α_T = 0.85
α/α_T = 0.25-0.75

NOTE NUMBERS ARE VALUES
OF (α/α_T) X 10² FOR
DATA POINTS

$\frac{h_P}{H_T}$

ENERGY GRADIENT

H_T

q

R

h_P $α_T$
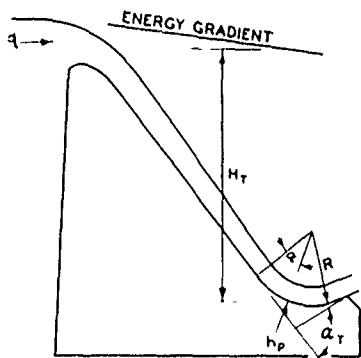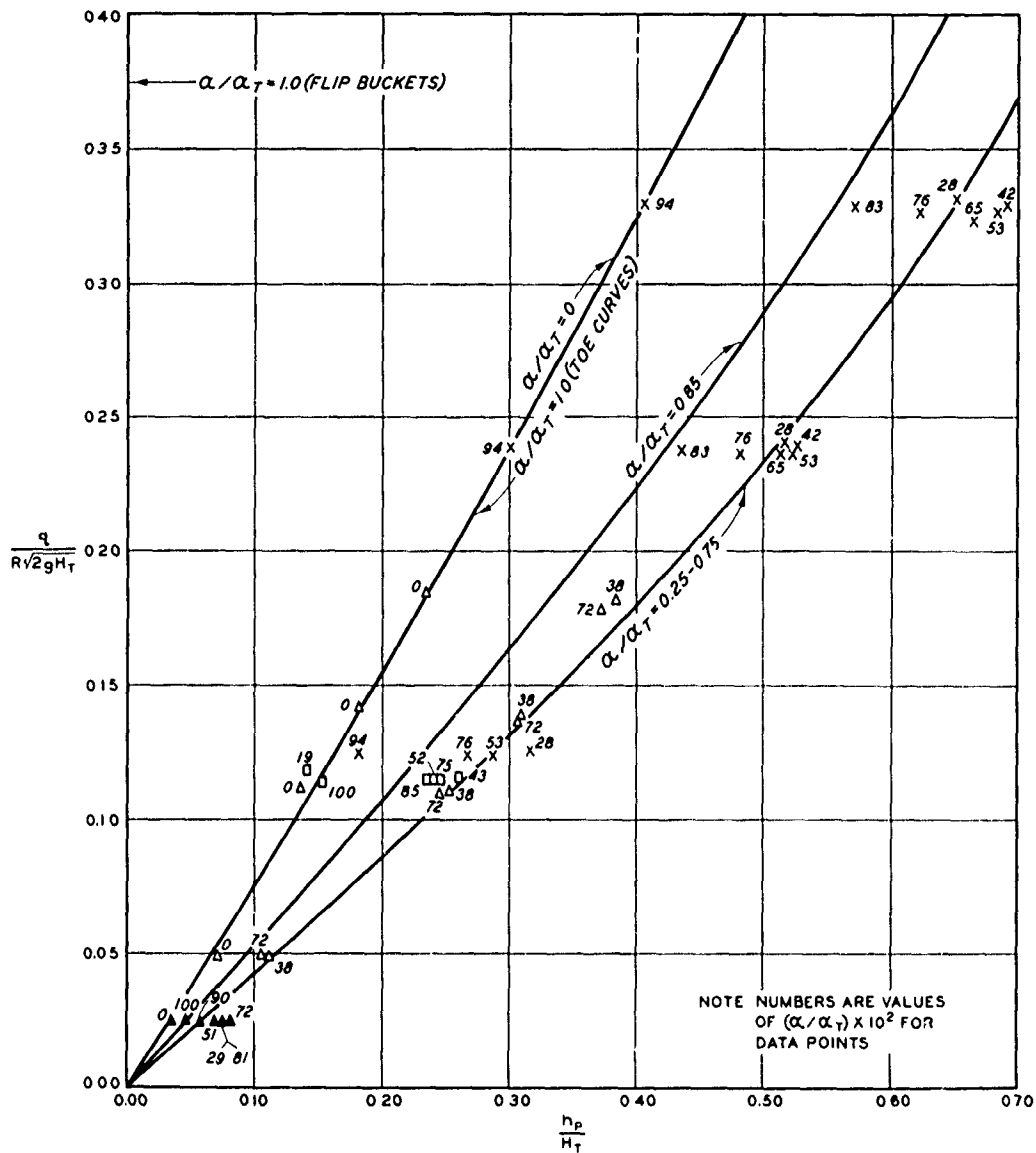
DEFINITION SKETCH

LEGEND

△ PINE FLAT MODEL
X HARTWELL MODEL
▲ PINE FLAT PROTOTYPE
□ ES 801 (TOE CURVE)

HIGH OVERFLOW DAMS

ENERGY DISSIPATORS

FLIP BUCKET AND TOE CURVE PRESSURES

HYDRAULIC DESIGN CHART 112-7

REV 1-64

WES 10-61

PREPARED BY U. S. ARMY ENGINEER WATERWAYS EXPERIMENT STATION, VICKSBURG, MISSISSIPPI

HIGH OVERFLOW DAMS

ENERGY DISSIPATORS

FLIP BUCKET THROW DISTANCE

1. For economy, flip bucket or ski-jump energy dissipators are some-times used when spray from the jet can be tolerated and erosion by the plunging jet will not be a problem. Flip buckets have caused trouble in climates where spray from the jet resulted in icing of nearby roadways or electrical equipment. The major amount of energy dissipation occurs in the region where the jet plunges into the tailwater; a minor amount occurs as the jet frays after leaving the bucket.

2. Factors affecting the horizontal throw distance from the bucket lip to point of jet impact are the initial velocity of the jet, the bucket lip angle, and the difference in elevation between the lip and the tailwater.

3. HDC 112-8 presents throw-distance curves for lip angles of 0 to 45 degrees. The horizontal throw distance X and the vertical drop from the bucket lip to tailwater Y are expressed in terms of the jet velocity head H_V. The following expression based on the theoretical equations for trajectories was used for developing the curves:

$$X/H_V = \sin 2\theta + 2 \cos \theta \sqrt{\sin^2 \theta + Y/H_V}$$

where

X = throw distance, ft
Y = vertical drop from lip to tailwater surface, ft
H_V = velocity head of jet at bucket lip, ft
θ = bucket lip angle, deg

4. HDC 112-8 is a guide for judging the point of impact of the jet. The throw distance may be substantially less than indicated, depending upon spillway energy losses. Prototype measurements of spillway energy losses are needed to permit a comparison of theoretical and actual throw distances.

EQUATION

$$\frac{X}{H_V} = \text{SIN } 2\theta + 2 \text{ COS } \theta \sqrt{\text{SIN}^2\theta + \frac{Y}{H_V}}$$
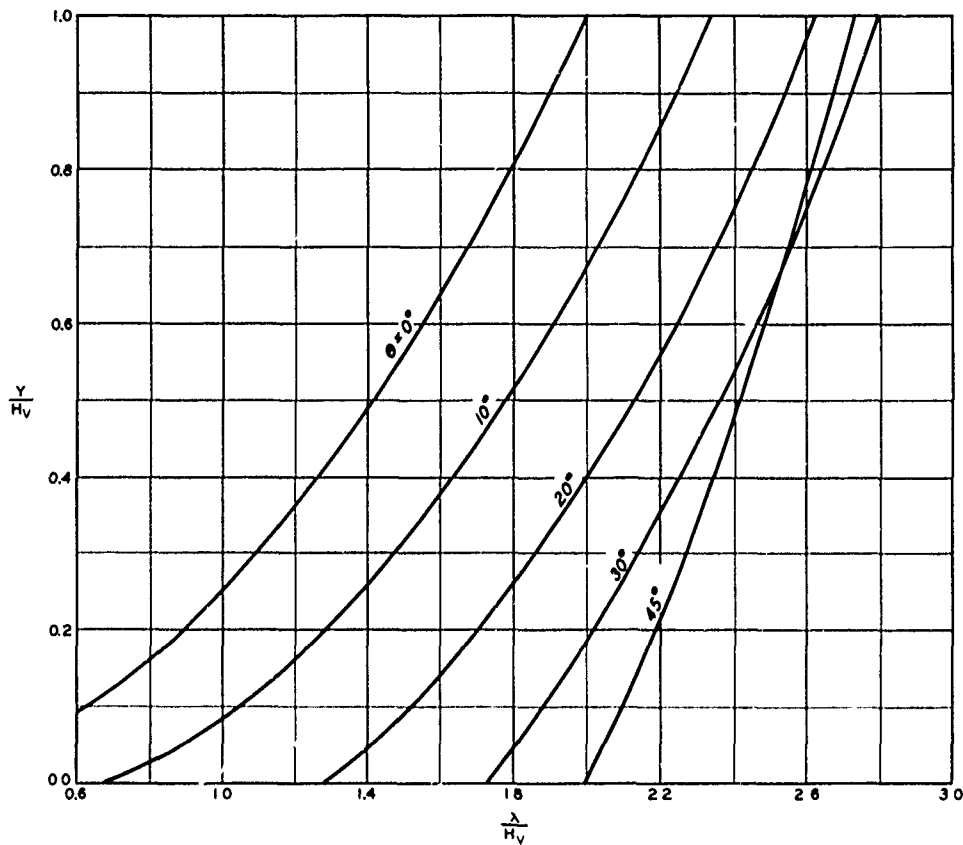
WHERE

X = THROW DISTANCE, FT

θ = BUCKET LIP ANGLE

H_V = VELOCITY HEAD AT BUCKET LIP, FT

Y = VERTICAL DROP FROM LIP TO TAILWATER SURFACE, FT
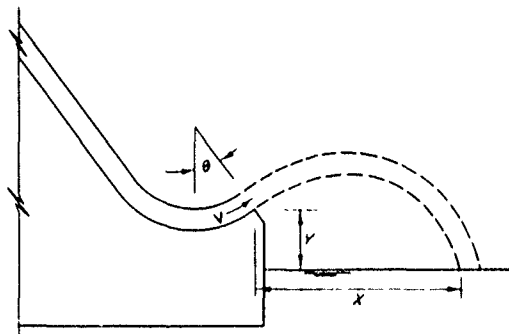
DEFINITION SKETCH

HIGH OVERFLOW DAMS

ENERGY DISSIPATORS
FLIP BUCKET THROW DISTANCE

HYDRAULIC DESIGN CHART 112-8

WES 10-61

LOW OGEE CREST

DISCHARGE COEFFICIENTS

APPROACH DEPTH EFFECTS

1. Bureau of Reclamation (USBR) Tests. Figure 15B of the USBR Boulder Canyon report* shows the relation between discharge coefficient C and the ratio of head to height of crest. As the coefficients are derived from the tests of a sharp-crested weir, the shape of the lower surface varies as the velocity of the approach flow is varied.

2. WES Tests. Tests at the WES to determine approach depth effects on discharge coefficients were conducted with a standard crest based on a design head of 0.75 ft. The velocity of the approach flow was varied by raising or lowering the false floor in the model which simulated the bottom of the approach channel. Negative pressures were found on the crest at the higher velocities of approach flow and the resulting coefficients are higher than the corresponding USBR coefficients based on sharp-crested weir flows. The portions of the curves for values of $H_e/H_d > 0.5$ in HDC 122-1 represent the WES test data. The basis of the portions of the curves for $H_e/H_d < 0.5$ is the prototype data plotted in HDC 111-3. The curve for $P/H_d = 1.33$ is identical with the curve for high overflow dams shown in HDC 111-3. The curves of P/H_d versus C at the top of HDC 122-1 are included to facilitate interpolation between the three basic curves.

3. The purpose of HDC 122-1 is to show the effects of approach depth on the discharge coefficient for the standard spillway shape shown in HDC 111-1 to 111-2/1.

---

* U. S. Bureau of Reclamation, Studies of Crests for Overfall Dams, Boulder Canyon Project. Final Reports, Part VI-Hydraulic Investigations, Bulletin 3, Denver, Colo., 1948.
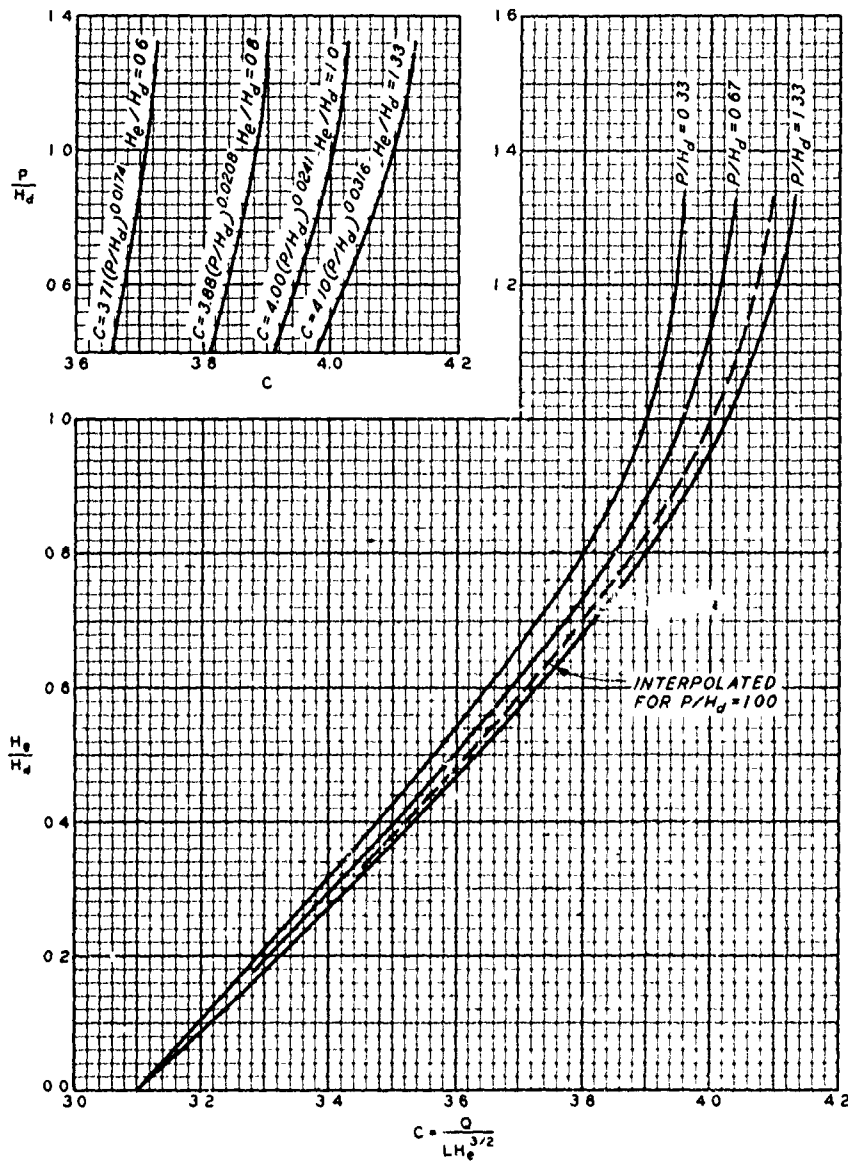
NOTE H_e = ENERGY HEAD ON CREST, FT
       H_d = DESIGN HEAD ON CREST, FT
       C = DISCHARGE COEFFICIENT
       Q = DISCHARGE, CFS
       L = NET LENGTH OF CREST, FT
       P = HEIGHT OF CREST ABOVE
           APPROACH CHANNEL, FT

LOW OGEE CREST
DISCHARGE COEFFICIENTS
APPROACH DEPTH EFFECTS

HYDRAULIC DESIGN CHART 122-1

REV 1-64   REV 6-57   WES 4-52

PREPARED BY U S ARMY ENGINEER WATERWAYS EXPERIMENT STATION, VICKSBURG, MISSISSIPPI

SPILLWAY CREST

LOW OGEE CREST DISCHARGE COEFFICIENTS

1. Purpose. Hydraulic Design Chart 122-1/1 may be used for preliminary economic studies in which a number of crest lengths and heights are to be investigated. This chart shows the effects of spillway approach depth and apron elevation on the discharge coefficient for $H_e = H_d$.

2. Basic Data. The basic data resulting in the curve shown on Chart 122-1/1 were obtained from tests made on the standard crest shape at the Waterways Experiment Station under CW 801, "General Spillway Investigations." Approach depths of 0.2 to 1.33 H_d and apron heights of 0.13 to 1.0 H_d were used in the investigation. Toe curve radii of 0.0, 0.5, and 1.0 H_d were studied.

3. Discharge coefficients were determined first for various approach depths with the apron low and then for various apron elevations with the approach floor low for the crest shape shown. The ratios of the coefficients for different approach depths to the coefficient for an approach depth of 1.33 H_d were computed. These ratios were multiplied by the discharge coefficients for numerous apron elevations to estimate coefficients reflecting the combined effect of approach depths and apron heights.

4. Adequacy of Curve. The curve shown on Chart 122-1/1 is believed to be the best estimate of a coefficient for low ogee crests that can be made until test data become available for actual combinations of shallow approach depths and high apron elevations.

122-1/1

1.4

1.2

1.0

P/H_d 0.8

0.6

0.4

0.2

3.60   3.70   3.80   3.90   4.00   4.10

$C = Q/LH_e^{3/2}$

$H_e = H_d$

$X^{1.85} = 2.0 H_d^{0.85} Y$

$R = 0.5 H_d$

P
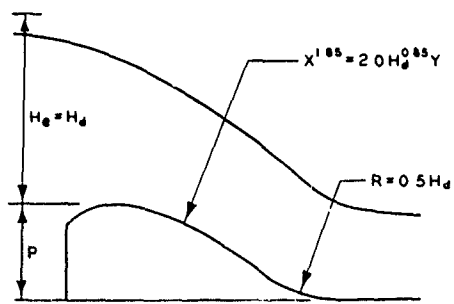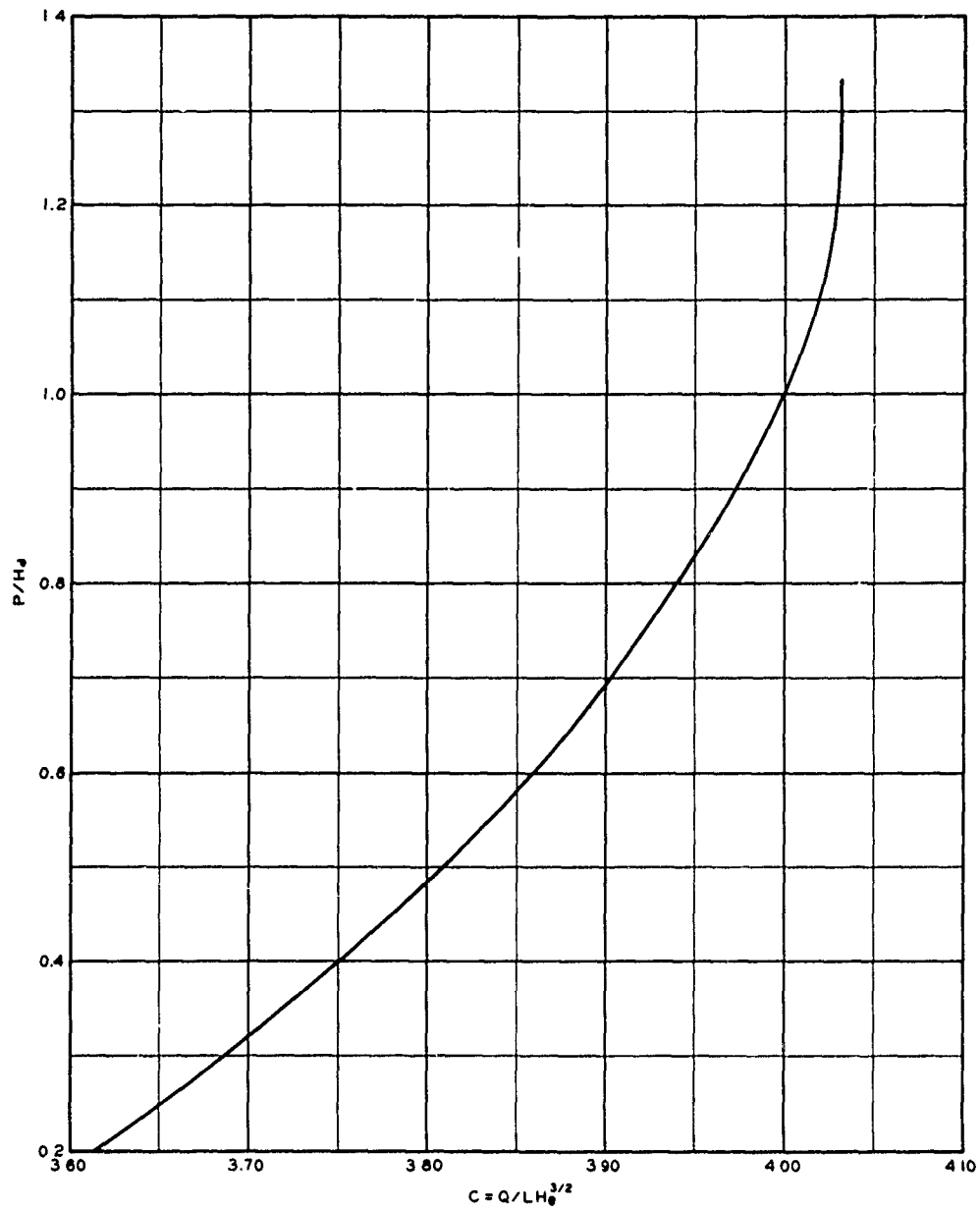
LOW OGEE CRESTS
DISCHARGE COEFFICIENTS
DESIGN HEAD

HYDRAULIC DESIGN CHART 122-1/1

WES 6-57

HYDRAULIC DESIGN CRITERIA

SHEET 122-1/2

OVERFLOW SPILLWAYS

DISCHARGE COEFFICIENTS

DESIGN HEAD

1. **Purpose.** Hydraulic Design Chart 122-1/2 can be used for selecting the spillway design head for upstream spillway face slope and approach depth conditions not covered by other Hydraulic Design Criteria charts. The chart, used in conjunction with the USBR[1] extensive tables of lower and upper nappe surface coordinate data for weirs sloping downstream and for vertical weirs, should permit optimization of spillway crest shape design for free overfall spillways having upstream face slope ratios from 3V on 12H to vertical and approach depths from 0.15 to 10 times the design head (H_d).

2. **Background.** The USBR tests were made in a 2-ft-wide, 9-ft-deep rectangular flume. Approach depths varied from less than 0.1 ft to 5 ft. Heads on the sharp-crested weirs ranged from about 0.1 to 1.0 ft. Discharge coefficients have been converted into values applicable to heads on the rounded crest. USBR coordinates of the upper and lower nappes of the weir overflow are in terms of the head on the sharp-crested weir. Comparable presentations of Bazin's[2] data for weirs sloping downstream (3V on 6H and 3V on 12H) are also included on the chart and in the USBR tabulation. A plot of the WES experimental data (Chart 122-1) for $H/H_d = 1$ and $P/H_d = 0.3$ to 1 is included for comparison. The WES discharge coefficients for rounded crests have consistently b..n about 3 percent higher than comparable USBR coefficients for sharp-crested weirs (HDC 122-4). The use of the USBR coefficients for the design of unmodeled spillways should result in conservative design.

3. **Application.** The spillway design flow Q_d is computed using an appropriate coefficient from Chart 122-1/2 and pier and abutment contraction coefficients from other applicable charts (see Charts 111-3/1, 111-3/2, 111-5, 116-6, and 122-2). The spillway design head H_d and the computed design discharge Q_d are then used with Chart 111-3/3 to develop a spillway rating curve for uncontrolled flow as described in paragraph 5a of Sheet 111-3/3.

4. **References.**

(1)   U. S. Bureau of Reclamation, Studies of Crests for Overfall Dams; Hydraulic Investigations. Bulletin 3, Part VI, Boulder Canyon Project Final Reports, Denver, Colo., 1948

(2)   Bazin, M., "Recent experiments on the flow of water over weirs." Annales des Ponts et Chaussees, October 1888.

OVERFLOW SPILLWAYS
DISCHARGE COEFFICIENTS
DESIGN HEAD

HYDRAULIC DESIGN CHART 122-1/2
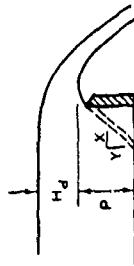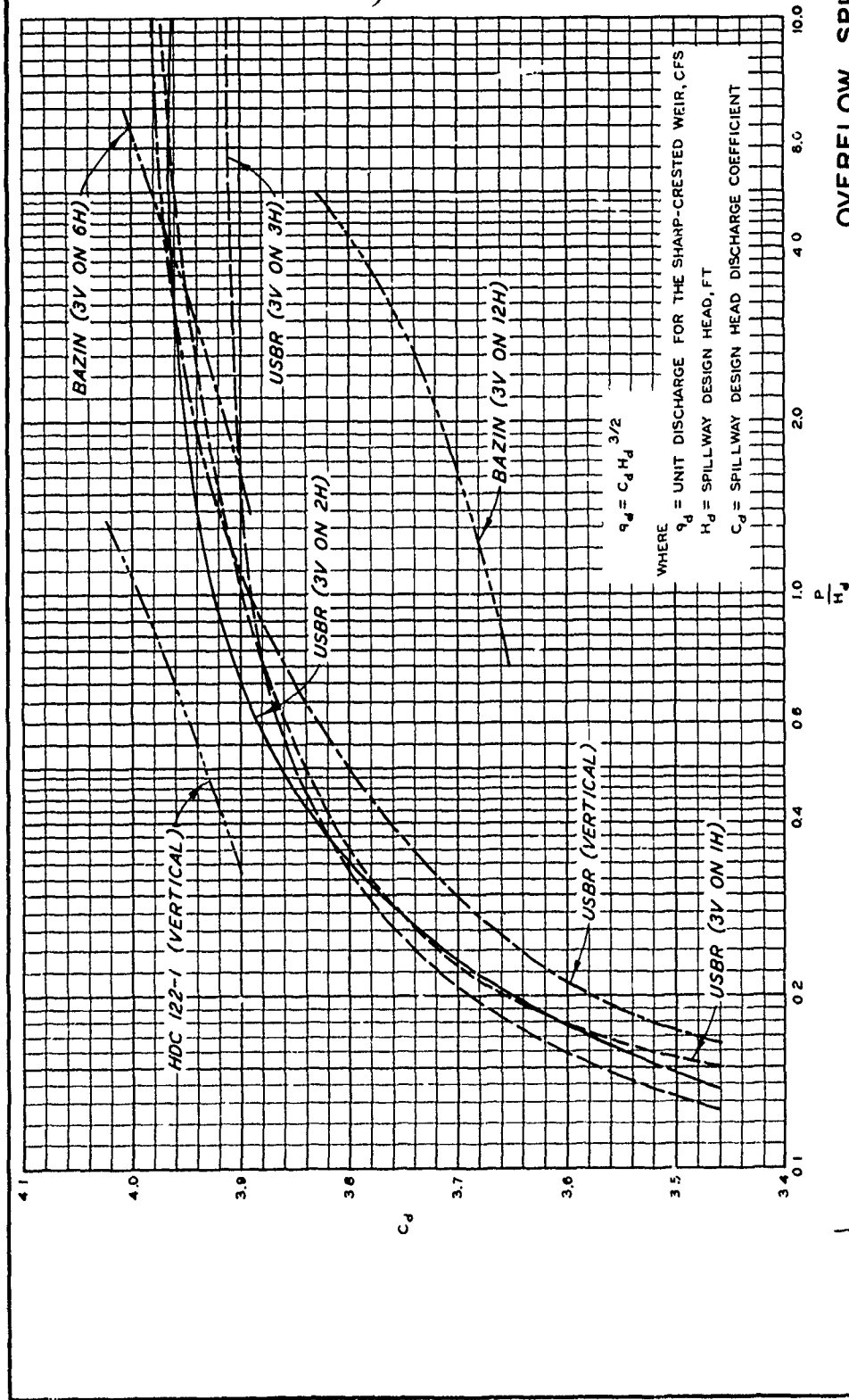
WES 2-72

NOTE   CURVES BASED ON FIGURES 15 AND 21, BULLETIN 3,
PART VI, BOULDER CANYON PROJECT, FINAL REPORT.
USBR 1948.

$$q_d = C_d H_d^{3/2}$$

WHERE

q_d = UNIT DISCHARGE FOR THE SHARP-CRESTED WEIR, CFS

H_d = SPILLWAY DESIGN HEAD, FT

C_d = SPILLWAY DESIGN HEAD DISCHARGE COEFFICIENT

BAZIN (3V ON 6H)

USBR (3V ON 3H)

USBR (3V ON 2H)

HDC 122-1 (VERTICAL)

USBR (VERTICAL)

USBR (3V ON 1H)

BAZIN (3V ON 12H)

$\frac{P}{H_d}$

C_d

LOW OGEE CRESTS

PIER CONTRACTION COEFFICIENTS

1. The data shown on Hydraulic Design Chart 122-2 were derived from the same series of CW 801 tests which are represented on Charts 111-5 and 111-6. The general remarks on Sheets 111-5 and 111-6 are equally applicable to the accompanying chart. The purpose of Chart 122-2 is to show the effect of velocity head of approach upon the pier contraction coefficient. The elevation of the approach floor was varied to produce various approach velocities with the type 2 pier. The effect of the approach depth on the coefficient for other pier types has not been determined. In the absence of adequate experimental data, pier contraction coefficients for types 1, 3, and 4 piers may be obtained by proportioning from Chart 111-5.

TYPE 2 PIER

0.133 H_d RAD

0.267 H_d

TYPE 2 PIER

H_d = DESIGN HEAD

$X^{1.85} = 2H_d^{0.85} Y$

0.5 H_d RAD

0.2 H_d RAD

AXIS OF SPILLWAY CREST

0.200 H_d

0.333 H_d

0.667 H_d

1.333 H_d

RATIO OF VERTICAL DISTANCE TO DESIGN HEAD

RATIO OF HORIZONTAL DISTANCE TO DESIGN HEAD

1.333 H_d

6.667 H_d

0.333 H_d

0.667 H_d

0.200 H_d

DESIGN HEAD

RATIO OF HEAD ON CREST TO DESIGN HEAD — H_e/H_d

COEFFICIENT OF PIER CONTRACTION — K
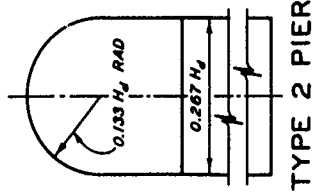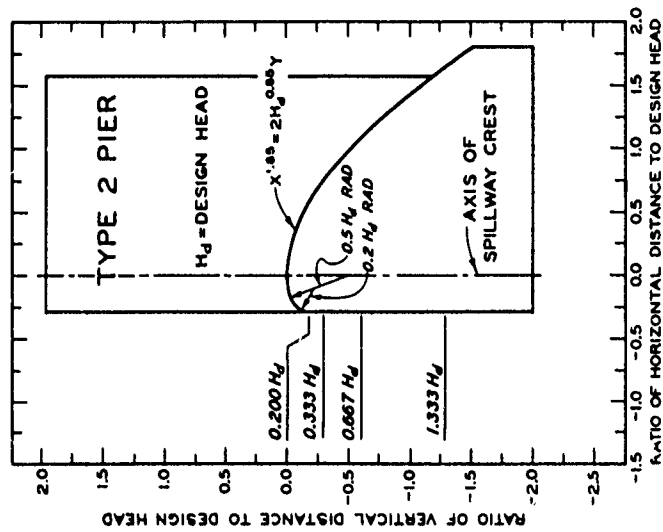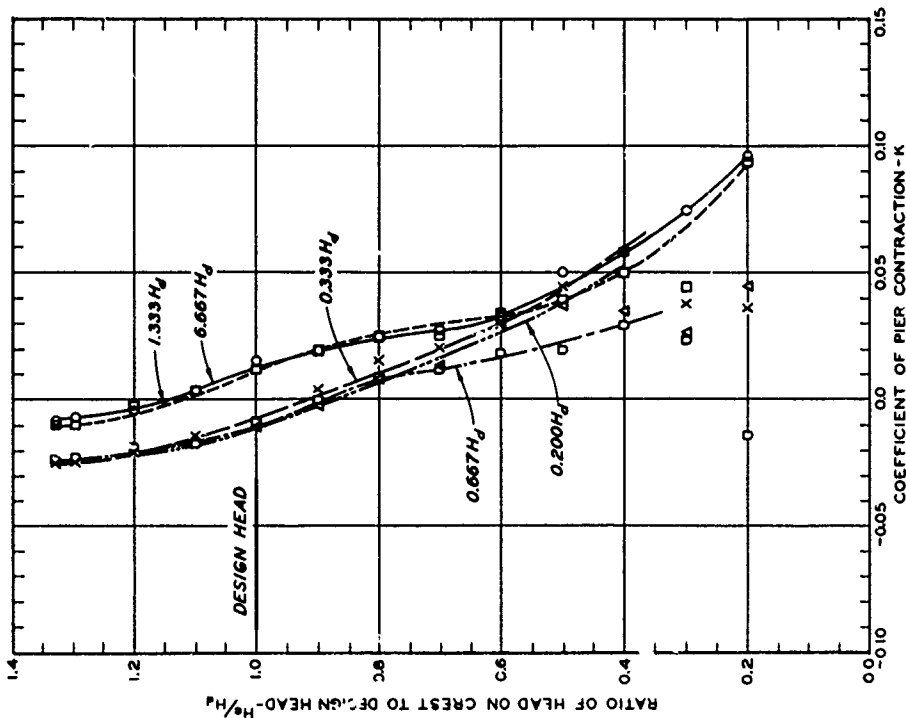
LOW GATED OGEE CRESTS
PIER CONTRACTION COEFFICIENTS
EFFECT OF APPROACH DEPTH

HYDRAULIC DESIGN CHART 122-2

WES 4-1-53

CHART 122-2

1. <u>General.</u> The upstream face of low, ogee spillway crests subjected to high heads are often sloped for structural stability. Coordinates of the lower nappe profile for sharp-crested weirs sloping 45 degrees downstream and various approach depths have been determined and published by the USBR.[1] The published coordinates are in terms of the head on the sharp-crested weir.

2. For low, ogee crests, the head is defined as the total energy head upstream from the spillway crest, and the approach depth as the height of the spillway crest above the approach channel bottom. For convenience of design, the shape downstream from the apex of the crest is considered separately from the shape upstream. The USBR[2] has published curves for determining the location of the apex of the crest, and for selecting coefficients and powers applicable to the general downstream-quadrant crest shape equation of a somewhat different form from that used by the Corps of Engineers.

$$\frac{Y}{H_d} = K \left(\frac{X}{H_d} \right)^n \qquad \text{USBR form}$$

$$X^n = \frac{1}{K} H_d^{(n-1)} Y \qquad \text{Corps of Engineers form}$$

The published curves have been confirmed by an independent WES study of the USBR data for weirs sloping 45 degrees downstream.

3. <u>Preferred Shapes.</u> HDC 122-3 shows the relation between the approach depth P and the approach velocity head h_a in terms of the design head H_d based on the USBR data.[1] The increments of h_a/H_d used in the original study were fairly close together, although the actual shape change is not great until the velocity of the approach flow becomes substantial. Three preferred shapes which would be considered reasonable for a range of h_a/H_d, and their corresponding values of P/H_d are indicated in HDC 122-3. These three selected crest shapes are suggested for projects subject to model testing to provide information systematically and economically on pressure characteristics and discharge coefficients. For cases in which model studies are not contemplated, use of the published USBR

data[1] for crest shape design may be desirable pending model confirmation of the preferred shapes.

4. <u>Downstream Quadrant Shape.</u> HDC 122-3/1 presents the published USBR curves for the coefficient K and exponent n of the downstream-quadrant shape equation. The curves are applicable to approach velocity head-design head ratios h_a/H_d of 0.00 to 0.20. The USBR curves of X_e/H_d and Y_e/H_d for locating the apex of the crest are also given in the chart. Downstream quadrant equations for spillways having approach velocity head-design head ratios of 0.08 and 0.12 are given in HDC 122-3/2 and 122-3/3, respectively. The condition of $h_a/H_d = 0.00$ is presented in HDC 111-9. The coefficients in the equations given in these charts as noted in paragraph 2 are reciprocals of those given in HDC 122-3/1. Tables of the functions required in the evaluation of the equations are not available elsewhere; consequently, they are included in the charts to assist the designer in computing the required coordinates. Tabulations of the slope of the downstream quadrant shape are also included in the charts to facilitate location of the beginning of the toe curve or the tangent section.

5. <u>Upstream Quadrant Shape.</u> Upstream quadrant shapes have frequently been defined by circular arcs fitted to the experimental data. This procedure usually results in a surface of discontinuity where the curved crest meets the sloping upstream face. The possible effects of this surface of discontinuity are discussed in paragraph 4 of HDC Sheets 111-1 to 111-2/1. The WES has derived upstream quadrant equations based on the USBR[1] basic data for 45-degree downstream sloping weirs. HDC 122-3/4 gives the general form of the equation in terms of the sharp-crested weir. Curves of the coefficients and the exponents required for evaluation of the equation are given in this chart and in HDC 122-3/1. The curves are applicable to approach velocity head-design head ratios h_a/H_d of 0.00 to 0.20. Upstream quadrant shapes based on these curves should satisfy the crest location criteria given in HDC 122-3/1, result in zero slope at the spillway crest, minimize the discontinuity at the 45-degree upstream face, and result in good agreement with the experimental data.

6. The solution of the equation in HDC 122-3/4 gives coordinates in terms of the sharp-crested weir. Transfer of the coordinate origin to the spillway crest and the reference head to the design head results in the cumbersome general equation shown in HDC 122-3/5. Upstream quadrant coordinates referenced to the crest apex and design head are tabulated in this chart for h_a/H_d values of 0.08 and 0.12 to simplify the design procedure.

7. The crest shapes defined in HDC 122-3 to 122-3/5 have not been tested in the laboratory for determination of pressures and discharge coefficients.

122-3 to 122-3/5
Revised 1-64

8. <u>References</u>.

(1) U. S. Bureau of Reclamation, <u>Studies of Crests for Overfall Dams,
Boulder Canyon Project.</u> Final Reports, Part VI-Hydraulic Investiga-
tions, Bulletin 3, Denver, Colo., 1948.

(2) _____, <u>Design of Small Dams.</u> U. S. Government Printing Office,
1960.

Chart axes:
- Y-axis: $\dfrac{h_a}{H_d}$ (0.00 to 0.20)
- X-axis: $\dfrac{P}{H_d}$ (0.0 to 3.2)

SUB-MERGED | USE $\dfrac{h_a}{H_d} = 0.12$ | USE $\dfrac{h_a}{H_d} = 0.08$ | USE NEGLIGIBLE $\dfrac{h_a}{H_d}$

NOTE DATA FROM TABLE 8, BOULDER CANYON
REPORT, BULLETIN 3, USBR, 1948

h_a
CREST AXIS
H_d
P
45°
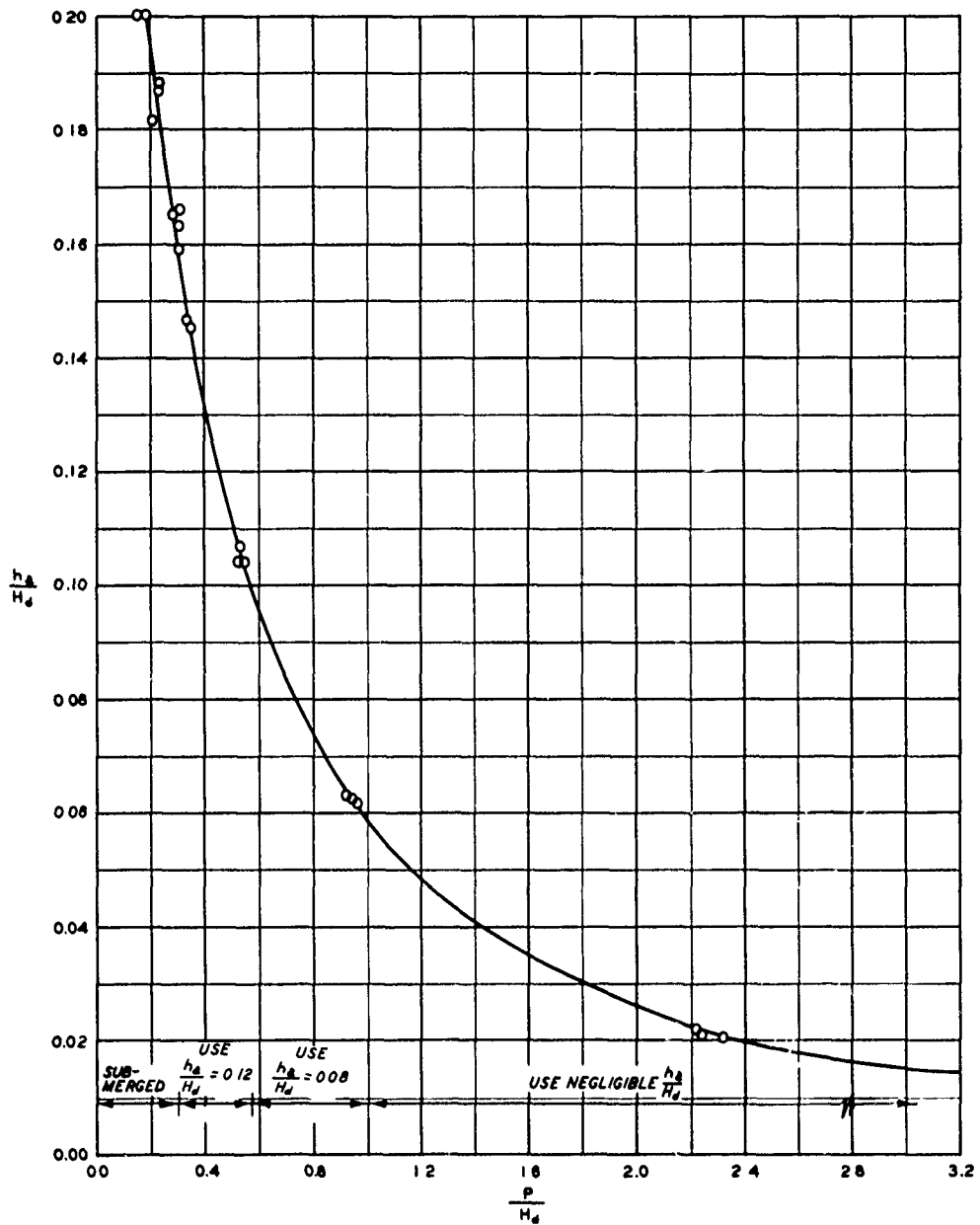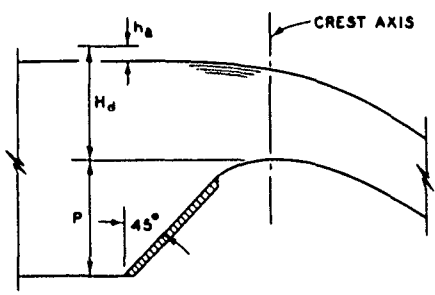
DEFINITION SKETCH

LOW OGEE CRESTS
45-DEGREE UPSTREAM SLOPE
APPROACH HYDRAULICS

HYDRAULIC DESIGN CHART 122-3
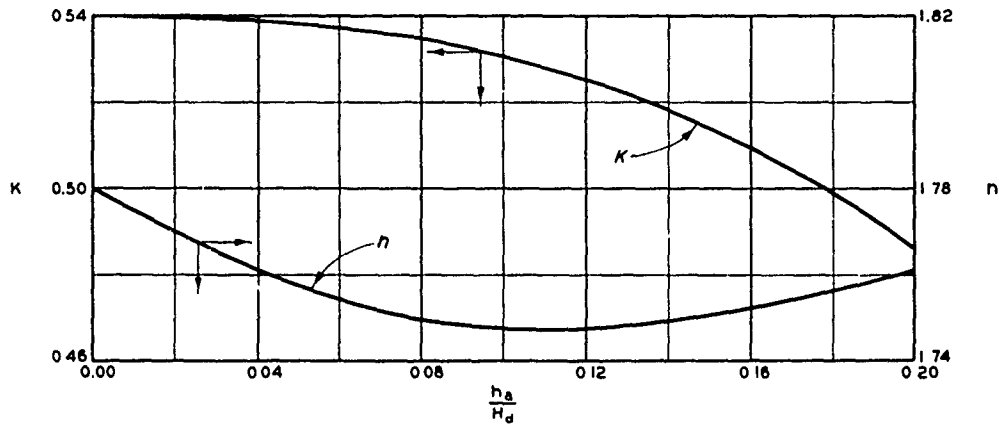
A. CONSTANTS OF DOWNSTREAM QUADRANT EQUATIONS
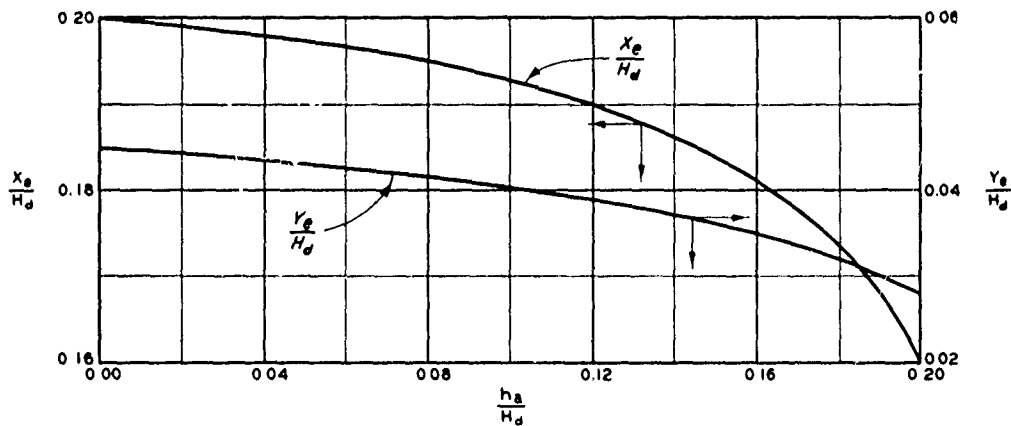
B. WEIR NAPPE GEOMETRY

NOTE CURVES REPRODUCED FROM
FIGURE 187, DESIGN OF SMALL
DAMS, USBR, 1960.
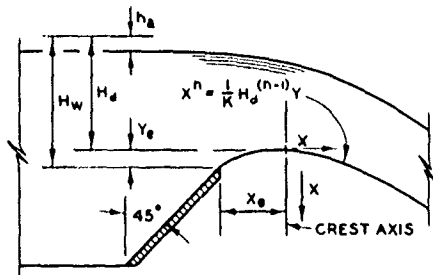
DEFINITION SKETCH

LOW OGEE CRESTS
45-DEGREE UPSTREAM SLOPE
CREST SHAPE FACTORS

HYDRAULIC DESIGN CHART 122-3/1

REV 1-64   WES 10-61

$h_a = 0.08 H_d$

H_d

ORIGIN OF COORDINATES

UPSTREAM QUADRANT (SEE HDC 122-3/5)

DOWNSTREAM QUADRANT

$X^{1.75} = 1.869 H_d^{0.75} Y$

$P = 0.75 H_d$

SHARP-CRESTED WEIR

CREST AXIS

X

Y

dX

dY

$\dfrac{X}{H_d} = 1.092 \left(\dfrac{dY}{dX}\right)^{\frac{1}{0.75}}$

45°
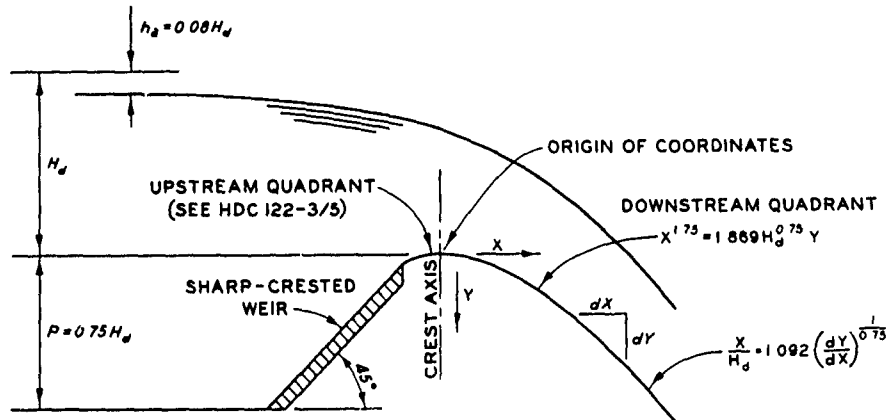
NOTE: EQUATION BASED ON USBR CURVES, HDC 122-3/1

DOWNSTREAM QUADRANT DATA   SLOPE DATA

| X	$X^{1.75}$	X	$X^{1.75}$	H_d	$\dfrac{1.869}{H_d^{0.75}}$	H_d	$\dfrac{1.869}{H_d^{0.75}}$	$\dfrac{dY}{dX}$	$\dfrac{X}{H_d}$
0.10	0.0177	6	23.002	1	1869	26	21 522	0.50	0.435
0.15	0.0361	7	30.125	2	3 144	27	22 139	0.60	0.553
0.20	0.0598	8	38.055	3	4 261	28	22 752	0.70	0.679
0.25	0.0883	9	46.765	4	5 287	29	23 358	0.80	0.811
0.30	0.1216	10	56.234	5	6 250	30	23 960	0.90	0.949
0.35	0.1592	12	77.369	6	7 166	31	24 557	1.00	1.092
0.40	0.2011	14	101.327	7	8 044	32	25 148	1.05	1.165
0.45	0.2472	16	128.000	8	8 891	33	25 735	1.10	1.240
0.50	0.2973	18	157.299	9	9 712	34	26 318	1.15	1.315
0.60	0.4090	20	189.148	10	10 511	35	26 897	1.20	1.392
0.70	0.5356	25	279.508	11	11 290	36	27 471	1.25	1.470
0.80	0.6767	30	384.5?9	12	12 051	37	28 041	1.30	1.549
0.90	0.8316	35	503.639	13	12 797	38	28 608	1.35	1.629
1.00	1.000	40	636.217	14	13 528	39	29 171	1.40	1.710
1.20	1.376	45	781.847	15	14 247	40	29 730	1.45	1.792
1.40	1.802	50	940.151	16	14 953	41	30 285	1.50	1.875
1.60	2.276	55	1110.797	17	15 649	42	30 838	1.60	2.043
1.80	2.797	60	1293.495	18	16 334	43	31 387	1.70	2.215
2.00	3.364	65	1487.984	19	17 010	44	31 933	1.80	2.391
2.50	4.970	70	1694.032	20	17 677	45	32 475		
3.00	6.839	75	1911.425	21	18 336	46	33 015		
3.50	8.956	80	2139.969	22	18 987	47	33 552		
4.00	11.314	90	2629.810	23	19 631	48	34 086		
4.50	13.903	100	3162.278	24	20 268	49	34 617		
5.00	16.719			25	20 898	50	35 146		

LOW OGEE CRESTS

45-DEGREE UPSTREAM SLOPE
DOWNSTREAM QUADRANT – $h_a = 0.08 H_d$

HYDRAULIC DESIGN CHART 122-3/2

WES 1-64

$h_a = 0.12 H_d$

ORIGIN OF COORDINATES

DOWNSTREAM QUADRANT

$X^{1.747} = 1.905 H_d^{0.747} Y$

UPSTREAM QUADRANT (SEE HDC 122-3/5)

SHARP-CRESTED WEIR

$P = 0.45 H_d$

$\dfrac{X}{H_d} = 1.123 \left(\dfrac{dY}{dX}\right)^{\frac{1}{0.747}}$
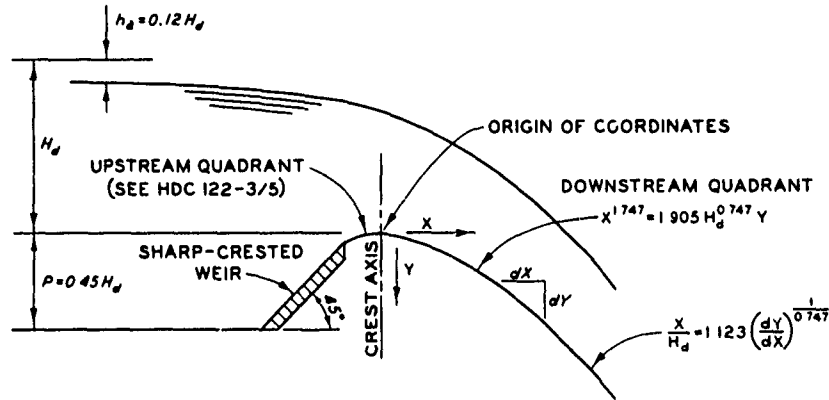
NOTE. EQUATION BASED ON USBR CURVES, HDC 122-3/1.

DOWNSTREAM QUADRANT DATA — SLOPE DATA

X	$X^{1.747}$	X	$X^{1.747}$	H_d	$\dfrac{1.905\,x}{H_d^{0.747}}$	H_d	$\dfrac{1.905\,x}{H_d^{0.747}}$	$\dfrac{dY}{dX}$	$\dfrac{X}{H_d}$
0.10	0.0179	6	22.879	1	1.905	26	21.718	0.50	0.444
0.15	0.0363	7	29.949	2	3.197	27	22.339	0.60	0.567
0.20	0.0601	8	37.818	3	4.328	28	22.954	0.70	0.696
0.25	0.0887	9	46.458	4	5.365	29	23.564	0.80	0.833
0.30	0.1220	10	55.847	5	6.338	30	24.169	0.90	0.975
0.35	0.1597	12	76.794	6	7.263	31	24.768	1.00	1.123
0.40	0.2017	14	100.528	7	8.149	32	25.362	1.05	1.198
0.45	0.2478	16	126.940	8	9.004	33	25.952	1.10	1.275
0.50	0.2979	18	155.941	9	9.832	34	26.537	1.15	1.354
0.60	0.4096	20	187.456	10	10.638	35	27.118	1.20	1.433
0.70	0.5362	25	276.822	11	11.422	36	27.695	1.25	1.514
0.80	0.6771	30	380.654	12	12.190	37	28.267	1.30	1.595
0.90	0.8318	35	498.295	13	12.941	38	28.836	1.35	1.678
1.00	1.000	40	629.215	14	13.677	39	29.401	1.40	1.762
1.20	1.375	45	772.969	15	14.401	40	29.963	1.45	1.846
1.40	1.800	50	929.182	16	15.112	41	30.520	1.50	1.932
1.60	2.273	55	1097.523	17	15.812	42	31.075	1.60	2.106
1.80	2.792	60	1277.704	18	16.502	43	31.626	1.70	2.284
2.00	3.357	65	1469.466	19	17.182	44	32.174	1.80	2.466
2.50	4.957	70	1672.578	20	17.853	45	32.718		
3.00	6.816	75	1886.828	21	18.516	46	33.260		
3.50	8.923	80	2112.021	22	19.170	47	33.799		
4.00	11.267	90	2594.548	23	19.818	48	34.334		
4.50	13.841	100	3118.889	24	20.458	49	34.867		
5.00	16.638			25	21.091	50	35.397		

LOW OGEE CRESTS
45-DEGREE UPSTREAM SLOPE
DOWNSTREAM QUADRANT — $h_a = 0.12 H_d$

HYDRAULIC DESIGN CHART 122-3/3

WES 1-64
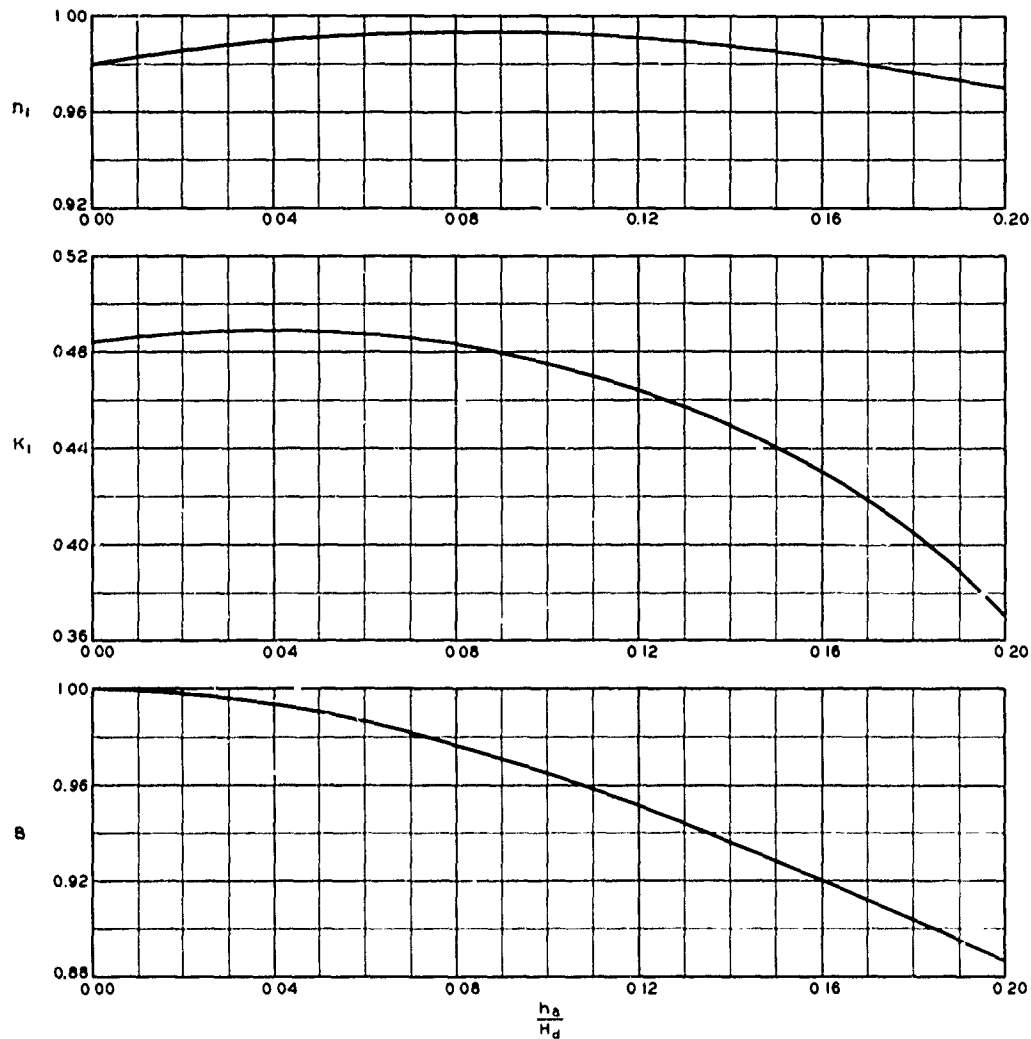
NOTES: 1 CURVES BASED ON USBR DATA
IN BOULDER CANYON REPORT,
BULLETIN 3, PART VI, 1948, AND
ON USBR CURVES ON HYDRAULIC
DESIGN CHART 122-3/1

2. n IS THE SAME IN BOTH UPSTREAM
AND DOWNSTREAM QUADRANT
EQUATIONS

$$\frac{Y}{H_W} = K_1\left(\frac{X}{H_W}\right)^{n_1} - B\left(\frac{X}{H_W}\right)^{n}$$
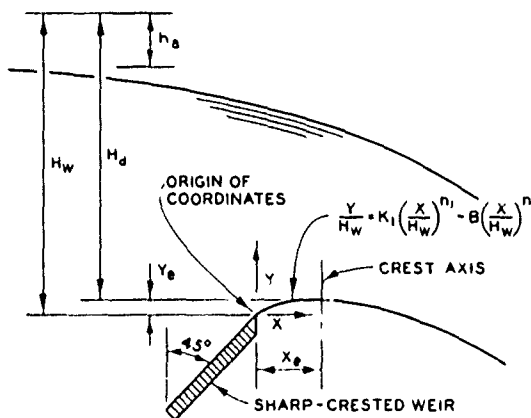
DEFINITION SKETCH

LOW OGEE CRESTS

45-DEGREE UPSTREAM SLOPE
UPSTREAM QUADRANT FACTORS

HYDRAULIC DESIGN CHART 122-3/4

WES 1-64

$$\frac{Y}{H_d} = \frac{Y_\theta}{H_d} + B_2\left(\frac{X}{H_d} + \frac{X_\theta}{H_d}\right)^n - K_2\left(\frac{X}{H_d} + \frac{X_\theta}{H_d}\right)^{n_1}$$

ORIGIN OF COORDINATES

DOWNSTREAM QUADRANT
(SEE HDC 122-3/2 & 122-3/3)

SHARP-CRESTED WEIR
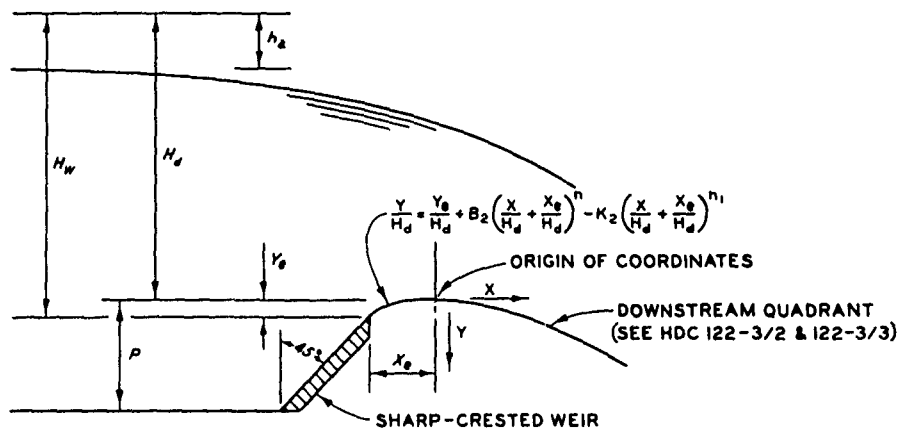
	Y/H_d			Y/H_d	
X/H_d \ h_c/H_d	0 08	0 12	X/H_d \ h_c/H_d	0 08	0 12
-0 000	0 0000	0 0000	-0 150	0 0235	0 0231
-0 020	0 0004	0 0004	-0 155	0 0252	0 0248
-0 040	0 0016	0 0015	-0 160	0 0270	0 0265
-0 060	0 0035	0 0035	-0 165	0 0288	0 0284
-0 080	0 0064	0 0062	-0 170	0 0308	0 0303
-0 100	0 0101	0 0099	-0 175	0 0326	0 0323
-0 110	0 0122	0 0120	-0 180	0 0349	0 0344
-0 120	0 0147	0 0144	-0 185	0 0372	0 0366
-0 130	0 0174	0 0170	-0 190	0 0395	0 0390
-0 140	0 0203	0 0199	-0 195	0 0420	
-0 145	0 0219	0 0215			

NOTE COORDINATES BASED ON
HDC 122-3/1 AND 122-3/4

LOW OGEE CRESTS

45-DEGREE UPSTREAM SLOPE
UPSTREAM QUADRANT COORDINATES

HYDRAULIC DESIGN CHART 122-3/5

WES 1-64

LOW OGEE CRESTS

WATER-SURFACE PROFILES

45-DEGREE UPSTREAM SLOPE

1. The shapes of the upper nappe profiles for low, ogee crests are required for the design of spillway abutment and pier heights and for the selection of trunnion elevations for tainter gates. Coordinates for the upper nappe profile for sharp-crested weirs sloping 45 degrees downstream have been determined and published by the USBR.* The published coordinates apply, in a strict sense, only to the unsupported free-falling jet. When the jet is supported, the development of the turbulent boundary layer will influence the thickness of the jet. The jet thickness will also be affected if the beginning of the toe curve or the tangent chute is close to the crest. However, the published data can be used for estimating the water-surface profile in the vicinity of the spillway crest for the design.

2. For low, ogee crests, the head is defined as the total energy head upstream from the spillway crest, and the approach depth as the height of the spillway crest above the approach channel invert. HDC 122-3/9 shows the relation between the design head-approach channel depth ratio $\left(\dfrac{H_d}{P_w + Y_e}\right)$ and the approach velocity parameter $\left(\dfrac{h_a}{H_w}\right)$ used by the USBR. This chart can be used in conjunction with HDC 122-3 and 122-3/1 for selection of the most appropriate upper nappe profile coordinates from the published data.

3. The published data are in the terms of the head on the sharp-crested weir with the origin of the data at the weir crest. For design purposes, coordinates are expressed in terms of the head on the crest with their origin at the crest apex. The necessary conversion can be accomplished using the relation between the weir head and the design head

$$H_w = H_d + Y_e$$

and the values of X_e/H_d and Y_e/H_d given in HDC 122-3/1. HDC 122-3/10 illustrates the computations required for this conversion.

---

* U. S. Bureau of Reclamation, Studies of Crests for Overfall Dams, Boulder Canyon Project. Final Reports, Part VI-Hydraulic Investigations, Bulletin 3, Denver, Colo., 1948.

$\dfrac{h_a}{H_W}$

0.20

0.16

0.12

0.08

0.04

0.00

0.0   1.0   2.0   3.0   4.0

$\dfrac{H_d}{P_W + Y_e}$

NOTE DATA FROM TABLE 8, BOULDER CANYON
REPORT, <u>BULLETIN 3</u>, USBR, 1948

h_a

H_W H_d

Y_e

$\dfrac{X}{H_W}$

P_W 45°

$-\dfrac{Y}{H_W}$
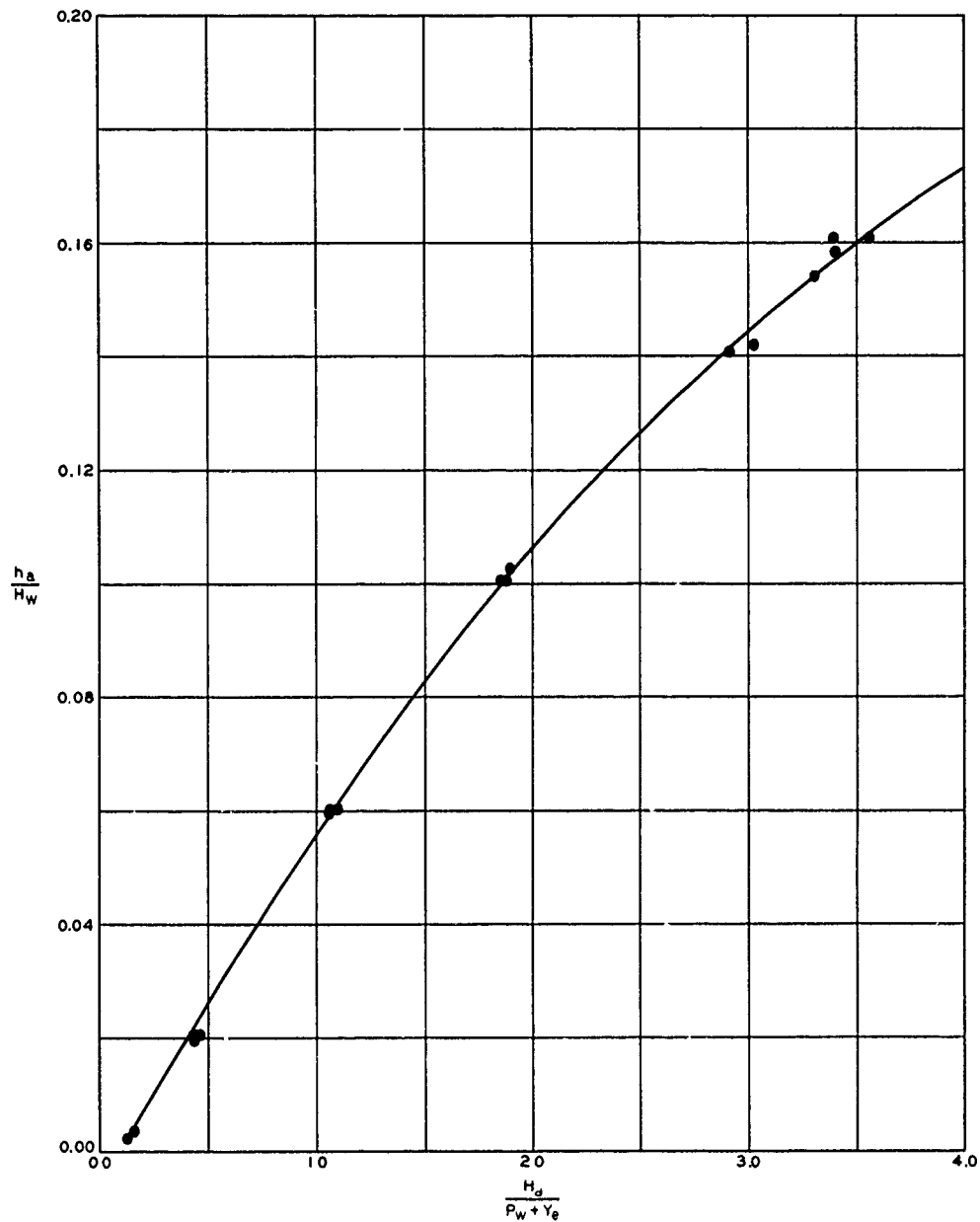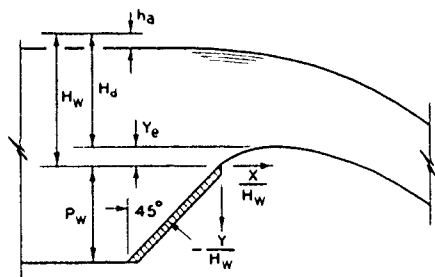
<u>DEFINITION SKETCH</u>

LOW OGEE CRESTS

45-DEGREE UPSTREAM SLOPE
APPROACH VELOCITY

HYDRAULIC DESIGN CHART 122-3/9

WES 1-64

PREPARED BY U S ARMY ENGINEER WATERWAYS EXPERIMENT STATION VICKSBURG MISSISSIPPI

JOB: _____ES 804_____ PROJECT: _____John Doe Dam_____ SUBJECT: _____Spillway_____

COMPUTATION: _____Upper Water Surface Profile_____

COMPUTED BY: ___RGC___ DATE: ___1/6/64___ CHECKED BY: ___MBB___ DATE: ___1/10/64___

GIVEN:

Spillway Crest

$$H_d = 20 \text{ ft}$$
$$\left.\begin{array}{l} P/H_d = 0.74 \\ h_a/H_d = 0.08 \end{array}\right\} \text{HDC } 122\text{-}3$$
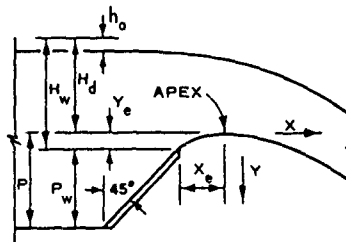
REQUIRED:

Coordinates for upper nappe profile for design head (H_d), origin at crest apex.

COMPUTE:

1. Required relationships

   $Y_e/H_d = 0.042$ (HDC 122-3/1)

   $X_e/H_d = 0.195$ (HDC 122-3/1)

   $h_a/H_w = 0.076$ (HDC 122-3/9)

   $H_w = H_d + Y_e$ (Definition sketch)

   $\dfrac{H_w}{H_d} = 1 + \dfrac{Y_e}{H_d} = 1 + 0.042 = 1.042$

   $\dfrac{X}{H_d} = 1.042 \dfrac{X}{H_w}; \quad \dfrac{Y}{H_d} = 1.042 \dfrac{Y}{H_w}$ (Origin at sharp crest)

   $\dfrac{X}{H_d} = 1.042 \dfrac{X}{H_w} - \dfrac{X_e}{H_d}; \quad \dfrac{Y}{H_w} = 1.042 \dfrac{Y}{H_w} + \dfrac{Y_e}{H_d}$ (Origin at crest apex)

2. Coordinates – Upper water-surface profile

	Origin at Weir Crest				Origin at Crest Apex		
(1)	(2)	(3)	(4)	(5)	(6)	(7)	(8)
X/H_w*	Y/H_w**	X/H_d	Y/H_d	X/H_d	Y/H_d	X	Y
		$(1.042 \times (1))$	$(1.042 \times (2))$	$((3) - 0.195)$	$((4) + 0.042)$	(ft)	(ft)
−4.00	−0.910	−4.168	−0.948	−4.363	−0.906	−87.26	−18.12
−3.00	−0.906	−3.126	−0.944	−3.321	−0.902	−66.42	−18.04
−2.00	−0.899	−2.084	−0.937	−2.279	−0.895	−45.58	−17.90
−1.00	−0.881	−1.042	−0.918	−1.237	−0.876	−24.74	−17.52
0.00	−0.760	0.000	−0.792	−0.195	−0.750	−3.90	−15.00
0.50	−0.580	0.521	−0.604	0.326	−0.562	6.52	−11.24
1.00	−0.257	1.042	−0.268	0.847	−0.226	16.94	−4.52
1.50	0.247	1.563	0.257	1.368	0.299	27.36	5.98
2.00	0.931	2.084	0.970	1.889	1.012	37.78	20.24

*From Table 21, p. 80, Boulder Canyon report, Bulletin 3, USBR, 1948

**From Table 21, cited above, interpolated for $h_a/H_w = 0.076$

LOW OGEE CRESTS

45-DEGREE UPSTREAM SLOPE
UPPER WATER-SURFACE PROFILE
SAMPLE COMPUTATION

HYDRAULIC DESIGN CHART 122-3/10

LOW OGEE CRESTS

DESIGN HEAD DISCHARGE COEFFICIENT

45-DEGREE UPSTREAM FACE

1. Discharge coefficients for low spillways with 45-deg upstream faces have not been subjected to general laboratory investigation. However, the Bureau of Reclamation (USBR)[1] has published discharge coefficient data for sharp-crested weirs and the Waterways Experiment Station (WES) has done extensive testing on the ogee crest shape defined in HDC 111-1 to 111-2/1. The WES discharge coefficient data presented in HDC 122-1 and the USBR data were used as a basis for the discharge coefficient curve defined by the dashed line in HDC 122-4. This curve should serve for preliminary design purposes and be helpful in studying the economics of low crests with 45-deg upstream faces. The discharge coefficient for design head is plotted as a function of the approach depth-design head ratio in the chart. The sharp flexure in the curve at a P/H_d of about 0.4 indicates that the coefficient reduces rapidly for lower crest heights. The estimated values should not be considered applicable for crests with toe curves set high enough to increase the pressure cn the crest and produce a submerged effect.
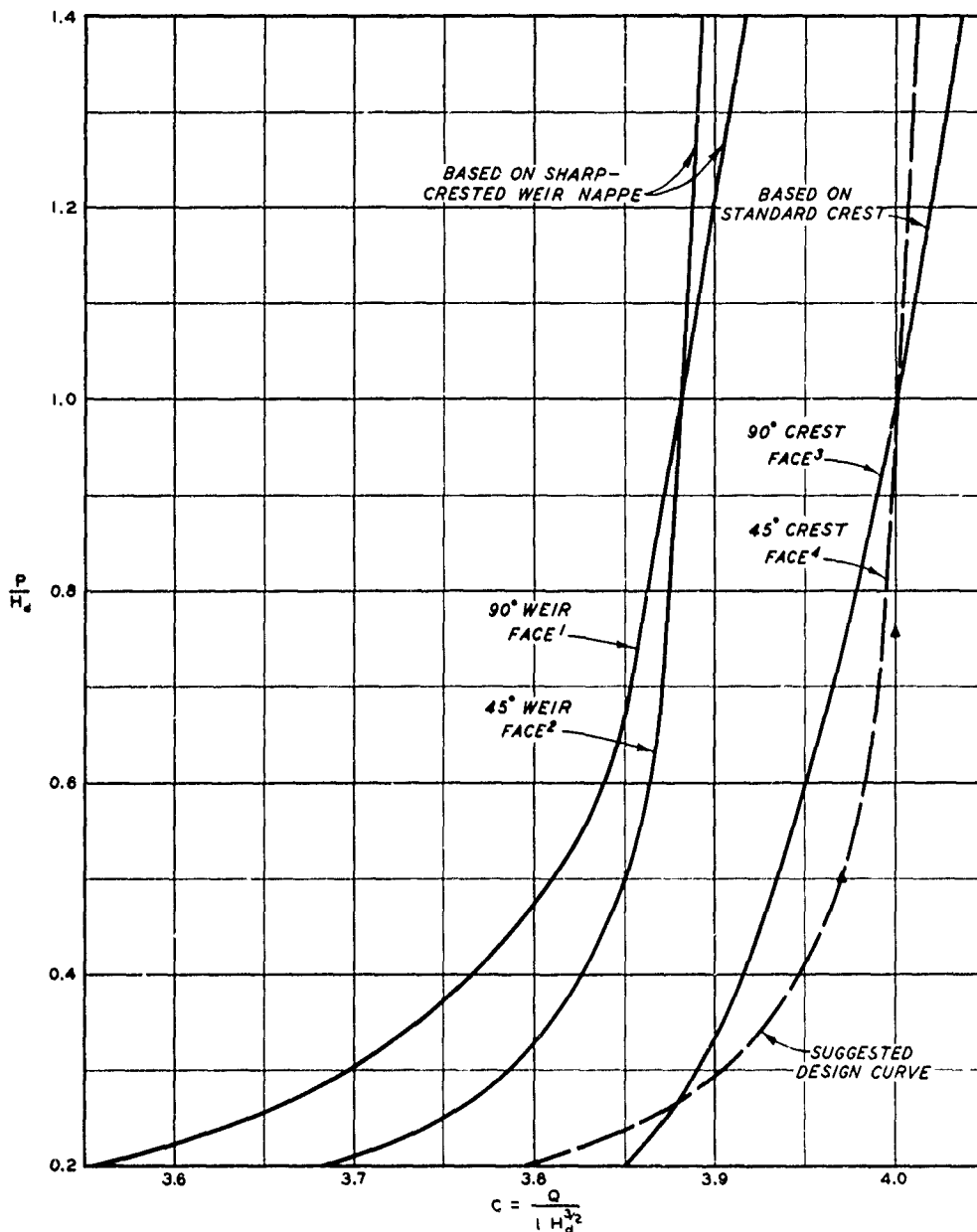
2. Study of the WES and USBR data indicates that the crest shape defined in HDC 111-1 to 111-2/1 is about 3 percent more efficient than the comparable sharp-crested weir. This factor was applied to the USBR data for a 45-deg sloping weir to obtain the suggested design curve shown in HDC 122-4.

3. Available literature indicates that the geometry of spillway crests with 45-deg upstream faces does not usually conform to the theoretical lower-nappe profile of the free jet. In most cases that were model-tested, abnormal approach- and exit-channel conditions existed which affected the spillway discharge. The Proctor Dam[2] type 3 spillway crest shape closely approximates the theoretical shapes for approach depth-design head ratios of 0.50 and 0.76. The model data indicate that the design head discharge coefficients were not affected by exit-channel tailwater. These coefficients are plotted in HDC 122-4 and appear to generally confirm the usefulness of the suggested design curve. The USBR coefficient curves for sharp-crested weirs with vertical and 45-deg sloping faces and the WES curve for the crest shape defined in HDC 111-1 to 111-2/1 are also shown for comparison.

4. References.

(1) U. S. Bureau of Reclamation, Studies of Crests for Overfall Dams, Boulder Canyon Project. Final Reports, Part VI-Hydraulic Investigations, Bulletin 3, Figs. 15 and 21, Denver, Colo., 1948.

(2) U. S. Army Engineer Waterways Experiment Station, CE, <u>Spillway for Proctor Dam, Leon River, Texas; Hydraulic Model Investigation,</u> by E. S. Melsheimer and T. E. Murphy. Technical Report No. 2-645, Vicksburg, Miss.. March 1964.

BASED ON SHARP-
CRESTED WEIR NAPPE

BASED ON
STANDARD CREST

90° CREST
FACE[3]

45° CREST
FACE[4]

90° WEIR
FACE[1]

45° WEIR
FACE[2]

SUGGESTED
DESIGN CURVE

$$C = \dfrac{Q}{L\,H_d^{3/2}}$$

$\dfrac{P}{H_d}$

LEGEND

▲ WES PROCTOR MODEL TR NO 2-645
Q = DISCHARGE
H_d = DESIGN HEAD
L = CREST LENGTH

[1] BOULDER CANYON REPORT, FIG 15, BULLETIN 3, USBR, 1948
[2] BOULDER CANYON REPORT, FIG 21b, BULLETIN 3, USBR, 1948
[3] HDC 122-1, WES, REV 1-64
[4] WES ESTIMATE

h_a

H_d

P

45°

90°
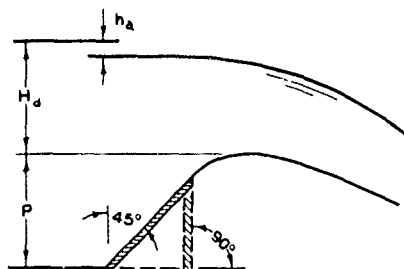
DEFINITION SKETCH

LOW OGEE CREST
DESIGN HEAD
DISCHARGE COEFFICIENT
45° UPSTREAM FACE

HYDRAULIC DESIGN CHART 122-4

LOW OGEE CRESTS

TOE CURVE PRESSURES

1. **Purpose.** Experimental laboratory data indicate that toe cu've pressures for low ogee crests are approximately a maximum from the third point to the end of the toe curve. Analytical and flow net studies further indicate that the toe curve affects the boundary pressure immediately upstream and downstream from the curve. The relatively high pressure at the end of the curve may be transmitted to the underside of the chute slabs immediately downstream. Also, for low ogee crests the toe curve may have a submergence effect upon the flow over the crest. Therefore, estimates of boundary pressure relating to toe curves may be useful in studies of the structural design of the curve, the stability of the slabs immediately downstream, and the capacity of the spillway. HDC 122-5 can be used as a guide in estimating the pressure distribution on toe curves for low ogee spillways.

2. **Design Criteria.** The results of a Waterways Experiment Station (WES)[1] semiempirical study on flip bucket and toe curve pressures for high overflow spillways have been published and are summarized in HDC 112-7. The study included analysis of data from five hydraulic model investigations of low ogee spillways (Gavins Point,[2] Dickinson,[3] Fresno,[4] Bonny,[5] and Keyhole[6] Dams). The parameters defined in HDC 112-7 were used in the analysis. Reasonable correlation of the data for ratios of toe curve radius-total head $R/H_T \le 1.0$ was obtained as shown in HDC 122-5. The curves in the chart are based on HDC 112-7. For R/H_T ratios > 1.0, the dimensionless pressure term can be expressed as $h_p/H_T + \Delta(h_p/H_T)$ where h_p/H_T is the value of the pressure parameter from HDC 122-5 and $\Delta(h_p/H_T)$ is an additive value from the insert graph in the chart. Revision of the curves in this chart may be desirable as additional data become available.

3. **Application.** The values of the parameters $q/R\sqrt{2gH_T}$, α/α_T , and R/H_T are computed for the design or maximum flow as the case may be. The notation is defined in HDC 112-7 and in the definition sketch in HDC 122-5. The values of h_p/H_T for α/α_T of 0.0 and 0.25 to 1.00 are read directly from the chart if $R/H_T < 1.0$. Values of $\Delta(h_p/H_T)$ from the chart insert should be added to the values read from the chart proper if $R/H_T > 1.0$. The pressure upstream and downstream from the toe curve reduces rapidly to the normal hydrostatic pressure and can be evaluated by a flow net or model study. However, an estimate of these pressures can be obtained by graphical extrapolation of the pressure pattern of the toe curve.

4. **References.**

(1) U. S. Army Engineer Waterways Experiment Station, CE, *An Investigation*

of Spillway Bucket and Toe Curve Pressures. Miscellaneous Paper No. 2-625, Vicksburg, Miss., February 1964.

(2) U. S. Army Engineer Waterways Experiment Station, CE, Spillway for Gavins Point Dam, Missouri River, Nebraska; Hydraulic Model Investigation. Technical Memorandum No. 2-404, Vicksburg, Miss., May 1955.

(3) Beichley, G. L., Hydraulic Model Studies of Dickinson Dam Spillway. Hydraulic Laboratory Report No. HYD-267, U. S. Bureau of Reclamation, 30 December 1949.

(4) Ball, J. W., and Besel, R. C., Hydraulic Model Studies of the Spillway and Outlets for the Fresno Dam, Milk River Project. Hydraulic Laboratory Report No. HYD-177, U. S. Bureau of Reclamation, 6 July 1945.

(5) Rusho, E. J., Hydraulic Model Studies of the Overflow Spillway and the Hale Ditch Irrigation Outlet, Bonny Dam, Missouri River Basin Project. Hydraulic Laboratory Report No. HYD-331, U. S. Bureau of Reclamation, 31 January 1952.

(6) Beichley, G. L., Hydraulic Model Studies of Keyhole Dam Spillway, Missouri River Project. Hydraulic Laboratory Report No. HYD-271, U. S. Bureau of Reclamation, 8 January 1952.

$$\Delta\left(\frac{h_p}{H_T}\right) = \left(\frac{h_p}{H_T}\right)_{OBS} - \left(\frac{h_p}{H_T}\right)_{CURVE}$$

H_{max}

$\frac{R}{H_T}$

$\frac{q}{R\sqrt{2gH_T}}$

$\alpha/\alpha_T = 0$

$0.25 < \alpha/\alpha_T < 1.00$

BASED ON
HDC 112-7

NOTE: NUMBERS ARE VALUES
OF $(\alpha/\alpha_T) \times 10^2$

$\frac{h_p}{H_T}$
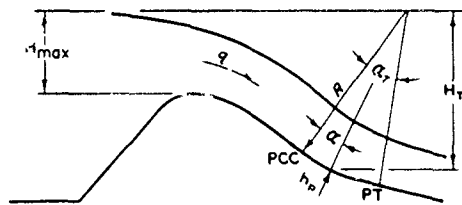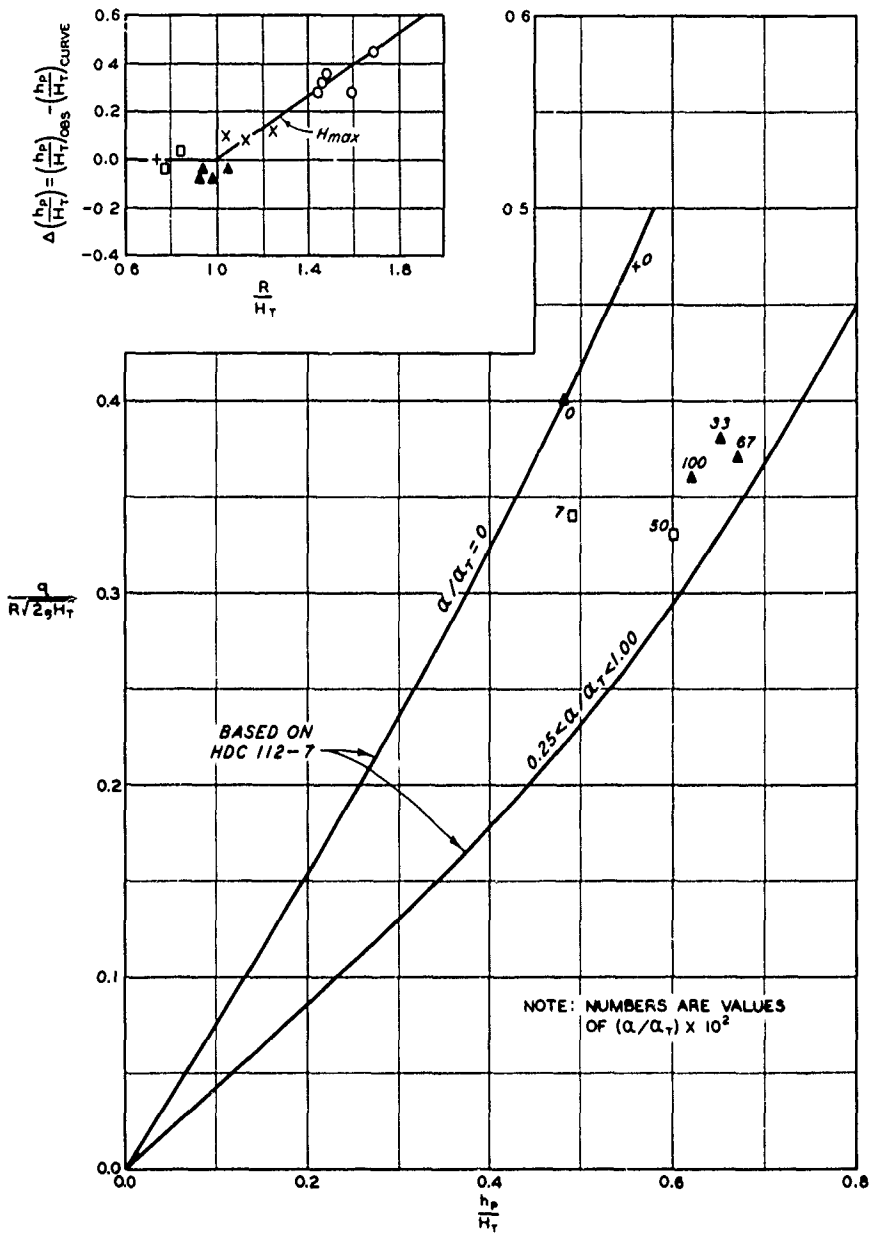
LEGEND

X GAVINS POINT DAM
▲ DICKINSON DAM
O FRESNO DAM
□ BONNY DAM
+ KEY HOLE DAM

H_{max}

q

R

α_T

α

PCC

h_p

PT

H_T

DEFINITION SKETCH

LOW OGEE CRESTS
TOE CURVE PRESSURES

HYDRAULIC DESIGN CHART 122-5

1. **General.** The design procedure to determine the water-surface profile in a spillway chute often employs the step method of computation. The curve can be solved by use of the varied flow function. The method devised by Bakhmeteff[1] is preferred by some engineers and the type of profile is classified as the S_1 curve. However, when the step method is employed, a trial-and-error procedure is normally used to resolve the total energy into depth and velocity head from the equation:

$$E = d + \frac{V^2}{2g}$$

where E is the energy in feet and is the difference between the energy gradient and the bottom of the chute, d is the depth of flow and $V^2/2g$ is the velocity head.

2. **Energy-depth Curves.** A graph with energy and depth as ordinates and a family of curves representing various rates of flow per unit width (q) greatly facilitates the step method. This type of graph is not new.

3. **Sample Computation.** The sample computation chart (123-6) is included only to demonstrate the application of the energy-depth curves. Many different arrangements of the computation form have been used. The sample computation is carried to one-hundredths of a foot to indicate that the last significant figure can be estimated from the energy-depth curve. The starting station of the water-surface profile is commonly taken to be the tangent point of the chute to the ogee. If one assumes no energy loss between the reservoir pool and the starting station, the initial energy is the difference in elevation between the reservoir and the chute floor at the starting station. Entering the energy-depth graph with the initial energy and the proper discharge per unit width, the depth can be determined. Subtracting the depth from the energy, the velocity head is found. The energy-depth curves are then used at each successive phase of the computation after a new energy value is determined. Reproductions of the energy-depth curves on double size sheets are available upon request.

---

[1] Boris A. Bakhmeteff, Hydraulics of Open Channels (McGraw-Hill, 1932).
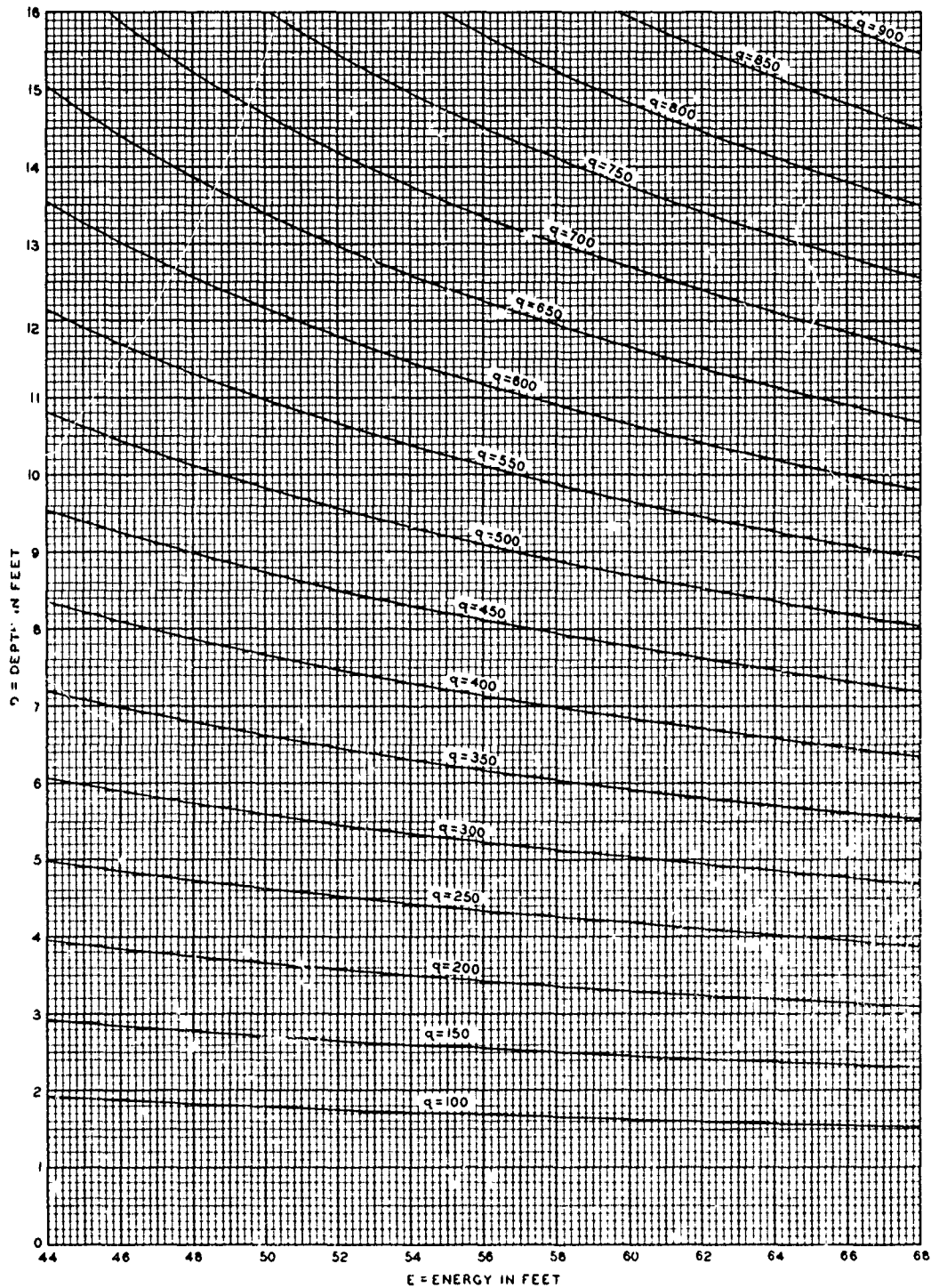
D = DEPTH IN FEET
D_c = CRITICAL DEPTH IN FEET
q = DISCHARGE PER FOOT OF WIDTH IN CFS
E = ENERGY IN FEET $\left(E = D + \frac{V^2}{2g}\right)$.
V = VELOCITY IN FT PER SEC

ENERGY-DEPTH CURVES
SUPERCRITICAL FLOW
ENERGY - 44 TO 68 FEET
HYDRAULIC DESIGN CHART 123-3

WES 4 52

D = DEPTH IN FEET

E = ENERGY IN FEET

D = DEPTH IN FEET
D_c = CRITICAL DEPTH IN FEET
q = DISCHARGE PER FOOT OF WIDTH IN CFS
E = ENERGY IN FEET $\left(E = D + \dfrac{V^2}{2g} \right)$
V = VELOCITY IN FT PER SEC

ENERGY-DEPTH CURVES
SUPERCRITICAL FLOW
ENERGY–68 TO 92 FEET
HYDRAULIC DESIGN CHART 123-4
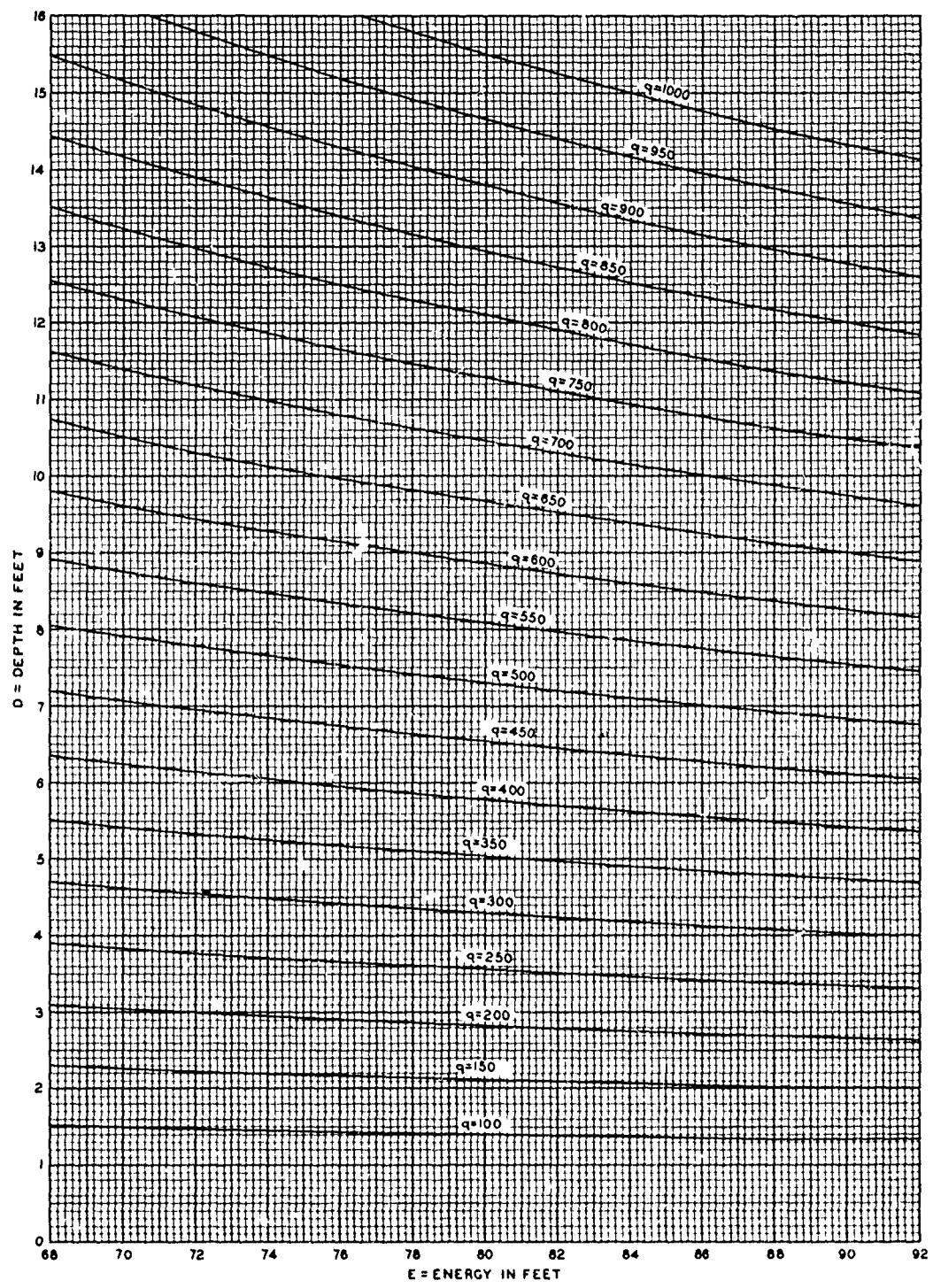
WES 4 1 52

D = DEPTH IN FEET

E = ENERGY IN FEET

D = DEPTH IN FEET
D_c = CRITICAL DEPTH IN FEET
q = DISCHARGE PER FOOT OF WIDTH IN CFS
E = ENERGY IN FEET $\left(E = D + \frac{V^2}{2g}\right)$
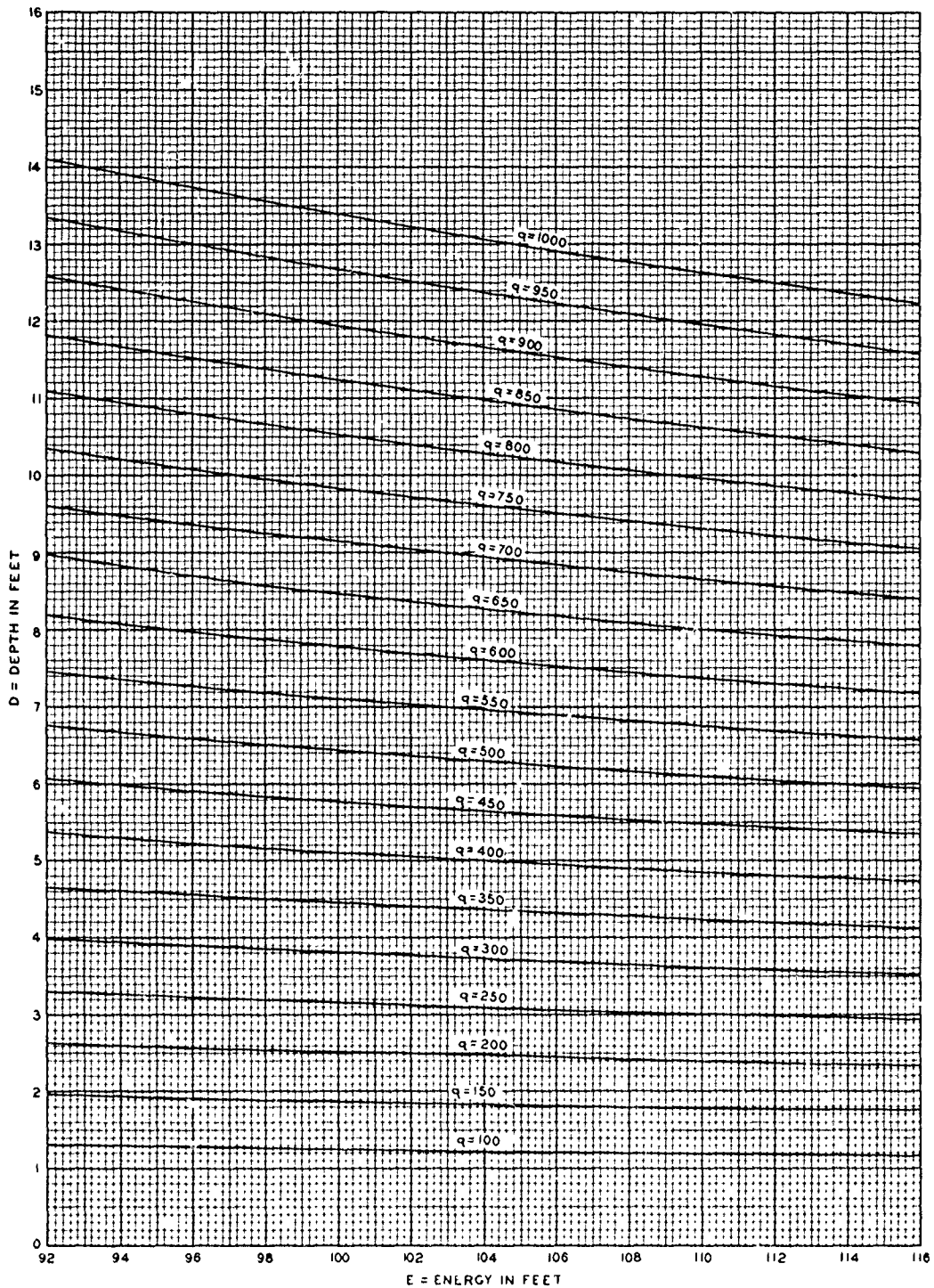V = VELOCITY IN FT PER SEC

ENERGY-DEPTH CURVES
SUPERCRITICAL FLOW
ENERGY-92 TO 116 FEET

HYDRAULIC DESIGN CHART 123-5

WES 4-52

WATERWAYS EXPERIMENT STATION
COMPUTATION SHEET

Job: *CW-804* Project: *JOHN DOE DAM* Subject: *CHUTE SPILLWAY*
Computations: *WATER SURFACE PROFILE*
Computed By: *A.A.Mc.* Date: *4-1-52* Checked By: *B.G.* Date: *4-1-52*

GIVEN:

$Q = 120,000 \, cfs$
$W = 400 \, ft$
$n = 0.013$
$\Delta L = 100 \, ft$
Chute Slope = 0.10
Initial Energy = 28.0 ft

FORMULAS:

$$\Delta h_f = \Delta L n^2 \left(\frac{V^2}{2.21 R^{4/3}} \right)$$

$\Delta L n^2 = 0.0169$
$q = Q/W = 300 \, cfs$

STATION	FLOOR ELEV	ENERGY GRAD ELEV	E	d	R	$\frac{V^2}{2g}$	V	$\frac{V^2}{2.21 R^{4/3}}$	Δh_f
10+50	599.25	627.25	28.0	8.45	8.11	19.55	35.5	34.92	0.590 [2]
		626.66 [1]							0.908 [4]
11+50	589.25	626.34 [3]	37.41	6.78	6.56	30.63	44.5	72.57	1.226
		625.11							1.568
12+50	579.25	624.77	45.86	5.92	5.75	39.94	50.7	113.01	1.910
		622.86							2.273
13+50	569.25	622.50	53.61	5.35	5.21	48.26	55.81	155.95	2.636
		619.86							2.972
14+50	559.25	619.53	60.61	5.00	4.88	55.61	59.82	195.71	3.308
		616.22							3.647
15+50	549.25	615.88	66.97	4.72	4.61	62.25	63.44	235.85	3.986
								$\Sigma \Delta h_f = 11.368$	

Check Energy Gradient Elev 627.25
$\qquad$ 615.88 + 11.368 = 627.248 Check

[1] First estimate of energy gradient based on Δh_f from station 10 + 50 [2]
[3] Adjusted energy gradient based on average of Δh_f between 10 + 50 & 11 + 50 [4]

NOTATION:

d = Depth of Flow in Chute - ft
E = Energy = $d + V^2/2g$ - ft
Δh_f = Increment of Friction Loss - ft
ΔL = Increment of Chute Length - ft
n = Manning's Friction Coefficient
q = Discharge per foot of width - cfs
Q = Discharge - cfs
R = Hydraulic Radius - ft
V = Velocity - ft/sec
W = Width of Chute - ft

CHUTE SPILLWAYS
ENERGY – DEPTH CURVES
SAMPLE COMPUTATION

HYDRAULIC DESIGN CRITERIA

SHEETS 123-7 TO 123-9

CHUTE SPILLWAY

COMPUTATION AIDS

1. The curves on Hydraulic Design Chart 123-7 to 123·9 were prepared as design aids for problems similar to the one given in the sample computation on Chart 123-6 previously issued. The first two charts facilitate the determination of the hydraulic radius for a given rectangular chute width when the depth becomes known. Chart 123-7 is for widths from 10 to 120 ft and Chart 123-8 is for widths from 100 to 1200 ft. The last chart enables the designer to find the velocity and the function $V^2/2.21 R^{4/3}$ after the velocity head has been computed.

HYDRAULIC RADIUS IN FEET

WIDTH IN FEET

BASIC EQUATION

$$R = \frac{Wd}{W+2d}$$

WHEPE

W = WIDTH OF CHUTE
d = DEPTH OF WATER
R = HYDRAULIC RADIUS

CHUTE SPILLWAYS
HYDRAULIC RADIUS –
WIDTH–DEPTH CURVES
WIDTH 10 TO 120 FT

HYDRAULIC DESIGN CHART 123-7

WES 4-1-53

HYDRAULIC RADIUS IN FEET (y-axis)

WIDTH IN FEET (x-axis)

Curves labeled: d=16, d=15, d=14, d=13, d=12, d=11, d=10, d=9, d=8, d=7, d=6, d=5, d=4, d=3, d=2, d=1
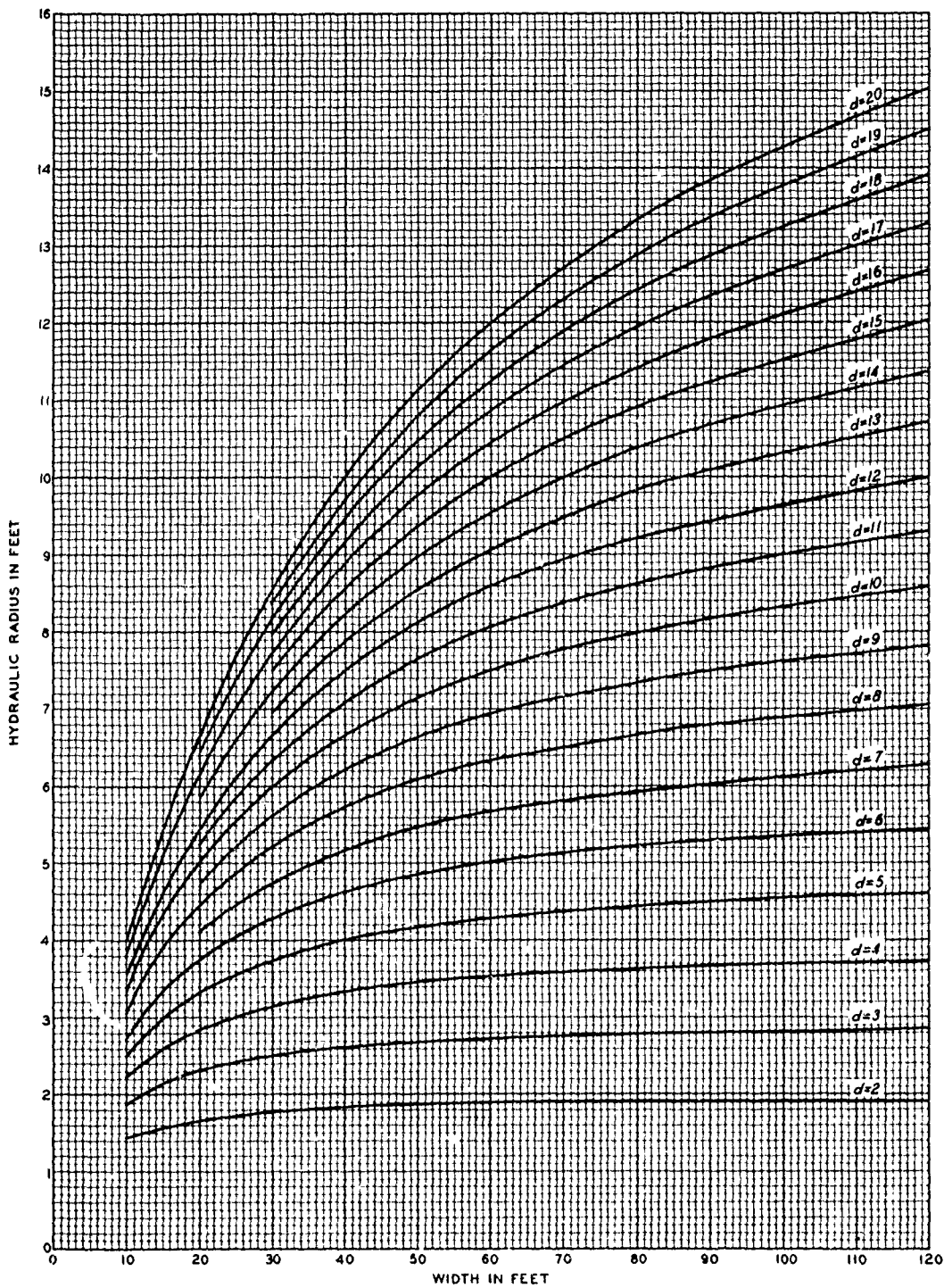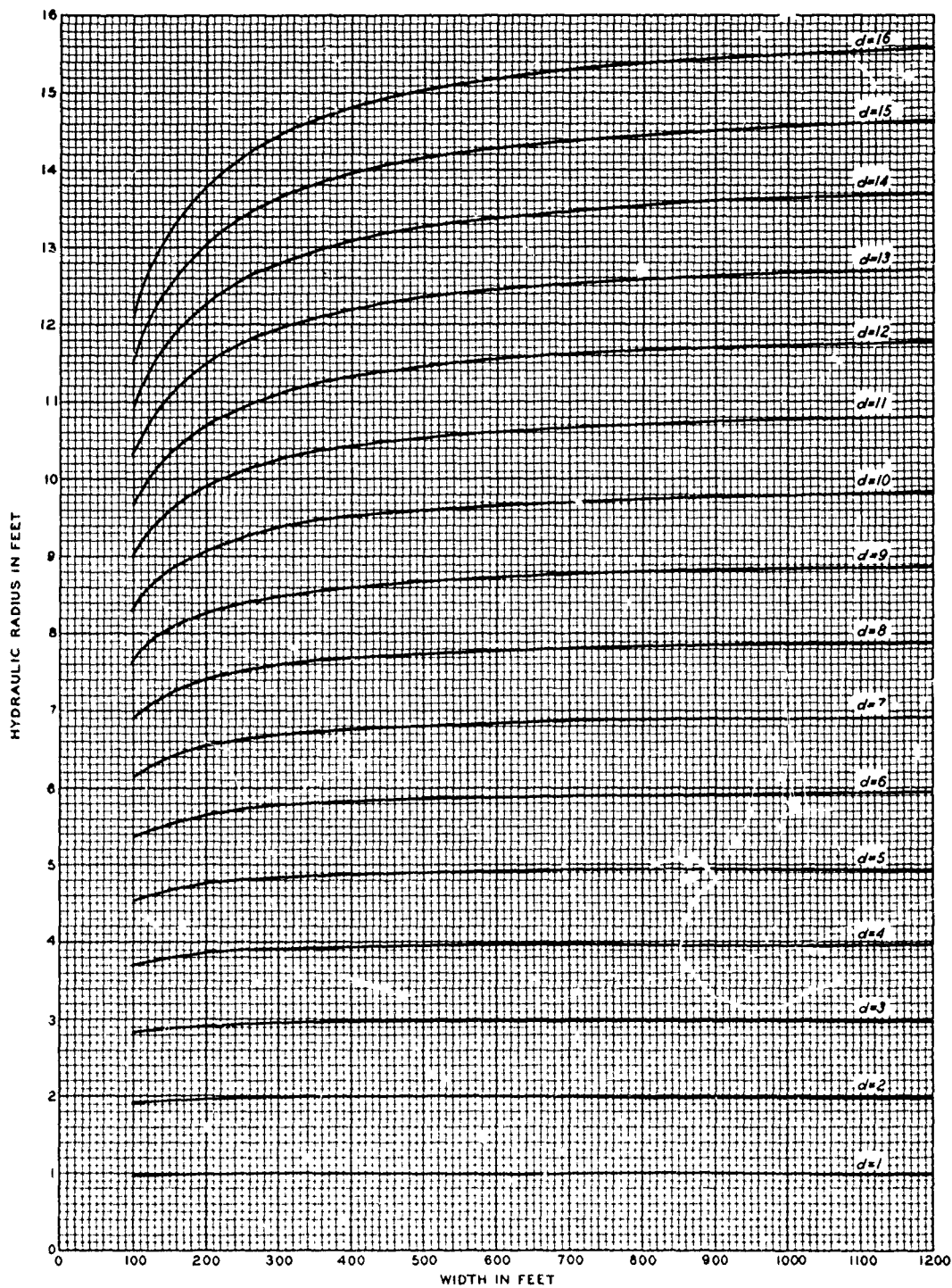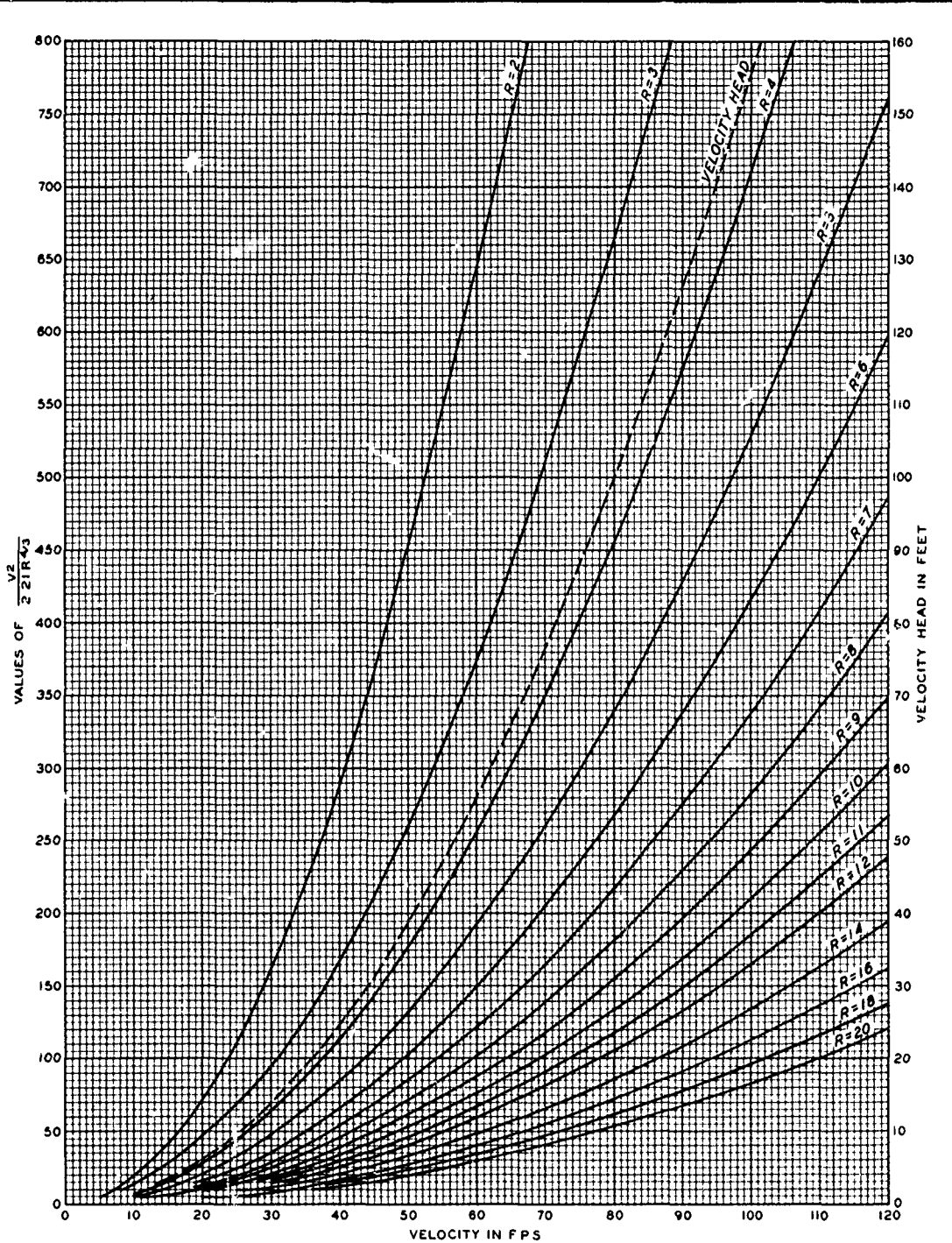
BASIC EQUATION

$$R = \frac{Wd}{W+2d}$$

WHERE

W = WIDTH OF CHUTE
d = DEPTH OF WATER
R = HYDRAULIC RADIUS

CHUTE SPILLWAYS
HYDRAULIC RADIUS-
WIDTH-DEPTH CURVES
WIDTH 100 TO 1200 FT

HYDRAULIC DESIGN CHART 123-8

WES 4-1-53

CHUTE SPILLWAYS

VELOCITY–HEAD AND $\dfrac{V^2}{2.21\,R^{4/3}}$ CURVES

HYDRAULIC DESIGN CHART 123-9

HYDRAULIC DESIGN CRITERIA

SHEETS 124-1 TO 124-1/1

CHUTE SPILLWAYS

STILLING BASINS

LENGTH OF HYDRAULIC JUMP

1. **Purpose.** The hydraulic jump is commonly used for energy dissipation at the end of spillway chutes. The jump may occur on the sloping chute, on both the sloping chute and the horizontal apron, or on the horizontal apron, depending upon tailwater conditions. In each case it is necessary to determine the length of the stilling basin walls required to confine the jump. HDC 124-1 can be used to estimate jump lengths when excess tailwater forces the jump to occur entirely on the chute slope. HDC 124-1/1 is applicable when the length of the jump spans the intersection of the sloping chute and the horizontal apron.

2. **Laboratory Investigation.** Laboratory experiments on the hydraulic jump on sloping aprons have been conducted by Bakhmeteff and Matzke,[1] Kindsvater,[2] Lin and Priest,[3] and Bradley and Peterka.[4,5] Difficulty has been found in correlating the results of various investigations of length of a jump on a sloping floor. The apparent reason for this is differences in the definition of the jump length used by the investigators. Bradley and Peterka[4] define the end of the jump as "The point where the high velocity jet begins to lift from the floor, or a point on the tailwater surface immediately downstream of the surface roller, whichever occurs farthest downstream." Bradley and Peterka's jump-length curves have been reproduced as HDC 124-1 and 124-1/1 and are recommended for design purposes because of the extensiveness of the tests compared with those of other investigators. The experimental data points have been omitted from the charts to simplify their use. Data points for existing basins with sloping aprons are plotted in HDC 124-1/1 and show good agreement with the curves. These points, selected from project tabulations published by Bradley and Peterka,[4] are limited to those cases where the locations of the jumps are dimensionally defined.

3. The length L of the jump in terms of the theoretical depth d_2 for zero slope is plotted as a function of the entering Froude number F_1 in HDC 124-1. Jump-length curves for continuous slopes of 0.0 to 0.33 are given. The tailwater depth d_2' required for the jump to occur completely on the sloping apron is shown by the insert graph.

4. For noncontinuous slopes, the length L_t of that portion of the jump occurring on the slope is given as a function of the tailwater depth TW in HDC 124-1/1. The theoretical depths d_2 for the horizontal apron jump have been used to develop the dimensionless curves for apron slopes of 0.05 to 0.33.

5. <u>Application.</u> HDC 124-1 and 124-1/1 can be used in the following manner:

    <u>a.</u> <u>Continuous Slope.</u> Compute the Froude number of the entering flow and the theoretical depth d_2 for the jump on a horizontal floor. The latter can be estimated from HDC 112-3 or 112-4 and 112-5. From the insert graph in HDC 124-1, determine the tailwater depth d_2' for the slope of interest. This depth locates the end of the jump. From the chart proper determine the jump length for the entering Froude number and the chute slope. Locate the toe of the jump using the computed tailwater depth d_2' and jump length L . Check the Froude number at the toe of the jump against the Froude number computed for the entering flow and repeat the computations if necessary.

    <u>b.</u> <u>Noncontinuous Slope.</u> For a noncontinuous slope, the procedure is similar to that for continuous slopes. If the existing tailwater depth TW is less than the d_2' obtained from the insert graph in HDC 124-1 but greater than the theoretical depth d_2 , the hydraulic jump will occur partly on the slope and partly on the horizontal apron. The length of the portion of the jump on the slope is readily determined from HDC 124-1/1. The computed length L_t locates the toe of the jump. If the Froude number used in the computation does not approximate that existing at the toe of the jump, the computations should be repeated using the new Froude number at the toe of the jump. Bradley and Peterka suggest that the jump length curves given in HDC 124-1 for continuous slopes are also applicable, with negligible error, to non-continuous slopes.

6. <u>References.</u>

(1) Bakhmeteff, B. A., and Matzke, A. E., "The hydraulic jump in terms of dynamic similarity." <u>Transactions, American Society of Civil Engineers,</u> vol 101 (1936), pp 630-680.

(2) Kindsvater, C. E., "The hydraulic jump in sloping channels." <u>Transactions, American Society of Civil Engineers,</u> vol 109 (1944), pp 1107-1120.

(3) Lin, Kuang-ming, and Priest, M. S., <u>The Hydraulic Jump Over a Plane Inclined Bottom.</u> Alabama Polytechnic Institute, Engineering Experiment Station Bulletin 30, April 1958.

(4) Bradley, J. N., and Peterka, A. J., "Hydraulic design of stilling basins: stilling basin with sloping apron (basin V)." <u>ASCE Hydraulics Division Journal,</u> vol 83, HY 5 (October 1957), pp 1-32.

(5) U. S. Bureau of Reclamation, <u>Hydraulic Design of Stilling Basins and Bucket Energy Dissipators,</u> revised July 1963, by A. J. Peterka. Engineering Monograph No. 25.
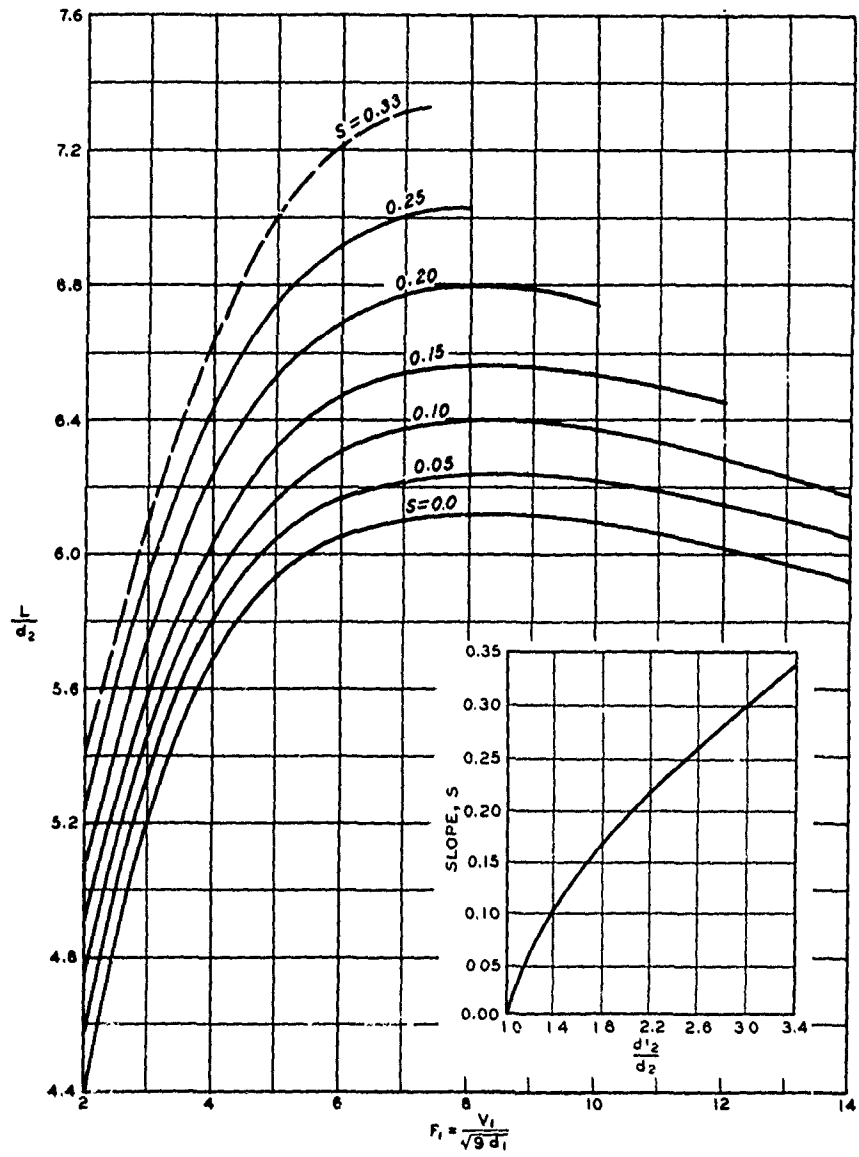
$$\frac{d_2}{d_1} = \frac{1}{2}\left(\sqrt{1+8F_1^2}-1\right)$$

NOTE CURVES DEVELOPED BY BRADLEY
AND PETERKA FROM EXPERIMENTAL
DATA DATA POINTS OMITTED TO
SIMPLIFY CHART
CURVE FOR S=0 33 EXTRAPOLATED
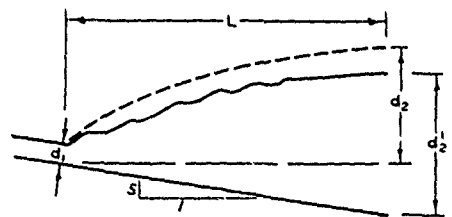
DEFINITION SKETCH

CHUTE SPILLWAYS
STILLING BASINS
CONTINUOUS SLOPE
LENGTH OF HYDRAULIC JUMP

HYDRAULIC DESIGN CHART 124-1

WES 1-66

LEGEND

O	NORRIS	S= 0.25
●	BHAKRA	S= 0.10
X	MADDEN	S= 0.25
□	FRIANT	S= 0.143
△	DICKINSON	S= 0.125

Vertical axis: $\dfrac{TW}{d_2}$

Horizontal axis: $\dfrac{L_1}{d_2}$

Curve labels: S=0.33, 0.30, 0.25, 0.20, 0.15, 0.10, S. 0.05

$$\frac{d_2}{d_1} = \frac{1}{2}\left(\sqrt{1 + 8F_1^2} - 1\right)$$
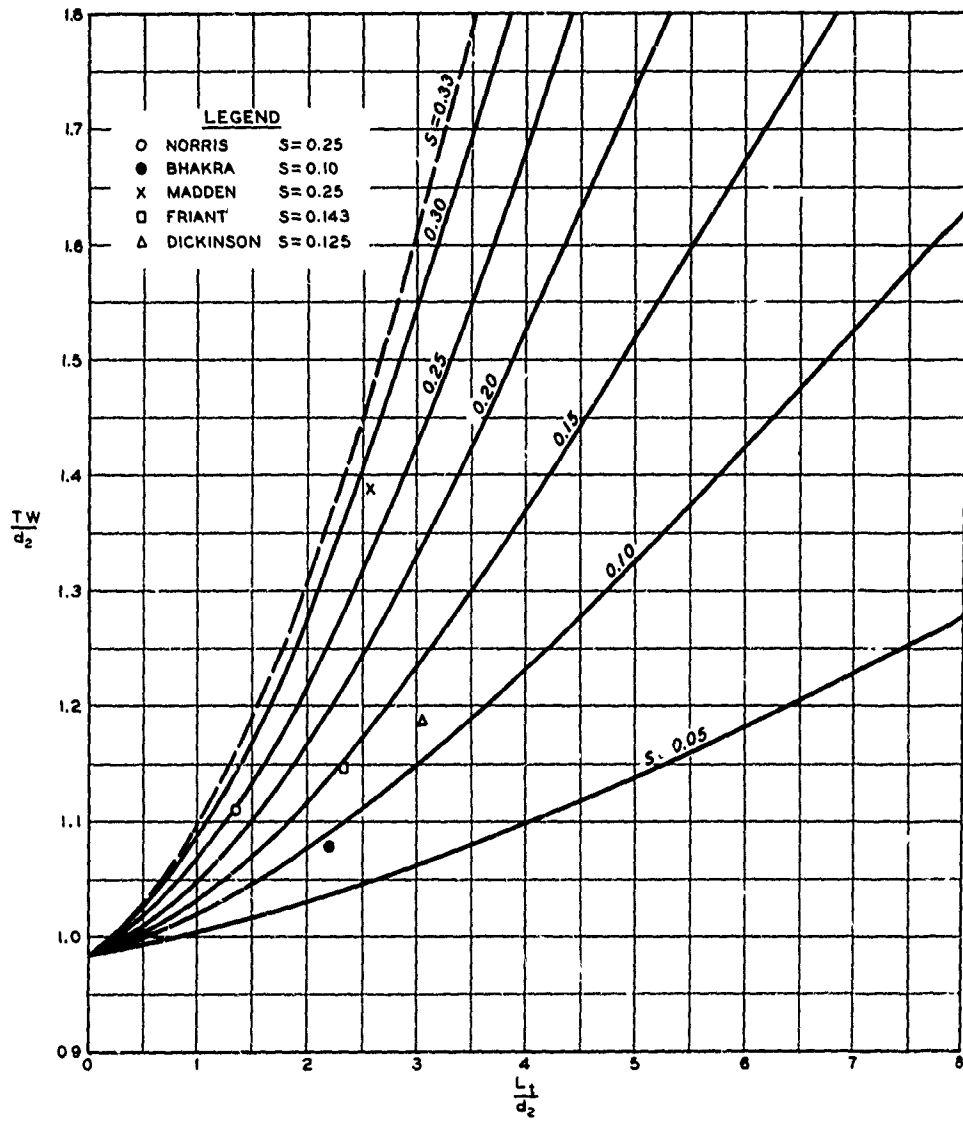
$$F_1 = \frac{V_1}{\sqrt{g\,d_1}}$$

NOTE CURVES DEVELOPED BY BRADLEY AND
PETERKA FROM EXPERIMENTAL DATA.
DATA POINTS OMITTED TO SIMPLIFY
CHART.
CURVE FOR S=0.33 EXTRAPOLATED

DEFINITION SKETCH

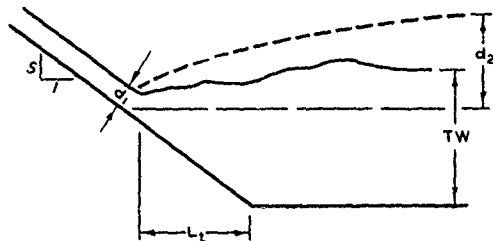**CHUTE SPILLWAYS
STILLING BASINS**

NONCONTINUOUS SLOPE
JUMP LENGTH ON SLOPE

HYDRAULIC DESIGN CHART 124-1/1

WES 1-68

HYDRAULIC DESIGN CRITERIA

SHEETS 140-1 TO 140-1/8

MORNING GLORY SPILLWAYS

1. __Background.__ Morning glory or shaft spillways utilize a crest circular in plan. The outflow is carried by a vertical or sloping shaft to a horizontal tunnel at approximately streambed level. The capacity of the morning glory spillway is limited by the size of the circular crest that can be fitted to the topography and by the head on the crest. Under various hydraulic conditions, the flow may be controlled by the crest, the throat, or the friction of the entire system flowing under pressure. A recent design of the USBR includes an inclined shaft with a vertical bend at the bottom that has a radius five times the diameter.[2] The USBR recommends that the horizontal tunnel of morning glory spillways be designed to flow only 75 percent full to eliminate instability.[8]

2. __Laboratory Investigation.__ Laboratory investigations by Camp,[3,4] Wagner,[9] Lazzari,[5] and others on flow over circular sharp-crested weirs have been used as the basis for design of morning glory spillways. The most complete study was that made by Wagner on a 20-in.-diameter weir. The results of this study have been used for the development of HDC's 140-1 to 140-1/8.

3. __Design Discharge.__ Morning glory spillways are generally designed for crest control or free-flow conditions. Laboratory tests indicate that submergence begins to affect the discharge when the ratio of the head to weir radius is greater than 0.45. The discharge may be determined by a modified weir equation:

$$Q = C \ (2\pi R) \ H_d^{3/2}$$

where

Q = discharge, cfs
C = discharge coefficient
R = radius of sharp crest, ft
H_d = design head on spillway crest, ft

HDC 140-1 permits a preliminary estimate of the discharge-head-radius relation for deep approach and free-flow crest conditions. The discharge curves on this chart are for head-radius ratios of 0.20, 0.30, and 0.40.

4. The experimental discharge coefficients are for the head on the circular, sharp-crested weir. Discharge coefficient curves for design head on the spillway crest have been published by the USBR[8] and are reproduced in HDC 140-1/1 for use with the equation given in paragraph 3. Curves for

three approach depth conditions are shown.

5. **Crest Shape.** HDC's 140-1/2 to 140-1/5 present dimensionless crest profiles and coordinates in terms of the head on the sharp crest. Tabulations are included for ratios of head to weir radius of 0.2 to 2.0 and ratios of approach depth to radius of 2, 0.30, and 0.15. The ratio of head (H_s) to weir radius (R) is required for use of these charts. This relation can be determined from a USBR design aid[8] reproduced as HDC 140-1/6.

6. **Crest Shape Equations.** Equations of the lower surface of the nappe have been determined for a limited number of conditions. The converging flow over the crest results in complex equations for morning glory spillway crest shapes. Upstream and downstream quadrant shape equations for three approach depth conditions and for three ratios of head to radius for each depth are given in HDC 140-1/7. The equations are considered adequate for defining crest shapes within the limits indicated on the chart.

7. **Transition Shape.** The crest shape is generally connected to the vertical shaft by a transition section. A procedure which can be used for transition shape design has been published by the USBR.[8]

8. **Application Procedure.** HDC 140-1/8 is a sample computation illustrating the use of HDC's 140-1/1 to 140-1/7 in morning glory spillway design. In this computation the horizontal tunnel was considered as flowing 75 percent full.

9. **Design Factors.** A number of problems encountered in the design and operation of morning glory spillways have been reported.[1,2,6,7] In the design of these structures the engineer is sometimes concerned with flow regulation by crest gates. Information may also be required on discharge coefficients and crest pressures for less than design flow and possible effects of adjacent topography on radial flow to the crest. Therefore, in some cases a model study may be required before selection of the final design.

10. **References.**

(1) Abecasis, F. N., "The behavior of morning glory shaft spillways." IAHR, Proceedings of the Sixth General Meeting, The Hague, 1955, vol 3, pp C8-1-C8-10.

(2) Bradley, J. N., "Prototype behavior," in "Morning glory shaft spillways: A symposium." Transactions, American Society of Civil Engineers, vol 121 (1956), pp 312-344.

(3) Camp, C. S., Determination of Shape of Nappe and Coefficient of Discharge of a Vertical Sharp-crested Weir, Circular in Plan with Radially Inward Flow. State University of Iowa thesis, 1937.

(4) Camp, C. S., and Howe, J. W., "Tests of circular weirs." Civil

Engineering, vol 9, No. 4 (April 1939), pp 247-248.

(5) Lazzari, E., "Ricerca sperimentale sullo sfioratore a pianta circolare." L'Energia Elettrica (November 1954), pp 838-840.

(6) Peterka, A. J., "Performance tests on prototype and model," in "Morning glory shaft spillways: A symposium." Transactions, American Society of Civil Engineers, vol 121 (1956), pp 385-409.

(7) U. S. Bureau of Reclamation, "Tests on preliminary designs of spillways," in Model Studies of Spillways. Boulder Canyon Project Final Reports, Part VI, Hydraulic Investigations, Bulletin 1 (Denver, Colo., 1938), Chapter II.

(8) _____, Design of Small Dams, 1st ed. 1960.

(9) Wagner, W. E., "Shaft spillways: determination of pressure-controlled profiles." Transactions, American Society of Civil Engineers, vol 121 (1956).
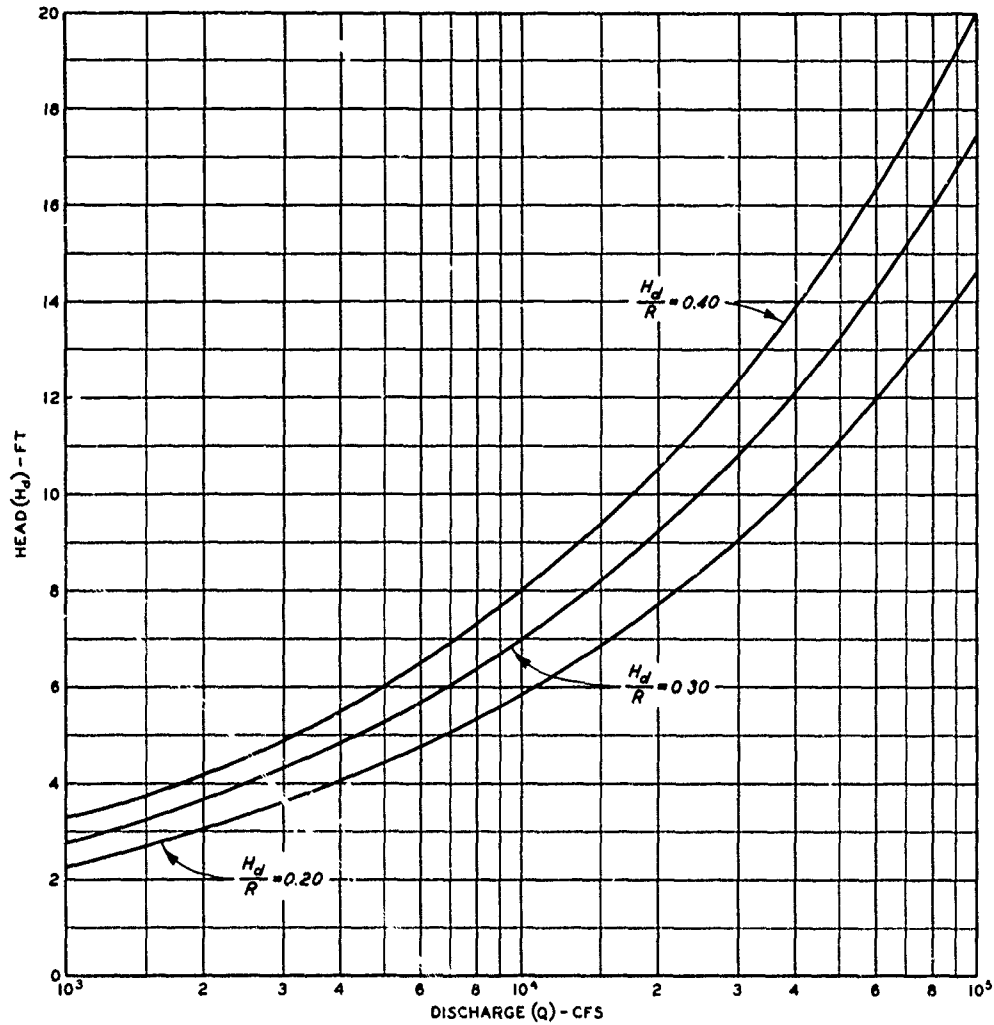
HEAD (H_d) - FT

DISCHARGE (Q) - CFS

$\frac{H_d}{R} = 0.40$

$\frac{H_d}{R} = 0.30$

$\frac{H_d}{R} = 0.20$

DEFINITION SKETCH

EQUATION

$$Q = C\,(2\pi R)\,H_d^{3/2}$$

WHERE.
Q = DISCHARGE, CFS
C = DISCHARGE COEFFICIENT
R = RADIUS OF SHARP CREST, FT
H_d = DESIGN HEAD ON SPILLWAY CREST, FT
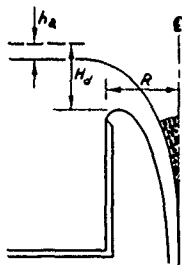
MORNING GLORY SPILLWAYS
DEEP APPROACH – CREST CONTROL
DESIGN DISCHARGE

HYDRAULIC DESIGN CHART 140-1
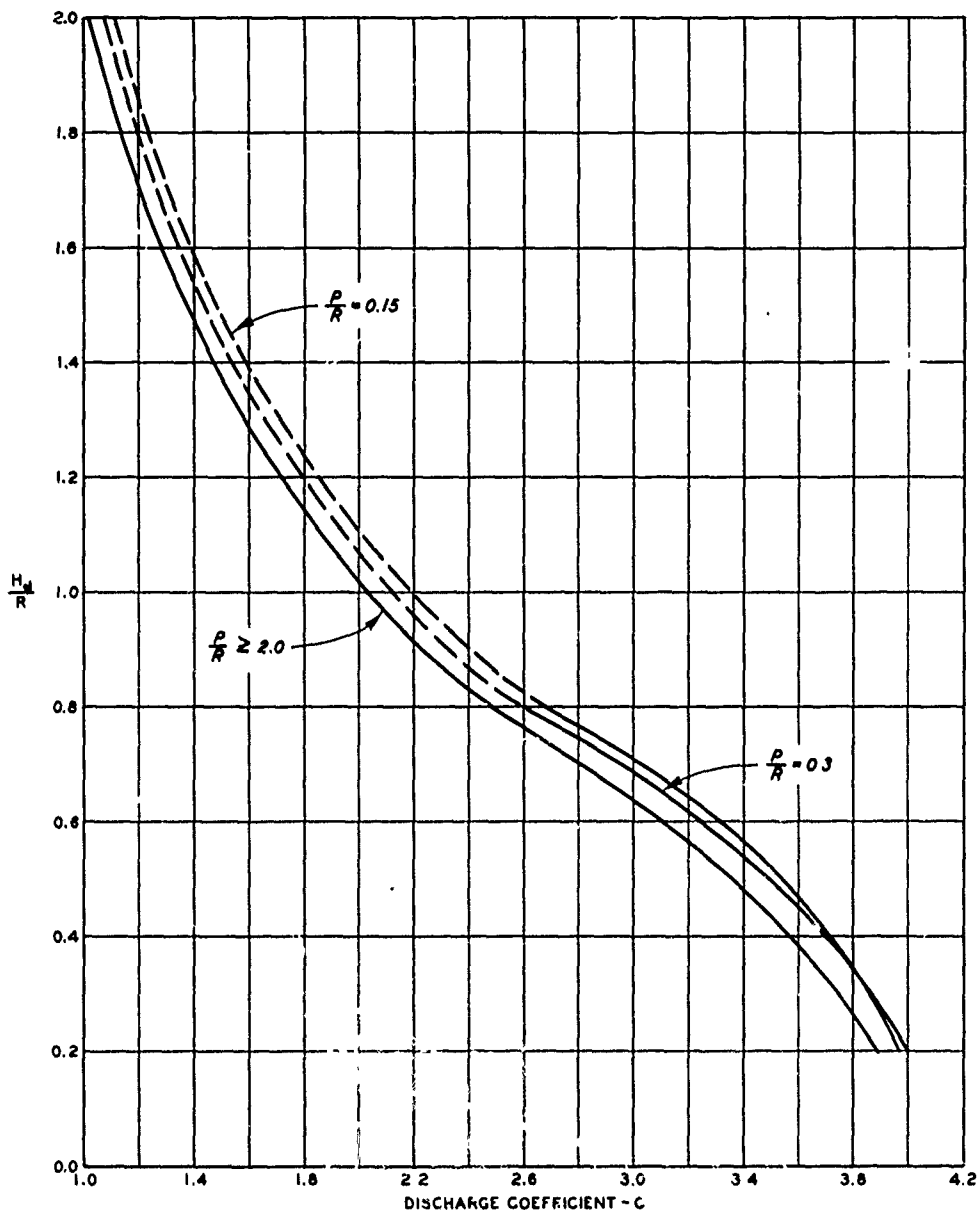
WES 10-61

$\dfrac{H_d}{R}$

DISCHARGE COEFFICIENT - C

$\dfrac{P}{R} = 0.15$

$\dfrac{P}{R} \geq 2.0$

$\dfrac{P}{R} = 0.3$

EQUATION

$$Q = C(2\pi R) H_d^{3/2}$$

WHERE:
  Q = DISCHARGE, CFS.
  C = DISCHARGE COEFFICIENT.
  R = RADIUS OF SHARP CREST, FT
  H_d = DESIGN HEAD ON SPILLWAY
       CREST, FT

NOTE. CURVES ARE TAKEN FROM USBR DESIGN OF
SMALL DAMS AND ARE BASED ON WAGNER'S
DATA FOR FULLY AERATED FLOW OVER A
SHARP-CRESTED WEIR.

DASHED CURVES ARE BASED ON EXTRAPOLATED
VALUES OF H_d/R (CHART 140-1/6).

P = APPROACH DEPTH TO SHARP CREST, FT.

MORNING GLORY SPILLWAYS
DISCHARGE COEFFICIENT
DESIGN HEAD

HYDRAULIC DESIGN CHART 140-1/1

WES 10-61

MORNING GLORY SPILLWAYS
LOWER NAPPE PROFILES

HYDRAULIC DESIGN CHART 140-1/2
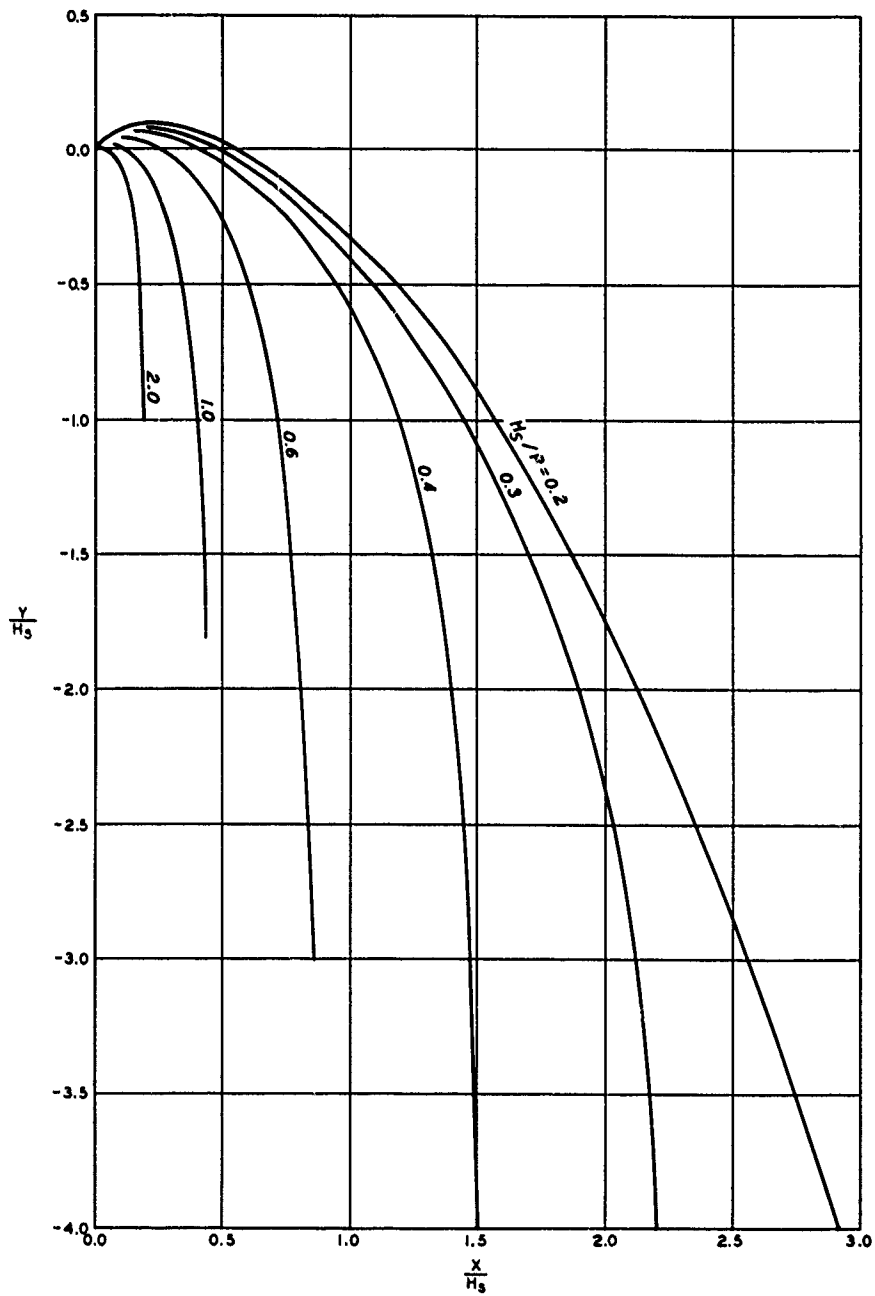
NOTE: $\frac{P}{R} \geq 2$, NEGLIGIBLE VELOCITY OF APPROACH. NAPPE AERATED.

DEFINITION SKETCH

$\dfrac{H_s}{R}$	0.20	0.30	0.40	0.50	0.60	1.00	1.50	2.00
$\dfrac{X}{H_s}$			$\dfrac{Y}{H_s}$ FOR PORTION OF PROFILE ABOVE WEIR CREST					
0.000	0.0000	0.0000	0.0000	0.0000	0.0000	0.0000	0.0000	0.0000
.010	.0133	.0128	.0122	.0116	.0112	.0095	.0077	.0070
.020	.0250	.0236	.0225	.0213	.0202	.0159	.0115	.0090
.030	.0350	.0327	.0308	.0289	.0270	.0198	.0126	.0085
.040	.0435	.0403	.0377	.0351	.0324	.0220	.0117	.0050
.050	.0506	.0471	.0436	.0402	.0368	.0226	.0092	
.060	.0570	.0521	.0489	.0448	.0404	.0220	.0053	
.070	.0627	.0584	.0537	.0487	.0432	.0201	.0001	
.080	.0677	.0630	.0578	.0521	.0455	.0172		
.090	.0722	.0670	.0613	.0549	.0471	.0135		
.100	.0762	.0705	.0642	.0570	.0482	.0089		
.120	.0826	.0758	.0683	.0596	.0483			
.140	.0872	.0792	.0705	.0599	.0460			
.160	.0905	.0812	.0710	.0585	.0418			
.180	.0927	.0820	.0705	.0559	.0361			
.200	.0938	.0819	.0688	.0521	.0292			
.250	.0926	.0773	.0596	.0380	.0068			
.300	.0850	.0668	.0446	.0174				
.350	.0750	.0540	.0280					
.400	.0620	.0365	.0060					
.450	.0450	.0170						
.500	.0250							
.550	.0020							
.600								
.650								

| $\dfrac{Y}{H_s}$			$\dfrac{X}{H_s}$ FOR PORTION OF PROFILE BELOW WEIR CREST					
0.000	0.554	0.487	0.413	0.334	0.262	0.116	0.070	0.048
-.020	.592	.526	.452	.369	.293	.145	.096	.074
-.040	.627	.563	.487	.400	.320	.165	.115	.088
-.060	.660	.596	.519	.428	.342	.182	.129	.100
-.080	.692	.628	.549	.454	.363	.197	.140	.110
-.100	.722	.657	.577	.478	.381	.210	.150	.118
-.150	.793	.725	.641	.531	.423	.238	.170	.132
-.200	.860	.790	.698	.575	.459	.260	.184	.144
-.250	.919	.847	.750	.613	.490	.280	.196	.153
-.300	.976	.900	.797	.648	.518	.296	.206	.160
-.400	1.079	1.000	.880	.706	.562	.322	.220	.168
-.500	1.172	1.087	.951	.753	.598	.342	.232	.173
-.600	1.260	1.167	1.012	.793	.627	.359	.240	.179
-.800	1.422	1.312	1.112	.854	.673	.384	.253	.184
-1.000	1.564	1.440	1.189	.899	.710	.402	.260	.188
-1.200	1.691	1.553	1.248	.933	.739	.417	.266	
-1.400	1.808	1.653	1.293	.963	.760	.423		
-1.600	1.918	1.742	1.330	.988	.780	.430		
-1.800	2.024	1.821	1.358	1.008	.797	.433		
-2.000	2.126	1.891	1.381	1.025	.810			
-2.500	2.354	2.027	1.430	1.059	.838			
-3.000	2.559	2.119	1.468	1.086	.853			
-3.500	2.749	2.171	1.489	1.102				
-4.000	2.914	2.201	1.500					
-4.500	3.053	2.220	1.509					
-5.000	3.178	2.227						
-5.500	3.294	2.229						
-6.000	3.405	2.232						

NOTE   NEGLIGIBLE VELOCITY OF APPROACH
NAPPE AERATED   TABLE BY WAGNER,
TRANSACTIONS, ASCE, 1956

MORNING GLORY SPILLWAYS
LOWER NAPPE SURFACE COORDINATES
$P/R \geq 2$

HYDRAULIC DESIGN CHART 140-1/3

WES 10-61

$\frac{H_s}{R}$	0.20	0.30	0.40	0.50	0.60	0.80
$\frac{X}{H_s}$	$\frac{Y}{H_s}$ FOR PORTION OF PROFILE ABOVE WEIR CREST					
0.000	0.0000	0.0000	0.0000	0.0000	0.0000	0.0000
.010	.0130	.0130	.0120	.0115	.0110	.0100
.020	.0245	.0240	.0225	.0195	.0180	.0170
.030	.0340	.0330	.0300	.0270	.0240	.0210
.040	.0415	.0390	.0365	.0320	.0285	.0240
.050	.0495	.0455	.0420	.0370	.0325	.0245
.060	.0560	.0505	.0460	.0405	.0350	.0250
.070	.0610	.0550	.0500	.0440	.0370	.0245
.080	.0660	.0590	.0530	.0460	.0385	.0235
.090	.0705	.0625	.0550	.0480	.0390	.0215
.100	.0740	.0660	.0575	.0500	.0395	.0190
.120	.0800	.0705	.0600	.0510	.0380	.0120
.140	.0840	.0735	.0615	.0515	.0355	.0020
.160	.0870	.0750	.0610	.0500	.0310	
.180	.0885	.0755	.0600	.0475	.0250	
.200	.0885	.0745	.0575	.0435	.0180	
.250	.0855	.0685	.0480	.0270		
.300	.0780	.0580	.0340	.0050		
.350	.0660	.0425	.0150			
.400	.0495	.0240				
.450	.0300	.0025				
.500	.0090					
.550						

$\frac{Y}{H_s}$	$\frac{X}{H_s}$ FOR PORTION OF PROFILE BELOW WEIR CREST					
0.000	0.519	0.465	0.384	0.310	0.238	0.141
-.020	.560	.495	.423	.345	.272	.174
-.040	.598	.532	.458	.376	.300	.198
-.060	.632	.567	.491	.406	.324	.220
-.080	.664	.600	.522	.432	.343	.238
-.100	.693	.631	.552	.456	.363	.254
-.150	.760	.701	.618	.510	.412	.290
-.200	.831	.763	.677	.558	.451	.317
-.250	.893	.826	.729	.599	.483	.341
-.300	.953	.880	.779	.634	.510	.362
-.400	1.060	.981	.867	.692	.556	.396
-.500	1.156	1.072	.938	.745	.595	.424
-.600	1.242	1.153	1.000	.760	.627	.446
-.800	1.403	1.301	1.101	.845	.672	.478
-1.000	1.549	1.430	1.180	.892	.707	.504
-1.200	1.680	1.543	1.240	.930	.733	.524
-1.400	1.800	1.647	1.287	.959	.757	.540
-1.600	1.912	1.740	1.323	.983	.778	.551
-1.800	2.018	1.821	1.353	1.005	.797	.560
-2.000	2.120	1.892	1.380	1.022	.810	.569
-2.500	2.351	2.027	1.428	1.049	.837	
-3.000	2.557	2.113	1.464	1.081	.852	
-3.500	2.748	2.167	1.489	1.099		
-4.000	2.911	2.200	1.499			
-4.500	3.052	2.217	1.507			
-5.000	3.173	2.223				
-5.500	3.290	2.228				
-6.000	3.400					
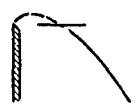
NOTE   APPRECIABLE VELOCITY OF APPROACH
NAPPE AERATED   TABLE BY WAGNER,
TRANSACTIONS ASCE, 1956

MORNING GLORY SPILLWAYS
LOWER NAPPE SURFACE COORDINATES
## P/R = 0.30

HYDRAULIC DESIGN CHART 140-1/4

$\frac{H_s}{R}$	0 20	0 30	0 40	0 50	0 60	0 80
$\frac{X}{H_s}$	$\frac{Y}{H_s}$ FOR PORTION OF PROFILE ABOVE WEIR CREST
0 000	0 0000	0 0000	0 0000	0 0000	0 0000	0 0000
.010	0120	.0115	0110	0105	0100	0090
.020	0210	0195	0185	0170	0160	.0140
.030	0285	.0265	.0250	0225	.0200	.0165
.040	0345	.0325	0300	.0265	0230	0170
050	0405	.0375	0345	.0300	0250	0170
.060	.0450	0420	0380	.0330	0265	0165
.070	0495	0455	0410	.0350	0270	0150
.080	0525	.0485	0435	0365	0270	0130
090	.0560	0510	.0455	0370	0265	0100
.100	.0590	0535	0465	0375	0255	0065
120	0630	0570	0480	0365	0220	
.140	0660	0585	.0475	0345	0175	
.160	.0670	0590	.0460	0305	0110	
180	0675	0580	.0435	.0260	.0040	
.200	0670	.0560	.0395	0200		
250	0615	0470	.0265	0015		
300	.0520	.0930	0100			
.350	0380	0165				
.400	0210					
.450	0015					
500						
.550						

$\frac{Y}{H_s}$	$\frac{X}{H_s}$ FOR PORTION OF PROFILE BELOW WEIR CREST
0 000	0 454	0 392	0.325	0 253	0 189	0 116
- 020	.499	437	369	292	228	149
- 040	540	478	407	326	259	174
- 060	.579	516	443	.356	286	195
- 080	615	550	476	.386	310	213
- 100	650	584	506	412	331	228
-.150	.726	660	577	.468	376	263
-.200	795	729	639	516	413	293
- 250	862	790	692	.557	445	319
- 300	922	.843	741	594	474	.342
- 400	1.029	947	828	656	523	381
- 500	1.128	1 040	902	710	567	413
- 600	1 220	1 129	967	753	601	439
- 800	1 380	1 285	1 060	827	655	473
-1.000	1 525	1 420	1 164	878	696	498
-1 200	1.659	1 537	1 228	917	725	517
-1 400	1 760	1.639	1 276	949	750	531
-1.600	1 897	1.729	1 316	973	770	544
-1 800	2 003	1 809	1 347	937	787	553
-2 000	2 104	1 879	1 372	1 013	801	560
-2.500	2 340	2 017	1 423	1 049	827	
-3 000	2 550	2 105	1 457	1 073	840	
-3 500	2 740	2 153	1 475	1 086		
-4.000	2 904	2 160	1 487			
-4 500	3 048	2 198	1 491			
-5 000	3 169	2 207				
-5 500	3 286	2 210				
-6 000	3 396					

NOTE APPRECIABLE VELOCITY OF APPROACH
NAPPE AERATED   TABLE BY WAGNER,
<u>TRANSACTIONS</u>, <u>ASCE</u>, 1956

MORNING GLORY SPILLWAYS
LOWER NAPPE SURFACE COORDINATES
P/R = 0.15

HYDRAULIC DESIGN CHART 140-1/5
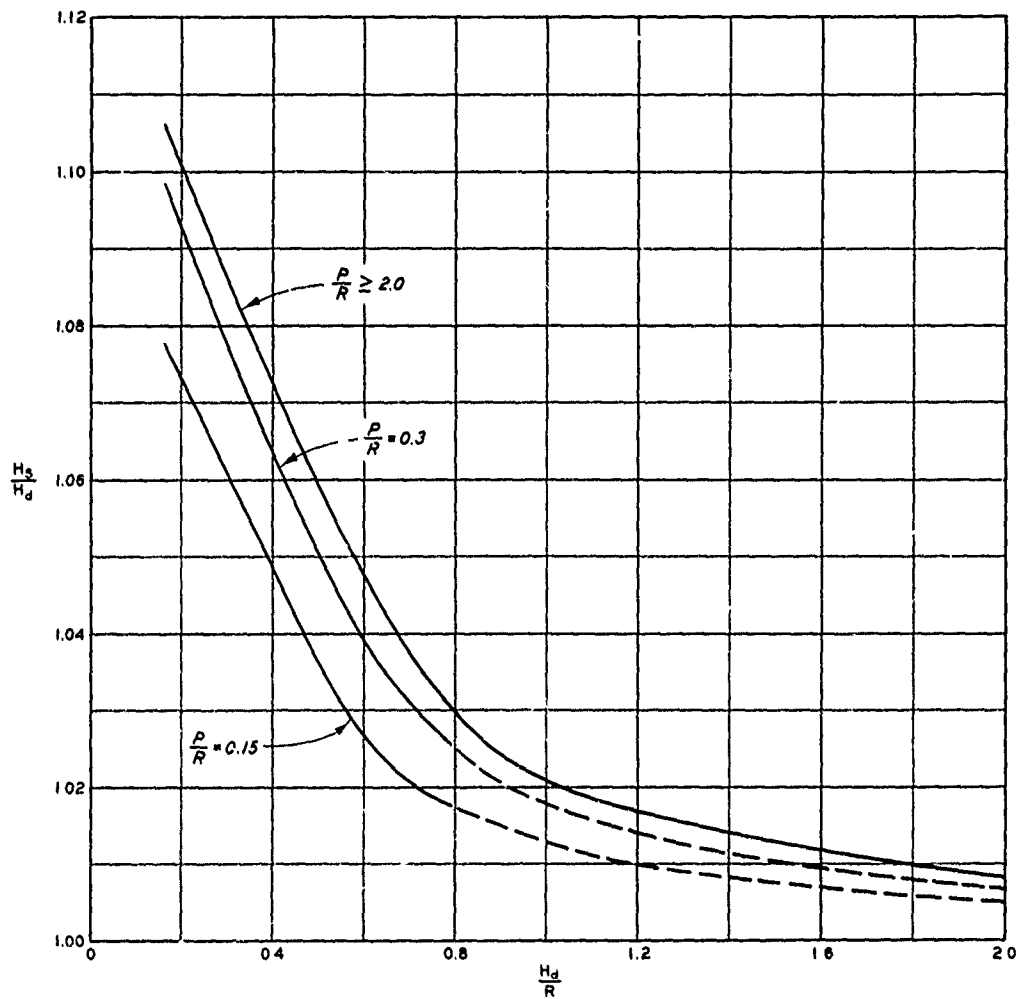
NOTE P = DEPTH OF APPROACH TO SHARP CREST
      R = RADIUS OF SHARP CREST.
      H_s = DESIGN HEAD ON SHARP CREST
      H_d = DESIGN HEAD ON SPILLWAY CREST
      CURVES ARE TAKEN FROM USBR <u>DESIGN OF
      SMALL DAMS</u>
      DASHED LINES ARE BASED ON EXTRAPOLATION
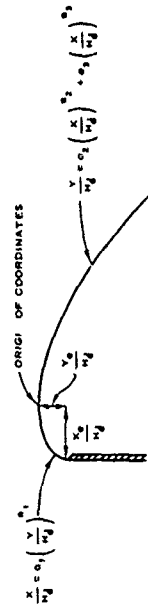   OF DATA.

MORNING GLORY SPILLWAYS

$$\frac{H_s}{H_d} \text{ VS } \frac{H_d}{R}$$

HYDRAULIC DESIGN CHART 140-1/8

MORNING GLORY SPILLWAYS
CREST SHAPE EQUATIONS

$\dfrac{P}{R}$	$\dfrac{H_s}{R}$	$\dfrac{X_s}{H_d}$	$\dfrac{Y_s}{H_d}$	UPSTREAM QUADRANT EQUATIONS	LIMITING $\dfrac{X}{H_d}$	DOWNSTREAM QUADRANT EQUATIONS	LIMITING $\dfrac{X}{H_d}$
≥2	0.2	-0.237	0.1035	$\dfrac{X}{H_d} = -0.635\left(\dfrac{Y}{H_d}\right)^{0.410}$	-0.190	$\dfrac{Y}{H_d} = 0.610\left(\dfrac{X}{H_d}\right)^{1.85}$	3.20
	0.3	-0.209	0.0893	$\dfrac{X}{H_d} = -0.568\left(\dfrac{Y}{H_d}\right)^{0.387}$	-0.166	$\dfrac{Y}{H_d} = 0.665\left(\dfrac{X}{H_d}\right)^{1.86} + 0.000009\left(\dfrac{X}{H_d}\right)^{13.6}$	2.25
	0.4	-0.174	0.0764	$\dfrac{X}{H_d} = -0.538\left(\dfrac{Y}{H_d}\right)^{0.424}$	-0.145	$\dfrac{Y}{H_d} = 0.830\left(\dfrac{X}{H_d}\right)^{1.85} + 0.035\left(\dfrac{X}{H_d}\right)^{12.2}$	1.45
0.30	0.2	-0.219	0.0972	$\dfrac{X}{H_d} = -0.622\left(\dfrac{Y}{H_d}\right)^{0.418}$	-0.155	$\dfrac{Y}{H_d} = 0.590\left(\dfrac{X}{H_d}\right)^{1.73} + 0.00375\left(\dfrac{X}{H_d}\right)^{4.73}$	3.50
	0.3	-0.189	0.0817	$\dfrac{X}{H_d} = -0.637\left(\dfrac{Y}{H_d}\right)^{0.431}$	-0.140	$\dfrac{Y}{H_d} = 0.650\left(\dfrac{X}{H_d}\right)^{1.73} + 0.00174\left(\dfrac{X}{H_d}\right)^{8.68}$	2.15
	0.4	-0.156	0.0655	$\dfrac{X}{H_d} = -0.556\left(\dfrac{Y}{H_d}\right)^{0.440}$	-0.120	$\dfrac{Y}{H_d} = 0.725\left(\dfrac{X}{H_d}\right)^{1.73} + 0.140\left(\dfrac{X}{H_d}\right)^{6.93}$	1.35
0.15	0.2	-0.192	0.0724	$\dfrac{X}{H_d} = -0.625\left(\dfrac{Y}{H_d}\right)^{0.450}$	-0.160	$\dfrac{Y}{H_d} = 0.600\left(\dfrac{X}{H_d}\right)^{1.73} + 0.00375\left(\dfrac{X}{H_d}\right)^{4.77}$	3.45
	0.3	-0.164	0.0627	$\dfrac{X}{H_d} = -0.665\left(\dfrac{Y}{H_d}\right)^{0.476}$	-0.125	$\dfrac{Y}{H_d} = 0.660\left(\dfrac{X}{H_d}\right)^{1.73} + 0.0008\left(\dfrac{X}{H_d}\right)^{10.0}$	2.15
	0.4	-0.132	0.0504	$\dfrac{X}{H_d} = -0.540\left(\dfrac{Y}{H_d}\right)^{0.451}$	-0.105	$\dfrac{Y}{H_d} = 0.760\left(\dfrac{X}{H_d}\right)^{1.73} + 0.155\left(\dfrac{X}{H_d}\right)^{6.67}$	1.35

ORIGIN OF COORDINATES

$$\frac{X}{H_d} = a_1 \left(\frac{Y}{H_d}\right)^{a_2}$$

$$\frac{Y}{H_d} = a_1 \left(\frac{X}{H_d}\right)^{a_2} + a_3 \left(\frac{X}{H_d}\right)^{a_4}$$

HYDRAULIC DESIGN CHART 140-1/7

WES 10-61

CHART 140-1/7

U. S. ARMY ENGINEER WATERWAYS EXPERIMENT STATION

COMPUTATION SHEET

GIVEN:

Design discharge $(Q) = 10,000$ cfs
Design head $(H_d) = 10$ ft
Approach depth $(P) \geq 2R$
Conduit to be designed for free flow

REQUIRED:

Spillway shape with minimum crest radius

COMPUTE:

1. Crest radius required to pass design discharge.

   Assume $R = 16.4$ ft

   $$\frac{H_d}{R} = \frac{10}{16.4} = 0.61$$

   For $\frac{H_d}{R} = 0.61$ and $\frac{P}{R} \geq 2$

   $C = 3.08$ (HDC 140-1/1)

   $$Q = C\,(2\pi R)\,H_d^{3/2}$$
   $$= 3.08 \times 6.28 \times 16.4 \times 10^{3/2}$$
   $$= 10,030 \text{ cfs*}$$

2. Ratio of head on weir to crest radius (H_s/R)

   For $\frac{H_d}{R} = 0.61$ and $\frac{P}{R} \geq 2$

   $$\frac{H_s}{H_d} = 1.047 \text{ (HDC 140-1/6)}$$

   $H_s = 1.047 \times 10 = 10.47$ ft

   $$\frac{H_s}{R} = \frac{10.47}{16.4} = 0.64 \text{ (Partial submergence, } 0.45 < H_s/R < 1.00)$$

3. Crest profile for $H_s/R = 0.64$ by interpolation from table on HDC 140-1/3.

*If computed discharge does not closely approximate design discharge, assume new radius and repeat computation.
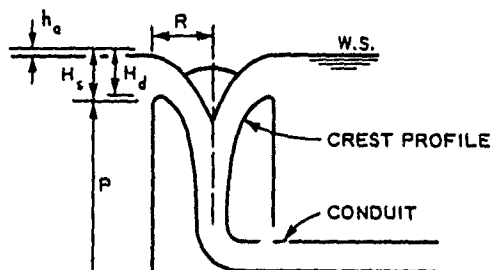
MORNING GLORY SPILLWAYS
SPILLWAY DESIGN
SAMPLE COMPUTATION

HYDRAULIC DESIGN CHART 140-1/8

SLUICE ENTRANCES FLARED ON FOUR SIDES

PRESSURE-DROP COEFFICIENTS

1. **Purpose.** The objectives in sluice entrance design are positive pressures at all flows to preclude cavitation, smoothly varying pressures to minimize entrance losses, and small size for stop-log closure. Hydraulic Design Charts 211-1 to 211-1/2 give pressure-drop data for several shapes of entrances to rectangular sluices.

2. **Theory.** The pressure drop (H_d) from the reservoir surface to any point on the pressure gradient for an entrance curve can be expressed as a function of the velocity head in the conduit proper:

$$H_d = C(V^2/2g)$$

where

H_d = pressure drop, ft

C = dimensionless pressure-drop coefficient

V = average velocity in conduit proper, fps.

3. **Experimental Data.** The pressure data on Chart 211-1 to 211-1/2 were obtained from tests conducted at the Waterways Experiment Station under CW 802, Conduit Intake Model Tests.* The laboratory test section represented a prototype sluice 5.67 ft wide by 10 ft high (h/w = 1.765) with the elliptical and combination elliptical entrance curves shown on the charts. The value of D in the curve equations is equal to the conduit height for the top and bottom curves and the conduit width for the side curves. The Pine Flat prototype data** shown on Chart 211-1/2

---

* Entrances to Conduits of Rectangular Cross Section; Investigation of Entrance Flared in Four Directions. U. S. Army Engineer Waterways Experiment Station, CE, TM 2-428, Report No. 1, Vicksburg, Miss., March 1956.

** Vibration, Pressure and Air-Demand Tests in Flood-control Sluice, Pine Flat Dam, Kings River, California. U. S. Army Engineer Waterways Experiment Station, CE, Miscellaneous Paper No. 2-75, Vicksburg, Miss., February 1954, and subsequent unpublished test data.

are for a 5-ft-wide by 9-ft-high (h/w = 1.80), horizontal sluice with elliptical entrance curves at the 20-on-1 sloping upstream face. These data are averages obtained for 14 pool elevations between 113 and 302 ft above the sluice center line.

4. The CW 802 data are from laboratory tests in which the discharge was closely controlled. The Pine Flat prototype data are based on a discharge curve developed from stream measurements. The pressure-drop coefficients are sensitive to small inaccuracies in discharge, and the discrepancy between the laboratory and prototype data is attributed to such small inaccuracies. A 2 per cent adjustment in the basic discharge data would result in close agreement.

5. Sluice Entrance Pressures. The dimensionless pressure-drop coefficients given on Charts 211-1 to 211-1/2 can be used to compute the pressure gradient elevations for the given entrance shapes. The pressure gradient for any combination of pool elevation and discharge then can be compared with the entrance profile to determine the pressures on the entrance surfaces. The elliptical shape should normally be used, but for high dams with insufficient back pressures use of the longer combination elliptical curve may be necessary to prevent occurrence of negative pressures.
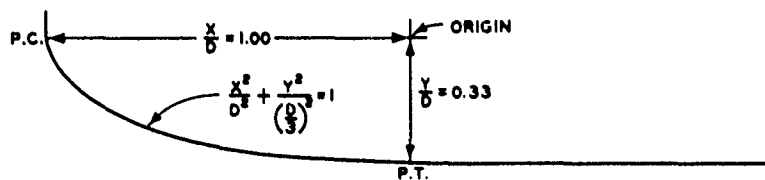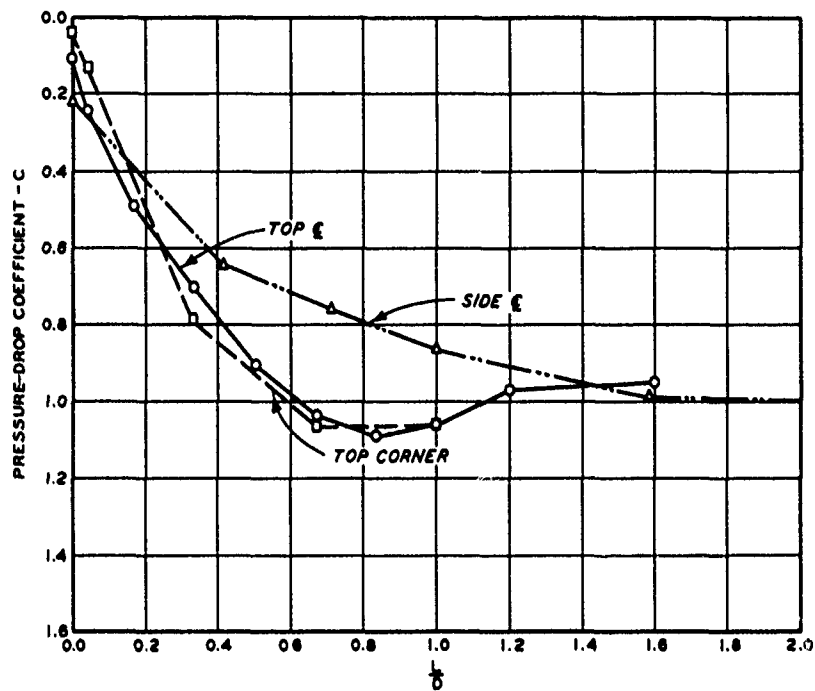
BASIC EQUATION

$$C = \frac{H_D}{\frac{V^2}{2g}}$$

WHERE:

C = PRESSURE-DROP COEFFICIENT
H_D= PRESSURE DROP FROM POOL IN FT
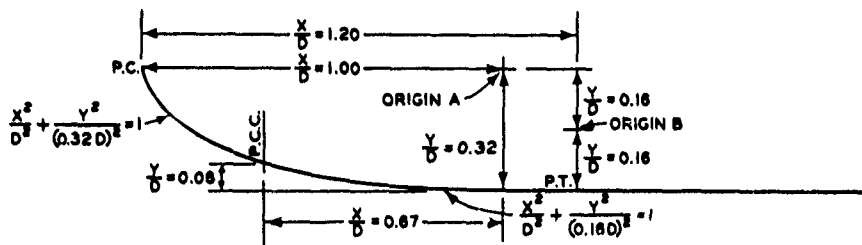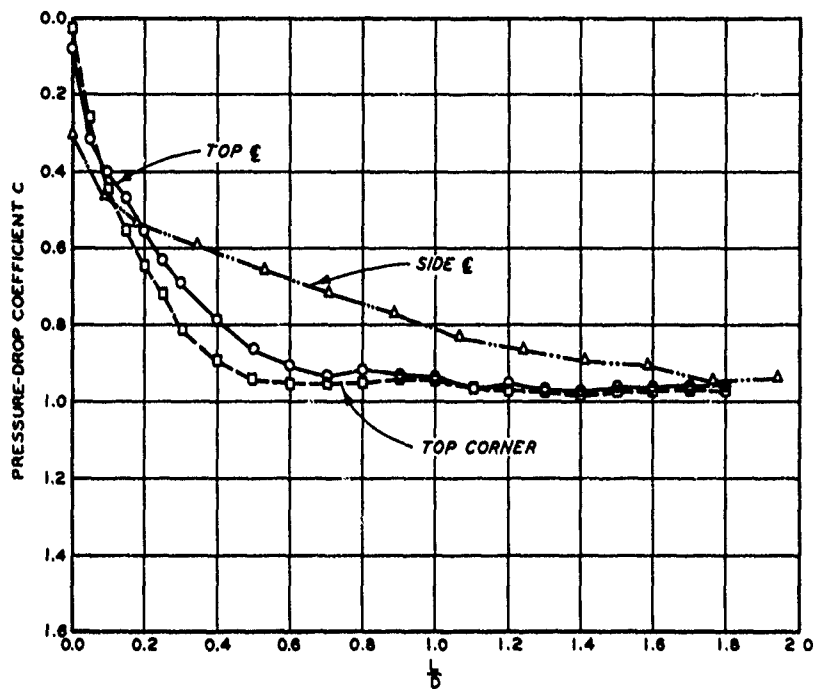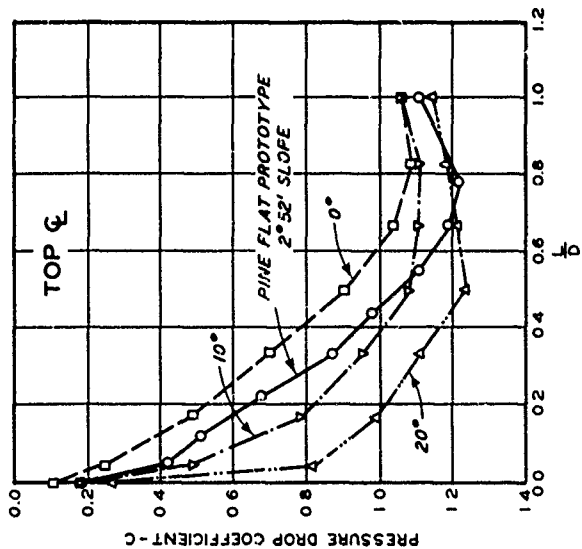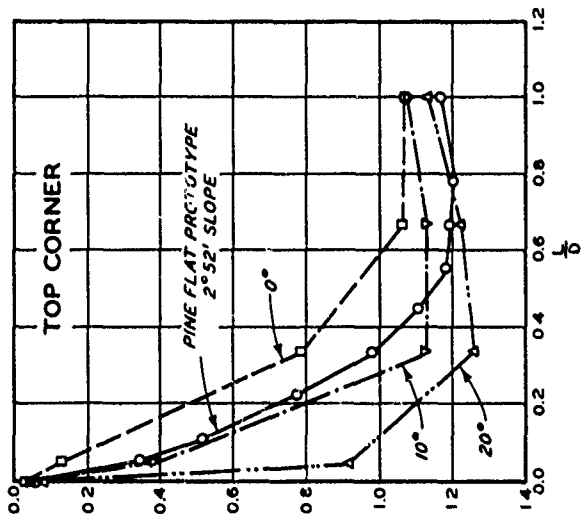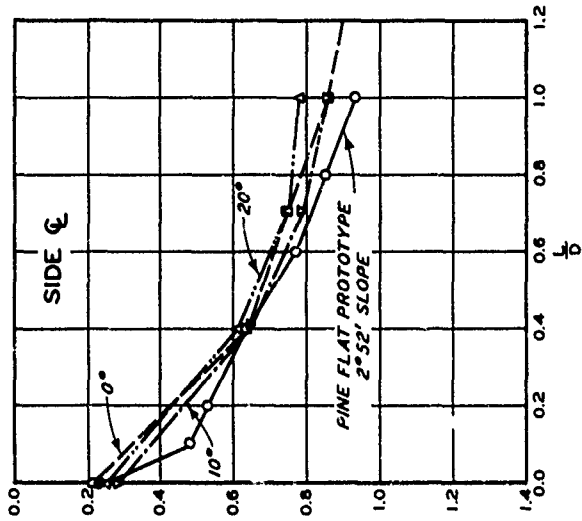V = AVERAGE VELOCITY IN CONDUIT
  PROPER IN FT PER SEC

NOTE:

  RESULTS BASED ON CW 802
  TEST DATA (h/w = 1.765).

D = DIMENSION OF CONDUIT IN DIRECTION
  CONCERNED IN FT
L = DISTANCE ALONG CONDUIT IN FT
h = HEIGHT OF CONDUIT PROPER
w = WIDTH OF CONDUIT PROPER

SLUICE ENTRANCES
PRESSURE-DROP COEFFICIENTS
ELLIPTICAL SHAPE

HYDRAULIC DESIGN CHART 211-1

PRESSURE-DROP COEFFICIENT C

TOP ℄

SIDE ℄

TOP CORNER

$\frac{L}{D}$

$\frac{X}{D} = 1.20$

$\frac{X}{D} = 1.00$

P.C.

ORIGIN A

$\frac{Y}{D} = 0.16$

ORIGIN B

$\frac{X^2}{D^2} + \frac{Y^2}{(0.32D)^2} = 1$

$\frac{Y}{D} = 0.32$

$\frac{Y}{D} = 0.16$

P.C.C.

$\frac{Y}{D} = 0.08$

P.T.

$\frac{X}{D} = 0.67$

$\frac{X^2}{D^2} + \frac{Y^2}{(0.16D)^2} = 1$

BASIC EQUATION

$$C = \frac{H_0}{\frac{V^2}{2g}}$$

WHERE:

C = PRESSURE-DROP COEFFICIENT
H_0 = PRESSURE DROP FROM POOL, FT
V = AVERAGE VELOCITY IN CONDUIT
    PROPER, FT PER SEC

NOTE:

RESULTS BASED ON ES 802
TEST DATA (h/w = 1.765).

D = DIMENSION OF CONDUIT IN DIRECTION
    CONCERNED, FT
L = DISTANCE ALONG CONDUIT, FT
h = HEIGHT OF CONDUIT PROPER, FT
w = WIDTH OF CONDUIT PROPER, FT

SLUICE ENTRANCES
PRESSURE-DROP COEFFICIENTS
COMBINATION ELLIPTICAL SHAPE

HYDRAULIC DESIGN CHART 211-1/1

SLUICE ENTRANCES
PRESSURE DROP COEFFICIENTS
ELLIPTICAL SHAPE
EFFECT OF ENTRANCE SLOPE
HYDRAULIC DESIGN CHART 211-1/2

BASIC EQUATION

$$C = \frac{H_D}{\frac{V^2}{2g}}$$

WHERE:

C = PRESSURE DROP COEFFICIENT
H_D = PRESSURE DROP FROM POOL IN FT
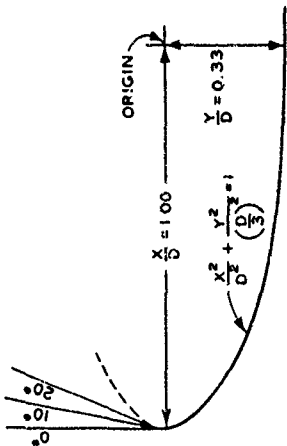V = AVERAGE VELOCITY IN CONDUIT
    PROPER IN FT PER SEC

D = DIMENSION OF CONDUIT IN DIRECTION
    CONCERNED IN FT
L = DISTANCE ALONG CONDUIT IN FT
h = HEIGHT OF CONDUIT PROPER
w = WIDTH OF CONDUIT PROPER

NOTE

COEFFICIENTS BASED ON CW802 MODEL
TEST DATA (h/w=1.785). PINE FLAT
PROTOTYPE DATA FOR HORIZONTAL
SLUICE (h/w=1.800) WITH ENTRANCE
AT 20 ON 1 (2°52') SLOPING UPSTEAM
FACE

DEFINITION SKETCH

$$\frac{X}{D} = 1.00$$

$$\frac{X^2}{D^2} + \frac{Y^2}{\left(\frac{D}{3}\right)^2} = 1$$

$$\frac{Y}{D} = 0.33$$

ORIGIN

WES 6-57

CHART 211-1/2

HYDRAULIC DESIGN CRITERIA

SHEETS 212-1 TO 212-1/2

GATE SLOTS

PRESSURE COEFFICIENTS

1. **Background.** Flow past gate slots results in a decrease in pressure on the conduit walls immediately downstream from the slot. Cavitation erosion can occur downstream from the slot when high-velocity flow is accompanied by insufficient pressure in the general region. One of the variables involved is the ratio of the slot width to depth. Another important variable is the conduit geometry downstream from the slot. Undesirable pressure conditions on the conduit walls can be improved to some degree by offsetting the downstream edge of the slot and returning gradually to the original conduit wall alignment.

2. **Basic Data.** Hydraulic Design Chart 212-1 presents pressure coefficients for rounded corner gate slots with a width-depth ratio equal to 2.1. Similar data for a ratio of 1.8 are presented in Chart 212-1/1 for slots with the rounded downstream corners combined with a 1:12 taper to the original conduit alignment. The coefficients shown were computed using the equation

$$H_d = CH_v$$

where

H_d = pressure difference from reference pressure, ft

C = pressure coefficient

H_v = conduit velocity head at reference pressure station, ft

The reference pressure station noted above is shown in the definition sketch in each chart. The coefficients shown in the charts result from U. S. Army Engineer Waterways Experiment Station (WES) laboratory tests made on 1-to-6-scale models of gate slot designs for Bull Shoals Dam.[1]

3. Chart 212-1/2 presents coefficients for computing the minimum pressure in and downstream from square-edged slots with ratios of width to depth ranging from 0.5 to 2.5. The chart is based on tests by the U. S. Bureau of Reclamation (USBR)[2] with supporting data by Spengo.[3] The USBR tests also included study of the effects of rounding the upstream corner of the gate slot, decreasing the downstream wall convergence rate to 1:24 and 1:36, and using convergences shaped to circular arcs. Rounding of the upstream corner of the slot appears to have little effect on the pressures in or near the slot unless the rounding is appreciable.
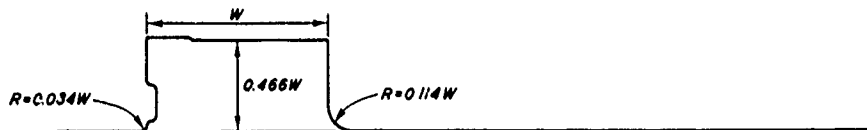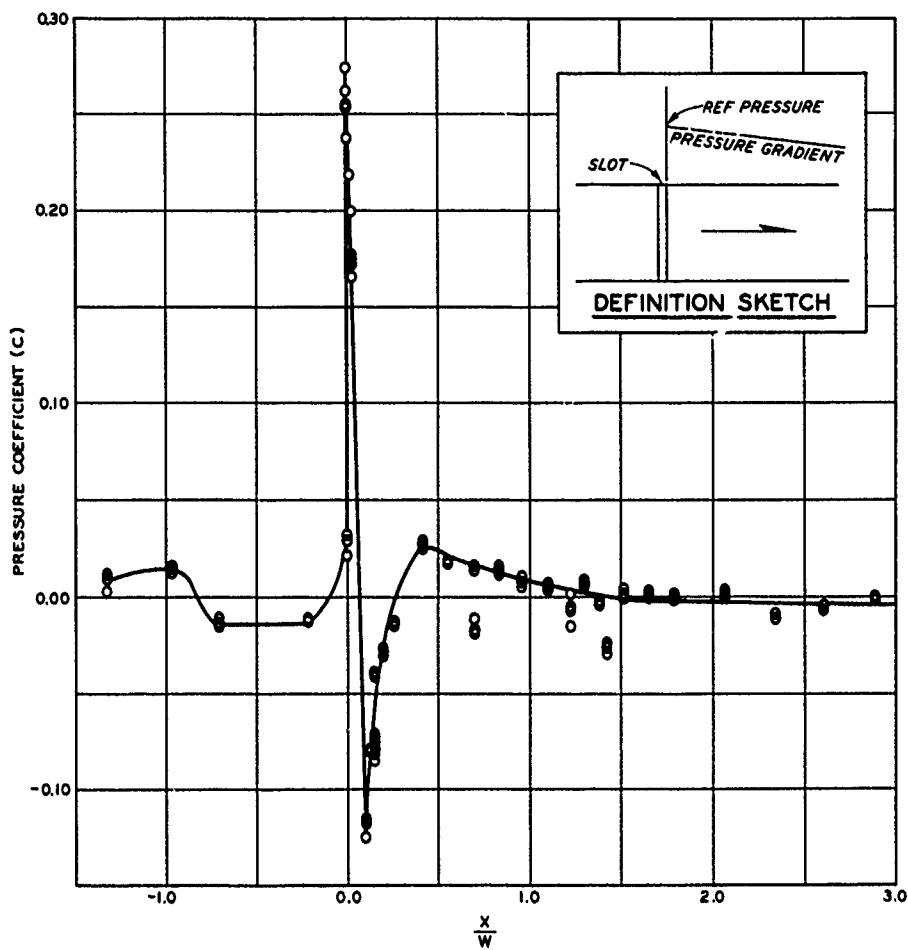
In this case expansion of the flow into the slot can result in greater downstream flow contraction accompanied by greater pressure reduction on the downstream walls. Changing the downstream convergence rate to 1:24 and 1:36 effects a downstream movement of the minimum pressure location with no appreciable pressure changes. The USBR tests also showed that convergences shaped to circular arcs are hydraulically superior to those formed by tangents.

4. The coefficients shown in Charts 212-1 through 212-1/2 are based on mean piezometric measurements and do not reflect local pressure fluctuations caused by turbulence in the flow. It is suggested that the minimum computed pressure be limited to at least atmospheric pressure to reduce the possibility of cavitation in the prototype. Prototype data from electric pressure transducers are needed for firm criteria.

5. Design Criteria. Charts 212-1 through 212-1/2 should be used as guides for estimating minimum pressure conditions in the vicinity of gate slots for full tunnel flow. The rounding of the upstream edge of the gate slot shown in the charts can be eliminated with no apparent adverse hydraulic or structural effects. The 1:12 downstream taper shown in Chart 212-1/1 has been generally adopted for design and found satisfactory. In practice, the radius of the downstream corner of the gate slot has been appreciably decreased over that shown in the charts to reduce gate span and slot depth, thereby effecting savings in costs. Experience indicates that for part-gate operation cavitation erosion mainly occurs 6 to 8 in. downstream from the beginning of the 1:12 taper rather than at the end of the taper, as inferred from Chart 212-1/1. If the gates are to be operated appreciably at part-gate openings under high heads, consideration should be given to using stainless steel for the first 6 to 8 in. of the taper. The design criteria above is recommended for high head structures. The simpler gate slot design given in Chart 212-1 should be adequate for low heads when the conduit back pressure results in a minimum computed average local pressure approximating atmospheric pressure.

6. References.

(1) U. S. Army Engineer Waterways Experiment Station, CE, Model Studies of Conduits and Stilling Basin, Bull Shoals Dam, White River, Arkansas. Technical Memorandum No. 2-234, Vicksburg, Miss., June 1947.

(2) Ball, J. W., "Hydraulic characteristics of gate slots." ASCE, Hydraulics Division, Journal, vol 85, HY 10 (October 1959), pp 81-114.

(3) Spengo, A., "Cavitation and Pressure Distribution at Gate Slots." M.S. thesis, University of Iowa, Iowa City, June 1949.

PRESSURE COEFFICIENT (C)

$\frac{X}{W}$

DEFINITION SKETCH

REF PRESSURE
PRESSURE GRADIENT
SLOT

TYPE 1 GATE SLOT (REFERENCE 1)

W

0.466W

R=0.034W

R=0.114W

NOTE: X/W = RATIO OF DISTANCE FROM
DOWNSTREAM EDGE OF SLOT TO
WIDTH OF SLOT

EQUATION

$H_d = CH_V$

WHERE:
H_d = PRESSURE DIFFERENCE FROM
REFERENCE PRESSURE, FT
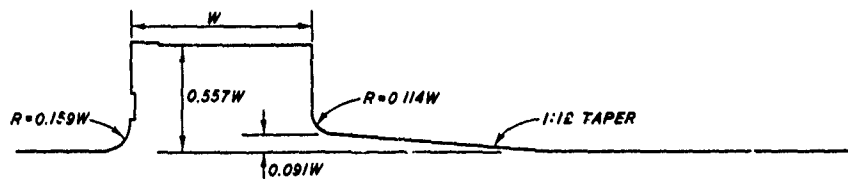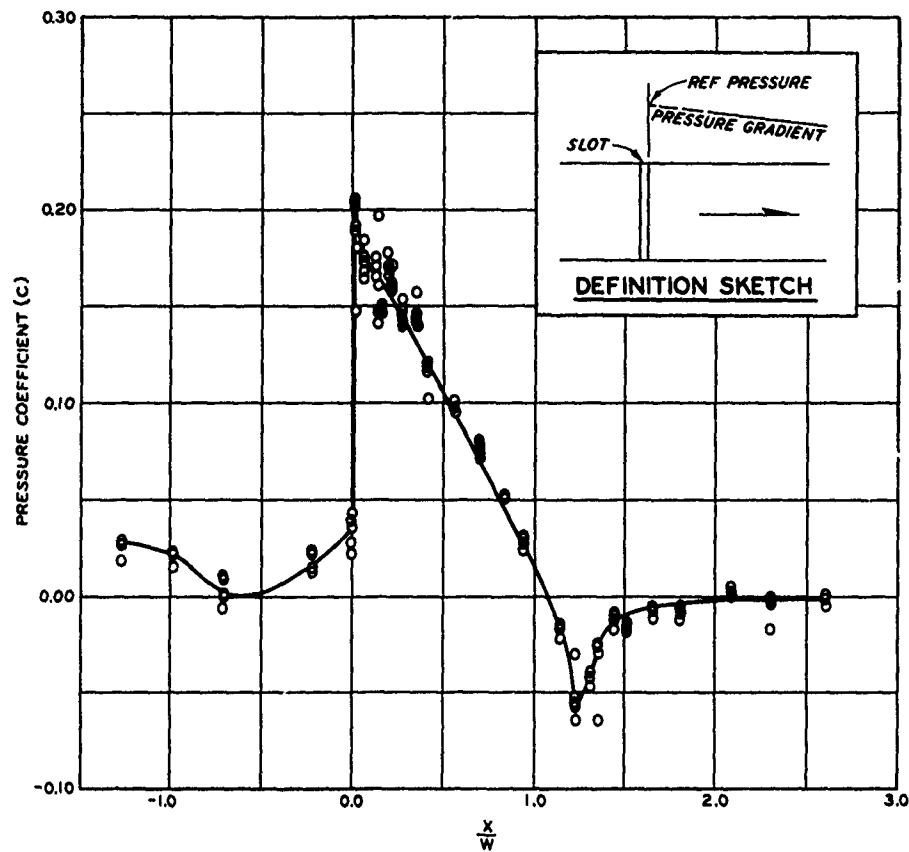C = PRESSURE COEFFICIENT
H_V = CONDUIT VELOCITY HEAD AT
REFERENCE PRESSURE STATION, FT

GATE SLOTS
WITHOUT DOWNSTREAM OFFSET
PRESSURE COEFFICIENTS

HYDRAULIC DESIGN CHART 212-1

DEFINITION SKETCH

TYPE 2 GATE SLOT (REFERENCE 1)

EQUATION

$$H_d = C H_V$$
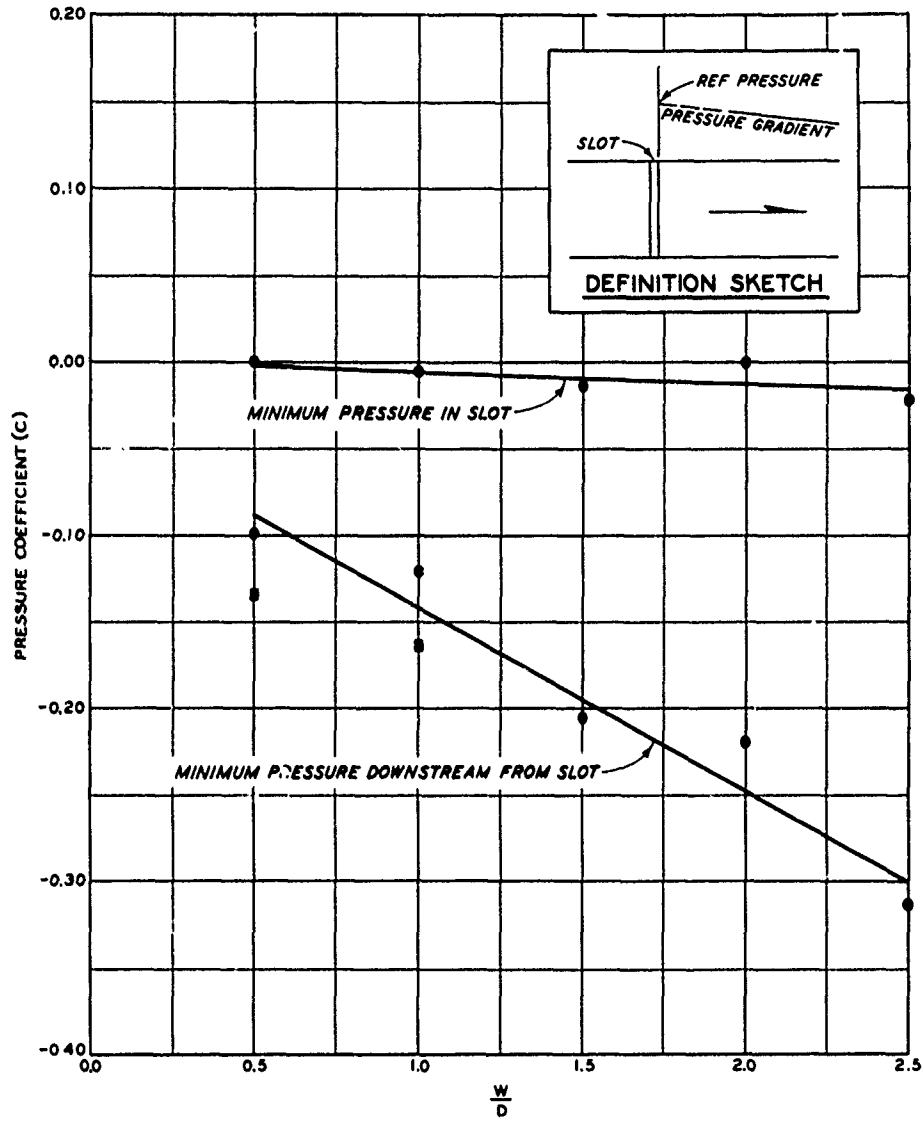
WHERE
H_d = PRESSURE DIFFERENCE FROM
REFERENCE PRESSURE, FT
C = PRESSURE COEFFICIENT
H_V = CONDUIT VELOCITY HEAD AT
REFERENCE PRESSURE STATION, FT

NOTE: X/W = RATIO OF DISTANCE FROM
DOWNSTREAM EDGE OF SLOT TO
WIDTH OF SLOT

GATE SLOTS
WITH DOWNSTREAM OFFSET
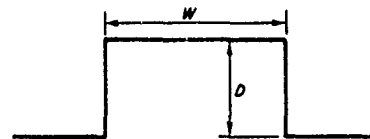PRESSURE COEFFICIENTS

HYDRAULIC DESIGN CHART 212-1/1

DEFINITION SKETCH

PRESSURE COEFFICIENT (C)

MINIMUM PRESSURE IN SLOT

MINIMUM PRESSURE DOWNSTREAM FROM SLOT

$\frac{W}{D}$

LEGEND

● USBR (REF 2)
■ SPENGO, SUI (REF 3)

EQUATION

$H_d = CH_V$

WHERE:
H_d = PRESSURE DIFFERENCE FROM REFERENCE PRESSURE, FT
C = PRESSURE COEFFICIENT
H_V = CONDUIT VELOCITY HEAD AT REFERENCE PRESSURE STATION, FT

GATE SLOTS
WITHOUT DOWNSTREAM OFFSET
PRESSURE COEFFICIENTS
EFFECT OF SLOT WIDTH-DEPTH RATIO

HYDRAULIC DESIGN CHART 212-1/2

WES 10-61

HYDRAULIC DESIGN CRITERIA

SHEET 221-1

CONCRETE CONDUITS

INTAKE LOSSES

1. **Chart 221-1.** The chart presents intake losses determined from model and prototype investigations of single, double, and triple intakes. It is only applicable to conduits flowing full.

2. **Theory.** For design purposes intake losses include trashrack, entrance, gate-slot, transition, and friction losses throughout the intake section. The total intake loss expressed as a function of the velocity head in the conduit proper is

$$h_e = K_e \ (V^2/2g)$$

where

h_e = intake loss, ft

K_e = loss coefficient

V = average velocity in conduit proper, ft/sec

g = acceleration due to gravity, ft/sec^2

3. Accurate experimental determination of intake losses is dependent upon the conduit being of sufficient length to permit a uniform friction gradient to be established based on fully developed turbulence. The intake loss is the total available head minus the velocity head and the friction loss of the conduit.

4. **Basic Data.** Chart 221-1, which summarizes the best available data, was developed from results of model and prototype investigations of conduits of sufficient length for turbulence to become fully developed. The data selected from model and prototype investigations for use in determining intake losses for the three types of intakes are described below.

    a. **Single intake.** The Pine Flat Dam[1] data used are prototype pressures observed in a rectangular concrete conduit. Other data[2] were obtained during a laboratory study of the effect of artificial stimulation of the turbulent boundary layer in a rectangular conduit conducted under Corps of Engineers Engineering Studies Item 802, Conduit Intake Model Tests. The laboratory intake section contained no gate slots. Data concerning the effects of gate slots on intake losses were
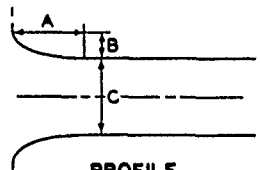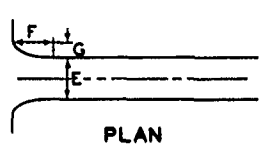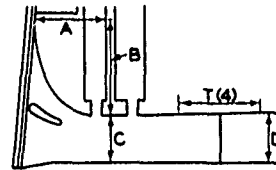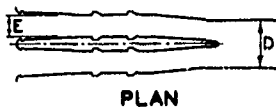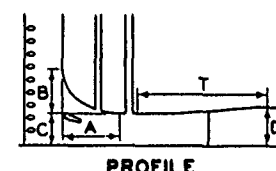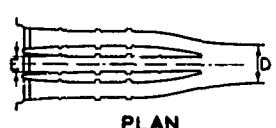
obtained in special tests made during the Bull Shoals Dam[3] model study; the data indicate that these effects are negligible.

    b. <u>Double intake.</u> Prototype pressure data were obtained at Denison[4] and Fort Randall Dams.[5] The Denison[6] and Fort Randall[7] models were built to a scale of 1 to 25. The friction losses in the Fort Randall model appeared normal. Those in the Denison model appeared excessively low. However, the relation between model and prototype intake losses is consistent.

    c. <u>Triple intake.</u> The Tionesta model[8] data are the only known data resulting from a study of a triple intake to a conduit of sufficient length to permit turbulence to become fully developed.

   5. <u>References.</u>

(1) U. S. Army Engineer Waterways Experiment Station, CE, <u>Vibration, Pressure and Air-Demand Tests in Flood-Control Sluice, Pine Flat Dam, Kings River, California.</u> Miscellaneous Paper No. 2-75, Vicksburg, Miss., February 1954.

(2) _____, <u>The Effect of Artificial Stimulation of the Turbulent Boundary Layer in Rectangular Conduits.</u> Miscellaneous Paper No. 2-160, Vicksburg, Miss., March 1956.

(3) _____, <u>Model Studies of Conduits and Stilling Basin, Bull Shoals Dam, White River, Arkansas.</u> Technical Memorandum No. 2-234, Vicksburg, Miss., June 1947.

(4) _____, <u>Pressure and Air Demand Tests in Flood-Control Conduit, Denison Dam, Red River, Oklahoma and Texas.</u> Miscellaneous Paper No. 2-31, Vicksburg, Miss., April 1953.

(5) _____, <u>Flow Characteristics in Flood-Control Tunnel 10, Fort Randall Dam, Missouri River, South Dakota; Hydraulic Prototype Tests.</u> Technical Report No. 2-626, Vicksburg, Miss., June 1963.

(6) _____, <u>Hydraulic Model Studies of the Control Structures for the Denison Dam, Red River.</u> Technical Memorandum No. 161-1, Vicksburg, Miss., April 1940.

(7) _____, <u>Spillway and Outlet Works, Fort Randall Dam, Missouri River, South Dakota; Hydraulic Model Investigation.</u> Technical Report No. 2-528, Vicksburg, Miss., October 1959.

(8) Carnegie Institute of Technology, <u>Report on Hydraulic Model Tests of Spillway and Outlet Works for Tionesta Creek Reservoir Dam, Tionesta, Pennsylvania.</u> Hydraulic Laboratory, Pittsburgh, Pa., September 1938.

SHAPE	PROJECT (1)	CONDUIT PROPER LENGTH DIAM (2)	CONDUIT PROPER REYNOLDS NUMBER (2)	CONDUIT PROPER VELOCITY HEAD (1)	AVERAGE INTAKE COEFFICIENT K_e
	SINGLE INTAKE (CONCRETE DAM CONDUITS)				

PROFILE

PLAN

SHAPE	PROJECT (1)	LENGTH DIAM (2)	REYNOLDS NUMBER (2)	VELOCITY HEAD (1)	K_e
	PINE FLAT (PROTOTYPE) A=90, B=30 C=9.0, E=5.0 F=5.0, G=1.7	54	$2.9-3.6 \times 10^7$ (PROTOTYPE)	65-81	0 16
	ES 802 (1:20 MODEL) A=7.5, B=2.5 C=10.0, E=5.7 F=4.3, G=1.4	83	6.7×10^5 (MODEL)	97	007 (3)

DOUBLE INTAKE (EARTH DAM TUNNEL)

PROFILE

PLAN

	DENISON (PROTOTYPE) A=25.0, B=390 C=190, D=200 E= 9.0, T=53.0	40	1.2×10^6 (PROTOTYPE)	66	0.19
	DENISON (1:25 MODEL) (SEE ABOVE)	47	$8.2-96 \times 10^5$ (MODEL)	81-82	0.12
	FT RANDALL (5) (PROTOTYPE) A=24.0, B=16.0 C=23.0, D=220 E=11.0, T=490	39	$07-1.5 \times 10^6$ (PROTOTYPE)	16-72	0 25
	FT RANDALL (1:25 MODEL) (SEE ABOVE)	39	$0.9-1.0 \times 10^6$ (MODEL)	46-86	0 16

TRIPLE INTAKE (EARTH DAM TUNNEL)

PROFILE

PLAN

	TIONESTA (1:36 MODEL) A=300, B=220 C=16.0, D=19.0 E= 7.5, T=660	98	$1.5-4.1 \times 10^5$ (MODEL)	7-50	0 33

INTAKE HEAD LOSS

$$h_e = K_e \frac{V^2}{2g}$$

V = VELOCITY IN CONDUIT PROPER

(1) DIMENSIONS IN PROTOTYPE FEET
(2) EQUIVALENT DIAMETER FOR NONCIRCULAR SECTIONS BASED ON HYDRAULIC RADIUS
(3) DOES NOT INCLUDE GATE-SLOT LOSSES
(4) LENGTH OF TRANSITION
(5) ROOF CURVE MAJOR AXIS HORIZONTAL

CONCRETE CONDUITS
INTAKE LOSSES
HYDRAULIC DESIGN CHART 221-1

HYDRAULIC DESIGN CRITERIA

SHEET 221-1/1

CONCRETE CONDUITS

INTAKE LOSSES

THREE-GATE-PASSAGE STRUCTURES

1. **Background.** It may be necessary to operate multiple-gate-passage intake structures with one or more passages inoperative. It is therefore desirable to determine the reservoir stage required to pass the design flow with one or more gate passages inoperative as well as with all passages operative. Hydraulic Design Chart 221-1/1 summarizes available head loss data for intake structures with three gate passages. Loss coefficients are given for three-passage operation as well as for the condition of an inoperative center passage. Comparable data for one inoperative side passage are not available. Chart 221-1/1 is only applicable to conduits flowing full.

2. **Theory.** For design purposes the intake loss is usually expressed in terms of the conduit velocity head as explained in Sheet 221-1. However with one gate passage inoperative, more consistent results are obtained if the coefficients are expressed in terms of the gate passage velocity head. Therefore, the values given in the chart are in terms of gate passage velocity head. Conversion into terms of the conduit velocity head can be accomplished by multiplying the coefficients given in the chart by the square of the ratio of the conduit flow area to the effective gate passage flow area. The intake loss is equal to the total available energy head minus the velocity head and the resistance and other losses in the conduit proper. Accurate experimental determination of the intake loss is dependent upon the conduit being of sufficient length to permit the resistance gradient to be established for fully developed turbulent flow. For a constant discharge, the increase in pool stage resulting with one or more gates inoperative is equal to the additional intake loss. This increase in head loss can be determined from measured rating curves and added to the head loss for the condition of all gate passages operative to obtain the total estimated head loss with one or more passages inoperative. However, in each case it is necessary that the downstream conduit flow full.

3. **Basic Data.** Chart 221-1/1 was developed from model investigations of intake structures with three gate passages. The following subparagraphs briefly describe the model data and the procedure used to obtain loss coefficients presented in the chart. The basic intake geometry is given in the chart. The gate area used to compute the intake loss coefficient may not necessarily be the minimum passage area in the intake section.

   a. **Wappapello.**[1] The tunnel is D-shaped and has an equivalent L/D (length-diameter) ratio of 13. The model scale was 1:25. The K_e (loss coefficient) values shown are based on model

discharge rating curves, computed energy losses using the smooth pipe curve in Chart 224-1, and Chart 225-1.

b. Tionesta.[2] The tunnel is circular and has an L/D ratio of 98. The model scale was 1:36. K_e values shown are based on measured model resistance gradients and discharge rating curves.

c. Arkabutla.[3] The tunnel is egg shaped with an equivalent L/D ratio of 20. The model scale was 1:25. The K_e values shown are based on measured model pressures near the end of the tunnel, the theoretical resistance loss using the smooth pipe curve in Chart 224-1, and the model rating curves.

4. Results. The sketches and dimensions given in Chart 221-1/1 for the three structures indicate considerable variation in geometry and size. The large K_e values computed for Arkabutla are attributed to the unusual intake geometry. The values given in the chart can be used as a guide for selecting entrance loss coefficients for three-gate-passage structures with all passages operative or with only the side passages operative. Prototype confirmation of the model intake loss coefficient is desirable. Limited available data indicate that prototype loss coefficients are appreciably higher than model loss coefficients (Chart 221-1).

5. References.

(1) U. S. Army Engineer Waterways Experiment Station, CE, Model Study of the Outlet Structures for the Wappapello Dam. Technical Memorandum No. 134-1, Vicksburg, Miss., August 1938.

(2) Carnegie Institute of Technology, Hydraulic Laboratory, Report, Hydraulic Model Tests of Spillway and Outlet Works for Tionesta Creek Reservoir Dam, Tionesta, Pennsylvania. Pittsburgh, Pa., September 1938.

(3) U. S. Army Engineer Waterways Experiment Station, CE, Model Study of the Outlet Structures for Arkabutla Dam, Coldwater River. Technical Memorandum No. 167-1, Vicksburg, Miss., December 1940.
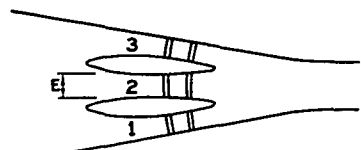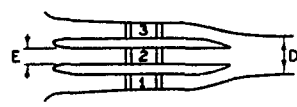
PLAN
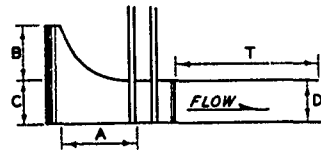
PROFILE

WAPPAPELLO*

(1:25 MODEL)

A = 31', B = 25'

C = 20', D = 20'

E = 10', T = 50'

K_e (THREE GATES) = 0.50

K_e (GATES 1 & 3) = 0.37

PLAN
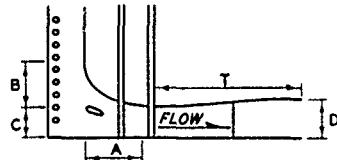
PROFILE

TIONESTA

(1:36 MODEL)

A = 30', B = 22'

C = 16', D = 19'

E = 7.5', T = 66'

K_e (THREE GATES) = 0.53

K_e (GATES 1 & 3) = 0.45

PLAN

NO 2

NOS. 1 & 3
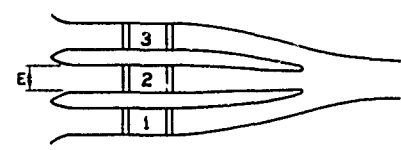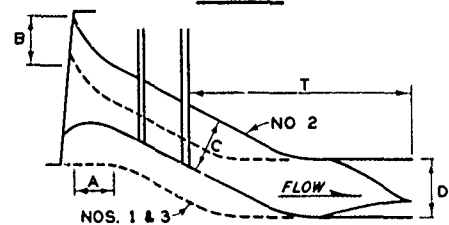
PROFILE

ARKABUTLA*

(1 25 MODEL)

A = 10.5', B = 16'

C = 17', D = 18.25'

E = 8.5', T = 75'

K_e (THREE GATES) = 0.79

K_e (GATES 1 & 3) = 0.68

*CONDUIT NOT CIRCULAR

INTAKE HEAD LOSS h_e

$$h_e = K_e \frac{V^2}{2g}$$

WHERE:

K_e = LOSS COEFFICIENT

V = GATE PASSAGE VELOCITY

g = ACCELERATION, GRAVITATIONAL

NOTE: TO CONVERT LOSS COEFFICIENTS INTO TERMS OF CONDUIT VELOCITY HEAD, MULTIPLY K_e BY THE SQUARE OF THE RATIO OF THE CONDUIT AREA TO THE GATE PASSAGE FLOW AREA $\Sigma(C \times E)$ OF THE GATES CONCERNED

CONCRETE CONDUITS

INTAKE LOSSES

THREE-GATE-PASSAGE STRUCTURES

HYDRAULIC DESIGN CHART 221-1/1

WES 1-68

1. Hydraulic Design Chart 221-1/2 presents loss coefficients for intakes with two and four gate passages. Values are given for the condition of one passage inoperative as well as for the condition of all passages operative. Reference is made to paragraphs 1, 2, and 3 of Sheet 221-1 and to paragraphs 1 and 2 of Sheet 221-1/1 for background, theory, and procedures used for developing the loss coefficients presented in Chart 221-1/2. The loss coefficients are in terms of gate passage velocity head for the reasons stated in paragraph 2 of Sheet 221-1/1. The chart is only applicable to full conduit flow.

2. **Basic Data.** Chart 221-1/2 was developed from model and prototype investigations of structures with two and four gate passages. The following subparagraphs briefly describe the model data and procedures used to obtain the loss coefficients given in the chart. The gate passage area used in computing the loss coefficients may not necessarily be the minimum area in the intake section. Structures with two gate passages are not usually designed to flow full with one gate passage inoperative.

    a. East Branch.[1] The intake has two gate passages. The circular outlet conduit has an L/D (length-diameter) ratio of 125. Two horizontal bends having R/D (curve radius/conduit diameter) values of 25 are separated by an 800-ft-long tangent. The model scale was 1:25. The resistance coefficient, based on the measured model pressure gradients in the 800-ft-long tangent, correlates with the smooth pipe curve of the resistance diagram shown in Chart 224-1. The measured pressure gradients in the tangent section were therefore accepted as the resistance gradient in computing the intake losses. Chart 228-1 was used to estimate the additional loss resulting from the upstream horizontal bend.

    b. Fort Randall.[2,3] The intake has two gate passages. The basic intake geometry is given in Chart 221-1. The circular outlet tunnel has an L/D ratio of 39 and a rated downstream control gate. The computed prototype loss coefficients are based on pressure observations at seven piezometer rings in the circular tunnel.

    c. Sardis.[4] The intake has four gate passages. The circular outlet tunnel has an L/D ratio of 31. The model scale was 1:25. Theoretical friction gradients, based on Charts 224-1

and 225-1, indicated that the measured tunnel pressure gradients closely approximate theoretical model resistance losses. K_e (loss coefficient) values are based on the theoretical and measured resistance gradients and the model rating curves.

3. <u>Results.</u> The K_e values in Chart 221-1/2 are in terms of the gate passage velocity heads for the reasons stated in paragraph 2 of Sheet 221-1/1. The values given in the chart can be used as a guide for selection of entrance loss coefficients for intake structures with two and four passages with all gates operative as well as with one gate inoperative. Conversion into terms of the conduit velocity head can be accomplished by multiplying the coefficients given in the chart by the square of the ratio of the conduit flow area to the area of the gate passages concerned. Prototype confirmation of the model loss coefficients is desirable. Limited data indicate appreciably higher prototype losses than those observed in models (Chart 221-1).

4. <u>References.</u>

(1) U. S. Army Engineer Waterways Experiment Station, CE, <u>Spillway and Outlet Works, East Branch Reservoir, Clarion River, Pennsylvania; Model Investigation.</u> Technical Memorandum No. 2-325, Vicksburg, Miss., July 1951.

(2) _____, <u>Flow Characteristics in Flood-Control Tunnel 10, Fort Randall Dam, Missouri River, South Dakota; Hydraulic Prototype Tests,</u> by J. V. Dawsey, Jr., C. J. Huval, and W. C. Blanton. Technical Report 2-626, Vicksburg, Miss., June 1963.

(3) U. S. Army Engineer Division, Omaha, CE, <u>Flow Characteristics in Flood-Control Tunnel 10 for 1 and 2 Gate Operation, Fort Randall Dam, Missouri, South Dakota,</u> 1967. (Unpublished supplement to Technical Report No. 2-626, reference 2 above.)

(4) U. S. Army Engineer Waterways Experiment Station, CE, <u>Model Study of Proposed Outlet Structures for Sardis Dam.</u> Technical Memorandum No. 123-2, Vicksburg, Miss., 17 November 1937.
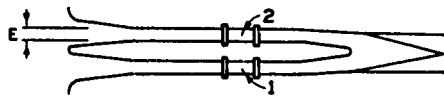
PLAN
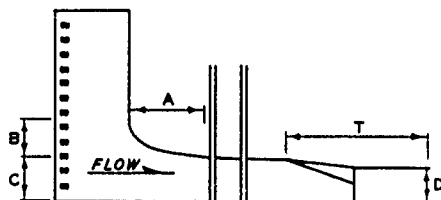
PROFILE

EAST BRANCH
(1:25 MODEL)

A= 23', B= 8'
C= 12', D= 10'
E= 3.33', T= 42.5'

K_e (TWO GATES) = 0.23
K_e (ONE GATE) = 0.45

SEE CHART 221-1 FOR
DIMENSIONS OF FORT
RANDALL INTAKE

FORT RANDALL
(PROTOTYPE)

K_e (TWO GATES) = 0.44
K_e (ONE GATE) = 0.73
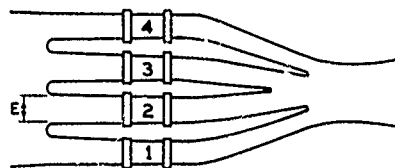
PLAN
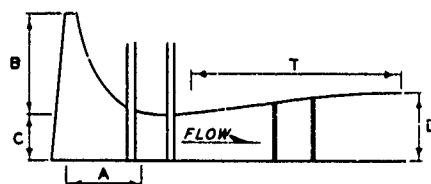
PROFILE

SARDIS
(1:25 MODEL)

A= 16', B= 23.5'
C= 12', D= 17'
E= 6', T= 62.5'

K_e (FOUR GATES) = 0.32
K_e (GATES 1, 2, & 3) = 0.33
K_e (GATES 1, 3, & 4) = 0.37

INTAKE HEAD LOSS h_e

$$h_e = K_e \frac{V^2}{2g}$$

WHERE:
  K_e = LOSS COEFFICIENT
  V = GATE PASSAGE VELOCITY
  g = ACCELERATION, GRAVITATIONAL

NOTE TO CONVERT LOSS COEFFICIENTS
  INTO TERMS OF CONDUIT VELOCITY
  HEAD, MULTIPLY K_e BY THE SQUARE OF
  THE RATIO OF THE CONDUIT AREA TO
  THE GATE PASSAGE FLOW AREA $\Sigma(C \times E)$
  OF THE GATES CONCERNED.

CONCRETE CONDUITS
INTAKE LOSSES
TWO- AND FOUR-
GATE-PASSAGE STRUCTURES

HYDRAULIC DESIGN CHART 221-1/2

WES 1-68

HYDRAULIC DESIGN CRITERIA

SHEET 221-1/3

CONCRETE CONDUITS

MIDTUNNEL CONTROL STRUCTURE LOSSES

1. Hydraulic Design Chart 221-1/3 presents head loss data for mid-tunnel control structures with three, two, and one gate passages. Such structures usually have appreciable tunnel lengths upstream and downstream from the control structure. Where applicable, head loss coefficients are given for the condition of one gate passage inoperative as well as for the condition of all passages operative.

2. The basic theory and procedure described in paragraphs 1, 2, and 3 of Sheet 221-1 and in paragraphs 1 and 2 of Sheet 221-1/1 for conduit intakes were used in the development of the loss coefficients (K_e) presented in Chart 221-1/3. However, the energy loss for midtunnel control towers is defined as the difference in the elevation of the resistance gradients at the beginning of the upstream and the end of the downstream transitions. The chart is only applicable to full conduit flow. Conduits with two gate passages are not usually designed to flow full with one gate inoperative.

3. **Basic Data.** Chart 221-1/3 summarizes the only known available data on loss coefficients for midtunnel control structures. The following subparagraphs briefly describe the model data and the procedures used to obtain the coefficients presented in the chart.

    a. <u>Youghiogheny.</u>[1] The control tower has three gate passages. The circular conduit has a downstream L/D (length-diameter) ratio of 64 and an upstream L/D of 34. The upstream conduit contains a 207-ft-long horizontal bend formed by a 200-ft radius. The model scale was 1:36. The loss coefficients presented in the chart are based on the observed model pressure gradients. The resistance coefficients computed from these pressure gradients plot slightly above the smooth pipe curve shown in Chart 224-1.

    b. <u>Abiquiu.</u>[2] The control structure has two gate passages. The circular conduit has a downstream L/D ratio of 71 and an upstream L/D ratio of 25. The model scale was 1:20. The observed pressure gradient used to develop the coefficient given in Chart 221-1/3 agrees closely with the theoretical resistance gradient based on the smooth pipe curve shown in Chart 224-1. The downstream conduit does not flow full with one gate passage operating.

    c. <u>Oahe.</u>[3] The control tower has a single gate passage. The circular conduit has a downstream L/D ratio of 60.8 and an

u.stream L/D ratio of 77. The upstream conduit contains a horizontal bend having a length of 802 ft and an R/D (curve radius-conduit diameter) ratio of 108. The upstream and downstream conduits were studied independently on 1:25-scale models. The gate passage loss coefficients given in the chart are based on pressure gradients observed in the model conduits. Computations indicated that the model pressure gradients closely approximate the theoretical resistance gradient based on the smooth pipe curve shown in Chart 224-1.

4. Results. Sketches and dimensions are given in Chart 221-1/3 for midtunnel control towers with three, two, and one gate passages. The K_e values presented are in terms of the gate passage velocity head for the reasons stated in paragraph 2 of Sheet 221-1/1. The values presented can be used as guides in the selection of loss coefficients for midtunnel control towers with all passages operative as well as with one passage inoperative. For design convenience, the K_e values given in the chart can be converted into terms of the conduit velocity head by multiplying the given values by the square of the ratio of the conduit area to the effective gate passage flow area of the passages concerned. Prototype confirmation of the model loss coefficients is desirable. Limited data for conduit intakes indicate that prototype losses are appreciably higher than model losses (Chart 221-1).

5. References.

(1) Carnegie Institute of Technology, Hydraulic Laboratory, Report on Hydraulic Model Tests of Spillway and Outlet Works of Youghiogheny River Dam, Confluence, Pennsylvania. Pittsburgh, Pa., March 1941.

(2) U. S. Army Engineer Waterways Experiment Station, CE, Outlet Works for Abiquiu Dam, Rio Chama, New Mexico; Hydraulic Model Investigation. Technical Report No. 2-513, Vicksburg, Miss., June 1959.

(3) _____, Outlet Works, Oahe Dam, Missouri River, South Dakota; Hydraulic Model Investigation, by D. R. Bucci and T. E. Murphy. Technical Report No. 2-557, Vicksburg, Miss., September 1960.
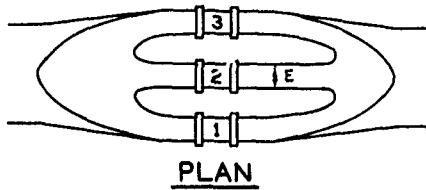
PLAN
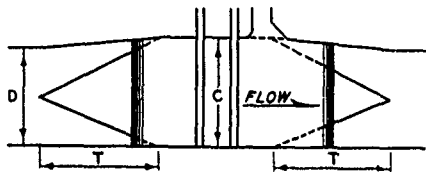
PROFILE

YOUGHIOGHNEY

(1:36 MODEL)

C=20', D=18'

E=4.25', T=24'

K_e(THREE GATES)=0.29

K_e(GATES 1 & 3)=0.41
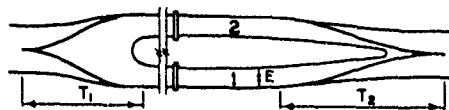
PLAN
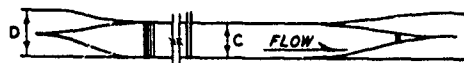
PROFILE

ABIQUIU

(1:20 MODEL)

C=9', D=12'

E=5', T_1=36'

T_2=45'

K_e(TWO GATES)=0.30
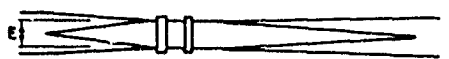
PLAN
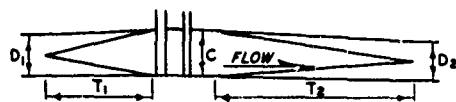
PROFILE

OAHE

(1:25 MODEL)

C=22', D_1=19.75'

D_2=18.25', E=13'

T_1=54', T_2=100'

K_e=0.44

CONTROL STRUCTURE HEAD LOSS h_e

$$h_e = K_e \frac{V^2}{2g}$$

WHERE:

K_e = LOSS COEFFICIENT

V = GATE PASSAGE VELOCITY

g = ACCELERATION, GRAVITATIONAL

NOTE TO CONVERT LOSS COEFFICIENTS
INTO TERMS OF CONDUIT VELOCITY
HEAD, MULTIPLY K_e BY THE SQUARE OF
THE RATIO OF THE CONDUIT AREA TO
THE GATE PASSAGE FLOW AREA $\Sigma(C \times E)$
OF THE GATES CONCERNED

CONCRETE CONDUITS

MIDTUNNEL CONTROL
STRUCTURE LOSSES

HYDRAULIC DESIGN CHART 221-1/3

WES 1-68

EARTH DAM OUTLET WORKS

ENTRANCE WITH ROOF CURVE ONLY

PRESSURE-DROP COEFFICIENTS

1. **General.** Intake structures for earth dam outlet works are designed to avoid flow separation and unsatisfactory pressure conditions. Entrance roofs are formed to smooth curves, and the invert is approximately level with the approach channel floor. The sidewalls are generally parallel with slight flare or curvature upstream from the roof curve. The sidewalls or piers should extend approximately one conduit height into the low-velocity flow area, with the upstream ends (noses) rounded and extending nearly vertically well above the roof curve. The general entrance geometry is shown in Hydraulic Design Chart 221-2. In the region of the roof curve where rapid flow acceleration occurs, the flow approaches two dimensional and the pressure across the roof is essentially uniform at any section as shown in Chart 221-2/1.

2. **Theory.** The pressure drop H_d from the reservoir surface to the pressure gradient for any point on the entrance boundary can be expressed as a function of the velocity head in the uniform section of the intake gate passage

$$H_d = C \frac{V^2}{2g}$$

where

H_d = pressure drop, ft

C = dimensionless pressure-drop coefficient

V = average velocity in uniform section of gate passage, ft/sec

g = gravitational acceleration, ft/sec^2

The magnitude of the reservoir head appears to have little effect upon the pressure-drop coefficients as long as the entrance is submerged several times its height.[1]

3. **Data Sources.** Tests have been made at the U. S. Army Engineer Waterways Experiment Station (WES) to develop entrance shapes of minimum length and cross-section area conducive to satisfactory boundary surface pressure distribution and to economical construction. In addition, model investigations have been made on specific projects. Applicable results

from selected available study reports have been analyzed and summarized in reference 1. The three entrances developed during the Fort Randall,[2] Garrison,[3] and Blakely Mountain[4] model investigations are basically similar except for the geometry of the upstream face of the intake tower. The results of these model studies together with comparable data from reference 5 are presented in Chart 221-2.

4. <u>Upstream Face Geometry.</u> Chart 221-2 presents pressure-drop coefficients for intakes of similar entrance geometry but with appreciably different upstream face geometry. In each case the roof curve for all practical purposes is formed to the equation

$$\frac{X^2}{D^2} + \frac{Y^2}{(2/3\ D)^2} = 1$$

where

$\quad$ D = conduit height at the uniform section

$\quad$ X and Y = coordinates of an ellipse with its origin as shown in the chart

Parallel sidewalls or piers extend upstream approximately 1D from the upstream end of the roof curve. Intake types 2, 3, and 4 (Blakely Mountain,[4] Fort Randall,[2] and Garrison,[3] respectively) have bulkhead slots immediately upstream of the intake curve. Type 1[5] has neither bulkhead nor gate slots.

5. The pressure-drop coefficient curves in Chart 221-2 indicate that the geometry of the upstream face of the intake has negligible effect upon the pressure distribution along the roof curve. For entrances with roof flare only, it is suggested that the vertical upstream face extend 0.5D above the beginning of the roof curve. Above this elevation the most economical structural geometry should be used.

6. <u>Roof Curve Shape.</u> The entrance curve shape given in Chart 221-2 is suggested for use in designing entrances curved in one direction only. This shape should be adequate for earth dam outlet works having appreciable tunnel length. For short tunnels with less back pressure the curve given in Chart 221-2/1 should result in more favorable pressure conditions. The pressure-drop coefficients are based on average pressures, and the local pressure fluctuations criteria given in paragraph 4 of Sheets 534-2 and 534-2/1 should be considered in selecting the final roof curve design.

7. <u>Application.</u> The pressure-drop coefficient is a function of the velocity head in the uniform gate passage section which in turn is a function of the outlet works length, the intake and other geometric losses, and the total available head. Local pressure conditions as effected by gate and bulkhead slots are discussed in HDC 212-1 to 212-1/2 and in reference 1.

8. The adequacies of the entrance geometry and the resulting

pressure gradient are dependent to a large extent upon the tunnel length. The optimum entrance geometry for a short tunnel is not necessarily the same as that for a long conduit. Also, closure of one or more gates in multiple-passage intakes may result in unsatisfactory pressure conditions (no back pressure). The pressure-drop coefficients in Chart 221-2 result from studies of conduit height-width ratios of 1.36 to 2.09. Application of these data should be limited to reasonably similar ratios.

9. Chart 221-2/2 is an example computation for evaluating the adequacy of entrance geometry.

10. References.

(1) U. S. Army Engineer Waterways Experiment Station, CE, Characteristic Pressure Distribution in Outlet Works Inlets, by R. G. Cox and Y. H. Chu. Miscellaneous Paper H-69-8, Vicksburg, Miss., September 1969.

(2) _____, Spillway and Outlet Works, Fort Randall Dam, Missouri River, South Dakota; Hydraulic Model Investigation, by T. E. Murphy. Technical Report No. 2-528, Vicksburg, Miss., October 1959.

(3) _____, Outlet Works and Spillway for Garrison Dam, Missouri River, North Dakota; Hydraulic Model Investigation. Technical Memorandum No. 2-431, Vicksburg, Miss., March 1956.

(4) _____, Flood-Control Outlet Works for Blakely Mountain Dam, Ouachita River, Arkansas; Hydraulic Model Investigation. Technical Memorandum No. 2-347, Vicksburg, Miss., June 1952.

(5) _____, Entrances to Conduits of Rectangular Cross Section; Investigation of Entrances Flared in Three Directions and One Direction, by T. E. Murphy. Technical Memorandum No. 2-428, Report 2, Vicksburg, Miss., June 1959.

PRESSURE-DROP COEFFICIENT-C

L/D

DEPTH-D

L/D

$$\frac{X^2}{D^2} + \frac{Y^2}{\left(\frac{20}{3}\right)^2} = 1$$

FLOW

NOTE: D = HEIGHT OF RECTANGULAR
GATE SECTION
L = DISTANCE ALONG CONDUIT, FT
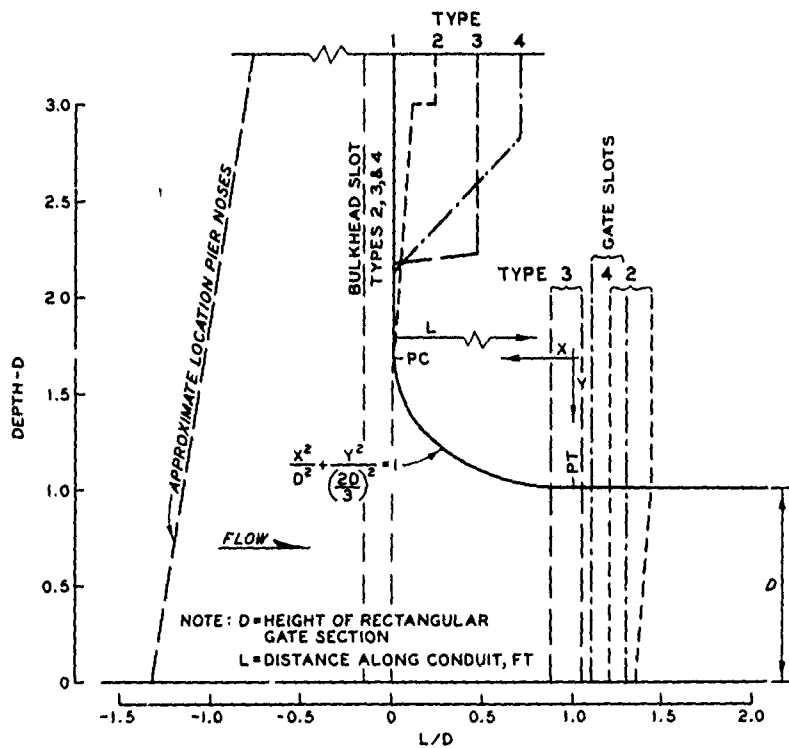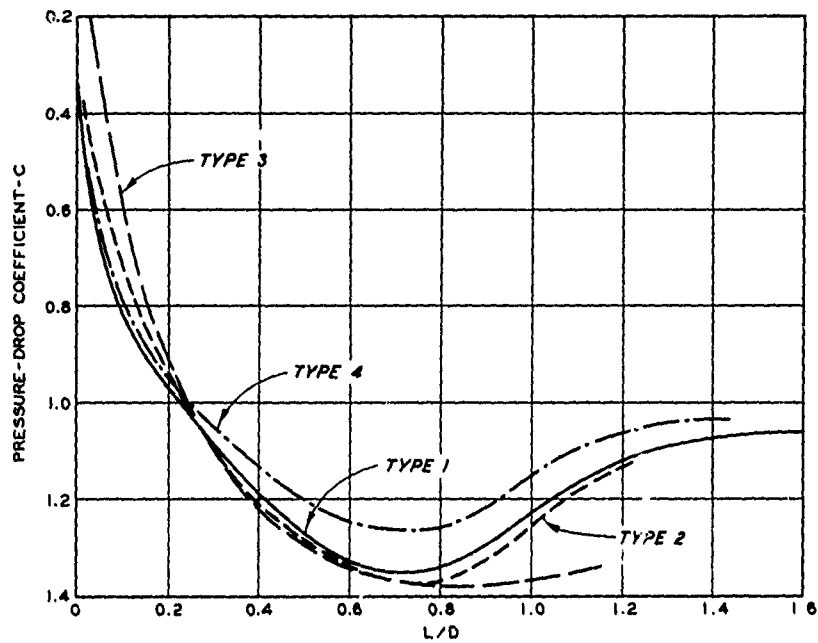
EQUATION

$$H_d = C\frac{V^2}{2g}$$

WHERE.

H_d = PRESSURE DROP FROM POOL, FT

C = PRESSURE-DROP COEFFICIENT

$\frac{V^2}{2g}$ = VELOCITY HEAD IN RECTANGULAR
GATE SECTION, FT

EARTH DAM OUTLET WORKS
ENTRANCE WITH ROOF CURVE ONLY
PRESSURE-DROP COEFFICIENTS
UPSTREAM FACE EFFECTS

HYDRAULIC DESIGN CHART 221-2

RESULTS BASED ON ES802
TEST DATA (GATE SECTION
HEIGHT-WIDTH RATIO = 1.765)

PRESSURE-DROP COEFFICIENT – C

TOP CORNER

TOP ℄

$\dfrac{L}{D}$

$\dfrac{X}{D} = 1.5$

P.C.

ORIGIN

$\dfrac{X^2}{(1.5D)^2} + \dfrac{Y^2}{\left(\dfrac{2D}{3}\right)^2} = 1$

$\dfrac{Y}{D} = 0.67$

P.T.

$\dfrac{D}{2}$

℄

L

NOTE: D = HEIGHT OF RECTANGULAR
GATE SECTION, FT
L = DISTANCE ALONG CONDUIT, FT

EQUATION

$$H_d = C \frac{V^2}{2g}$$

WHERE:
H_d = PRESSURE DROP FROM POOL, FT
C = PRESSURE-DROP COEFFICIENT
$\dfrac{V^2}{2g}$ = VELOCITY HEAD IN RECTANGULAR GATE SECTION, FT

EARTH DAM OUTLET WORKS
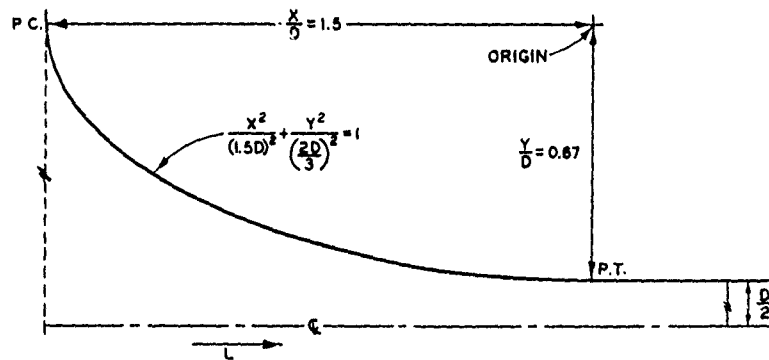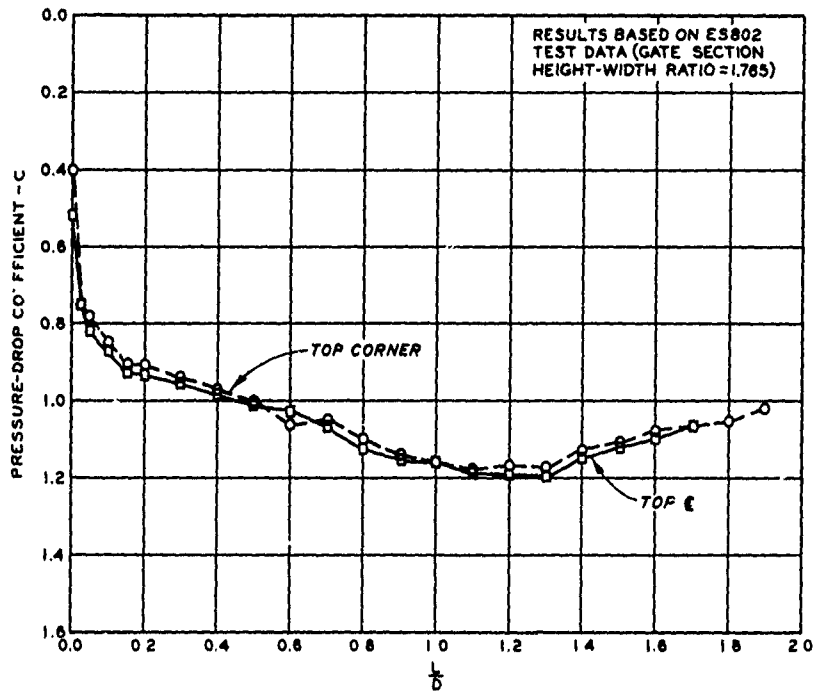ENTRANCE WITH ROOF CURVE ONLY
PRESSURE-DROP COEFFICIENTS
LONG ELLIPTICAL SHAPE

HYDRAULIC DESIGN CHART 221-2/1

TWO GATES FULLY OPEN

GIVEN:

Reservoir pool el = 181 ft msl
Intake invert el = 100 ft msl
Gate passages
  No. = 2
  Height (D) = 23 ft
  Width (W) = 11 ft
  Discharge (Q) = 20,600 cfs
  Both gates open full

REQUIRED:

Roof curve el at L = 1, 5, 10, 15, 20, and 30 ft
Gate passage velocity head
Pressures on roof at L = 1, 5, 10, 15, 20, and 30 ft

COMPUTE:

Roof curve elevations

Basic equation: $\dfrac{X^2}{529} + \dfrac{Y^2}{235} = 1$ or $Y = (235 - 0.444\,X^2)^{1/2}$
              with $X = 23 - L$

L (ft)	L/D	X (ft)	X^2	$0.444\,X^2$	Y^2	Y (ft)	Roof el (138.3 − Y) (ft msl)
1	0.04	22	484	215	20	4.5	133.8
5	0.22	18	324	144	91	9.5	128.8
10	0.44	13	169	75	160	12.7	125.6
15	0.65	8	64	28	207	14.4	123.9
20	0.87	3	9	4	231	15.2	123.1
23	1.00	0	0	0	235	15.3	123.0
30	1.30	−7					123.0

Gate passage velocity head

$$V = \frac{Q}{A} = \frac{20,600}{2 \times 11 \times 23} = 40.7 \text{ fps}$$

$$\frac{V^2}{2g} = \frac{(40.7)^2}{2 \times 32.2} = 25.7 \text{ ft}$$

Pressure on roof (assume conservative values of C from Chart 221-2)

Basic equation: $H_d = C\,\dfrac{V^2}{2g}$

L/D	C	H_d (ft)	Pool − H_d (ft msl)	Roof el (ft msl)	Roof Pressure (ft)
0.04	0.66	17.0	164.0	133.8	30.2
0.22	0.98	25.2	155.8	128.8	27.0
0.44	1.26	32.4	148.6	125.6	23.0
0.65	1.36	35.0	146.0	123.9	22.1
0.87	1.38	35.5	145.5	123.1	22.4
1.00	1.36	35.0	146.0	123.0	23.0
1.30	1.26	32.4	148.6	123.0	25.6

Note: Roof pressures satisfactory
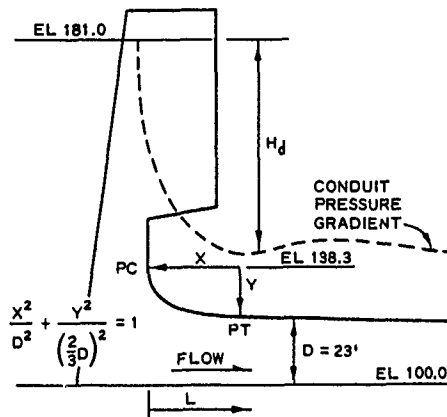
EARTH DAM OUTLET WORKS
ENTRANCE WITH ROOF CURVE ONLY
PRESSURE-DROP COEFFICIENTS
PRESSURE COMPUTATION

HYDRAULIC DESIGN CHART 221-2/2

HYDRAULIC DESIGN CRITERIA

SHEETS 221-3 AND 221-3/1

EARTH DAM OUTLET WORKS

ENTRANCE WITH ROOF CURVE AND SIDE FLARE OR CURVE

1. **General.** Dividing walls and piers for intake structures with multiple flow passages vary in thickness from 4 to 10 ft depending upon structural and foundation requirements. The design of entrances to these structures generally requires the use of curved or flared sidewalls or piers. When the side curve occurs at or downstream from the beginning of the entrance roof curve, the intake should be designed as a three-dimensional inlet rather than the two-dimensional type described in Hydraulic Design Criteria (HDC) 221-2 to 221-2/2.

2. In three-dimensional inlets, the sidewalls are curved horizontally and the roof curved vertically. The invert is level. Local acceleration of the flow in a lateral direction in addition to that in the vertical direction results in more rapid pressure reduction along the inlet roof corners than along the roof center line. In most designs, the roof is curved and the sides of the projecting pier walls are flared linearly. A short transition curve is used to join the sidewall taper with the uniform conduit section. When both the roof and sidewall flares are curvilinear they are shaped to an elliptical equation of the type given in paragraph 4 of Sheets 221-2 to 221-2/2. The term D of this equation is the dimension of the conduit (height or width) in the direction concerned.

3. **Linear Sidewall Flare.** Entrances of inlets with mild sidewall flare (less than 1 to 10) can be considered two-dimensional if the sidewalls are straight and extend appreciably upstream into the low-velocity flow area. For this condition, use of the equation given in Chart 221-2 for the roof curve should result in satisfactory inlet pressures for conduit lengths resulting in appreciable back pressure. An estimate of the roof center-line and corner pressures can be obtained by using the pressure-drop coefficient given in Chart 221-2 adjusted by the square of the ratio of the areas at each section, as described below. Chart 221-3 presents a plot of experimentally determined pressure-drop coefficients for an inlet having linear sidewall flare and curved roof.[1] Both top center-line and top corner data are given for the condition of all passages operating as well as for the side passages closed. Also shown in the chart is a pressure-drop coefficient curve for a two-dimensional inlet having the same roof curve.[2] The results of adjusting the two-dimensional inlet coefficients to the three-dimensional case is included in the chart.[3] Reasonable agreement with the experimental data is obtained.

4. **Coefficient Adjustment.** The basic equations used to adjust the two-dimensional pressure coefficients for three-dimensional use are:

<u>a</u>. The continuity equation:

$$Q = A_2 V_2 = A_3 V_3 \qquad (1)$$

giving

$$\frac{V_3}{V_2} = \frac{A_2}{A_3}$$

where

Q = discharge

A = cross-section area of the inlet at any section
    concerned

V = average velocity at this section

The subscripts 2 and 3 refer to entrances of the same design with and without sidewall flare, respectively, in the closed inlet section.

<u>b</u>. The energy equation:

$$H = P_2 + \frac{V_2^2}{2g} = P_3 + \frac{V_3^2}{2g} \qquad (2)$$

where

H = total head referenced to the point of
    interest on the roof curve

P and V = pressure and velocity, respectively,
    at this point

g = acceleration of gravity

<u>c</u>. The pressure-drop equation:

$$H_d = H - P \qquad (3)$$

with

$$H_{d2} = \frac{V_2^2}{2g} = C_2 \frac{V^2}{2g} \quad \text{and} \quad H_{d3} = \frac{V_3^2}{2g} = C_3 \frac{V^2}{2g} \qquad (4)$$

where

H_d = pressure drop from the reservoir water surface to
    the local pressure gradient elevation

C = pressure-drop coefficient

$\frac{V^2}{2g}$ = uniform conduit section velocity head

5. Equations 1 through 4 can be combined to give the relation

$$C_3 = C_2 \left(\frac{A_2}{A_3}\right)^2 \tag{5}$$

Equation 5 can be used with Chart 221-2 or 221-2/1 to estimate roof curve pressures for inlets with mild sidewall flare (up to 5 deg). The procedure given above is not applicable to inlets with side curves in which flow along the sidewall boundary has an appreciable lateral component and piers are not extended into the low-velocity-flow area.

6. <u>Curvilinear Sidewalls.</u> Inlets with roof and sidewall curves usually have elliptical equations to define these curves. The flow along the sidewalls has appreciable lateral components. Piers projecting upstream into the low-velocity-flow area are not provided. The inlet curve geometry and pressure-drop coefficients given in Chart 221-3/1 should result in satisfactory entrance pressures for inlets with curved roof and sidewalls and downstream conduits of appreciable length. The inlet design procedure described in paragraphs 4 and 5 above is not applicable to inlets of this type.

7. <u>Application.</u> The pressure-drop coefficients given in Charts 221-3 and 221-3/1 are based on average pressures. The general design philosophy discussed in Sheets 221-2 to 221-2/2 should be followed in the design of inlets with horizontal flare. Design adequacies discussed in paragraph 8 of that series should be considered in evaluating the final inlet design curves.

8. <u>References.</u>

(1) U. S. Army Engineer Waterways Experiment Station, CE, <u>Flood Control Outlet Structures for Tuttle Creek Dam, Big Blue River, Kansas; Hydraulic Model Investigation.</u> Technical Memorandum No. 2-396, Vicksburg, Miss., December 1954.

(2) _____, <u>Entrances to Conduits of Rectangular Cross Section; Investigation of Entrances Flared in Three Directions and One Direction,</u> by T. E. Murphy. Technical Memorandum No. 2-428, Report 2, Vicksburg, Miss., June 1959.

(3) _____, <u>Characteristic Pressure Distribution in Outlet Works Inlets,</u> by R. G. Cox and Y. H. Chu. Miscellaneous Paper H-69-8, Vicksburg, Miss., September 1969.

LOCATION
℄	CORNER	GATE OPERATION
○	●	ALL OPEN (HEAD = 131 FT)
□	■	ALL OPEN (HEAD = 71 FT)
△	▲	SIDE GATES CLOSED (HEAD = 71 FT)

NOTE: D = DIMENSION OF RECTANGULAR GATE SECTION IN DIRECTION CONCERNED, FT
L = DISTANCE ALONG CONDUIT, FT

EXPERIMENTAL
COMPUTED } THREE-DIMENSIONAL

TWO-DIMENSIONAL

EQUATION

$$H_d = C \frac{V^2}{2g}$$

WHERE:
H_d = PRESSURE DROP FROM POOL, FT
C = PRESSURE-DROP COEFFICIENT
$\frac{V^2}{2g}$ = VELOCITY HEAD IN RECTANGULAR GATE SECTION, FT

PLAN

ELEVATION

$$\frac{x^2}{D^2} + \frac{y^2}{(0.5D)^2} = 1$$
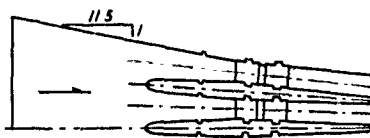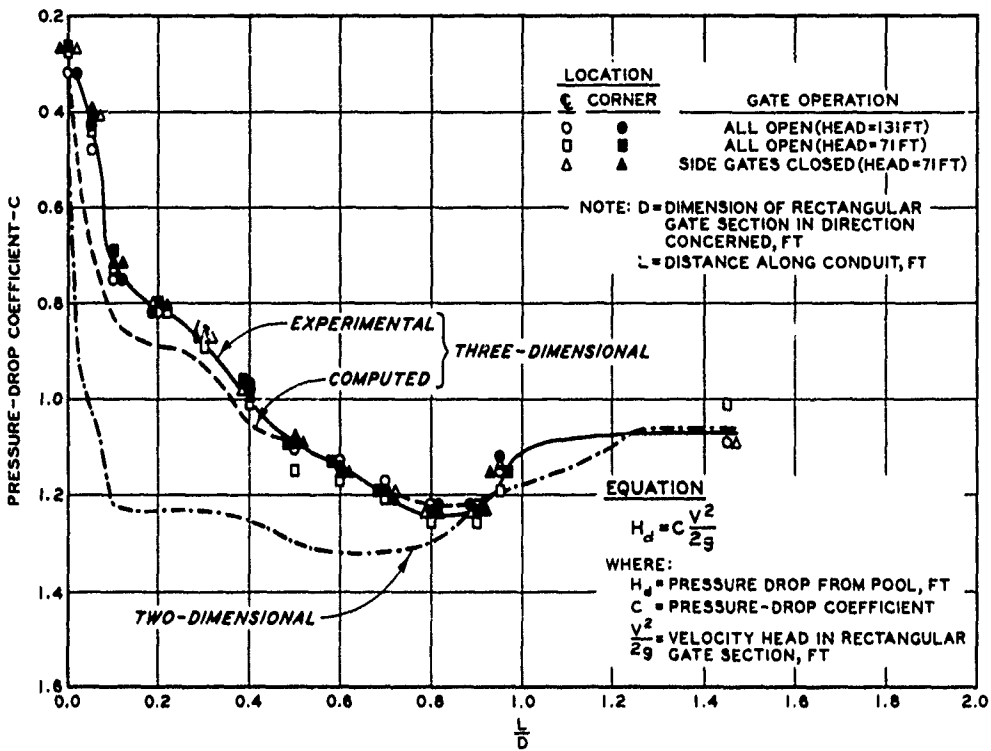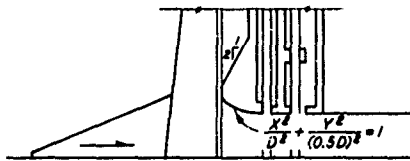
EARTH DAM OUTLET WORKS
ENTRANCE WITH TOP AND SIDES FLARED
PRESSURE-DROP COEFFICIENTS
STRAIGHT SIDEWALL FLARE

HYDRAULIC DESIGN CHART 221-3
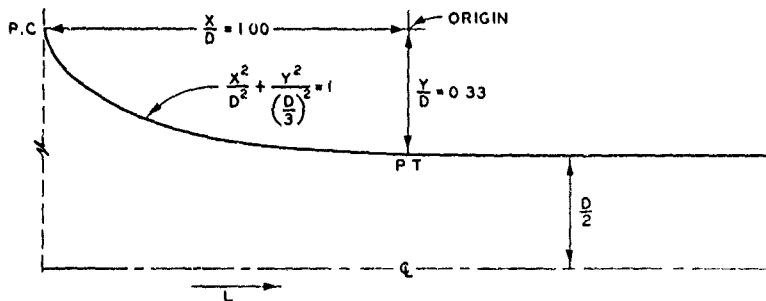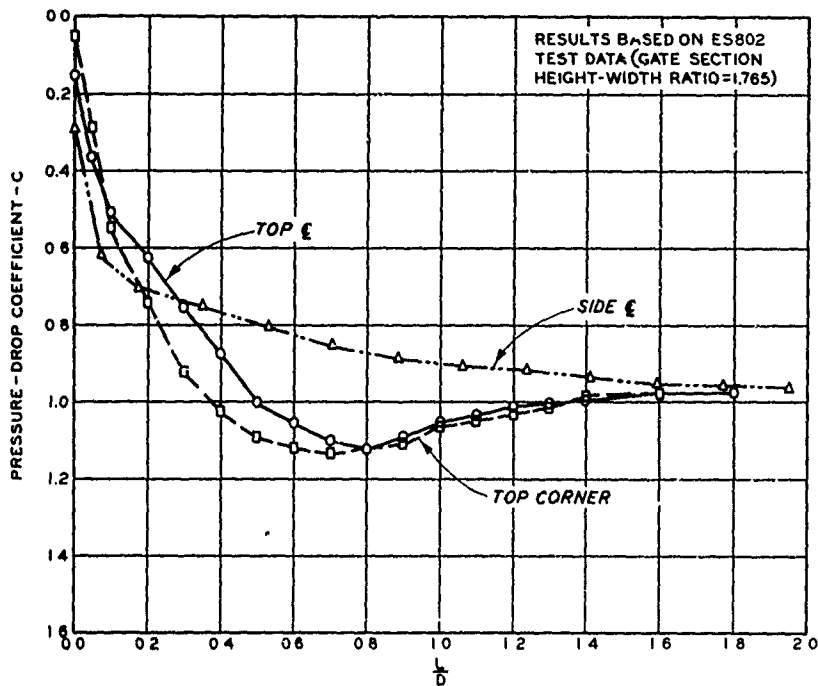
RESULTS BASED ON ES802
TEST DATA (GATE SECTION
HEIGHT-WIDTH RATIO=1.765)

EQUATION

$$H_d = C \frac{V^2}{2g}$$

WHERE

H_d = PRESSURE DROP FROM POOL, FT

C = PRESSURE-DROP COEFFICIENT

$\frac{V^2}{2g}$ = VELOCITY HEAD IN RECTANGULAR GATE SECTION, FT

NOTE D = DIMENSION OF RECTANGULAR
GATE SECTION IN DIRECTION
CONCERNED, FT
L = DISTANCE ALONG CONDUIT, FT

EARTH DAM OUTLET WORKS
ENTRANCE WITH TOP AND SIDES FLARED
PRESSURE-DROP COEFFICIENTS
ELLIPTICAL TOP AND SIDE FLARES

HYDRAULIC DESIGN CHART 221-3/1

RESISTANCE COEFFICIENTS

CONCRETE CONDUITS

1. **General.** The Kutter and Manning coefficients have been used extensively in the past by design engineers in the United States. Manning's n has found more favor in flood-control and irrigation design work because of its relative simplicity in the evaluation of resistance (friction) losses. A Manning's n value of 0.013 has been commonly used by engineers in the design of concrete conduits since publication of an article by Horton[1] in 1916 which was subsequently published in King's Handbook of Hydraulics. The Manning coefficient served a useful purpose for the design of conduits with Reynolds numbers that were small compared to those of large flood-control conduits. Tests at very high Reynolds numbers on the Oahe Dam flood-control conduit[2] where all joints and irregularities were ground smooth indicated a Manning's n of about 0.0098, illustrating that the older design values of the Manning's n can result in overdesign. However, because of possible deterioration of interior surfaces with time a Manning's n value of 0.014 is still used for capacity design by some engineers.

2. **Effect of Reynolds Number.** The variation of the resistance coefficient relative to the Reynolds number is expressed with the Darcy factor "f." This relation is normally plotted in the form of a general resistance diagram referred to as the Moody diagram.[3] Chart 224-1 is a Moody diagram on which have been plotted experimental data obtained on concrete conduits. The terms involved are defined on the chart. Nikuradse's study on pipes coated with uniform sand grains demonstrated that the resistance factor decreases with an increase in Reynolds number. Prandtl and Von Karman based the smooth pipe formula (Chart 224-1) upon theoretical considerations adjusted to the Nikuradse data. The heavy dashed line on the chart represents the limit of the transition from the smooth pipe formula to rough pipes with full turbulence. The resistance factor then becomes independent of Reynolds number and is only a function of the relative roughness. The lines in the transition region represent the Colebrook-White function[4] based on experiments with mixed roughness contrasted to uniform sand grains. The Colebrook-White function has been extrapolated considerably beyond the limits of the basic experimental data $R_e = 6 \times 10^5$. Observed values of f for the prototype flood-control conduits at Oahe and Denison Dams are considerably less than those computed for comparable Reynolds numbers using the Colebrook-White equation and field roughness measurements of the interior surface of the conduits. However, the relation between physical measurements of surface roughness and the hydraulic effective roughness has yet to be firmly established.

3. The velocity-diameter product VD for water at 60 F is included as a scale across the top of the graph. The VD scale is convenient for most design problems in which the effect of water temperature on capacity is neglected. Chart 001-1 shows the relation between kinematic viscosity and water temperature for use when it is desired to compute the effect of temperature.

4. _Effective Roughness._ Available test data on concrete pipes and conduits have been analyzed to correlate the effective roughness k_s with construction practices in forming concrete conduits and in treatment of interior surfaces. The following tabulation gives information pertinent to the data plotted in Chart 224-1. The type of construction and the resulting effective roughness can be used as guides in specific design problems. However, the k_s values listed are not necessarily applicable to other conduits of greatly different diameters.

Symbol	Project	Ref No.	Shape*	Size ft	k_s ft	Construction
				Precast Pipe		
●	Asbestos cement	5	C	1.2	0.00016	Steel mandril
▢	Asbestos cement	5	C	1.7	0.00008	Steel mandril
▽	Neyrpic	6	C	2.82	0.00030	19.7-ft steel form
⊕	Denver #10	7	C	4.5	0.00018	12-ft steel form
⊐	Umatilla River	8	C	3.83	0.00031	8-ft steel form
⊤	Prosser	8	C	2.54	0.00152	Oiled steel form
⊏	Umatilla Dam	8	C	2.5	0.00024	4-ft sheet steel on wood forms
⊥	Deer Flat	8	C	3.0	0.00043	6-ft steel form
✗	Victoria	8	C	3.5	0.00056	4-ft oiled steel forms
▲	Denver #3	9	C	2.5	0.00011	12-ft steel form
◣	Denver #13	9	C	5.0	0.00016	12-ft steel form
▼	Spavinaw	2	C	5.0	0.00013	12-ft steel form
				Steel Form Conduits		
○	Denison	10	C	20	0.00012	
△	Ontario	8	O	18	0.00001	Hand rubbed
▼	Chelan	11	C	14	0.00061	
■	Adam Beck	12	C	45	0.00018	Invert screeded and troweled
⊟	Fort Peck	13	C	24.7	0.00014	

(Continued)

* C = circular, O = oblate, R = round, and H = horseshoe.

224-1
Revised 8-60
Revised 1-64
Revised 9-70

Symbol	Project	Ref No.	Shape	Size ft	k_s ft	Construction
			Wood Form Conduits			
●	Oahe	14	C	18.3	0.00004	Joints ground
+	Enid	15	C	11	0.00160	
◐	Pine Flat 52	16	R	5 × 9	0.00103	Longitudinal planking
◑	Pine Flat 56	16	R	5 × 9	0.00397	
			Miscellaneous			
◉	Quabbin	17	H	11 × 13	0.00015	Unknown

5. **Design Criteria.**

    a. **Capacity.** Conservative values should be used in designing for conduit capacity. The k_s values listed below are based on the data presented in paragraph 4 and are recommended for capacity design computations.

Type	Size ft	k_s ft
Asbestos cement pipe	Under 2.0	0.0003
Concrete pipe, precast	Under 5.0	0.0010
Concrete conduits (circular)		0.0020
Concrete conduits (rectangular)		0.0030

    b. **Velocity.** The smooth pipe curve in Chart 224-1 should be used for computing conduit flow velocity pertinent to the design of energy dissipators. It should also be used for all estimates for critically low pressures in transitions and bends, as well as for the effects of boundary offsets projecting into or away from the flow.

    c. **Model Studies.** Experimental results indicate that the resistance coefficients of models made of plastic closely approximate the smooth pipe curve at model flow Reynolds numbers in Chart 224-1. The curve should be used in computing boundary resistance losses for models of concrete and steel conduits in order to make any required model length adjustment.

    d. **Conduit Shape Effects.** A WES study[19] shows that the shape effects on resistance in noncircular conduits can be neglected for all practical purposes in the design of conduit shapes normally encountered in Corps of Engineers Civil Works projects. It is suggested that the concept of equivalent hydraulic diameter be used in the design of

noncircular conduits unless the aspect ratio (width/height) is less than 0.5 or greater than 2. Where unusual shapes are involved, model testing to evaluate shape effects may be required.

 e. **Equivalent Diameter.** The equivalent diameter concept assumes that the resistance loss and flow velocity in a noncircular conduit are equal to those in a circular conduit having a hydraulic radius, boundary roughness condition, and energy head equal to those of the noncircular conduit. The equivalent diameter is equal to four times the hydraulic radius of the noncircular conduit. The cross-section area of the noncircular conduit is used with the above-defined velocity to compute the flow discharge.

6. Acknowledgment is made to the following for permission to use the data shown in Chart 224-1.

 a. **Engineering News-Record,** Spavinaw Aqueduct and Denver Conduit No. 10 data, References 2 and 7.

 b. **Journal, American Water Works Association,** Denver Conduits Nos. 3 and 13 data, Reference 9.

 c. **American Society of Civil Engineers,** Quabbin and Chelan data, References 11 and 17.

 d. **La Houille Blanche,** Neyrpic tests, precast concrete data, Reference 6.

 e. **The Engineering Journal,** Sir Adam Beck tunnel data, Reference 12.

 f. **The University of New South Wales,** Asbestos cement data, Reference 5.

7. **References.**

(1) Horton, R. E., "Some better Kutter's formula coefficients." Engineering News, vol 75, No. 8 (24 February 1916), pp 373-374; discussion, vol 75, No. 18 (4 May 1916), pp 862-863.

(2) Scobey, F. C., "Flow of water in Tulsa 60-inch and 50-inch concrete pipe lines." Engineering News-Record, vol 94, No. 22 (May 28, 1925), pp 894-987.

(3) Moody, L. F., "Friction factors for pipe flows." Transactions, American Society of Mechanical Engineers, vol 66 (November 1944), pp 671-684.

(4)   Colebrook, C. F., "Turbulent flow in pipes with particular reference to the transition region between smooth and rough pipe laws." Journal, Institute of Civil Engineering, London, vol 12, No. 4 (1939), pp 133-156.

(5)   Foster, D. N., Field Study of Friction Loss in Asbestos Cement Pipe Lines. Water Research Laboratory Report No. 106, University of New South Wales, Australia, June 1968.

(6)   Barbe, R., "La mesure dans un laboratorie des pertes de charge de conduites industrielles." La Houille Blanche (May-June 1947), pp 191-204.

(7)   Scobey, F. C., "Flow of water in 54-inch concrete conduit, Denver, Colorado." Engineering News-Record, vol 96, No. 17 (April 29, 1926), pp 678-680.

(8)   _____, The Flow of Water in Concrete Pipe. U. S. Department of Agriculture Bulletin No. 852, October 1920.

(9)   Capen, C. H., "Trends in coefficients of large pressure pipes." Journal, American Water Works Association, vol 33, No. 1 (January 1941), pp 1-83.

(10) U. S. Army Engineer Waterways Experiment Station, CE, Pressure and Air Demand Tests in Flood-Control Conduit, Denison Dam, Red River, Oklahoma and Texas, by B. Guyton. Miscellaneous Paper No. 2-31, Vicksburg, Miss., April 1953.

(11) Fosdick, E. R., "Tunnel and penstock tests at Chelan Station, Washington." Transactions, American Society of Civil Engineers, vol 101, paper 1952 (1936), pp 1409-1439.

(12) Bryce, J. B. and Walker, R. A., "Head-loss coefficients for Niagara water supply tunnel." The Engineering Journal, Montreal, Canada (July 1955).

(13) U. S. Army Engineer Waterways Experiment Station, CE, Hydraulic Prototype Tests, Control Shaft 4, Fort Peck Dam, Missouri River, Montana, by B. Guyton. Technical Memorandum No. 2-402, Vicksburg, Miss., April 1955.

(14) _____, Prototype Performance and Model-Prototype Relationship, by F. B. Campbell and E. B. Pickett. Miscellaneous Paper No. 2-857, Vicksburg, Miss., November 1966.

(15) _____, Prototype Hydraulic Tests of Flood-Control Conduit, Enid Dam, Yocona River, Mississippi, by C. J. Huval. Technical Report No. 2-510, Vicksburg, Miss., June 1959.

(16) U. S. Army Engineer Waterways Experiment Station, CE, <u>Vibration, Pressure and Air-Demand Tests in Flood-Control Sluice, Pine Flat Dam, Kings River, California,</u> by B. Guyton. Miscellaneous Paper No. 2-75, Vicksburg, Miss., February 1954. Also unpublished data.

(17) Kennison, K. R., discussion of "Friction coefficients in a large tunnel," by G. H. Hickox, A. J. Peterka, and R. A. Elder. <u>Transactions, American Society of Civil Engineers,</u> vol 113 (1948), p 1053.

(18) U. S. Army, Office, Chief of Engineers, <u>Engineering and Design; Hydraulic Design of Reservoir Outlet Structures.</u> EM 1110-2-1602, Washington, D. C., 1 August 1963.

(19) U. S. Army Engineer Waterways Experiment Station, CE, <u>Resistance Losses in Noncircular Flood Control Conduits and Sluices,</u> by R. G. Cox. Miscellaneous Paper No. H-73-1, Vicksburg, Miss., February, 1973.
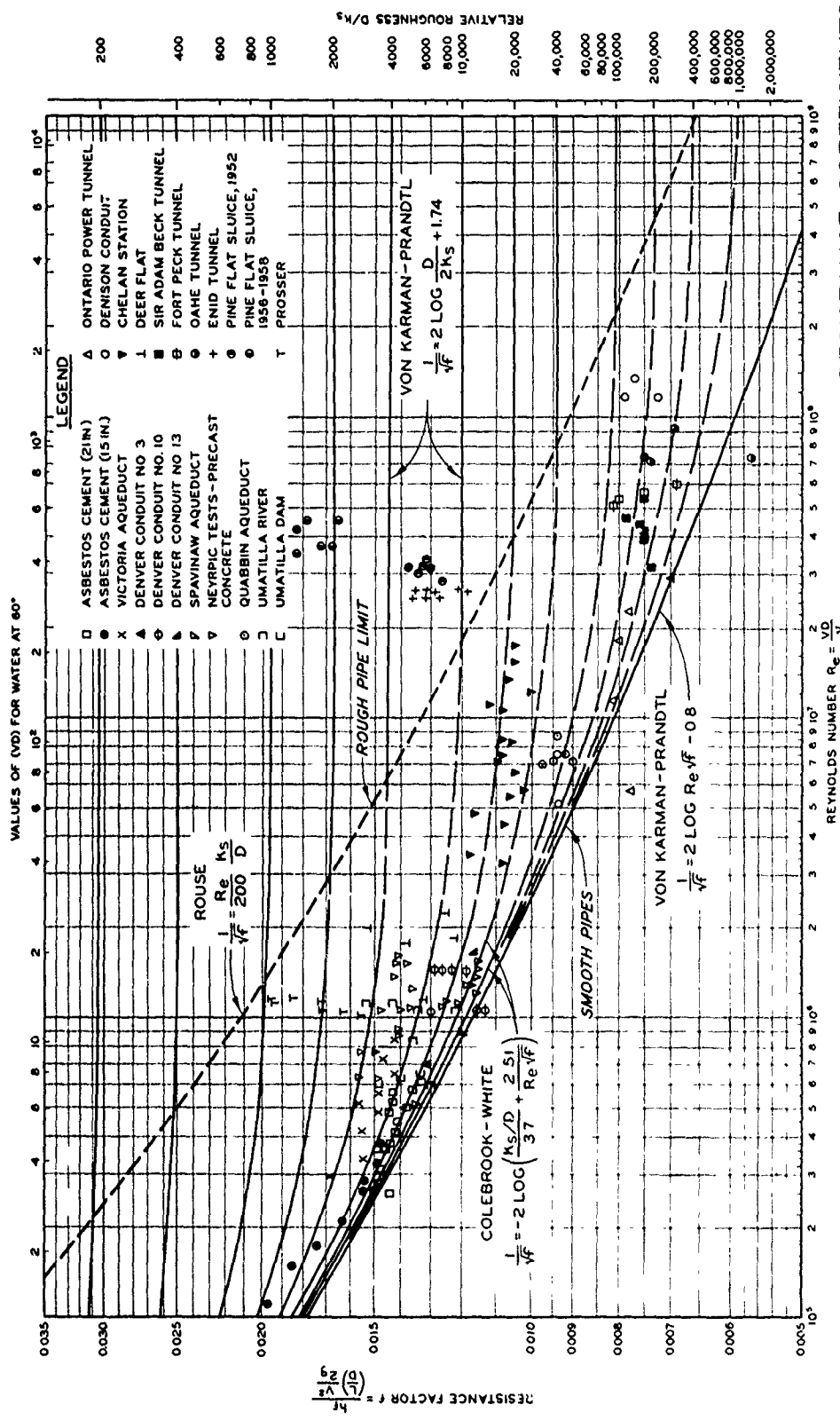
RESISTANCE COEFFICIENTS
CONCRETE CONDUITS

HYDRAULIC DESIGN CHART 224-1

REV 6-57, 8-60, 1-64, 9-70   WES 1-53

LEGEND

□	ASBESTOS CEMENT (21IN.)	△	ONTARIO POWER TUNNEL
●	ASBESTOS CEMENT (15 IN.)	○	DENISON CONDUIT
×	VICTORIA AQUEDUCT	▽	CHELAN STATION
▲	DENVER CONDUIT NO 3	⊥	DEER FLAT
◆	DENVER CONDUIT NO.10	■	SIR ADAM BECK TUNNEL
◇	DENVER CONDUIT NO 13	⊕	FORT PECK TUNNEL
▶	SPAVINAW AQUEDUCT	◉	OAHE TUNNEL
▽	NEYRPIC TESTS - PRECAST CONCRETE	+	ENID TUNNEL
⊖	QUABBIN AQUEDUCT	⊘	PINE FLAT SLUICE, 1952
⊓	UMATILLA RIVER	◎	PINE FLAT SLUICE, 1956-1958
⊏	UMATILLA DAM	T	PROSSER

VON KARMAN–PRANDTL

$$\frac{1}{\sqrt{f}} = 2 \text{ LOG } \frac{D}{2 k_s} + 1.74$$

ROUGH PIPE LIMIT

ROUSE

$$\frac{1}{\sqrt{f}} = \frac{Re}{200} \frac{k_s}{D}$$

VON KARMAN–PRANDTL

$$\frac{1}{\sqrt{f}} = 2 \text{ LOG } Re \sqrt{f} - 0.8$$

SMOOTH PIPES

COLEBROOK–WHITE

$$\frac{1}{\sqrt{f}} = -2 \text{ LOG } \left(\frac{k_s/D}{3.7} + \frac{2.51}{Re\sqrt{f}} \right)$$

NOTE h_f = RESISTANCE LOSS, FT
       L = LENGTH OF CONDUIT, FT
       D = DIAMETER FT
       k_s = EFFECTIVE ROUGHNESS FT
       V = VELOCITY, FPS
       ν = KINEMATIC VISCOSITY, FT²/SEC

PREPARED BY U S ARMY ENGINEER WATERWAYS EXPERIMENT STATION VICKSBURG MISSISSIPPI

HYDRAULIC DESIGN CRITERIA

SHEET 224-1/1

RESISTANCE COEFFICIENTS

STEEL CONDUITS

1. The magnitude of resistance (friction) loss in steel conduits is an important factor in the economics of design of pipelines, tunnels, and power penstocks. The concept of maximum and minimum design criteria is of importance in the design of flood-control outlet works and of surge tanks for power plants. It is desirable to use conservative resistance values in the design of flood-control conduits and water supply lines for hydraulic capacity and in the design of surge tanks for load acceptance. Conversely, minimum resistance values should be used for the design of stilling basins and of surge tanks for load rejection. The general comments in paragraphs 2 and 3 of HDC Sheet 224-1 apply to steel conduits.

2. **Resistance Factors.** Chart 224-1/1 is a plot of experimental data from tests made on steel conduits. The data are shown in the form of a Moody diagram where the resistance factor f is plotted as a function of the Reynolds number. The plotted points were selected principally from data compiled by the USBR.[1] The San Gabriel[2] test data were obtained from measurements on enamel-lined steel conduits and afford information for the higher Reynolds numbers. The Neyrpic tests,[3] the Milan tests,[4] and the Hoover Dam model tests[5] were hydraulic laboratory investigations involving fairly large Reynolds numbers. Corps of Engineers field tests at Fort Randall Dam in 1956[6] and 1959[7] afforded valuable information of the effects of surface treatment of 22-ft-diameter steel tunnels. The 1956 Fort Randall[6] and the 1957 Garrison[8] tests on vinyl-painted steel resulted in an average f value of 0.0075 for $R_e = 1.45 \times 10^7$ and an f value of 0.0071 for R_e of 2.5×10^7, respectively. The 1959 tests of brushed, tar-coated surface treatment resulted in an average f value of 0.0085 for $R_e = 1.01 \times 10^8$. The pipe flow theory indicates that experimental data should not plot below the smooth pipe curve in Chart 224-1/1.

3. **Effective Roughness.** The following tabulation summarizes the data plotted in Chart 224-1/1 and can be used as a guide in selecting k_s values for specific design problems. However, the k_s values listed do not necessarily apply to conduits having greatly different diameters.

Symbol	Project	Ref No.	Diameter ft	k_s ft	Remarks
□	Neyrpic	3	2.60	0.000010	Spun bitumastic coating
■	Neyrpic	3	2.61	0.000135	Uncoated
●	Milan	4	0.33	0.000039	Zinc coated
●	Milan	4	0.49	0.000026	Zinc coated
			(Continued)		

224-1/1
Revised 6-57
Revised 1-64
Revised 9-70

Symbol	Project	Ref No.	Diameter ft	k_s ft	Remarks
●	Milan	4	0.82	0.000071	Zinc coated
X	San Gabriel	2	10.25	0.000004	Enameled
△	San Gabriel	2	4.25	0.000152	Enameled
+	Hoover	5	0.83	0.000133	Galvanized pipe
▼	Fort Randall	9	22.00	0.000936	Tar coated
O	Fort Randall	7	22.00	0.000382	Tar coated
▲	Fort Randall	6	22.00	0.000008	Vinyl painted
▽	Garrison	8	24.00	0.000005	Vinyl painted

4. <u>Design Criteria</u>. The k_s values listed in the tabulation below are recommended for use in sizing cast iron and steel pipes and conduits to assure discharge capacity. The values for large steel conduits with treated interiors should also be useful in the design of surge tanks under load acceptance. The recommended values result from analysis of 500 k_s computations based on the data presented in Chart 224-1/1 and in table H of reference 1. The data are limited to continuous interior iron and steel pipe. The recommended values are approximately twice the average experimental values for the conditions indicated. The large increase in k_s values for large size tar- and asphalt-treated conduits results from heavy, brushed-on coatings.

Diameter ft	Treatment	k_s ft
Under 1.0	Tar dipped	0.0001
1 to 5	Tar coated	0.0003
Over 5	Tar brushed	0.0020
Under 6	Asphalt	0.0010
Over 6	Asphalt brushed	0.0100
All	Vinyl or enamel paint	0.0001
All	Galvanized, zinc coated or uncoated	0.0006

5. <u>Velocity</u>. The smooth pipe curve in Chart 224-1/1 is recommended for all design problems concerned with momentum and dynamic forces (water hammer, surge tanks for load rejection, critical low pressures at bends, branches, offsets, etc.).

6. <u>Aging Effects</u>. Interior treatment of pipes and conduits is of importance to their service life. Chemical, organic, and inorganic deposits in steel pipes and conduits can greatly affect the resistance losses and conduit capacity over a period of time. Data by Moore[10] indicate that over a 30-year period incrustation of iron bacteria up to 1 in. thick formed in uncoated 8-in. water pipe. Similar conditions prevailed in 10-in. pipe where the bond between the pipe and the interior coal tar enamel was poor. Computed k_s values for these pipes were 0.03 and 0.02 ft, respectively. Data compiled by Franke[11] indicate that organic and inorganic incrustations and deposits in steel conduits up to 6 ft in

diameter increased resistance losses by as much as 100 to 300 percent with k_s values increasing 100 percent. The data indicate that the interiors of some of the conduits were originally treated with a coat of bitumen. The changes occurred in periods of 5 to 17 years.

7. <u>Conduit Shape Effects.</u> (See paragraphs 5<u>d</u> and <u>e</u>, HDC Sheet 224-1.)

8. <u>References.</u>

(1) U. S. Bureau of Reclamation, <u>Friction Factors for Large Conduits Flowing Full,</u> by J. N. Bradley and L. R. Thompson. Engineering Monograph No. 7, Denver, Colo., March 1951 (revised 1965).

(2) Burke, M. F., <u>High Velocity Tests in a Penstock.</u> American Society of Civil Engineers Separate No. 297, October 1953.

(3) Barbe, R., "La mesure dans un laboratoire des pertes de charge de conduites industrielles." <u>La Houille Blanche</u> (May-June 1947), pp 191-204.

(4) Marchetti, A., "Perdite di carico per regime uniforme nelle condotte Dalmine di cemento-amianto con anima di acciaio, rivestite internamente di bitume centrifugato." <u>Memorie e Studi del'Istituto di Idraulica e Costruzioni Idrauliche del Politecnico di Milano,</u> No. 56, Milano (1944).

(5) U. S. Bureau of Reclamation, <u>Part VI - Hydraulic Investigations;</u> Bulletin 2, <u>Model Studies of Penstocks and Outlet Works.</u> Boulder Canyon Project Final Reports, Denver, Colo., 1938.

(6) U. S. Army Engineer District, Omaha, CE, <u>Friction Loss Tests in Penstock No. 8, Fort Randall Power Plant.</u> General Design Memorandum No. G-9, September 1956.

(7) U. S. Army Engineer Waterways Experiment Station, CE, <u>Flow Characteristics in Flood-Control Tunnel 10, Fort Randall Dam, Missouri River, South Dakota; Hydraulic Prototype Tests,</u> by J. V. Dawsey, Jr., C. J. Huval, and W. C. Blanton. Technical Report No. 2-626, Vicksburg, Miss., June 1963.

(8) U. S. Army Engineer District, Garrison, CE, <u>Friction Loss Tests in Penstock No. 1,</u> 1957.

(9) U. S. Army Engineer District, Omaha, CE, <u>Friction Loss Tests in Penstock No. 7, Fort Randall Power Plant.</u> General Design Memorandum No. G-7, 1955.

(10) Moore, M. O., "Incrustation in water pipelines." <u>ASCE, Pipeline Division, Journal,</u> vol 94, PL 1, paper 6161 (October 1968), pp 37-47.

(11) Franke, P. G., "Some roughness values of water pipelines." L'Energia
      Elettrica, vol 46, No. 2 (February 1969), pp 78-80.

224-1/1
Revised 6-57
Revised 1-64
Revised 9-70
Revised 3-73
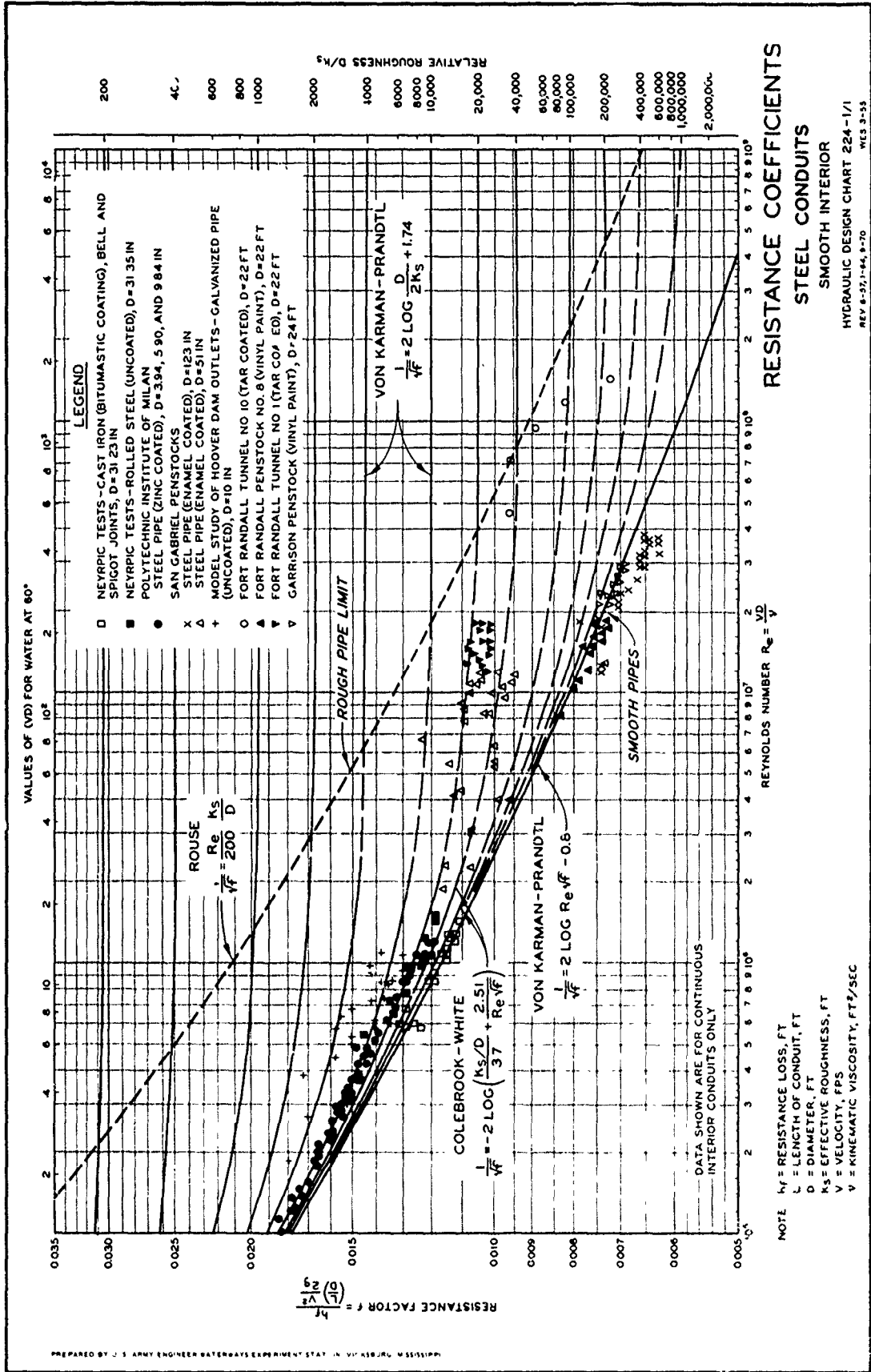
RESISTANCE COEFFICIENTS
STEEL CONDUITS
SMOOTH INTERIOR

HYDRAULIC DESIGN CHART 224-1/1

REV 8-57, 1-64, 8-70   WES 3-55

1.   Known hydraulic head loss investigations for corrugated metal pipe in the United States date back to 1914.[1] Extensive U. S. Department of Agriculture tests at Iowa[2] were published in 1926. The results of more recent tests at St. Anthony Falls Hydraulic Laboratory,[3] Bonneville Hydraulic Laboratory,[4] the U. S. Army Engineer Waterways Experiment Station (WES),[5] and others[6,7,8] have been summarized in Charts 224-1/2 to 224-1/4. These data are for full-pipe flow and large length-diameter ratios. Resistance data obtained in the Bonneville tests with paved inverts are also shown.

2.   Types of Corrugated Metal Pipe. Metal pipe with annular corrugations 0.5 in. deep spaced at intervals of 2.67 in. has been accepted as standard in the United States for many years (Chart 224-1/2). A new type of corrugated metal pipe having annular corrugations 1 in. deep spaced 3 in. apart is commercially available. Large diameter, field-assembled structural plate pipe having annular corrugations 2 in. deep spaced 6 in. apart has come into general use. Also, helical corrugated metal pipe in sizes of 6 to 96 in. is presently being manufactured.[9] The pitch and depth of the corrugations vary from 1.5 in. and 0.25 in., respectively, for the small size pipe to 3.0 in. and 1.0 in., respectively, for the large size pipe. Available limited test data indicate that the helical corrugated pipe is structurally superior to equivalent standard corrugated pipe.[10]

3.   The available experimental data for standard corrugated metal pipe are generally for full-scale tests using commercially fabricated pipe. Available experimental data for structural plate and the new type of corrugated pipe are basically limited to large-scale model tests. The 1:4- or quarter-scale model tests of standard 5-ft-diameter corrugated pipe at WES indicate somewhat higher resistance coefficients than the Bonneville 5-ft-diameter prototype tests (Chart 224-1/2). This is attributed to a minor difference in the relative corrugation size in the model and the prototype. The full-scale Alberta structural plate pipe test data, $K/D =$ 0.0339 (Chart 224-1/3) indicate about 10 percent higher f coefficients than comparable WES model test results adjusted 8 percent for field bolt effects.[5]

4.   Charts 224-1/2 and 224-1/3 show values of the Darcy-Weisbach resistance coefficient (f) versus Reynolds number (R_e) computed from the observed test data. The equations used for the plots are

$$f = \frac{h_f}{\left(\dfrac{L}{D}\right)\dfrac{V^2}{2g}}$$

and

$$R_e = \frac{VD}{\nu}$$

The symbols are defined in Chart 224-1/2.

5. Values of the Manning's n versus pipe diameter resulting from the test data and recommended for design are shown in Chart 224-1/4. The basic Manning equation is

$$n = \frac{1.486 S^{1/2} R^{2/3}}{V}$$

The terms are defined in the chart. The relation between f and n is given in Sheets 224-3 to 224-7. Recommended design curves of Manning's n for various pipe diameters are given in Chart 224-1/4. Also shown are limited experimental data[3] for standard corrugated pipe arches. The n values plotted in this chart are computed from the average maximum values of f observed on corrugated pipe. The 3-ft-diameter f vs R_e curve shape in Chart 224-1/2 was used to extrapolate to maximum f values for the smaller pipe sizes. A similar procedure was used to extrapolate to the maximum values for the data curves in Chart 224-1/3. The curves for structural plate pipe shown in the charts are principally based on results of WES tests on model pipe having a corrugation depth-to-pitch ratio of 1 to 3. The Bossy[5] procedure was used to adjust the WES model data for the additional resistance attributable to bolts required in field assembly of prototype pipe.

6. <u>Helical Corrugations.</u> Resistance coefficients have been reported by Chamberlain,[7] Garde,[8] and Rice[11] on small size helical and standard corrugated pipe of comparable size. The following tabulation summarizes their findings.

Pipe Size, in.	Type	K/D	f	n	Ref No.
8	Helical	0.03	0.037	0.013	11
12	Helical	0.04	0.042	0.015	11
12	Helical	0.04	0.048	0.016	8
12	Standard	0.08	0.126	0.026	8
12	Standard	0.08	0.117	0.026	7
12	Helical	0.04	0.040	0.015	7

All tests were made with Reynolds numbers from 10^5 to 10^6. The resistance coefficient was found to be essentially constant for each pipe tested.

7. The tabulation above indicates that the resistance coefficient for small-diameter helical corrugated pipe is about 33 percent of that for comparable standard corrugated pipe and about 58 percent in terms of Manning's n. These percentages will be different for other size pipe depending upon the corrugation pitch, depth, and inclination with the pipe axis. Presently available data are limited to small size pipe having corrugations inclined about 65 deg to the pipe axis. For large diameter helical corrugated pipe the n values given in Chart 224-1/4 for standard unpaved corrugated pipe are recommended for design.

8. <u>Application.</u> The Manning's n curves presented in Chart 224-1/4 are recommended for preliminary design purposes. The data presented in Charts 224-1/2 and 224-1/3 permit more accurate evaluation of resistance losses when the design Reynolds number is significantly different from that resulting in the peak values of the resistance coefficients. Resistance coefficients based on the model data curves in Chart 224-1/3 should be increased by 8 percent when used for field-assembled pipe. Caution should be used in extrapolating the data to other types of corrugations.
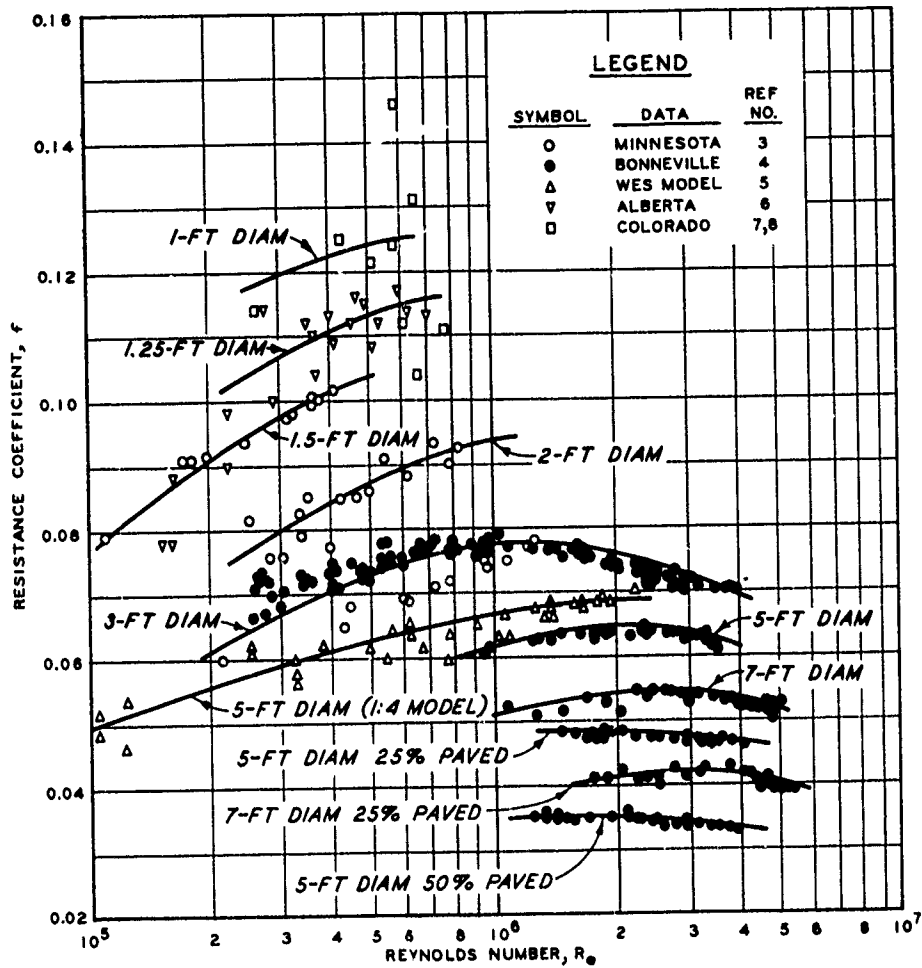
9. <u>References.</u>

(1) Cone, V. M., Trimble, R. E., and Jones, P. S., <u>Frictional Resistance in Artificial Waterways.</u> Bulletin No. 194, Colorado Agricultural Experiment Station, Fort Collins, 1914.

(2) Yarnell, D. L., Nagler, F. A., and Woodward, S. M., <u>Flow of Water Through Culverts.</u> Bulletin 1, Studies in Engineering, University of Iowa, Iowa City, 1926.

(3) Straub, L. G., and Morris, H. M., <u>Hydraulic Tests on Corrugated Metal Culvert Pipes.</u> Technical Paper No. 5, Series B, St. Anthony Falls Hydraulic Laboratory, University of Minnesota, Minneapolis, 1950.

(4) Bonneville Hydraulic Laboratory, Portland District, CE, <u>Friction Losses in Corrugated Metal Pipe; CWI 828.</u> Report No. 40-1, Portland, Oreg., July 1955.

(5) U. S. Army Engineer Waterways Experiment Station, CE, <u>Resistance Coefficients for Structural Plate Corrugated Pipe; Hydraulic Model Investigation,</u> by J. L. Grace, Jr. Technical Report No. 2-715, Vicksburg, Miss., February 1966.

(6) Neill, C. R., "Hydraulic roughness of corrugated pipes." <u>ASCE, Hydraulics Division, Journal,</u> vol 88, HY 3 (May 1962), pp 23-44; vol 88, HY 6 (November 1962), Discussions; vol 89, HY 1 (January 1962), Discussions; vol 89, HY 4 (January 1963), Closure.

(7) Chamberlain, A. R., <u>Effects of Boundary Form on Fine Sand Transport in Twelve-Inch Pipes.</u> Report CER No. 55, ARC 6, Department of Civil Engineering, Colorado State University, Fort Collins, 1955.

(8) Garde, R. J., <u>Sediment Transport Through Pipes.</u> Report CER No. 56,
     RJG 19, Department of Civil Engineering, Colorado State University,
     Fort Collins, 1956.

(9) American Iron and Steel Institute, <u>Handbook of Steel Drainage and
     Highway Construction Products.</u> New York, 1967.

(10) Armco Drainage and Metal Products, Inc., <u>Handbook of Drainage and
      Construction Products.</u> Middletown, Ohio, 1958.

(11) U. S. Department of Agriculture, <u>Friction Factors for Helical Corru-
      gated Pipe,</u> by C. E. Rice. ARS 41-119, Agricultural Research Service,
   Washington, D. C., February 1966.

Chart showing resistance coefficient f versus Reynolds number R_e for corrugated metal pipe of various diameters.

LEGEND

SYMBOL	DATA	REF NO.
O	MINNESOTA	3
●	BONNEVILLE	4
△	WES MODEL	5
▽	ALBERTA	6
□	COLORADO	7,8

Curve labels: 1-FT DIAM, 1.25-FT DIAM, 1.5-FT DIAM, 2-FT DIAM, 3-FT DIAM, 5-FT DIAM, 7-FT DIAM, 5-FT DIAM (1:4 MODEL), 5-FT DIAM 25% PAVED, 7-FT DIAM 25% PAVED, 5-FT DIAM 50% PAVED

Y-axis: RESISTANCE COEFFICIENT, f
X-axis: REYNOLDS NUMBER, R_e

BASIC EQUATIONS

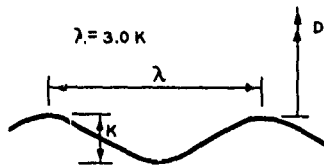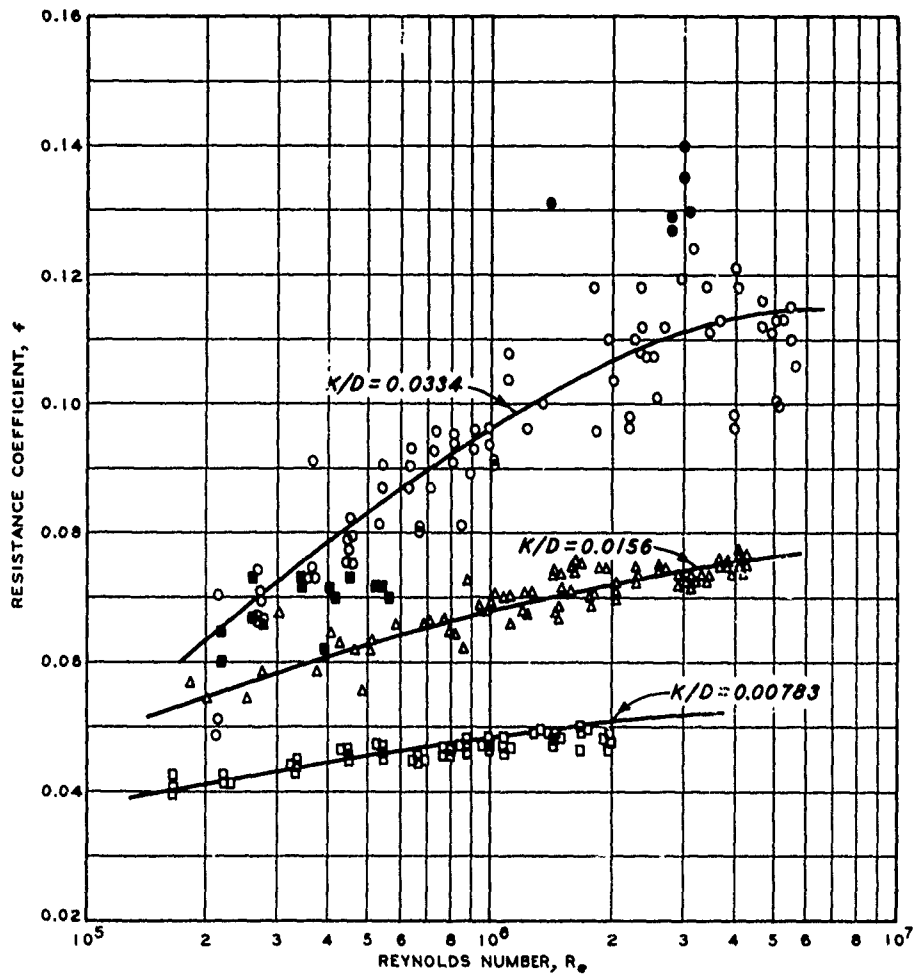$$f = \frac{h_f}{\left(\frac{L}{D}\right)\frac{V^2}{2g}} \quad ; \quad R_e = \frac{VD}{\nu}$$

WHERE:

f = DARCY RESISTANCE COEFFICIENT
h_f = FRICTION LOSS, FT
L = PIPE LENGTH, FT
D = PIPE DIAMETER, FT
V = AVERAGE VELOCITY, FPS
g = ACCELERATION, GRAVITATIONAL, FT/SEC^2
ν = KINEMATIC VISCOSITY, FT^2/SEC

K = 0.5 IN.
λ = 2.67 IN.
λ = 5.3K
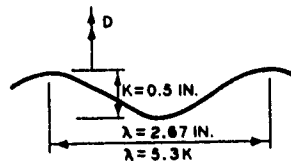
CORRUGATION DETAILS

RESISTANCE COEFFICIENTS
CORRUGATED METAL PIPE
λ = 5.3 K

HYDRAULIC DESIGN CHART 224-1/2

RESISTANCE COEFFICIENTS, f vs REYNOLDS NUMBER, R_e

λ = 3.0 K

CORRUGATION DETAILS

EQUIVALENT PIPE DIAMETER, FT

K/D	1- X 3-IN. CORRUGATION	2- X 6-IN. CORRUGATION
0.00783	10	20
0.0156	5	10
0.0334	2.5	5

NOTE CURVES ARE BASED ON MODEL DATA AND APPLY TO NEW TYPE SHOP-FABRICATED CORRUGATED METAL PIPE

INCREASE MODEL f BY 8 PERCENT FOR FIELD-ASSEMBLED STRUCTURAL PLATE PIPE.

LEGEND

SYMBOL	DATA	REF NO	MODEL SCALE	K/D
o	WES MODEL	5	1:2.2	0.0334
Δ	WES MODEL	5	1:8	0.0156
□	WES MODEL	5	1:16	0.00783
▪	ALBERTA MODEL	6	1:16.6	0.0333
●	ALBERTA PROT.	6	1:1	0.0339

RESISTANCE COEFFICIENTS
CORRUGATED METAL PIPE
λ = 3.0 K
HYDRAULIC DESIGN CHART 224-1/3

RESISTANCE COEFFICIENTS

CORRUGATED METAL PIPES

MANNING'S n

FULL PIPE FLOW

HYDRAULIC DESIGN CHART 224-1/4

WES 1-68

HYDRAULIC DESIGN CRITERIA

SHEETS 224-1/5 AND 224-1/6

RESISTANCE COEFFICIENTS

UNLINED ROCK TUNNELS

1. **Purpose.** Unlined rock tunnels have been built for flood flow diversion and for hydropower tunnels where the rock is of sound quality and not greatly jointed and fractured. Hydraulic Design Charts 224-1/5 and 224-1/6 summarize available flow resistance data for unlined rock tunnels and should be useful in estimating head losses resulting from boundary roughness.

2. **General.** The decision whether to line a water-carrying tunnel or to leave it unlined involves a number of factors that affect the economic aspects of a project. It will generally be found to be more economical to leave the tunnel unlined unless high flow velocities are involved, considerable rock remedial treatment is required, or lining in fractured rock zones is necessary. Operating experiences of over 60 years have shown that unlined power tunnels are economical both in initial construction and in maintenance.[1,2,3,4] However, the possibility of small rock falls resulting in turbine damage and penstock abrasion requires periodic tunnel inspection, especially during the first few years of operation.

3. Tunnel invert paving may be economically justified to (a) eliminate possible damage to downstream turbines or penstocks from migrating invert muck, thereby permitting greater flow velocities, and (b) facilitate tunnel inspection, maintenance, and rock trap clean out. In some cases it may be preferable to provide for tunnel invert cleanup using air and water jetting during construction. The proper balance between design velocity, provision of rock traps, and tunnel invert paving should be based on economic considerations.

4. **Tunnel Stability and Shape.** The determination of the structural stability of an unlined tunnel in rock and the need for partial or total tunnel lining depends on the findings of subsurface geologic exploration and a thorough study of the existing rock structure. The possible loss of flow through faults and fissures as well as heavy flows into the tunnel during construction should be investigated. Structural stability of the tunnel will usually require a rounded roof. A flat or nearly flat invert has been found to be advantageous for economical tunnel blasting and muck removal operations. The tunnel shape preferred by many contractors is the straight-legged horseshoe or some modified horseshoe shape.[5] The added hydraulic advantage of circular or nearly circular cross section has not generally justified the resulting increased tunneling complexity and cost. In the present study only one of 42 tunnels investigated was found to be circular in shape. Almost all the others were horseshoe or modified horseshoe shaped.

5. Overbreak. Overbreak as defined herein is the difference between the minimum allowable and the actual average tunnel dimensions. The sketch in Chart 224-1/6 graphically defines this terminology. The amount of overbreak determines to a great extent the tunnel roughness and thus resistance to the flow. There are many factors that influence the amount of overbreak, such as type and quality of rock, blasting technique, direction of driving relative to bedding planes, etc. The amount of overbreak varies from about 10 in. in the best granites to 18 in. in very blocky or laminated shales and sandstones.[5] More stringent control of overbreak usually results in higher costs.

6. Tunnel Hydraulics. Generally, velocities in unlined tunnels should not exceed 10 fps except during diversion flow when velocities to about 15 fps may be acceptable. For a tunnel with downstream turbines, penstocks, or valves, it has been recommended that velocities be limited to 5 fps or less[2] to prevent damage from migration of tunnel muck fines and rock falls. In addition, it is usually necessary to provide one or more rock or sand traps along the tunnel invert upstream of turbines to collect any migrating material. The development of satisfactory rock trap design and size is presented in references 6 and 7.

7. Theory. In unlined rock tunnels the resistance coefficient is independent of the Reynolds number because of the large relative roughness value usually obtained. Thus the Von Karman-Prandtl equation for fully rough flow based on the Nikuradse sand grain data should be applicable. This equation in terms of Darcy's f, pipe diameter D_m, and equivalent sand grain diameter k_s is

$$\frac{1}{\sqrt{f}} = 2 \log\left(\frac{D_m}{k_s}\right) + 1.14 \tag{1}$$

A measure of overbreak k (see reference 8) in unlined tunnels can be expressed as

$$k = D_m - D_n = \sqrt{\frac{4}{\pi}}\left(\sqrt{A_m} - \sqrt{A_n}\right) \tag{2}$$

where D_m and D_n are the equivalent diameters based on the areas A_m and A_n as shown in Chart 224-1/6. The relative roughness of the tunnel also can be expressed as

$$\frac{D_m}{k} = \frac{1}{1 - \sqrt{\frac{A_n}{A_m}}} \tag{3}$$

The k dimension is approximately twice the mean overbreak thickness and, therefore, is a parameter similar to the Nikuradse sand grain diameter k_s.

8. Resistance Coefficients. Considerable information on resistance in unlined rock tunnels as well as field experience has been published since 1953 (references 1, 2, 4, 5, 6, 7, 9, and 10). Data published in references 1, 2, 6, and 9-15 have been analyzed in accordance with equation 3 above, summarized in Chart 224-1/5, and plotted in Chart 224-1/6. The relation between Darcy's f, Manning's n, and tunnel diameter given on page 1 of Sheets 224-3 to 224-7 was used to convert the published resistance coefficients as required for tabulating and plotting. The relation between f, D_m, and k_s expressed by equation 1 above is also shown in Chart 224-1/6. The experimental data correlate well with the theoretical curve and indicate that k (equation 2) is a reasonably good measure of the tunnel roughness. The user is cautioned that the data presented in Charts 224-1/5 and 224-1/6 are in terms of the mean driven ("as built" average) tunnel areas (A_m).

9. Application.

a. Preliminary design. The average of the Manning's n values tabulated in Chart 224-1/5 is 0.033 and is based on the mean driven area A_m. This value can be used in preliminary design and economic analyses for average rock and blasting conditions.

b. Final design. Once a preliminary mean driven area is established, the final design can proceed, using Chart 224-1/6. An estimate of tunnel overbreak or relative roughness (D_m/k) is required for estimating resistance losses. An estimate of the overbreak depth k can be obtained from previous tunnel experience in similar geologic areas or by studying the data tabulated in Chart 224-1/5. Detailed studies of the local geology as well as the blasting experience of potential contractors are useful in estimating the expected tunnel roughness. The area obtained in the preliminary design should be used in the first trial of the computation to determine the required diameter for the given discharge, energy gradient, and surface roughness. After tunnel driving begins, the overbreak can be measured and a value of D_m/k computed to check the final design assumptions. Low values of f should be used in computations made to determine power tunnel surge tank stability and surge tank levels during load rejection. High values of f should be used to compute surge tank levels during power tunnel load acceptance.

10. References.

(1) Rahm, L., Flow Problems with Respect to Intakes and Tunnels of Swedish Hydro-Electric Power Plants. Bulletin No. 36, Institution of Hydraulics, Royal Institute of Technology, Stockholm, Sweden, 1953.

(2) Spencer, R. W., Laverty, B. R., and Barber, D. A., "Unlined tunnels of the Southern California Edison Company." ASCE, Power Division, Journal, vol 90, PO 3, paper 4087 (October 1964), pp 105-132.

(3) Groner, C. F., Snettisham Project, Alaska, First Stage Development, Formal Report on Power Tunnel Design. Oslo, Norway, October 1967.

(4) Thomas, H. H., and Whitman, L. S., "Tunnels for hydroelectric power in Tasmania." ASCE, Power Division, Journal, vol 90, PO 3, paper 4065 (October 1964), pp 11-28.

(5) Petrofsky, A. M., "Contractor's view on unlined tunnels." ASCE, Power Division, Journal, vol 90, PO 3, paper 4086 (October 1964), pp 91-104.

(6) Dann, H. E., Hartwig, W. P., and Hunter, J. R., "Unlined tunnels of the Snowy Mountains Hydro-Electric Authority, Australia." ASCE, Power Division, Journal, vol 90, PO 3, paper 4071 (October 1964), pp 47-79.

(7) Mattimoe, J. J., Tinney, E. R., and Wolcott, W. W., "Rock trap experience in unlined tunnels." ASCE, Power Division, Journal, vol 90, PO 3, paper 4067 (October 1964), pp 29-45.

(8) U. S. Army Engineer Waterways Experiment Station, CE, Prototype Performance and Model-Prototype Relationship, by F. B. Campbell and E. B. Pickett. Miscellaneous Paper No. 2-857, Vicksburg, Miss., November 1966.

(9) Report of Task Force on Flow in Large Conduits of the Committee on Hydraulic Structures, "Factors influencing flow in large conduits." ASCE, Hydraulics Division, Journal, vol 91, HY 6 (November 1965), pp 123-152.

(10) Rahm, L., "Friction losses in Swedish rock tunnels." Water Power, vol 10, No. 12 (December 1958), pp 457-464.

(11) Discussion of reference 9: Wright, D. E.; Anderson, D., and Palmer, P. M.; Angelin, S., and Larsen, P.; ASCE, Hydraulics Division, Journal, vol 92, HY 4 (July 1966).

(12) Johansen, F., "Head loss investigations in unlined rock tunnels," in Model Tests Completed in 1965, Articles and Summary of Project Reports. Bulletin No. 8E, River and Harbour Research Laboratory, University of Norway, Trondheim, 1966.

(13) Laverty, B. R., and Ludwig, K. R., "Design and performance of Mammoth Pool power tunnel." ASCE, Power Division, Journal, vol 89, PO 1, paper 3642 (September 1963), pp 9-43.

(14) Discussion of reference 6: Rufenacht, A., ASCE, Power Division, Journal, vol 91, PO 1 (May 1965), pp 120-123.

(15) Hickox, G. H., Peterka, A. J., and Elder, R. A., "Friction coefficients in a large tunnel." Transactions, ASCE, vol 113 (1948), pp 1027-1076.

(16) Elder, R. A., "Friction measurements in the Apalachia Tunnel." Transactions, ASCE, vol 123 (1958), pp 1249-1274.

No	Ref. No	Project	Location	Type of Rock	Invert Lining	A_n, Nominal or Design Area, ft²	A_m, Mean Driven Area, ft²	D_m/k	n_m	f_m
1	1, 10	Alfta	Sweden	Granite-gneiss	Negligible	323	364	17.3	0.036	0.086
2	10	Blasjon	Sweden	Gneiss-mica-schist	Asphalt paved	581	615	35.9	0.028[a]	0.047
3	10	Donje	Sweden	Gneiss	Concrete arches	1345	1521	16.8	0.034[a]	0.070
4	1, 10	Jarpstrommen	Sweden	Upper silurian slate horizontally stratified	Negligible	1130	1230	24.1	0.029	0.048
5	10	Krokstrommen	Sweden	Granite, with large amount of feldspar	Negligible	969	1094	17.0	0.029	0.048
6	1, 10	Nissastrom	Sweden	Granite-gneiss	Concrete arches	323	394	10.6	0.037[a]	0.101
7	1, 10	Porjus I	Sweden	Granite-gneiss	Negligible	53[p]	618	14.9	0.034	0.073
8	1, 10	Porjus II	Sweden	Granite-gneiss	Negligible	538	662	10.2	0.030	0.055
9	1, 10	Selsfors[b]	Sweden	Black slate with granite intrusions	NK[c]	753	866	14.8	0.044	0.114
10	1, 10	Sillre	Sweden	Vein gneiss	Negligible	54	71	7.7	0.034	0.102
11	1, 10	Sunnerstaholm	Sweden	Granite-gneiss	Minor	323	386	11.6	0.039	0.104
12[d]	10	Tasan	Sweden	Gneiss	Minor	183	185	170.6	0.033	0.081
13	1	Torpshammar	Sweden	Gneiss-granite and some diabase	NK	646	689	31.5	0.027	0.045
14	11	Stalon	Sweden	Sparagmite-quartzite	Negligible	645	705	23.0	0.030	0.055[a]
15	12	Tokke I	Norway	Variable-greenstone quartzite schist and metamorphic quartz sandstone	None	807	861	31.8	0.031	0.055[a]
16	12	Innset	Norway	NK	None	366	384	41.7	0.030	0.059[a]
17	12	Tunnsjo	Norway	Phyllite and mica schist	None	398	435	25.5	0.031	0.062[a]
18	12	Tunnsjodal	Norway	Greenstone, granite gabbro. Also phyllite and mica schist	None	484	508	41.7	0.030	0.055[a]
19	12	Tussa	Norway	NK	None	81	89	21.7	0.032	0.085[a]
20	12	Mykstufoss Head Race	Norway	Quartz, mica, and feldspar both granitic and gneissic	None	592	670	19.7	0.031	0.058[a]
21	12	Mykstufoss Tail Race	Norway	Gneiss, quartzite, and some micaceous amphibolite	None	592	639	26.9	0.035	0.074[a]
22[d]	12	Langvatn[g]	Norway	Silicates with limestone and dolomite sills	None	1507	1510	877	0.033	0.060[a]
23	6	Eucumbene-Tumut	Australia	36% granite, 64% metamorphized sedimentary	Concrete, paved flat	396	445	17.6	0.029	0.054
24	6	Tooma-Tumut	Australia	Granite	Concrete, paved flat	125	153	10.3	0.031	0.074
25	6	Murrumbidgee-Eucumbene[e]	Australia	10% granite, 90% metamorphized sedimentary	Smoothed muck	100	127	8.9	0.036	0.104
26	11	Eucumbene-Snowy[i]	Australia	94% granite, 6% metamorphized sedimentary	Concrete, paved flat	350	425	10.8	0.033	0.072
27	14	Kiewa No. 3	Australia	Granodiorite	Muck not sluiced	200	255	8.7	0.038	0.102[a]
28	14	Kiewa No. 4	Australia	Gneiss-intruded by granodiorite	Concrete	200	238	12.0	0.038	0.103[a]
29	14	Lower West Kiewa	Australia	Gneiss-intruded by granodiorite	Muck not sluiced, track left in	63	75	12.0	0.037	0.118[a]
30	14	Kiewa No. 1	Australia	Gneiss-intruded by granodiorite	Sluiced muck	150	200	7.5	0.041	0.122[a]
31	11	Telom	Malaysia	Closely-jointed granite	Compacted muck, track removed	87	105	11.0	0.030	0.081
32	9	Cresta	California	Granite	NK	578	656	16.3	0.035	0.075
33	9	West Point	California	Granite	NK	180	222	10.0	0.033	0.080
34	9	Bear River	California	Granite	NK	82	95	16.4	0.028	0.066
35	9	Balch	California	Granite	NK	144	169	13.0	0.032	0.079
36	9	Haas	California	Granite	NK	161	184	10.6	0.030	0.068
37	9	Cherry	California	Granite	NK	133	150	17.1	0.034	0.090
38	9	Jaybird	California	Granite	NK	177	195	21.0	0.032	0.077
39	2	Big Creek 3	California	Granite	Unlined	434	515	12.2	0.035	0.077[d]
40	2	Big Creek 4	California	Granite	Concrete paved	409	462	16.9	0.030	0.057[a]
41	2, 13	Mammoth Pool	California	Granite	Concrete paved	336	367	23.0	0.029	0.055[a]
42	15, 16	Apalachia	Tennessee	Quartzite and slate	Smoothed muck[h]	346[f]	403[f]	13.9	0.036	0.096

Notes

[a] Computed from $f_m = \dfrac{185\, n_m^2}{D_m^{1/3}}$

[b] Cross-section shape not constant
[c] NK not known
[d] Not plotted on HDC 224-1/6
[e] Tests may have been for free surface flow
[f] Average of 20- and 22-ft diameters
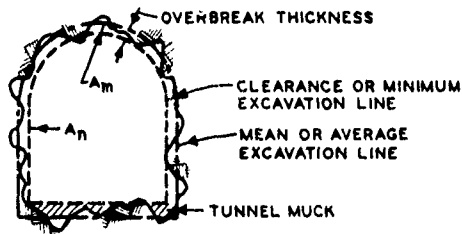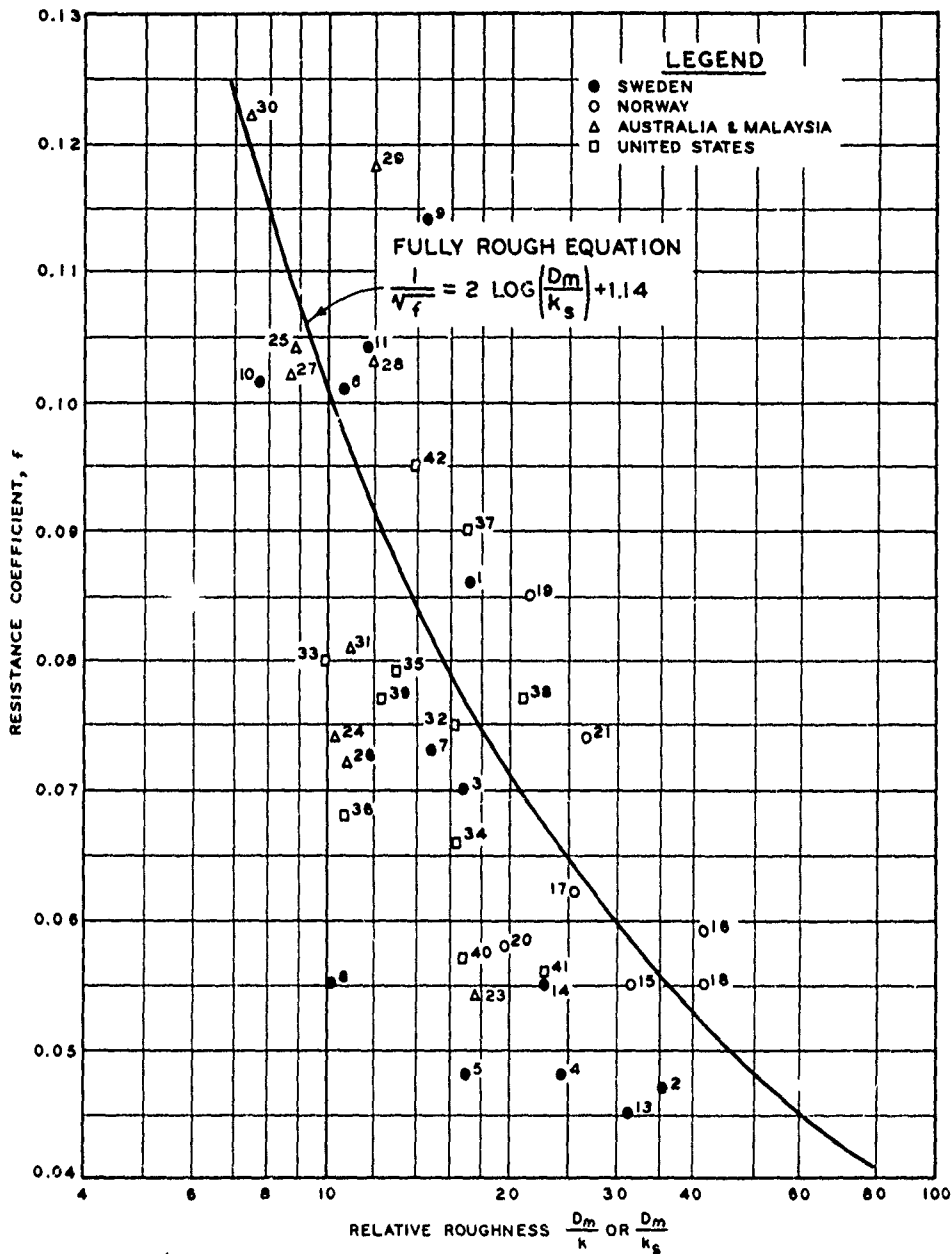[g] Cross-section area and hydraulic measurements are believed to be in error
[h] Muck (except for large rocks) cleaned out by flow
[i] Discharge measurements may be in error. Data being reanalyzed by contributor

RESISTANCE COEFFICIENTS

UNLINED ROCK TUNNELS

BASIC DATA

HYDRAULIC DESIGN CHART 224-1/5

RESISTANCE COEFFICIENTS
UNLINED ROCK TUNNELS
f-RELATIVE ROUGHNESS

HYDRAULIC DESIGN CHART 224-1/6

WES 1-66

CONDUIT SECTIONS

HYDRAULIC ELEMENTS

PRESSURE FLOW

1. The Darcy resistance factor, being expressed in terms of conduit diameter, is theoretically applicable only to conduits of circular cross section. However, the concept of equivalent hydraulic diameter has been devised by Schiller and Nikuradse* to make the Darcy f applicable to noncircular sections. This concept assumes that the resistance losses in a noncircular conduit are the same as those in a circular conduit having an equivalent hydraulic radius and boundary roughness. A WES study** has shown that the equivalent hydraulic diameter concept is applicable to all conduit shapes normally encountered in hydraulic structure design.
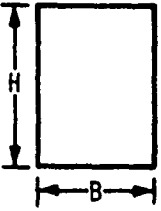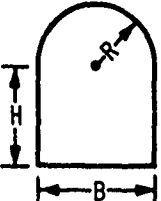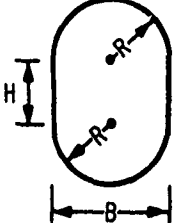
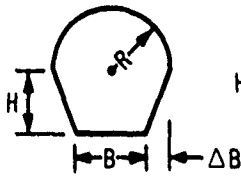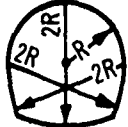2. The equivalent diameter is derived from

$$D = \qquad\qquad\qquad D = 4R = \frac{4A}{WP}$$

where R is the hydraulic radius of the noncircular conduit, A is the cross-sectional area, WP is the wetted perimeter, and D is the diameter of a circular conduit having the same hydraulic radius. Hydraulic Design Chart 224-2 is presented as an aid in the computation of equivalent hydraulic diameter for various common conduit shapes.

---

* Schlichting, H., _Boundary Layer Theory_, English translation by J. Kestin, McGraw-Hill Book Co., Inc., New York, 1960.
** U. S. Army Engineer Waterways Experiment Station, CE, _Resistance Losses in Noncircular Flood Control Conduits and Sluices_, by R. G. Cox. Miscellaneous Paper H-73-1, Vicksburg, Miss. January 1973.

SECTION	AREA (A)	WETTED PERIMETER (WP)	HYDRAULIC RADIUS (R)
	BH	$2(B+H)$	$\dfrac{BH}{2(B+H)}$
	$\dfrac{\pi D^2}{4}$	πD	$\dfrac{D}{4}$
	$BH + \dfrac{\pi R^2}{2}$	$B + 2H + \pi R$	$\dfrac{BH + \dfrac{\pi R^2}{2}}{B + 2H + \pi R}$
	$BH + \pi R^2$	$2(H + \pi R)$	$\dfrac{BH + \pi R^2}{2(H + \pi R)}$
	$H(B + \triangle B) + \dfrac{\pi R^2}{2}$	$B + 2(H^2 + (\triangle B)^2)^{\frac{1}{2}} + \pi R$	$\dfrac{H(B + \triangle B) + \dfrac{\pi R^2}{2}}{B + 2(H^2 + (\triangle B)^2)^{\frac{1}{2}} + \pi R}$
	$3.3172\,R^2$	$6.5338\,R$	$0.5077\,R$

HYDRAULIC ELEMENTS
CONDUIT SECTIONS
PRESSURE FLOW
HYDRAULIC DESIGN CHART 224-2
WES 5-75

STRAIGHT CIRCULAR CONDUIT DISCHARGE

1. The basic equation for discharge in an outlet works tunnel or conduit is:

$$Q = A_c \sqrt{\frac{1}{K + K_f + 1.0}} \sqrt{2 \, gH}$$

Where K is an intake coefficient which includes entrance losses, gate slot losses, and transition losses. The value K_f can be expressed in terms of the Darcy-Weisbach friction factor as follows:

$$K_f = \frac{fL}{D}$$

No simple equation is available for direct solution of the diameter required to pass a given discharge in view of the fact that the area of the conduit (A_c) and the friction coefficient (K_f) are both dependent upon the diameter (D). The design then requires successive approximations by computing the discharge for assumed values of diameter.

2. Hydraulic Design Chart 224-3 is a design aid for reducing the computation effort in determining the diameter required for passing a given discharge through a straight conduit. The Darcy-Weisbach friction factor "f" is used as the ordinate rather than Manning's "n" for simplicity in application. The f factor varies as the first power of the diameter whereas in Manning's formula, n varies as the two-thirds power of the diameter. The chart is prepared for an assumed K value of 0.10.

3. Many design engineers still prefer to use Manning's n instead of the Darcy-Weisbach friction factor f . Therefore, Hydraulic Design Chart 224-4 is included as an alternate design aid for reducing the computation effort in determining the diameter required for passing a given discharge. This chart presents a family of curves of various $L/D^{4/3}$ ratios plotted to show the relationship between Manning's n and the discharge coefficient K'.

4. Hydraulic Design Chart 224-5 is in the form of the Moody diagram with families of lines drawn to show the comparison of the Darcy-Weisbach f with the Manning's n for various values of the velocity-diameter ratio. The equation which relates f to n is expressed:

$$f = \frac{185n^2}{D^{1/3}}$$

This equation can be evaluated in terms of the VD product if the velocity is defined as so many diameters per second. The velocity-diameter product as used corresponds to a Reynolds number with water at 60° F.

5. A sample computation employing Charts 224-3 and 224-5 is given on Chart 224-6. An assumed diameter together with the required discharge fixes the velocity-diameter ratio and the velocity-diameter product. An alternate sample computation employing Chart 224-4 is given on Chart 224-7. The design aids presented facilitate an estimate of the required diameter, although it may be desirable to make the final determination of the discharge-head relationship analytically.
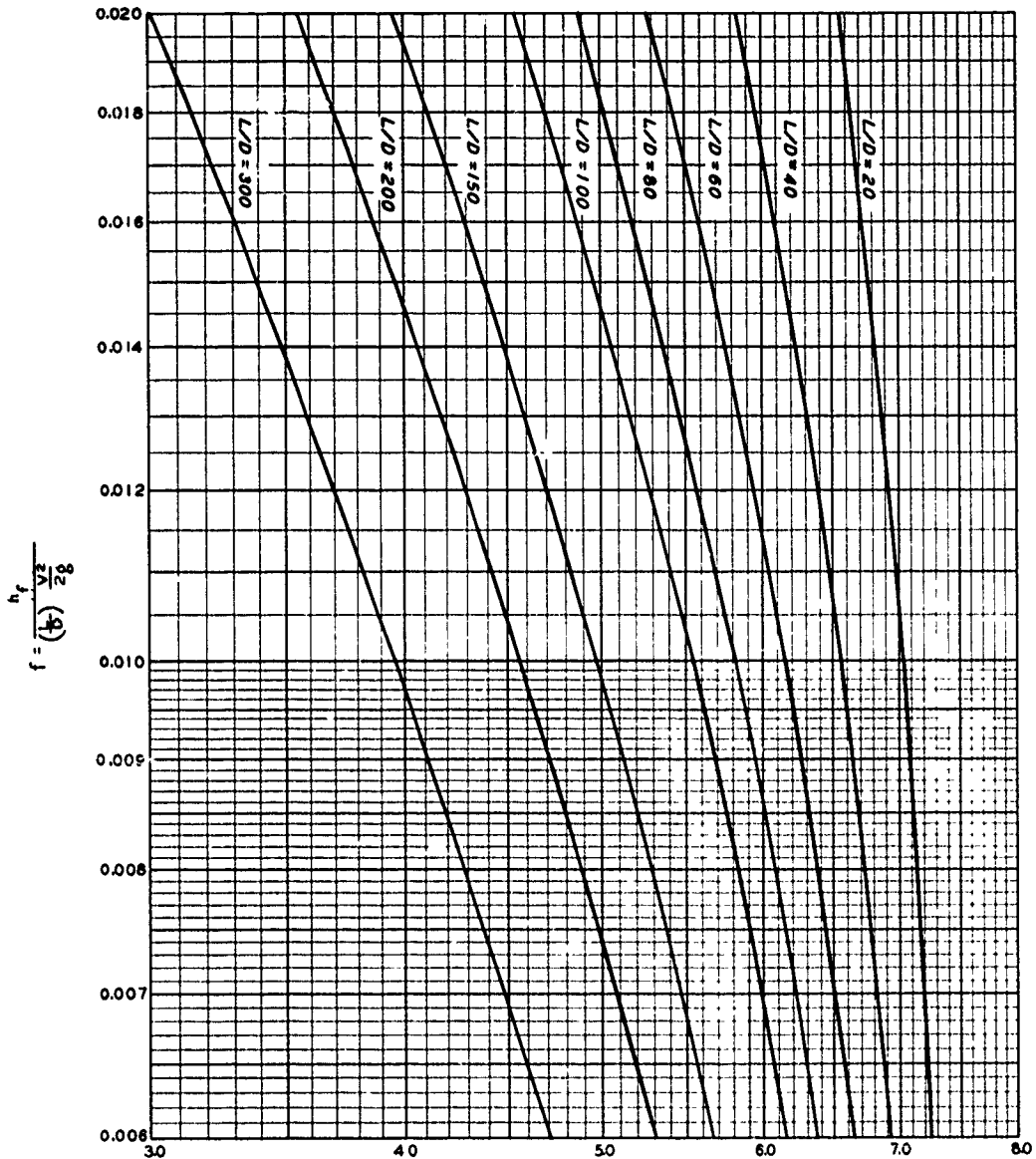
STRAIGHT CIRCULAR CONDUITS
DISCHARGE COEFFICIENTS
HYDRAULIC DESIGN CHART 224-3

STRAIGHT CIRCULAR CONDUIT DISCHARGE

Hydraulic Design Charts 224-3/1 to 224-3/4 are design aids for reducing computation effort in determining the diameter required for a given discharge through a straight conduit. These charts are presented as supplements to Chart 224-3. Chart 224-3 presents various L/D ratios as a function of the Darcy-Weisbach friction factor "f" and a discharge coefficient "K'." Chart 224-3 was prepared for a combined loss coefficient other than friction of 0.10. Charts 224-3/1 to 224-3/4 are based on combined loss coefficients of 0.20, 0.30, 0.40, and 0.50.

$$Q = A_c K' \sqrt{H}$$

WHERE:

Q = DISCHARGE IN CFS
A_c = AREA OF CONDUIT IN SQ FT
K' = DISCHARGE COEFFICIENT
H = AVAILABLE HEAD

K = 0.20

STRAIGHT CIRCULAR CONDUITS
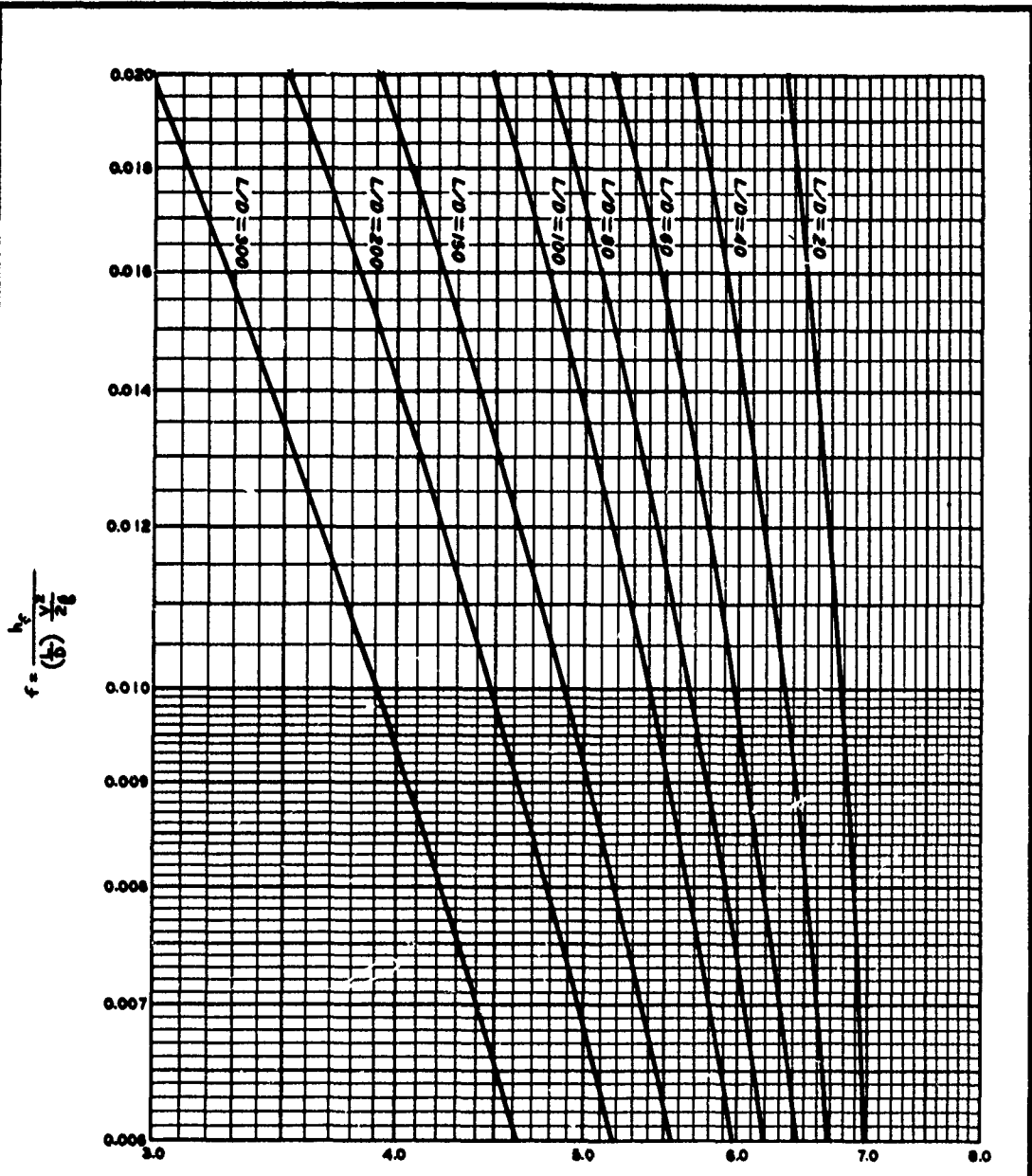## DISCHARGE COEFFICIENTS

HYDRAULIC DESIGN CHART 224-3/1

WES 2-54

$$f = \frac{h_f}{\left(\frac{L}{D}\right)\frac{V^2}{2g}}$$

$$K' = 8.02 \sqrt{\frac{1}{K+K_f+10}}$$

$$Q = A_c K' \sqrt{H}$$

WHERE:
Q = DISCHARGE IN CFS
A_c = AREA OF CONDUIT IN SQ FT
K' = DISCHARGE COEFFICIENT
H = AVAILABLE HEAD

$K = 0.30$

STRAIGHT CIRCULAR CONDUITS
DISCHARGE COEFFICIENTS
HYDRAULIC DESIGN CHART 224-3/2

WES 2-54

y-axis label: $f = \dfrac{h_f}{\left(\frac{L}{D}\right)\frac{V^2}{2g}}$

Curves labeled: $L/D=300$, $L/D=200$, $L/D=150$, $L/D=100$, $L/D=80$, $L/D=60$, $L/D=40$, $L/D=20$

x-axis label: $K' = 8.02 \sqrt{\dfrac{1}{K+K_f+1.0}}$
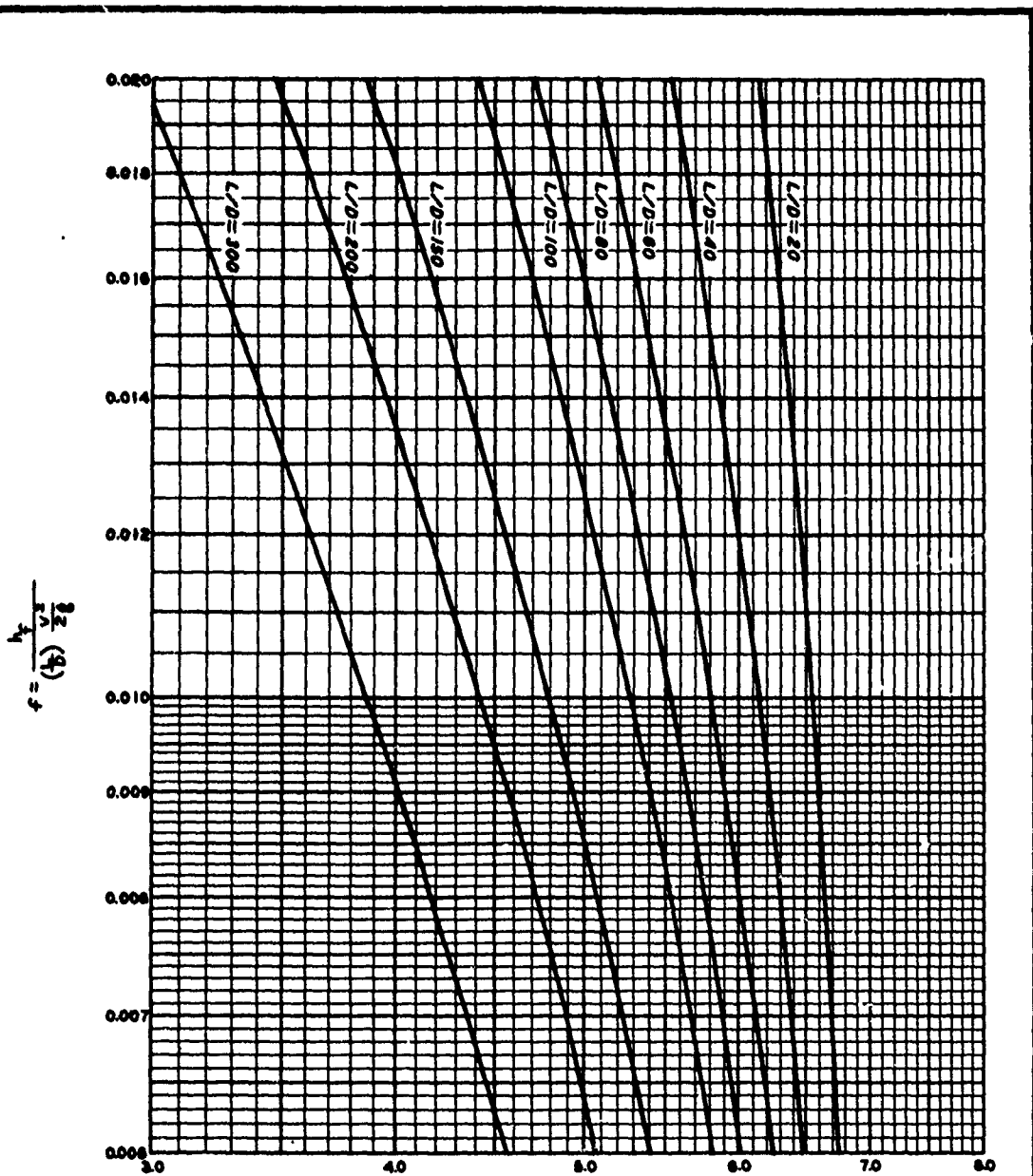
$Q = A_C K' \sqrt{H}$

WHERE:
  Q = DISCHARGE IN CFS
  A_C = AREA OF CONDUIT IN SQ FT
  K' = DISCHARGE COEFFICIENT
  H = AVAILABLE HEAD

$K = 0.40$

STRAIGHT CIRCULAR CONDUITS
DISCHARGE COEFFICIENTS

HYDRAULIC DESIGN CHART 224-3/3

WES 2-54

$$f = \left(\frac{v_c}{D}\right)\frac{v^2}{2g}$$
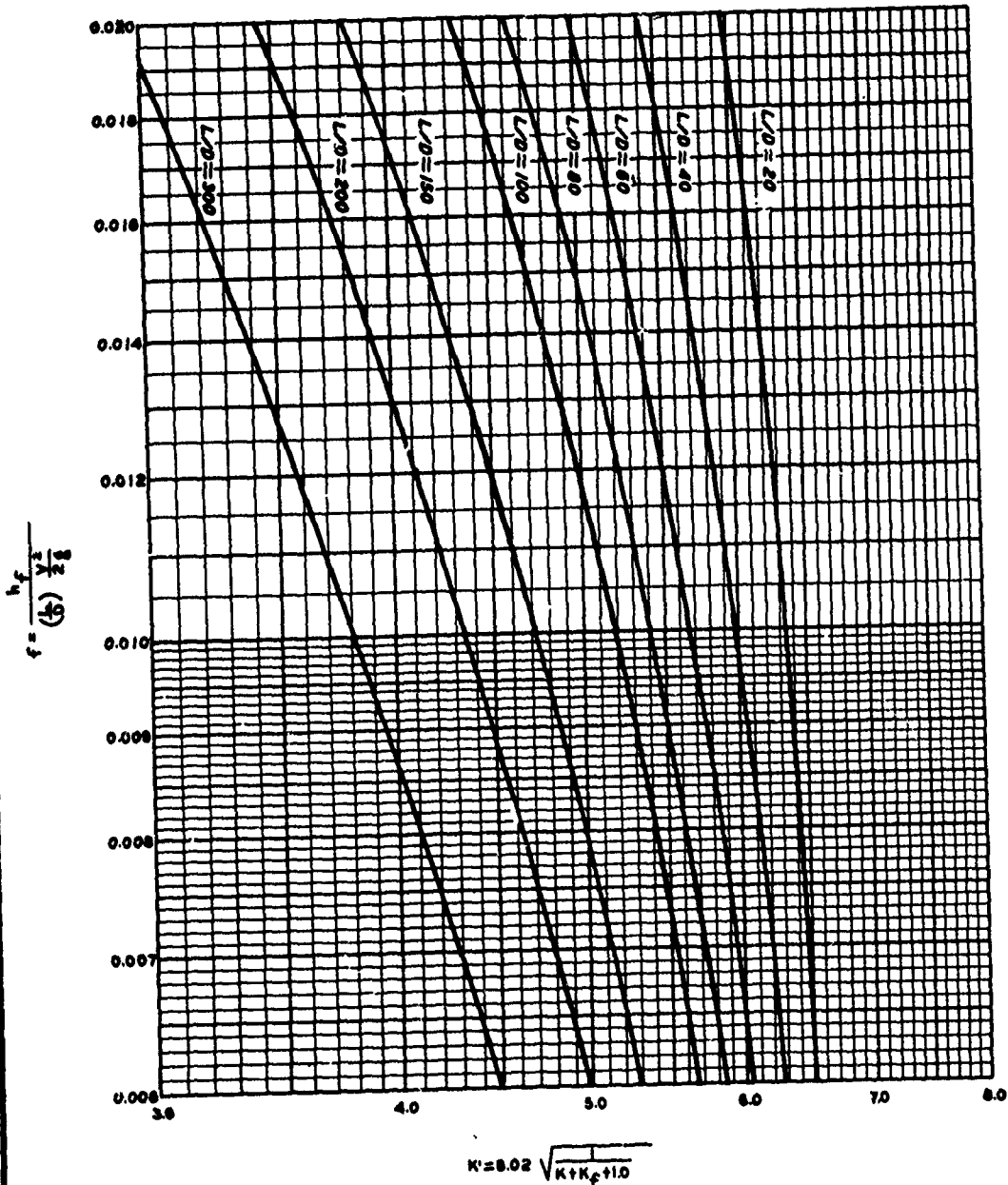
$$K' = 802\sqrt{\frac{1}{K + K_f + 10}}$$

$$Q = A_C K' \sqrt{H}$$

WHERE:

Q = DISCHARGE IN CFS
A_c = AREA OF CONDUIT IN SQ FT
K' = DISCHARGE COEFFICIENT
H = AVAILABLE HEAD

K = 0.50

STRAIGHT CIRCULAR CONDUITS
DISCHARGE COEFFICIENTS
HYDRAULIC DESIGN CHART 224-3/4

WES 2-54

$$Q = A_C K' \sqrt{H}$$
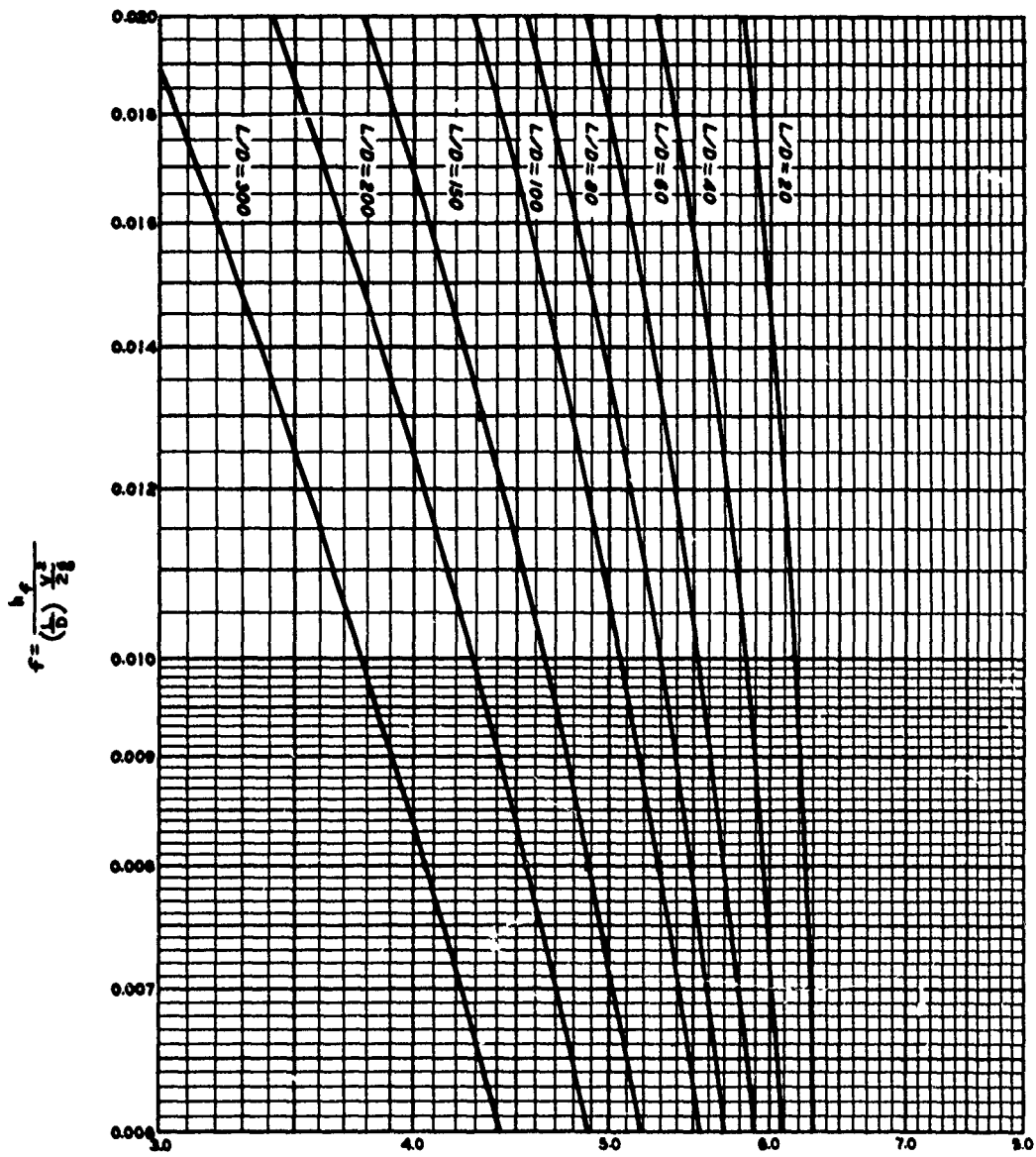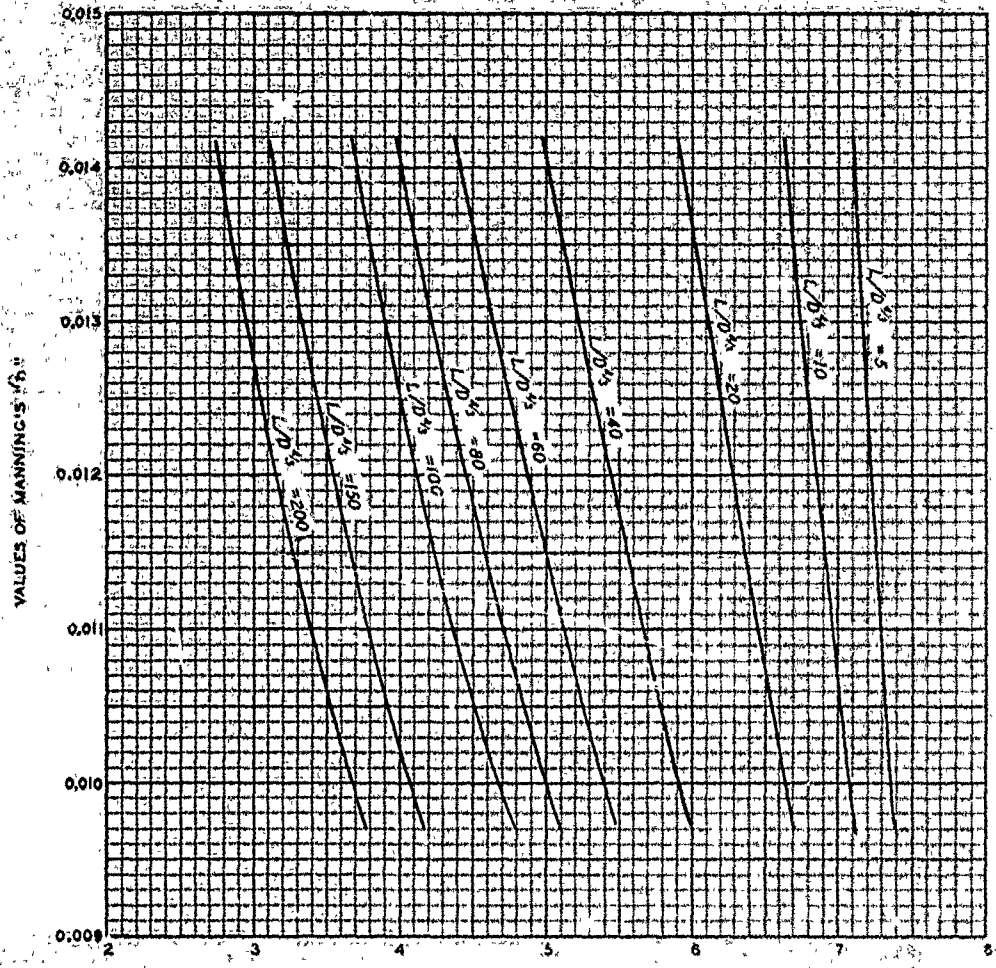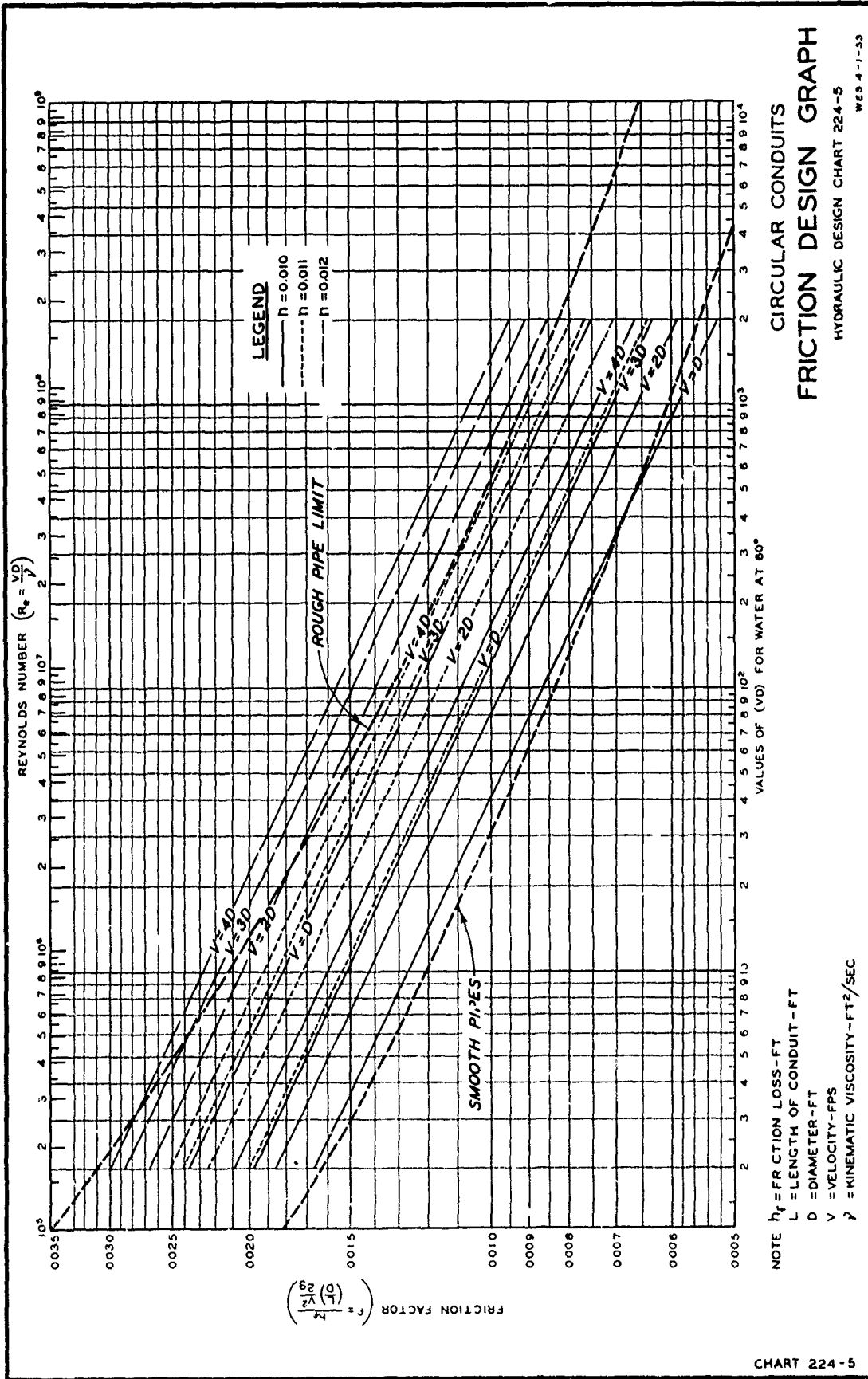
WHERE
Q = DISCHARGE IN CFS
A$_C$ = AREA OF CONDUIT IN SQ FT
K' = DISCHARGE COEFFICIENT
H = AVAIL. DIF HEAD

$K = 0.10$

STRAIGHT CIRCULAR CONDUITS
DISCHARGE COEFFICIENTS
HYDRAULIC DESIGN CHART 224-4

CIRCULAR CONDUITS
FRICTION DESIGN GRAPH

HYDRAULIC DESIGN CHART 224-5

WES 4-1-53

CHART 224-5

JOB: __CW 804__   PROJECT: __JOHN DOE DAM__   SUBJECT: __CIRCULAR CONDUITS__

COMPUTATIONS: __REQUIRED DIAMETER FOR DESIGN DISCHARGE__

COMPUTED BY: __RGC__   DATE: __10/22/52__   CHECKED BY: __AAMC__   DATE: __10-27-52__

DESIGN REQUIREMENTS

Discharge (Q) = 20,000 cfs
Length of conduit (L) = 1,000 ft
Available head (H) = 100 ft
Required conduit diameter (D) to be determined

DESIGN ASSUMPTIONS

Composite coefficient (K) = 0.10
Manning's "n" = 0.012

TRIAL COMPUTATIONS — Charts 224-3 and 224-5

Assume D = 20 ft

Then:

Area of conduit (A_c) = 314 sq ft

Velocity (V) = $\dfrac{20,000}{314}$ = 63.7 ft/sec

$\dfrac{V}{D}$ ratio = $\dfrac{63.7}{20}$ = 3.18

VD product = 63.7 × 20 = 1274

$\dfrac{L}{D}$ ratio = $\dfrac{1000}{20}$ = 50

Enter Hydraulic Design Chart 224-5 on Ordinate VD = 1274 locating V/D ratio value = 3.18 between line V/D = 3 and V/D = 4 having "n" value = 0.012. Read friction factor (f) value of 0.010 on scale at left side of chart. Enter Hydraulic Design Chart 224-3 from left side at friction factor value (f) = 0.010. Follow this "f" value across chart to L/D value of 50 between lines L/D = 40 and L/D = 60. Read discharge coefficient value of (K') = 6.35 on scale at bottom of chart. Use discharge formula on chart to compute conduit discharge.

$Q = A_c K' \sqrt{H}$

$Q = 314 \times 6.35 \sqrt{100}$ = 19,900 cfs

NOTE: If the computed discharge does not approximate the required design discharge, successive trial computations are required varying D until the design discharge is obtained.

STRAIGHT CIRCULAR CONDUITS
SAMPLE DISCHARGE COMPUTATION
HYDRAULIC DESIGN CHART 224-6
WES 4/1/53

JOB: __CW 804__   PROJECT: __JOHN DOE DAM__   SUBJECT: __CIRCULAR CONDUITS__

COMPUTATIONS: __REQUIRED DIAMETER FOR DESIGN DISCHARGE__

COMPUTED BY: __RGC__   DATE: __1/23/53__   CHECKED BY: __AAMC__ DATE: __2/3/53__

DESIGN REQUIREMENTS

Discharge (Q) = 20,000 cfs
Length of conduit (L) = 1000 ft
Available head (H) = 100 ft
Required conduit diameter (D) to be determined

DESIGN ASSUMPTIONS

Composite coefficient (K) = 0.10
Manning's "n" = 0.012

TRIAL COMPUTATION — Chart 224-4

Assume D = 20 ft

Then:

Area of conduit (A_c) = 314

K = 0.10

$D^{4/3} = (20)^{4/3} = 54.3$

$\dfrac{L}{D^{4/3}} = \dfrac{1000}{54.3} = 18.4$

Enter Hydraulic Design Chart 224-4 at left side with "n" value of 0.012. Traverse chart to point $\dfrac{L}{D^{4/3}} = 18.4$ between lines $\dfrac{L}{D^{4/3}} = 10$ and $\dfrac{L}{D^{4/3}} = 20$. Read discharge coefficient (K') = 6.4 on scale at bottom of chart. Use discharge formula on Chart 224-4 to compute conduit discharge.

$Q = A_c K' \sqrt{H}$

$Q = 314 \times 6.4 \times \sqrt{100} = 20,100$ cfs

NOTE: If computed discharge does not approximate the required design discharge successive trial computations are required varying D until the design discharge is obtained.

STRAIGHT CIRCULAR CONDUITS
SAMPLE DISCHARGE COMPUTATION
MANNING'S "N" METHOD
HYDRAULIC DESIGN CHART 224-7

WES 4/1/53

HYDRAULIC DESIGN CRITERIA

SHEETS 224-8 AND 224-9

CIRCULAR SECTIONS

FREE-SURFACE FLOW

1. Hydraulic Design Charts 224-8 and 224-9 are aids for reducing the computation effort in design of channels of circular section. Chart 224-8 is designed for use with Charts 610-1 and 610-1/1. Chart 224-9 is complete within itself. These charts can be used in conjunction with the method for nonuniform flow presented on Chart 010-2.

2. **Basic Equation.** Chart 224-8 can be used to determine normal depths (y_o) for any circular section. The curves on Chart 224-8 were developed using the equations stated in paragraph 2 of Sheets 610-1 to 610-7. Functions of the area and hydraulic radius, necessary for the solution of the equations, were obtained from published tables[1].

3. Chart 224-9 can be used to determine the critical depth-diameter ratio from which the critical depth can be computed; these curves are based on the critical depth formula[2]

$$Q = CD^{5/2}$$

4. **Application.** The ratio of normal-depth to diameter (y_o/D) for various sections can be determined from Chart 224-8 in the manner described in paragraph 3a, b, and c, Sheets 610-1 to 610-7. The ratio of critical depth to diameter can be determined directly from Chart 224-9 for a given discharge and diameter.

---

[1] H. W. King, Handbook of Hydraulics, 3d ed., New York, N. Y., McGraw-Hill Book Company (1939), tables 100 and 101, p 299.

[2] Ibid., Table 130, p 441.
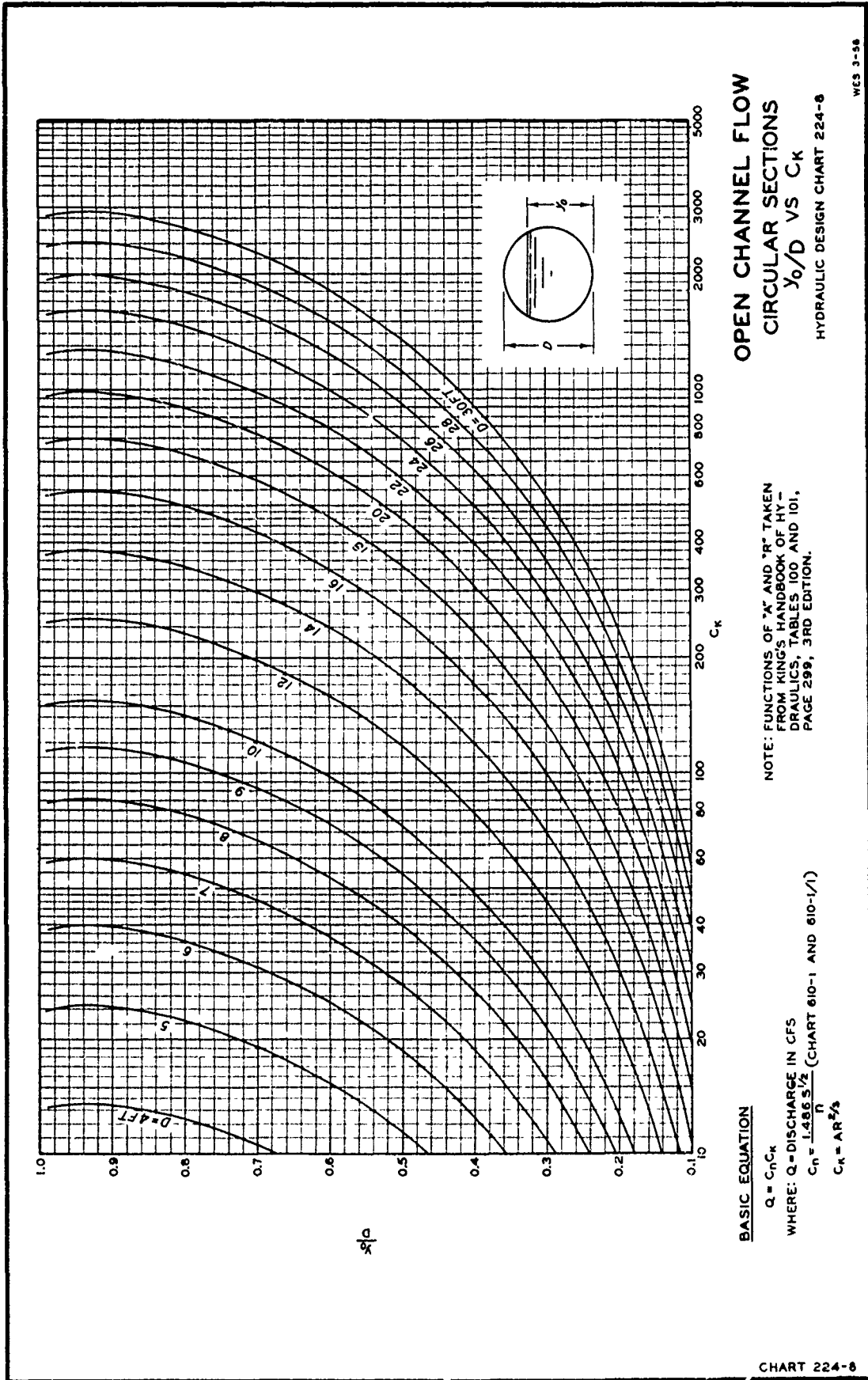
OPEN CHANNEL FLOW

CIRCULAR SECTIONS

Y_0/D VS C_K

HYDRAULIC DESIGN CHART 224-8

WES 3-56

NOTE: FUNCTIONS OF "A" AND "R" TAKEN
FROM KING'S HANDBOOK OF HY-
DRAULICS, TABLES 100 AND 101,
PAGE 299, 3RD EDITION.

BASIC EQUATION

$Q = C_n C_K$

WHERE: Q = DISCHARGE IN CFS

$C_n = \dfrac{1.486 \, S^{1/2}}{n}$ (CHART 610-1 AND 610-1/1)

$C_K = A R^{2/3}$

(y-axis) $\dfrac{y_0}{D}$

(x-axis) C_K

Curve labels: D = 4 FT, 5, 6, 7, 8, 9, 10, 12, 14, 16, 18, 20, 22, 24, 26, 28, D = 30 FT

CHART 224-8

OPEN CHANNEL FLOW
CIRCULAR SECTIONS
CRITICAL DEPTH AND DISCHARGE

HYDRAULIC DESIGN CHART 224-9

WES 3-56

BASIC EQUATION

$Q = CD^{5/2}$

WHERE Q = DISCHARGE IN CFS
       D = DIAMETER IN FT
       C = COEFFICIENT (KING'S HANDBOOK OF HYDRAULICS,
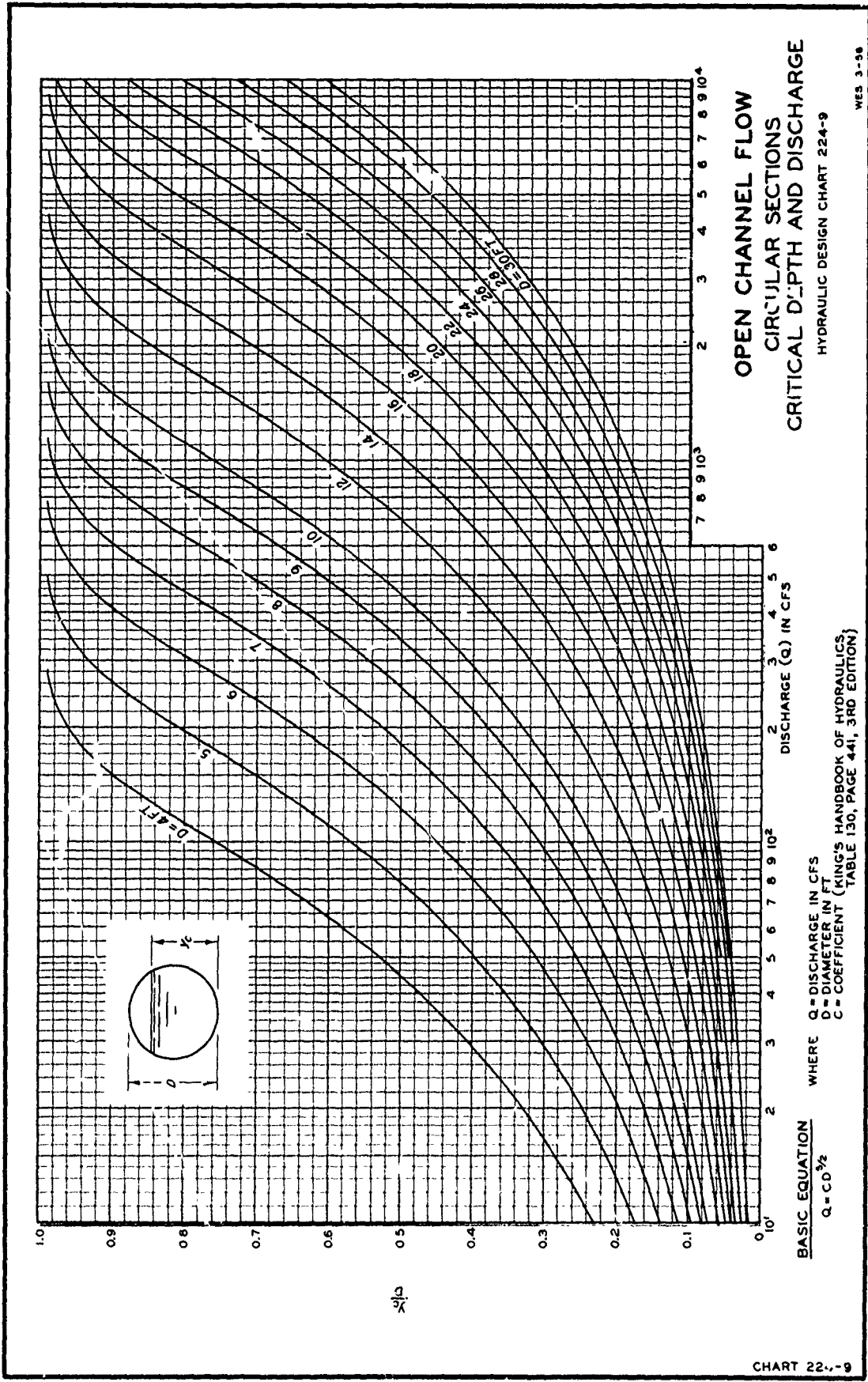   TABLE 130, PAGE 441, 3RD EDITION)

CHART 224-9

HYDRAULIC DESIGN CRITERIA

SHEET 224-10

HORSESHOE CONDUITS

HYDRAULIC ELEMENTS

1. Hydraulic Design Chart 224-10 presents curves of hydraulic elements as computed by the United States Bureau of Reclamation[*] for a standard horseshoe tunnel cross section. This conduit shape is identical with that presented at the bottom of Hydraulic Design Chart 224-2.

2. The flow cross-sectional area (A), water surface width (T), and wetted perimeter (P) can be expressed in terms of y/H, in which y is the central flow depth and H is the central height and width or in terms of the angle θ, which is the slope angle of the lower side arc radius line at the water surface intercept on the lower side arc. Angle θ equals $\sin^{-1}$ (0.5 - y/H). The flow section can be studied in three separate portions:

a. Value y varies from the bottom to the intersection of the lower side arcs, $0 \leq y/H < 0.0885$.

$$\frac{A}{H^2} = \cos^{-1}\left(1 - \frac{y}{H}\right) - \left(1 - \frac{y}{H}\right)\sqrt{\frac{y}{H}\left(2 - \frac{y}{H}\right)}$$

$$\frac{T}{H} = 2\sqrt{\frac{y}{H}\left(2 - \frac{y}{H}\right)}$$

$$\frac{P}{H} = 2\cos^{-1}\left(1 - \frac{y}{H}\right)$$

b. Value y varies from the intersection of the lower side arcs to half full, $0.0885 \leq y/H < 0.5$ or $0 \leq \theta < 0.4242$ rad.

$$\frac{A}{H^2} = 0.4366 - \theta + \frac{1}{2}\sin\theta\left(1 - \sqrt{1 + 8\sin^2\frac{\theta}{2} - 4\sin^2\theta}\right)$$

---

[*] Hu, Walter W., "Hydraulic Elements for the USBR Standard Horseshoe Tunnel," Transportation Engineering Journal of ASCE, Vol 99, No. TE4, Nov. 1973.

$$\frac{T}{H} = \sqrt{1 + 8 \sin^2 \frac{\theta}{2} - 4 \sin^2 \theta}$$

$$\frac{P}{H} = 1.6962 - 2\theta$$

<u>c</u>. Value y varies from half full to full, $0.5 \le y/H \le 1.0$.

$$\frac{A}{H^2} = 0.8293 - \frac{1}{4} \cos^{-1}\left(2\frac{y}{H} - 1\right) + \left(\frac{y}{H} - 0.5\right)\sqrt{\frac{y}{H}\left(1 - \frac{y}{H}\right)}$$

$$\frac{T}{H} = 2\sqrt{\frac{y}{H}\left(1 - \frac{y}{H}\right)}$$

$$\frac{P}{H} = 3.2670 - \cos^{-1}\left(2\frac{y}{H} - 1\right)$$

3. Other hydraulic elements included in Chart 224-10 are the hydraulic radius, $R = A/P$; hydraulic depth, $D = A/T$; section factor, $Z = A\sqrt{D}$; conveyance of Manning's formula, $K = 1.486\ AR^{2/3}$; and the critical slope for a given normal depth, S_{cn} . All are expressed as dimensionless ratios with respect to H except S_{cn} , which is expressed in the form

$S_{cn}/n^2 = 14.57 P^{4/3}/A^{1/3}T$, where n is the Manning's roughness.

CROSS—SECTIONAL GEOMETRY

$\dfrac{S_{cn}}{n^2}$

$\dfrac{P}{H}$

$\dfrac{Z}{H^{3/2}}$

$\dfrac{D}{H}$

$\dfrac{A}{H^2}$

$\dfrac{T}{H}$

$\dfrac{K}{H^{8/3}}$

$\dfrac{R}{H}$

$\dfrac{y}{H}$

LEGEND

A=CROSS-SECTIONAL AREA
D=HYDRAULIC DEPTH
H=CENTRAL HEIGHT AND WIDTH
K=CONVEYANCE OF MANNING'S FORMULA
n=MANNING'S ROUGHNESS
P=WETTED PERIMETER
R=HYDRAULIC RADIUS

S_{cn}=CRITICAL SLOPE FOR GIVEN NORMAL DEPTH
T =FREE WATER SURFACE WIDTH
y =CENTRAL FLOW DEPTH
Z =SECTION FACTOR
θ =SLOPE ANGLE OF LOWER SIDE ARC RADIUS LINE AT WATER SURFACE INTERCEPT ON SIDE ARC

HYDRAULIC ELEMENTS
HORSESHOE CONDUITS
HYDRAULIC DESIGN CHART 224—10

WES 5—75

CIRCULAR EXIT PORTAL

PRESSURE GRADIENTS

1. The elevation of the intersection of the pressure gradient with the plane of the exit portal is a factor in the computation of the discharge capacity of a flood-control conduit. The use of the center of the portal as the position of the pressure gradient yields fairly accurate discharge determination for unconstricted flow where the conduit is relatively small in relation to the design head. However, a closer determination of the pressure gradient intersection is pertinent to the discharge-capacity design where the conduit size is large in relation to the head.

2. **Theory.** A number of investigations have been made of velocity and pressure distribution in the vicinity of exit portals. Each investigator concluded that the intersection of the pressure gradient with the plane of the exit portal did not coincide with the center of the portal for a free discharging jet. D. Rueda-Briceno[2] determined the location of the pressure gradient as a function of Froude's number.

3. **Basic Data.** HDC 225-1 shows the relative position of the pressure gradient at an exit portal of circular section (Y_p/D) with respect to Froude's number (F). The plotted data show that the position of the pressure gradient varies with the support of the jet downstream from the portal plane as well as with Froude's number. The geometry of the jet support for the various investigations is summarized below:

    <u>a</u>. <u>State University of Iowa (Rueda-Briceno).</u>[2] Jet discharging into air.

    <u>b</u>. <u>Denison model.</u>[4] Jet discharging into transition having level invert and sidewalls flared 1 on 5.

    <u>c</u>. <u>Denison prototype.</u>[5] Jet discharging into transition having level invert and parallel sidewalls for 50 ft followed by 1-on-5 flared walls.

    <u>d</u>. <u>Garrison model.</u>[6] Jet discharging into transition having parabolic invert and sidewalls flared 8 on 35.

    <u>e</u>. <u>Youghiogheny model.</u>[1] Jet discharging into transition having 1-on-20 sloping invert and sidewalls flared 2 on 3 followed by elliptical curves.

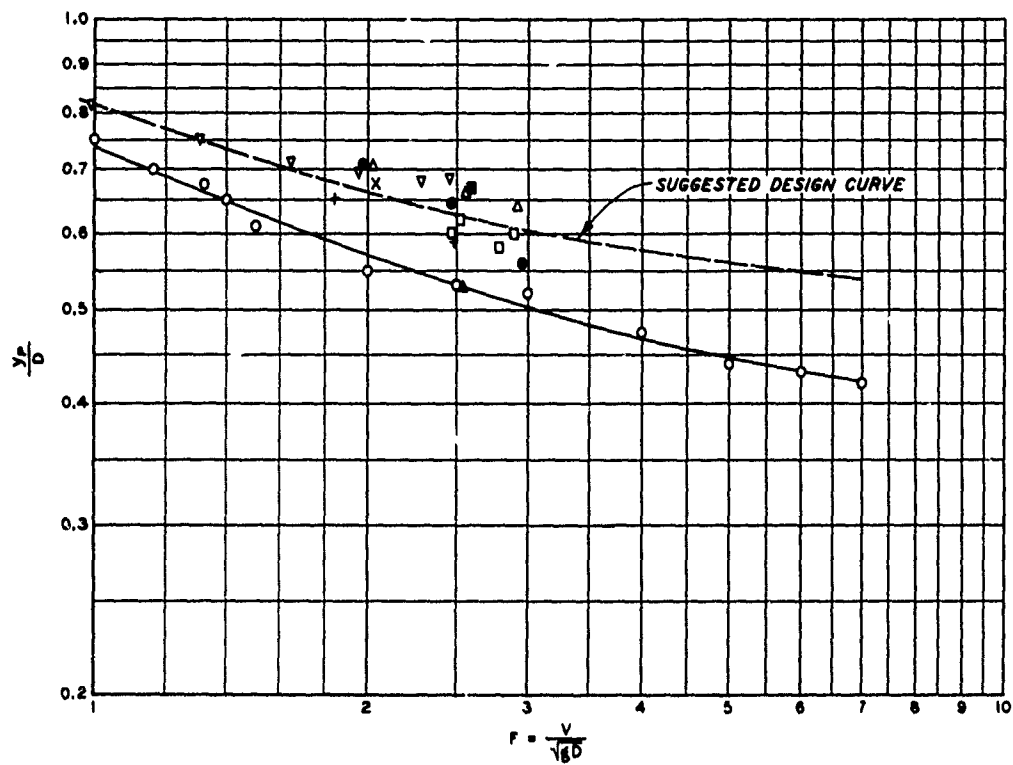   <u>f</u>. <u>Enid prototype.</u>[7] Jet discharging into transition having

parabolic invert and sidewalls flared with 100-ft radius
for 20 ft followed by flare of 1 on 4.5.

    g. <u>Fort Randall model and prototype.</u>[8,9] Jet discharging into
primary stilling basin having level invert and sidewalls
flared 1 on 6. The 500-ft-long primary basin is separated
from the secondary basin by a 25-ft-high ogee weir.

    h. <u>Oahe prototype.</u>[3] Jet discharging into transition having
parabolic invert and sidewalls flared 1 on 7.42.

    4. <u>Application.</u> The suggested design curve in HDC 225-1 applies to
circular conduits with some form of jet support below the exit portal. The
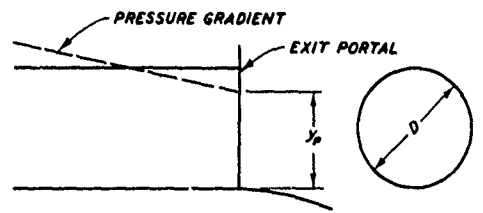solid-line curve is applicable only to exit portals having a free-falling
jet.

    5. <u>References.</u>

(1) Carnegie Institute of Technology, <u>Report on Hydraulic Model Tests of</u>
<u>Spillway and Outlet Works of Youghiogheny River Dam, Confluence,</u>
<u>Pennsylvania.</u> Hydraulic Laboratory, Pittsburgh, Pa., March 1941.

(2) Rueda-Briceno, D., <u>Pressure Conditions at the Outlet of a Pipe.</u>
State University of Iowa Master's Thesis, February 1954.

(3) U. S. Army Engineer District, Omaha, <u>Oahe Outlet Tunnel Prototype</u>
<u>Tests.</u> (Unpublished data.)

(4) U. S. Army Engineer Waterways Experiment Station, CE, <u>Hydraulic Model</u>
<u>Studies of the Control Structures for the Denison Dam, Red River.</u>
Technical Memorandum No. 161-1, Vicksburg, Miss., April 1940.

(5) _____, <u>Pressure and Air Demand Tests in Flood-Control Conduit,</u>
<u>Denison Dam, Red River, Oklahoma and Texas.</u> Miscellaneous Paper No.
2-31, Vicksburg, Miss., April 1953.

(6) _____, <u>Outlet Works and Spillway for Garrison Dam, Missouri</u>
<u>River, North Dakota; Hydraulic Model Investigation.</u> Technical
Memorandum No. 2-431, Vicksburg, Miss., March 1956.

(7) _____, <u>Prototype Hydraulic Tests of Flood-Control Conduit, Enid</u>
<u>Dam, Yocona River, Mississippi.</u> Technical Report No. 2-510, Vicksburg,
Miss., June 1959.

(8) _____, <u>Spillway and Outlet Works, Fort Randall Dam, Missouri</u>
<u>River, South Dakota; Hydraulic Model Investigation.</u> Technical
Report No. 2-528, Vicksburg, Miss., October 1959.

(9) _____, <u>Flow Characteristics in Flood-Control Tunnel 10, Fort</u>
<u>Randall Dam, Missouri River, South Dakota; Hydraulic Prototype Tests.</u>
Technical Report No. 2-626, Vicksburg, Miss., June 1963.

SUGGESTED DESIGN CURVE

$F = \dfrac{V}{\sqrt{gD}}$

$\dfrac{y_P}{D}$

PRESSURE GRADIENT

EXIT PORTAL

y_P

D

EXIT PORTALS
CIRCULAR CONDUITS
F VS y_P/D

HYDRAULIC DESIGN CHART 225-1

REVISED 1-64   REVISED 3-58   WES 9-54

BEND LOSS COEFFICIENTS

1. The purpose of this chart is for use in the design of flood-control conduits and tunnels. Most of the research work which has been conducted on bend loss is based on right-angle bends and is applicable principally to the problems of mechanical engineering design. Flood-control conduits are usually designed with a deflection angle (α) much smaller than 90 degrees. The work of Wasielewski[1] at Munich was applicable to a wide range of deflection angles and ratio of bend radii to pipe diameters (r/D). These experiments formed the basis of the curves on the attached chart.

2. The broken lines are suggested design curves formulated from the Wasielewski curves shown as solid lines. The bend loss coefficient (K_b) represents the loss in terms of velocity head caused by the bend only, excluding the friction loss within the bend. The experiments of Wasielewski employed approximately 55 diameters of pipe and should represent nearly complete decay of the turbulence caused by the bend. The Reynolds number for these tests was 225,000.

3. The maximum angle tested by Wasielewski was 75 degrees. His graph includes the data obtained by Hofmann[2] for losses caused by 90° bends. The design curves were adjusted by the use of the 90° curve shown in the upper right-hand corner of the chart. This curve also serves as an interpolation curve for the design curves on the chart. Although the coefficient K_b approaches zero very slowly as the r/D ratio becomes large, it was suggested by Professor J. S. McNown of State University of Iowa that a logarithmic function may fit the data. The equation shown produces a good fit for 90° with π used in the constants as indicated.

(1) Rudolph Wasielewski, "Loss in Smooth Pipe Bends with Bend Angles Less than 90°" (In German), Proceedings of the Hydraulic Institute of the Technical College of Munich, Issue 5 (1932), pp. 53-67.

(2) A. Hofmann, "Loss in 90 Degree Pipe Bends of Constant Circular Cross-Section," Transactions of the Hydraulic Institute of the Munich Technical University, Bulletin 3 (1929). Published in 1935 by the American Society of Mechanical Engineers, pp. 29-41.

4. The interpolation curve for $90°$ was developed independently on the basis of the Wasielewski data and was then compared with Anderson's and Straub's adjusted curve[3]. The two curves show a fair agreement. A careful analysis of Waterways Experiment Station data[4] for r/D = 1.5 and α = $90°$ gives a good verification of the design curve for that ratio. The experimental data by Beij[5] has been included on the graph. Dr. Beij has informed the Office, Chief of Engineers, that he considers his data applicable to rough pipe.

5. It was found further that the introduction of α in the equation as indicated, produced a family of curves which embraces the Wasielewski data fairly well. More experimental information is needed for the range of r/D greater than 4 and α less than $45°$. These data indicate the bend loss only and estimated friction for the length of bend should be added.
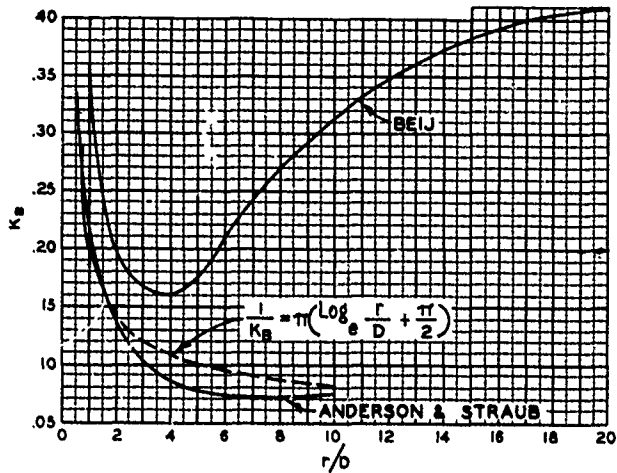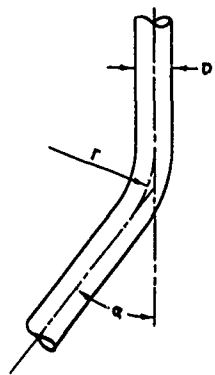
6. The data from the various experimenters on $90°$ bends show wide discrepancies. However, bend losses are usually small compared to friction losses in tunnels or conduits of substantial length. In the interest of conservatism, it is recommended that safety factors be applied to the dashed curves. The values on the graph should be increased 25% to 50% in the design for hydraulic capacity. The values indicated on the graph should be decreased by a comparable percentage in determining the maximum velocity entering a stilling basin at the downstream end of a tunnel. The selection of the actual percentage between the range given would depend upon the relative importance of hydraulic capacity and the effect upon cost.

---

[3] A. G. Anderson and L. G. Straub, "Hydraulics of Conduit Bends," St. Anthony Falls Hydraulic Laboratory Bulletin No. 1 (Minneapolis, Minnesota, December 1948).

[4] "Experiments to Determine the Pressure Loss in Pipe Bends," Waterways Experiment Station, Technical Memorandum No. 21-1 (Vicksburg, Miss., January 1932).

[5] K. Hilding Beij, "Pressure Losses for Fluid Flow in $90°$ Pipe Bends," Research Paper RP 1110, Journal of Research, National Bureau of Standards, Vol. 21 (July 1938).

K_B VS r/D FOR 90° BENDS

$$\frac{1}{K_B} = \pi \left(\log_e \frac{r}{D} + \frac{\pi}{2} \right)$$

BEIJ

ANDERSON & STRAUB

WASIELEWSKI CURVES
☐ T.M. 21.1-U.S. WES
SUGGESTED DESIGN CURVES

$$\frac{1}{K_B} = \frac{\pi^2}{2\alpha} \left(\log_e \frac{r}{D} + \alpha \right)$$

α = DEFLECTION ANGLE IN RADIANS

BEND COEFFICIENT K_B

DEFLECTION ANGLE α
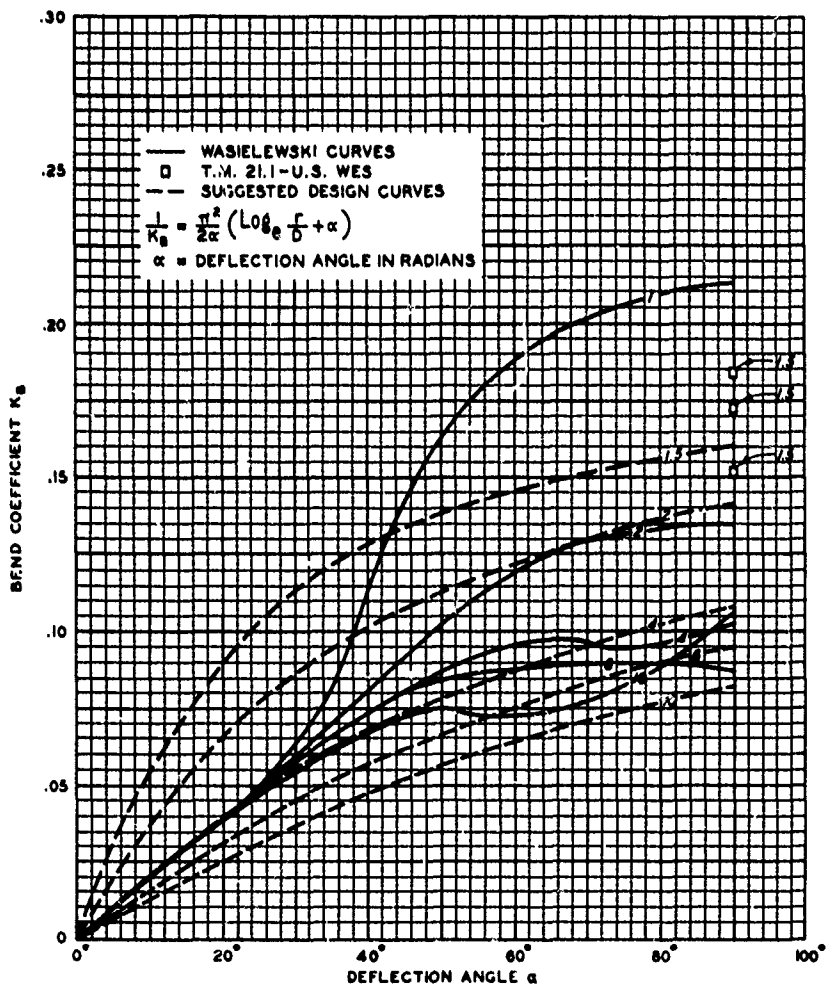
BASIC EQUATION = $h_L = K_B V^2/2g$

h_L = HEAD LOSS DUE TO BEND
K_B = BEND LOSS COEFFICIENT
V = VELOCITY IN PIPE

NOTE: FIGURES ON GRAPH INDICATE r/D RATIO.

BEND-LOSS COEFFICIENTS

HYDRAULIC DESIGN CHART 228-1

REVISED 8-58   WES 4-1-52

HYDRAULIC DESIGN CRITERIA

SHEETS 228-2 TO 228-2/1

MITER BENDS

BEND LOSS COEFFICIENTS

1. Hydraulic Design Chart 228-2 and 228-2/1 show bend loss coefficients (K_B) versus Reynolds number and deflection angle, respectively. The charts are based on laboratory tests made at Munich, Germany[1], and tests made on 90-degree bends at the Waterways Experiment Station[2]. The broken lines on Chart 228-2 are suggested design curves and are not the experimenters' interpretations. The bend loss coefficient (K_B) represents the loss in terms of velocity head caused by the bend only, excluding the friction loss within the bend.

2. Chart 228-2/1 is a plot of bend loss coefficients and deflection angles for three Reynolds numbers. The curves on this chart were used to establish the suggested design curves on Chart 228-2. The curves have been extended to assist the engineer in determining loss coefficients for smaller deflection angles.

[1] Hans Kirchbach, "Loss of Energy in Miter Bends," and Werner Schubart, "Energy Loss in Smooth and Rough Surfaced Bends and Curves in Pipe Lines," Transactions of the Hydraulic Institute of the Munich Tech. Univ. Bulletin 3, translation published by ASME, 1935.

[2] "Experiments To Determine the Pressure Loss in Pipe Bends," Waterways Experiment Station, Technical Memorandum No. 21-1, Vicksburg, Miss., January 1932.

VALUES OF (VD) FOR WATER AT 60°F
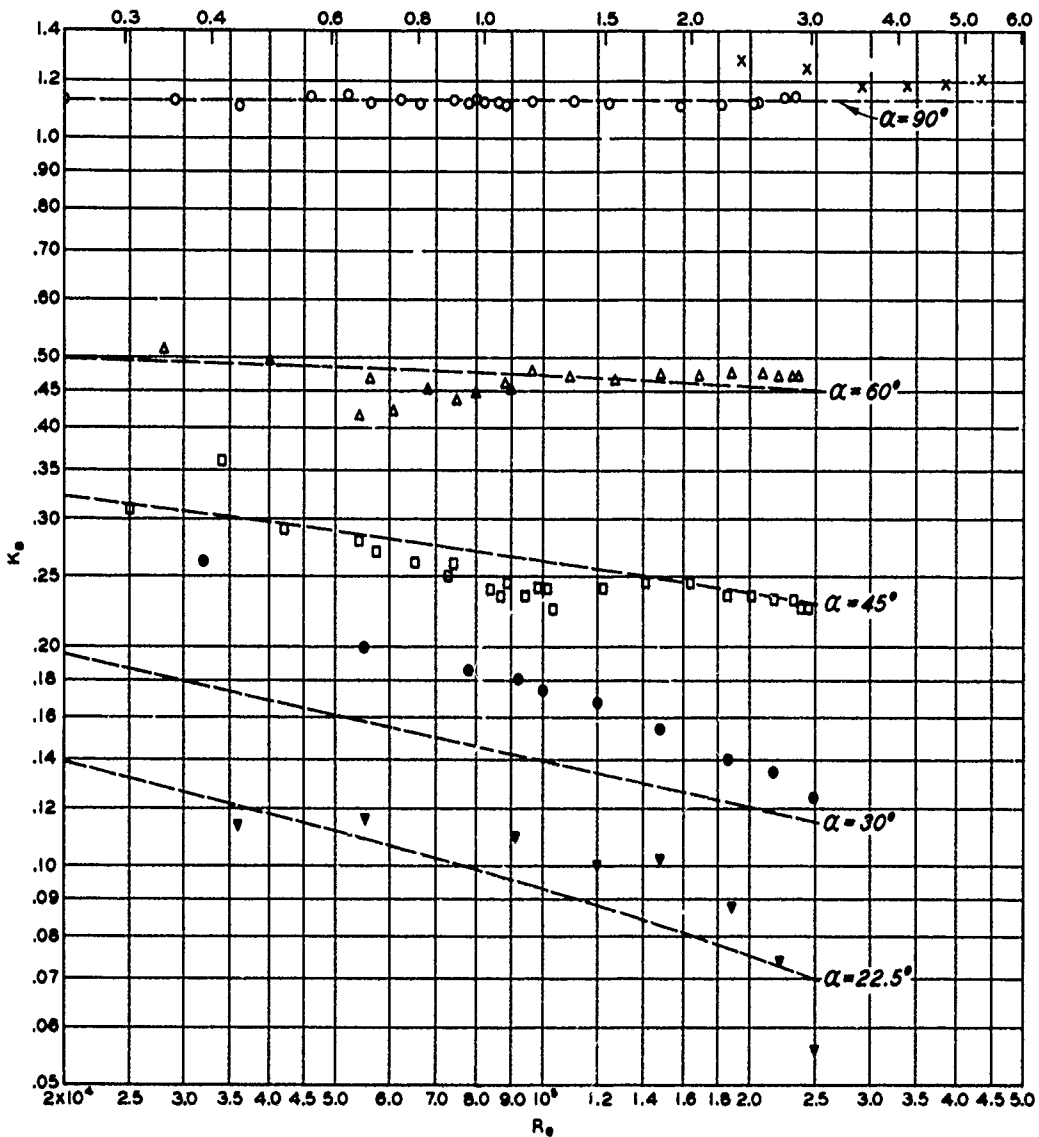
BASIC EQUATION

$$K_B = \frac{h_L}{V^2/2g}$$

WHERE K_B = BEND LOSS COEFFICIENT
        h_L = HEAD LOSS DUE TO BEND

LEGEND

x	WES DATA, $\alpha = 90°$
o	MUNICH DATA, $\alpha = 90°$
△	MUNICH DATA, $\alpha = 60°$
□	MUNICH DATA, $\alpha = 45°$
●	MUNICH DATA, $\alpha = 30°$
▼	MUNICH DATA, $\alpha = 22.5°$
—	SUGGESTED DESIGN CURVES

NOTE: WES DATA FROM 8" PIPE.
      MUNICH DATA FROM 1.69" PIPE.

**SINGLE MITER
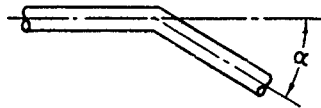BEND LOSS COEFFICIENTS
K_B VS R_e**

HYDRAULIC DESIGN CHART 228-2

K_B vs α chart

BASIC EQUATION

$$K_B = \frac{h_L}{V^2/2g}$$

WHERE K_B = BEND LOSS COEFFICIENT
h_L = HEAD LOSS DUE TO BEND

SINGLE MITER
BEND LOSS COEFFICIENTS
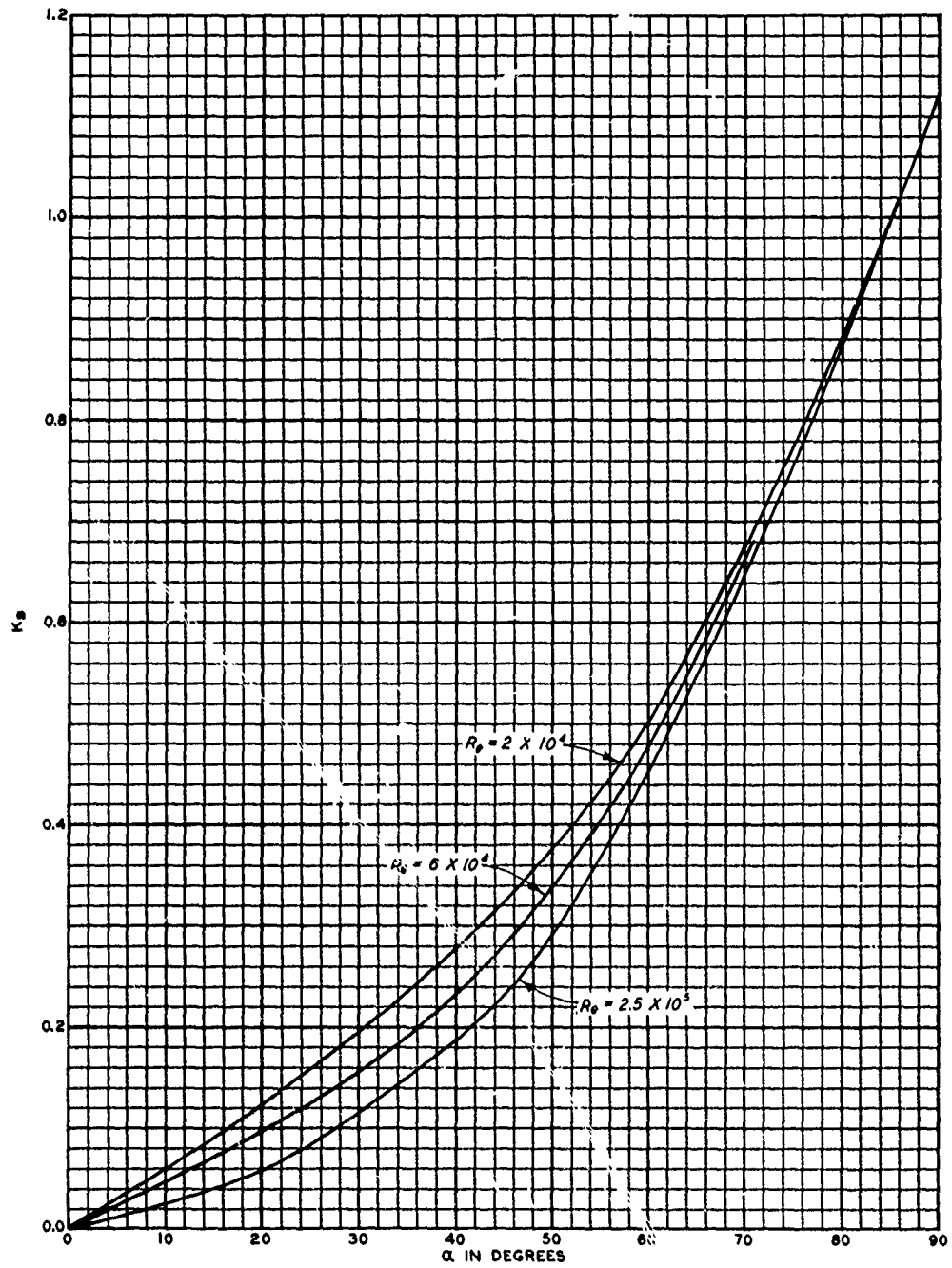K_B VS α

HYDRAULIC DESIGN CHART 228-2/1

WES 3-55

HYDRAULIC DESIGN CRITERIA

SHEET 228-3

PRESSURE FLOW

PIPE BENDS

MINIMUM PRESSURE

1. Flow around pipe bends results in a velocity acceleration along the inside of the bend accompanied by a local pressure reduction. This pressure reduction may be sufficient to result in cavitation in low flow and water supply pipes conducting discharges from reservoirs. Hydraulic Design Chart 228-3 should serve for estimating minimum pressures in standard pipe bends.

2. **Basic Data.** Available experimental data on minimum pressures in pipe bends are limited to those on 6-in. pipe bends of 45 to 180 deg by Yarnell.[1] These data show that the minimum pressure occurs 22.5 deg from the point of curvature compared with its occurrence 45 deg from the point of curvature for rectangular section conduits (HDC Sheets and Charts 534-2 and 534-2/1). The analytical procedure suggested by McPherson and Strausser[2] for determining the magnitude of the minimum pressure in a circular bend of rectangular conduits has been applied to pipe bends. The theoretical curve, Yarnell's data, and points computed from elbow meter data compiled by Taylor and McPherson[3] are shown in Chart 228-3. The elbow meter data are based on studies by Lansford,[4] Addison,[5] and Taylor and McPherson[3] (Lehigh data). Yarnell's[1] study showed that the pressure 45 deg from the point of curvature is only slightly higher than the minimum pressure that occurs at the 22.5-deg point. This is confirmed by the Lehigh data points in Chart 228-3. Data for both the 22.5- and 45-deg points correlate with the theoretical curve as shown in the chart. The data cover a range of pipe diameters from 4 to 12 in. and indicate a range of Reynolds numbers (R_e) of 10^4 to 10^5.

3. **Application.** The minimum bend pressure can be computed from the equation

$$C_p = \frac{H - H_i}{\frac{V^2}{2g}}$$

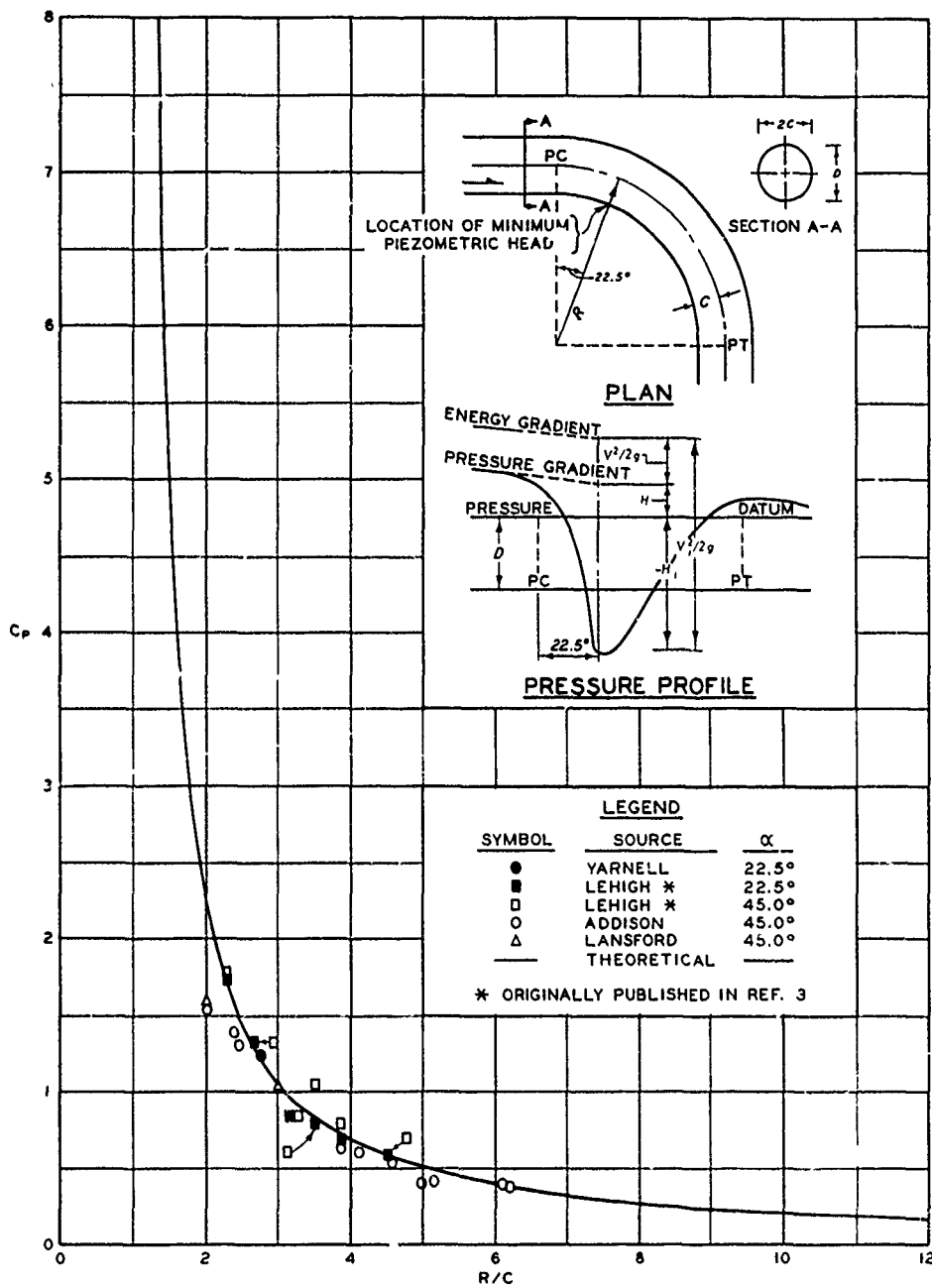The terms in the equation are defined in Chart 228-3. The equation for the theoretical curve shown in Chart 228-3 is given in Sheet 534-2.

4. The curve in Chart 228-3 can be used to estimate the minimum steady pressure in standard pipe bends of 45 to 180 deg. Cavitation occurs when the instantaneous pressure at any point in a flowing liquid drops to vapor pressure. Turbulence in flow causes local pressure

fluctuation. Therefore, an estimate should be made of the maximum expected fluctuation from the minimum computed steady pressure. A procedure for estimating the necessary average pressure or the permissible average velocity to prevent cavitation is given in paragraph 4 of Sheets 534-2 and 534-2/1. The sample computation shown in Chart 534-2/1 for rectangular conduits is also applicable to pipe bends.

5. References.

(1) U. S. Department of Agriculture, Flow of Water Through 6-Inch Pipe Bends, by D. L. Yarnell. Technical Bulletin No. 577, Washington, D. C. October 1937.

(2) McPherson, M. B., and Strausser, H. S., "Minimum pressures in rectangular bends." Proceedings, ASCE, vol 81, Separate Paper No. 747 (July 1955).

(3) Taylor, D. C., and McPherson, M. B., "Elbow meter performance." American Water Works Association Journal, vol 46, No. 11 (November 1954), pp 1087-1095. (Copyrighted by the American Water Works Association, Inc., N. Y.)

(4) Lansford, W. M., The Use of an Elbow in a Pipe Line for Determining the Rate of Flow in the Pipe. Bulletin No. 289, Engineering Experimental Station, University of Illinois, Urbana, December 1936.

(5) Addison, H., "The use of bends as flow meters." Engineering, vol 145 (4 March 1938), pp 227-229 (25 March 1938), p 324.

PLAN

PRESSURE PROFILE

LEGEND

SYMBOL	SOURCE	α
●	YARNELL	22.5°
■	LEHIGH *	22.5°
□	LEHIGH *	45.0°
○	ADDISON	45.0°
△	LANSFORD	45.0°
—	THEORETICAL	—

* ORIGINALLY PUBLISHED IN REF. 3

EQUATIONS

$$H + \frac{V^2}{2g} = H_1 + \frac{V_1^2}{2g}, \qquad \frac{H - H_1}{\frac{V^2}{2g}} = C_p$$

NOTE   α IS BEND ANGLE TO POINT OF MEASUREMENT.

WHERE

H = PIEZOMETRIC HEAD FROM PRESSURE GRADIENT EXTENSION, FT

V = AVERAGE VELOCITY, FT PER SEC

g = ACCELERATION, GRAVITATIONAL, FT PER SEC²

H_1 = MINIMUM PIEZOMETRIC HEAD, FT

V_1 = VELOCITY AT LOCATION OF H_1, FT PER SEC

C_p = PRESSURE DROP PARAMETER

PRESSURE FLOW PIPE BENDS

MINIMUM PRESSURE

HYDRAULIC DESIGN CHART 228-3

HYDRAULIC DESIGN CRITERIA

SHEET 228-4

IN-LINE CONICAL TRANSITIONS

LOSS COEFFICIENTS

1. **Purpose.** Hydraulic Design Chart (HDC) 228-4 presents coefficients for computing head losses through in-line expanding and contracting conical transitions frequently used in penstock and water supply design. This chart can also be used as a guide in estimating coefficients for computing head losses in flood control tunnel interior transitions.

2. **Background.**

   a. **Expansions.** Extensive data on energy losses in conical expansions were published by Gibson[1] in 1912. Although additional data were published by Peters[2] in 1934, design guidance given in Rouse[3] was limited to the earlier work by Gibson. Kalinske[4] and Robertson and Ross[5] also have investigated flow characteristics in conical diffusers. However, it was 1964 before additional data for head loss coefficients were published by Huang.[6] His study included both smooth and artificially roughened pipe. Reynolds numbers tested were from 0.3 to 1.5×10^5. Huang found very little difference in loss coefficients for smooth and rough pipe flow and no effect of Reynolds number on losses for in-line transitions.

   b. **Contractions.** Coefficient data for head losses in conical contractions are appreciably more limited than for expansions. The only known available study is that by Levin[7] in 1970. Levin's data are for diameter ratios of D_2/D_1 of 1.2 to 2.1 and were made at Reynolds numbers of 1×10^5 to 1×10^6.

   c. **Other shapes.** Loss coefficient curves for expansion transitions of many other cross-section shapes and installation locations have been published by Miller.[8]

3. **Theory.** Loss coefficient curves for conical expansions published by Rouse[3] are based on Gibson's data and described by equation 1.

$$K = \frac{2gH_L}{(V_1 - V_2)^2} \tag{1}$$

Comparable loss coefficients published by Huang, based on Gibson's, Peter's, and his own data are described by equation 2.

$$K_c = \frac{2gH_L}{V_1^2}$$ (2)

Loss coefficients published by Levin for conical contractions are also described by equation 2. In these equations, K and K_c are loss coefficients, H_L is the head loss effected by the transitions, V_1 is the average velocity in the smaller conduit (either upstream or downstream, respectively, depending upon whether the flow is expanding or contracting), V_2 is the average velocity in the larger conduit, and g is the acceleration of gravity.

    4. Coefficient values from Rouse's plots of Gibson's data were transposed into terms comparable to Huang's by use of the following equation:

$$K_c = K \left[1 - \left(\frac{D_1}{D_2} \right)^2 \right]^2$$ (3)

where D_1 is the smaller conduit diameter and D_2 is the larger conduit diameter.
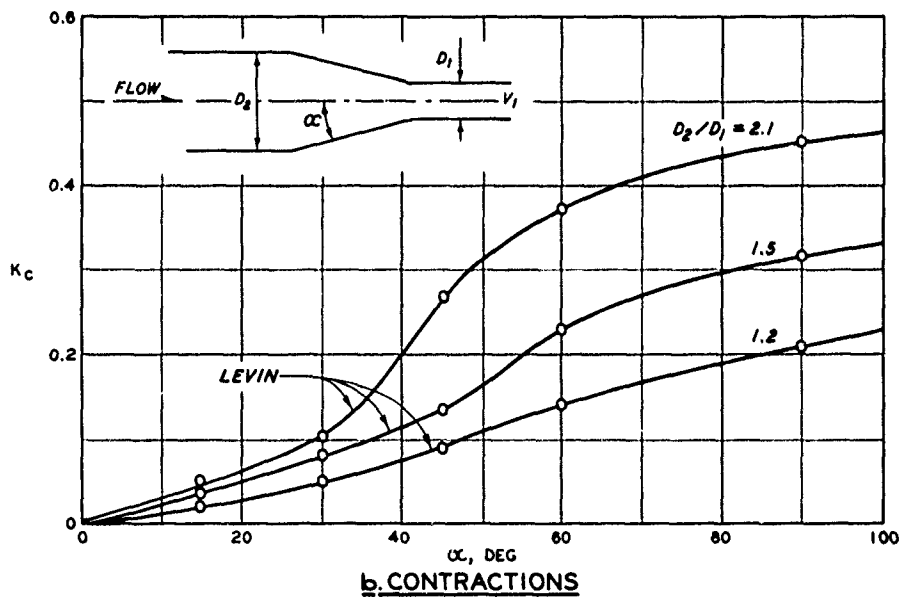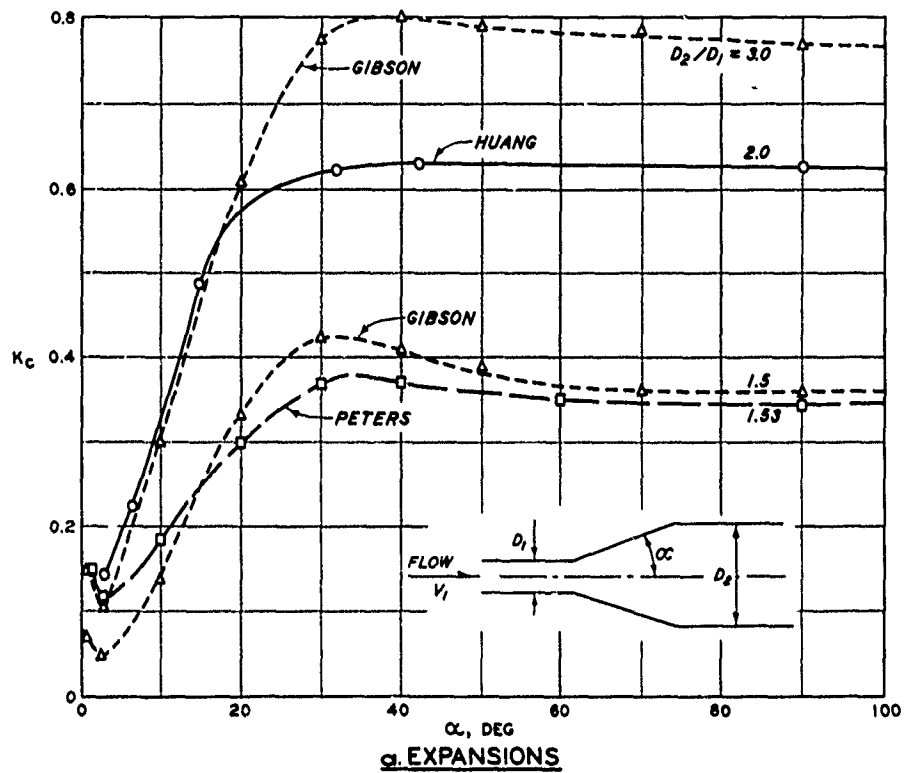
    5. <u>Design Criteria.</u>

        <u>a</u>. <u>Expansion coefficients.</u> Comparable plots of expansion loss coefficients based on tests by Gibson, Peters, and Huang are given in HDC 228-4a.

        <u>b</u>. <u>Contraction coefficients.</u> Contraction loss coefficients reproduced from Levin's plots are given in HDC 228-4b.

    6. <u>References.</u>

(1)   Gibson, A. H., "The conversion of kinetic to potential energy in the flow of water through passages having divergent boundaries." <u>Engineering,</u> vol 93 (1912), p 205.

(2)   Peters, H., <u>Conversion of Energy in Cross-Sectional Divergences Under Different Conditions of Inflow.</u> Technical Memorandum No. 737 (Translation), National Advisory Committee for Aeronautics, Washington, D. C., March 1934.

(3)   Rouse, H., <u>Engineering Hydraulics.</u> John Wiley and Sons, Inc., New York, N. Y., 1950, p 418.

(4) Kalinske, A. A., "Conversion of kinetic to potential energy in flow expansions." <u>Transactions, American Society of Civil Engineers,</u> vol 111 (1946), pp 355-374.

(5) Robertson, J. M. and Ross, D., <u>Water Tunnel Diffuser Flow Studies.</u> Parts I and II, Ordnance Research Laboratory, Pennsylvania State College, State College, Pa., 1949.

(6) Huang, T. T., <u>Energy Losses in Pipe Expansions.</u> Master of Science Dissertation, State University of Iowa, Iowa City, Iowa, 1964.

(7) U. S. Army Engineer Waterways Experiment Station, CE, <u>Study of Peculiar Head Losses in Conical Convergences,</u> by L. Levin. Translation No. 73-3, Vicksburg, Miss., January 1973.

(8) Miller, D. S., <u>Internal Flow, A Guide to Losses in Pipes and Duct Systems.</u> British Hydromechanics Research Association, Cranfield, Bedford, England, 1971.

a. EXPANSIONS

b. CONTRACTIONS

BASIC EQUATION

$$K_C = 2gH_L / V_1^2$$

WHERE:
- H_L = HEAD LOSS, FT
- g = ACCELERATION OF GRAVITY, FT/SEC^2
- V_1 = AVERAGE VELOCITY IN THE SMALLER CONDUIT, FPS

CONICAL TRANSITIONS
LOSS COEFFICIENTS

HYDRAULIC DESIGN CHART 228-4

WES 7-73

HYDRAULIC DESIGN CRITERIA

SHEET 228-5

PRESSURE CHANGE COEFFICIENTS

AND JUNCTION BOX HEAD LOSSES

FOR IN-LINE CIRCULAR CONDUITS

1. **Purpose.** Junction boxes are used extensively in the design of pressure storm drain systems where lateral drains flow into main-line drains. They are also included in long, continuous drains to provide ready access for conduit inspection and maintenance. In small, flow-control outlet works they have been used as wet wells for control gates. Hydraulic Design Chart (HDC) 228-5 presents design information on pressure change coefficients for junction boxes with in-line circular conduits. HDC 228-5a gives pressure change coefficients for junction boxes effecting expansions and contractions. HDC 228-5b shows the effects of box geometry on pressure change coefficient. A procedure for using these pressure change coefficients to compute junction box head losses is given in paragraph 5 below.

2. **Background.** Arbitrary loss coefficients were used for the design of junction boxes in storm drain systems for many years. In 1958 Sangster, et al.,[1] published the results of the first comprehensive hydraulic study on junction boxes for storm drain systems. In 1959 they published a selected summary of the basic tests.[2] The published reports also give design criteria applicable to multiple inflow junction boxes and to storm drain inlets.

3. **Theory.** Sangster applied the momentum theory to flows through junction boxes and developed the following equations describing pressure changes across a junction box with in-line conduits.

    <u>a</u>. **Expansions.**

$$K = 2 \left[1 - \left(\frac{D_1}{D_2} \right)^2 \right] \tag{1}$$

    <u>b</u>. **Contractions.**

$$K = 1 - \left(\frac{D_1}{D_2} \right)^4 + \left(\frac{1}{C_c} - 1 \right)^2 \tag{2}$$

where

$$K = \text{pressure change coefficient}$$
$$D_1 = \text{downstream conduit diameter, ft}$$
$$D_2 = \text{upstream conduit diameter, ft}$$
$$C_c = \text{downstream coefficient value for abrupt contraction according to Rouse[3]}$$

4. **Experimental Results.** Experimental studies were undertaken by Sangster to evaluate the effects of junction box geometry on the pressure change coefficient K. In each test the upstream and downstream friction pressure gradients were extended to the center of the junction box. The difference between the extended pressure gradients was divided by the velocity head in the downstream conduit to obtain the pressure change coefficient K. HDC 228-5a shows that K is a function of ratio of the diameters of the upstream and downstream conduits and that the junction box width has little effect on the coefficient value. HDC 228-5b shows the effects of junction box shape on pressure changes for in-line conduits of equal size. These plotted data show that for large ratios of b/D_2, pressure change coefficients up to 0.25 were obtained.

5. **Application.** The pressure change H across the junction box can be computed using the following equation:

$$H = K \left(\frac{V_1^2}{2g} \right) \tag{3}$$

where

$$V_1 = \text{downstream conduit velocity, fps}$$
$$g = \text{acceleration of gravity, ft/sec}^2$$

The head loss H_L across the junction box can be computed by use of the Bernoulli equation as follows:

$$H_L = H + \frac{V_2^2 - V_1^2}{2g} \tag{4}$$

where
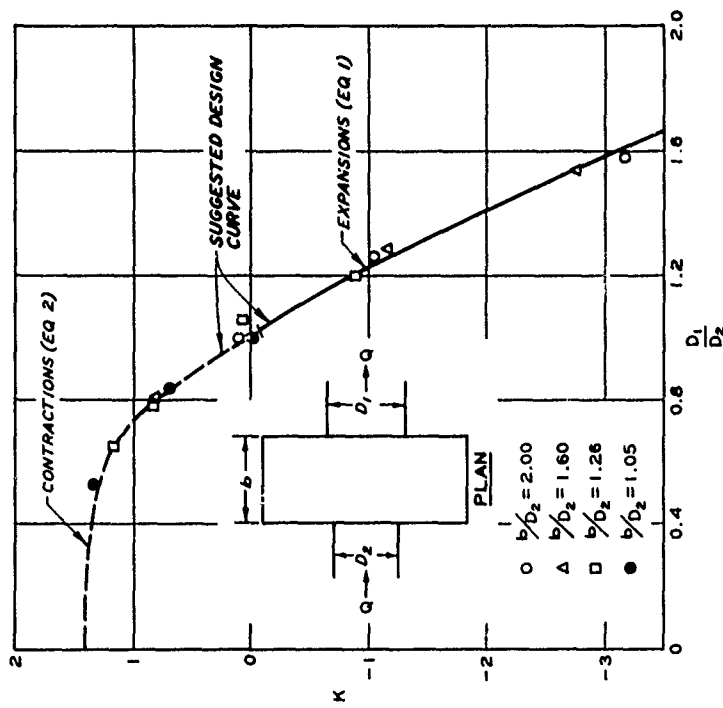
$$V_2 = \text{velocity in the upstream conduit, fps}$$

6. **References.**

(1)   Sangster, W. M. et al., Pressure Changes at Storm Drain Junctions. Engineering Series Bulletin No. 41, vol 59, No. 35, University of Missouri, Columbia, Mo., 1958.

(2)   Sangster, W. M. et al., "Pressure changes at open junctions in conduits." *Journal of the Hydraulics Division, American Society of Civil Engineers,* vol 85 (June 1959), pp 13-42.

(3)   Rouse, H., *Engineering Hydraulics.* John Wiley and Sons, Inc., New York, N. Y., 1950, p 34.

SQUARE BOX □ **RECTANGULAR BOX** △ **RECTANGULAR 90X RE-ENTRANT OUTLET** ▽ **ROUND BOX** ○

$\dfrac{D_1}{D_2} = 1$

NOTE: SYMBOLS DENOTE TWO—PIPE SYSTEM.

SUGGESTED DESIGN CURVE

b. EQUAL SIZE CONDUITS

$\dfrac{b}{D_2}$

K

---

a. TWO CONDUITS IN-LINE

CONTRACTIONS (EQ 2)

SUGGESTED DESIGN CURVE

EXPANSIONS (EQ 1)

$\dfrac{D_1}{D_2}$

K

PLAN

○ $b/D_2 = 2.00$
△ $b/D_2 = 1.60$
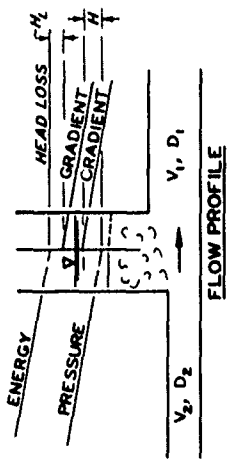□ $b/D_2 = 1.26$
● $b/D_2 = 1.05$

BASIC EQUATION

$$K = 2gH/V_1^2$$

WHERE:

K = PRESSURE CHANGE COEFFICIENT
g = ACCELERATION OF GRAVITY, FT/SEC²
H = PRESSURE CHANGE, FT
V_1 = DOWNSTREAM CONDUIT VELOCITY, FPS

ENERGY
GRADIENT
HEAD LOSS $\zeta \frac{V_1^2}{2g}$

PRESSURE
GRADIENT

V_2, D_2 V_1, D_1

FLOW PROFILE
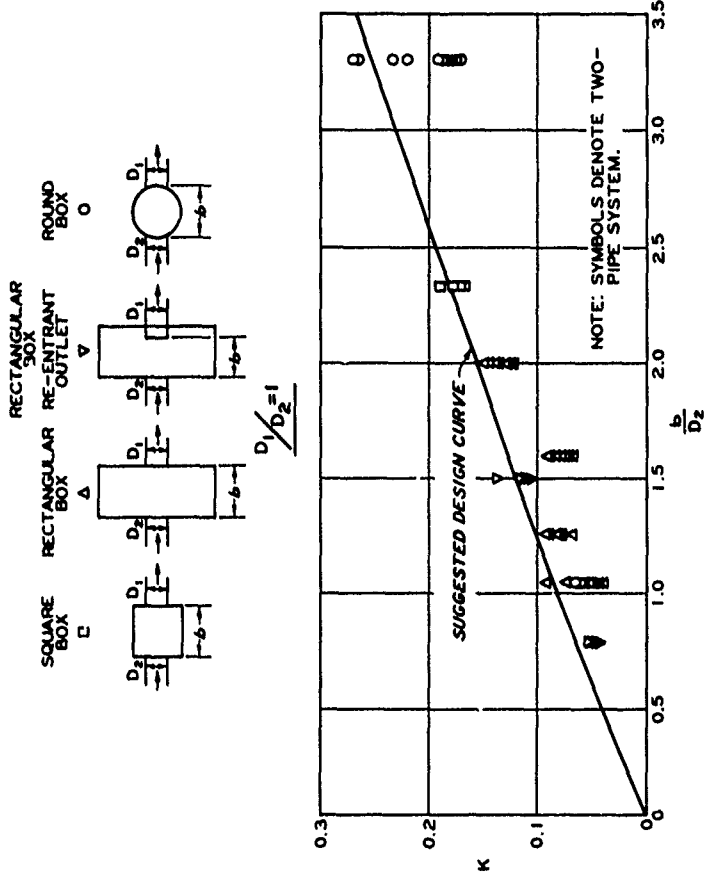
JUNCTION BOX

PRESSURE CHANGE COEFFICIENTS FOR IN-LINE CIRCULAR CONDUITS

HYDRAULIC DESIGN CHART 228-5

WES 7-73

RECTANGULAR CONDUITS

TRIPLE BEND LOSS COEFFICIENTS

1. **Purpose.** Multiple conduit bends are encountered in water supply and air venting systems and to some extent in lock culvert systems. Appreciable data are available for head losses for circular and rectangular conduits with single bends.[1,2,3,4] Composite head loss coefficients for multiple bends have been investigated and reported by Sprenger[5] for a rectangular conduit with an aspect ratio of two in the plane of the bend. Hydraulic Design Chart (HDC) 228-6 reproduces Sprenger's coefficients for triple bend systems with intermediate straight conduit lengths from zero to five times the equivalent hydraulic diameter of the conduit. Sprenger's data from tests on a single 90-deg bend are shown for comparison. The basic report[5] also contains head loss coefficients for many 90-deg bends of various cross sections for aspect ratios of 0.5 and 2.0 in the plane of the bend. Interaction coefficient factors for bends separated by short tangent lengths have also been published by Miller.[6]

2. **Theory.** The head loss associated with a single or multiple bend is defined as the difference in elevation between the uniform upstream and downstream pressure gradients when extended on the longitudinal axis of the conduit to the middle of the bend or bend system. This procedure assumes that normal resistance loss exists throughout the bend system and is computed independently of the geometric head loss. The observed pressure differences (head losses) were divided by the velocity head in the conduit flow to obtain a dimensionless coefficient:

$$K = \frac{H_L}{\frac{V^2}{2g}} \tag{1}$$

where

$\quad K$ = dimensionless head loss coefficient
$\quad H_L$ = observed pressure difference, ft
$\quad V$ = velocity of the conduit flow, fps
$\quad g$ = acceleration of gravity, ft/sec^2

3. The bend loss coefficient is similar to other form resistance coefficients and is a function of the flow Reynolds number:

$$R_e = \frac{VD_h}{\nu} \tag{2}$$

where

R_e = Reynolds number
D_h = equivalent hydraulic diameter of the conduit, ft
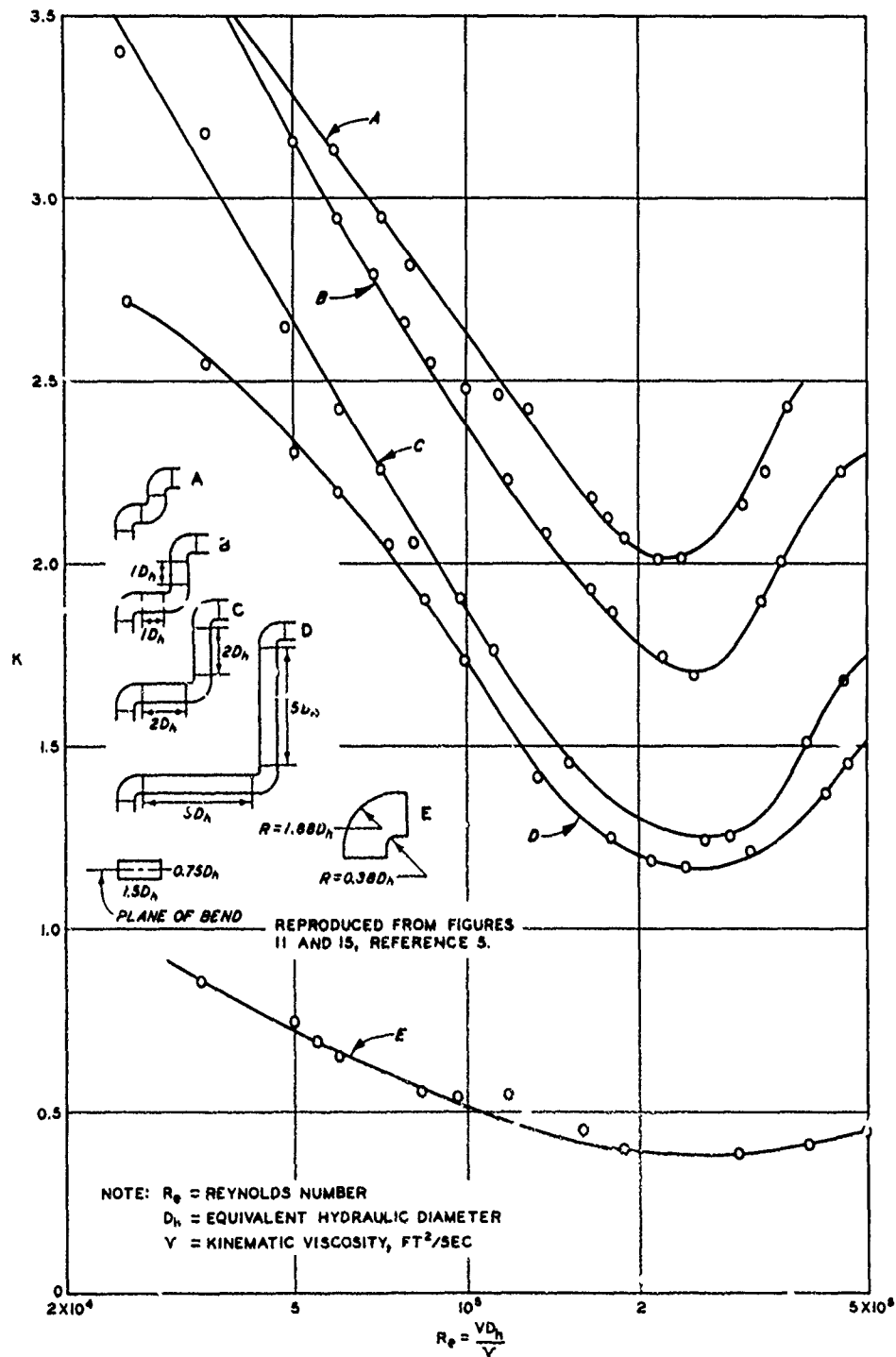ν = kinematic viscosity of the fluid, ft^2/sec

and V and g are as defined above.

4. The head loss coefficient decreases rapidly until it reaches a minimum value at a Reynolds number of about 2×10^5. From this point it increases in value until the Reynolds number reaches about 10^6, beyond which the coefficient probably remains fairly constant.[4]

5. Application. The head loss in a 90-deg rectangular bend with a large aspect ratio in the plane of the bend can be computed using equation 1 and the data given in HDC 228-6. Sprenger's experimental data on single 90-deg bends in rectangular conduits having aspect ratios of 0.5 in the plane of the bend indicate that head loss coefficients for this low aspect ratio are from 0.1 to 0.2 less than comparable values with high aspect ratios in the plane of the bend. It is recommended that the coefficient values given in HDC 228-6 be used for all rectangular conduits with multiple bends when designing for discharge.

6. References.

(1) Madison, R. D. and Parker, J. R., "Pressure losses in rectangular elbows." Transactions, American Society of Mechanical Engineers, vol 58 (1936), pp 167-176.

(2) Harper, J., "Tests on elbows of a special design." Journal of Aero Science (November 1947), pp 587-592.

(3) Silberman, E., The Nature of Flow in Elbows. Project Report No. 5, St. Anthony Falls Hydraulic Laboratory, University of Minnesota, Minneapolis, Minn., December 1947.

(4) Straub, L. G. and Anderson, A. G., Fluid Flow Diversion, A Summary and Bibliography of Literature. Project Report No. 1, St. Anthony Falls Hydraulic Laboratory, University of Minnesota, Minneapolis, Minn., August 1947, p 96.

(5) U. S. Army Engineer Waterways Experiment Station, CE, Head Losses in 90° Elbows for Rectangular Pipes, by H. Sprenger. Translation No. 70-3, Vicksburg, Miss., September 1970.

(6) Miller, D., Internal Flow, A Guide to Losses in Pipes and Duct Systems. British Hydromechanics Research Association, Cranfield, Bedford, England, 1971, p. 43.

3.5

3.0

2.5

K

2.0

1.5

1.0

0.5

0

A

B

C

D

E

$1D_h$

$1D_h$

$2D_h$

$2D_h$

$5D_h$

$5D_h$

$R=1.88D_h$

$R=0.38D_h$

$0.75D_h$

$1.5D_h$

PLANE OF BEND

REPRODUCED FROM FIGURES
11 AND 15, REFERENCE 5.

NOTE: R_e = REYNOLDS NUMBER
D_h = EQUIVALENT HYDRAULIC DIAMETER
Y = KINEMATIC VISCOSITY, FT²/SEC

2×10^4 5 10^5 2 5×10^5

$$R_e = \frac{VD_h}{Y}$$

BASIC EQUATION

$$H = KV^2/2g$$

WHERE:
H = HEAD LOSS, FT
V = CONDUIT VELOCITY, FPS
K = LOSS COEFFICIENT
g = ACCELERATION OF GRAVITY, FT/SEC²

RECTANGULAR CONDUITS
TRIPLE BEND LOSS COEFFICIENTS

HYDRAULIC DESIGN CHART 228-6

WES 7-73